Università degli studi di Genova

XXXI Ph.D. cycle in Science and Technology for Electrical Engineering, Naval Architecture, Complex Systems for Mobility.

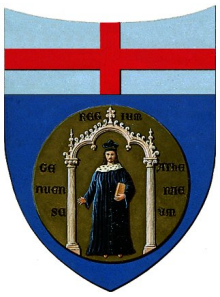

Second Generation Intact Stability criteria:

Analysis, Implementation and Applications to significant ship typologies

Doctoral Thesis in Naval Architecture

Coordinator:
Prof. Mario Marchesoni

Supervisor:
Prof. Paola Gualeni

Candidate:
Nicola Petacco

Genova, Italy
2019

Abstract

The following doctoral thesis addresses all the stability failures embraced by the Second-Generation Intact Stability criteria (SGISc). These criteria are under finalization within the sub-Committee at the International Maritime Organization (IMO). SGISc are one of the most discussed topic since the session in 2008 and they drew the attentions not only of the international scientific community but also of other stakeholders such as designers and shipyards. It is forecast that the second-generation criteria will be finalized and published in an official document at IMO by 2020 session. The new regulation has introduced a modern method to apply the criteria that is called multi-layered approach: it consist of three different vulnerability level with increasing accuracy and complexity.

One of the aims of this dissertation is to evaluate, both qualitatively and quantitatively, how the SGISc will affect existing vessels and new projects. To chase this main object, it has been necessary to develop a set of computational codes, for each stability failure and vulnerability level, integrated with an existing in-house software already developed. Before beginning to compile the codes, the phenomena physics behind each stability failure has been studied together with a detailed analysis of the regulations texts. Subsequently, a comprehensive campaign of application on a representative mega yacht unit and on a Ro-Ro pax ferry has been carried out in order to verify and validate the computational codes developed. Navy vessel and container-ship have been included in the analysis because they are deemed to be vulnerable to the phenomena addressed by SGISc. To identify a relationship between the stability failures and main design parameters, a set of parent hull variations has been carried out. To better understand which parameters are more relevant in each specific phenomenon, it has relied on a useful tool adopted in systems engineering: the Design Structure Matrix (DSM). Thanks to DSM it has been possible to classify the direction and the magnitude of relationships among parameters introduced by the SGISc.

Contents

Nomenclature

α	Linear coefficient of the roll damping, rad/sec.
δGM	Amplitude of the variation of metacentric height in wave, m.
γ	Cubic coefficient of the roll damping, sec/rad^2.
λ	Wave length, m.
∇	Volume of displacement at the considered loading condition, m^3.
∇_D	Volume of displacement at a waterline equal to D, m^3.
ω_ϕ	Natural roll frequency, rad/sec.
ω_{enc}	Encounter roll frequency between the ship and waves, rad/sec.
ϕ_S	Stable heel angle due to an external heeling lever, deg.
ϕ_V	Vanishing angle, deg.
ρ	Sea water density equal to 1.025 t/m.
ρ_{air}	Air density, equal to 1.222 t/m^3.
a	The linear coefficient of roll extinction curve, $-$.
A_k	Total overall projected area of the bilge keels, m^2.
A_W	Waterplane area at the considered loading condition, m^2.
B	Molded breadth of the ship, m.
C_m	Midship section coefficient of the fully loaded condition in calm water, $-$.
D	Molded depth at side to the weather deck, m.
d	Draught amidships at the considered loading condition, m.
d_{full}	Draught corresponding to the fully loaded condition, m.
Fn	Froude number, $-$.
g	Gravitational acceleration equal to 9.81 m/sec^2.

GM_C Metacentric height in calm water, m.

GM_{eq} Metacentric height in waves evaluated with the simplified method (§ 3.1.2), m.

GM_{max} Maximum metacentric height in waves, m.

GM_{min} Minimum metacentric height in waves, m.

$H_{1/3}$ Reference significant wave height for parametric roll criterion, m.

H_i 3% largest effective wave height for pure loss of stability criterion, m.

H_r Representative wave height for parametric roll criterion, m.

H_S Significant wave height obtained from the wave scatter diagram, m.

I Transversal moment of inertia of the waterplane, m^4.

L Length of the ship, m.

S_W Wave steepness defined as $S_W = \lambda/H$, $-$.

T_ϕ Natural roll period of the ship, sec.

T_{enc} Encounter period between the ship and waves, sec.

T_Z Zero-crossing period obtained from the wave scatter diagram, sec

V_S Service ship speed, m/sec.

$W2$ Statistical weighting factor of waves for surf-riding, $-$.

List of Acronyms

BSU Federal Bureau of Maritime Casualty Investigation

CAM Cambridge Advanced Modeler

CPM Critical Path Method

DE IMO Sub-Committee on Ship Design and Equipment

DSA Direct Stability Assessment

DSM Design Structure Matrix

FP IMO Sub-Committee on Fire Protection

GBS Goal Based Standard

IACS International Association of Classification Societies

IC/FBD Input in Column - Feedback Below Diagonal

IMCO Inter-Governmental Maritime Consultative Organization

IMO International Maritime Organization

IR/FAD Input in Row - Feedback Above Diagonal

ISEI Insufficient Stability Event Index

ITTC International Towing Tank Conference

L1 First vulnerability level

L2 Second vulnerability level

MIF Motion Induced Fatigue

MII Motion Induced Interruptions

MOD Ministry of Defense

MSC Maritime Safety Committee

MSI Motion Sickness Incidence

NATO North Atlantic Treaty Organization

NSc Naval Ship code

OG Operational Guidance

OL Operational Limitations

OM Operational Measures

OPV Offshore Patrol Vessel

PERT Program Evaluation and Review Technique

RAO Response Amplitude Operator

SDC IMO Sub-Committee on Ship Design and Construction

SFV Torremolinos international convention for the Safety of Fishing Vessels

SGISc Second Generation Intact Stability criteria

SLF IMO Sub-Committee on Stability and Load lines and on Fishing vessel safety

SOLAS International convention for Safety Of Life At Sea

SYBAS Super-yacht Builders ASsociation

TUHH Technischen Universität Hamburg-Harburg

UNIGE University of Genoa

Chapter 1

Introduction

The increasing of the maritime trade demand in terms of goods transport capacity, the need of short navigation time and less fuel consumption, lead to design a new generation of ships faster and with a larger deadweight than the previous one. The new hull shapes are apparently more sensitive to stability failures in a seaway. Suddenly, the first generation of intact stability criteria appears to be not exhaustive for the upcoming world fleet. They are based on a static approach and tuned on statistical data that in same cases are not fully representative for innovative ships. In this perspective, the International Maritime Organization (IMO) decided to proceed with the renovation of the Intact Stability Code and its integration. During the revision of the Code in 2008, it appeared the need to improve the current stability criteria starting from the basis. To do so, a significant change of the old prescriptive criteria was required. The IMO established an *ad hoc* agenda item to take on this push for innovation. It was decided that the new criteria would be based directly on the physics of the stability failures considered and not on a database of statistics and accidents, as it was for the previous criteria. The different approach leads the whole experts community to study and research new solutions and methodologies to deal with this new criteria. An other relevant difference from the old generation criteria is that, instead to consider the vessel in still water in a zero-speed condition, the new criteria address the interaction between hull and waves in a seaway condition. Thus, in the latest ten year, the development of the so-called Second Generation Intact Stability criteria (SGISc) has been one of the most challenges and important topics addressed by the IMO committee. Their finalization by the committee is forecast in early 2020, it is supposed that the new criteria will be issued as not mandatory and tested for a some years. At the end of this provisional trial period, the outcomes collected will be useful in order to tune and to improve the SGISc.

In light of this, in the thesis a comprehensive campaign of application of all new criteria has been carried out on a set of vessels. Different typologies have been analysed, such as a representative mega-yacht unit, a Ro-Ro pax ferry and some navy vessel. Actually, the latter typology of vessel is not involved in the development of the SGISc because it is not under the IMO regulations. Nevertheless, in the latest years many Navies are feeling the need to assess the vessel stability performance in extreme weather conditions using innovative tools

which go beyond the current specific navy regulations. Therefore, as done also by Grinnaert in [1], navy vessels have been included in the application of SGISc carried out in this thesis, because it has deemed that the new criteria could be a tool able to well fill the gap between the previous navy regulations and the performance-based oriented regulations desired by the Navies.

To do so, the development of assessment tools, able to apply the second generation criteria, has been required. Thus, during my PhD studies the SGISc have been studied from the physical point of view, but also the description of procedures to evaluate each criterion and to implement them has been tackled. This part of work required to follow the development at IMO committee meetings as well as the activities in the correspondence group of the experts. Since the new generation criteria topic is still under finalization, all the outcomes obtained in this thesis are updated to the available documents at the end of 2018. Starting from an in-house developed stability numerical tool available at University of Genoa (UNIGE), a set of computational tools have been developed by Matlab® software during the supervisory task on undergraduate students of MSc. in Naval Architecture and Marine Engineering at UNIGE. As an aid to the development process, a flow chart has been developed for every criterion, thus they have been included in the thesis.

When the new generation criteria will become effective, the designers and the shipbuilders shall be ready to tackle the new challenges and to implement the criteria in the ship design process since the early design phases. It is worth mentioning, an interesting PhD thesis defended in 2017 [2], which has tackled the new criteria too. In that work, the parametric roll failure has been studied taking into account the designer perspective to solve stability problems of volume carrier vessels. On the same stream, but in a comprehensive way embracing all the stability failures, this thesis wants to be a complete study of all the stability failure identified within the SGISc framework. The approaches and methodologies adopted in each criterion have been analysed keeping scientific publications as a reference to understand the origin of each formula introduced, even though, the designer's point of view has been fitted in order to understand the practical implication on the vessel design. In particular, it has been tried to identify such parameters which mostly characterize the design process in the early stages, i.e. those the designer can tune to begin well the ship design. To do so, it has been needed to select a tool able to manage and represent a large number of parameters and, most important, able to represent easily the inter-relationships among them. From the system engineering field, it has been borrowed a powerful technique which has been deemed as useful to the analysis of the new criteria. By means of a square matrix representation, all the criteria have been tackled and the set of most important parameters, shared by every stability failure, has been identified. Thereafter, to quantify the relationship between every selected parameters with the final value of each criterion, the representative mega-yacht hull has been modified in a systematic way changing individually the main dimensions, then the outcomes obtained have been analysed.

Finally, a focus on two specific topics has been conducted: how roll damping coefficient affects the second generation criteria and what is the relationship

between the new criteria and a direct assessment carried out with a complete time-domain tool. As concerns the roll damping coefficient influence on criteria, different methods all based on Ikeda's methodology have been presented and subsequently a blended version of them is formulated. The blended prediction method can be computed knowing just a few information about the design, thus it is usable by the designer as an early design tool. Furthermore, the proposed method has been substituted within the SGISc and a comparison with the original method has been carried out. With the aim to notice the differences between the new criteria and a direct analysis, the excessive acceleration failure has been evaluated by means of a direct assessment tool, kindly made available by the Technischen Universität Hamburg-Harburg (TUHH) during my study period in Hamburg. Again in this study, a set of vessels has been examined and the comparison between the outcomes obtained by the simulation tool and the SGISc application has been carried out.

Chapter 2

Regulatory context

The need of intact stability rules was not explicit until the modification of the International convention for Safety Of Life At Sea (SOLAS) in 1945 when it has been recognised a lack of regulations about this safety aspect. The first international intact stability rule has been issued after the SOLAS'60 modification when the Inter-Governmental Maritime Consultative Organization (IMCO) was recommended to initiate studies on ship stability relying on the SOLAS treaty. As a result, the General Stability Criteria based on righting arm characteristics has been adopted by the Sub-Committee on stability and subdivision of IMCO in 1968 [3],[4] for ships under 100 meters. These criteria are based on a statistical analysis of a large amount of ships already evaluated as safe or unsafe with regard to the stability performance carried out by Rahola [5]. Subsequently, in 1985 the Weather Criterion [6] was adopted by the IMO, who replaced IMCO in 1982, again thanks to recommendations within the SOLAS'74 modification. The criteria included in resolutions from 1962 to 1985 were recommended only, none of them was considered compulsory. Nevertheless they were extensively used as class requirements. In late eighties, in order to make some step forward, IMO decided to gather all resolutions and criteria already developed in one comprehensive document. The idea of an Intact Stability code was accepted by the Organization which developed the draft text. After discussion, the Intact Stability code was firstly adopted in 1993 by IMO Assembly [7] as recommended and, subsequently, revised and made mandatory in 2008 [8]. Very interesting and worth mentioning are papers of Francescutto and Kobyliński, respectively [9] and [10]. They give a complete description of the history of intact stability criteria, from the origin up to the current first generation intact stability criteria. Moreover, a detailed summary about the early stages of development of the so called second generation intact stability criteria is given.

2.1 Development of new generation intact stability criteria

Since the mid 70s of past century a set of new stability criteria was needed and eventually the experts felt that the existing criteria were unsatisfactory. They

asked for *rational* intact stability criteria not based only on statistics of casualty records. The new desire was to have criteria that consider the physic of the stability failure which may lead to a partial or total loss of stability. This approach was called *physical approach* and it considers the hydrodynamic aspects of a ship in a seaway condition. To improve the ship safety against capsizing, it is necessary to understand the actual behaviour of ships in extreme wave environment where the stability problems mostly arise [11], [12], [13], [14].

At the end of the finalization process of the Intact Stability code in 2008, the feel was that, notwithstanding the importance of the work already done, the most important part of the initial scope of the revision was still incomplete. The need of a new generation of intact stability criteria performance-based for a ship in a seaway condition was not satisfied. Nevertheless, the time spent by the Organization updating the existing stability criteria was in any case important to set the basis of the basic structure and dictionary, the relevant concepts and philosophy of the new criteria.

This is highlighted also within the general provisions of the mandatory part of Intact Stability code issued in 2010. Part A, Section 1.1 of the Code states as follows:

> *. . . some ships are more at risk of encountering critical stability situations in waves. Necessary precautionary provisions may need to be taken in the design to address the severity of such phenomena. The phenomena in seaways which may cause large roll angles and/or accelerations have been identified hereunder. [. . .]*

The phenomena identified by the Code are those recognized within the New generation intact stability criteria studies [15], [16], [17] and previously addressed also by IMO Circulars [18],[19]:

- Restoring moment variation due to waves profile (Parametric Roll and Pure Loss of Stability);
- Stability failure in the Dead Ship condition;
- Maneouvring-related stability failure (Surf-Riding and Broaching-to).

At the end of the 51st Session of the IMO Sub-Committee on Stability and Load lines and on Fishing vessel safety (SLF) in 2008, the *ad hoc* intersession correspondence group for the development of New generation intact stability criteria was established (§4.27 of [20]) and it started to examine the proposal submitted from the member state delegations. As a result, during the intersession period hard work have been carried out, so after the 52nd Session of SLF the multi-layered approach have been selected (adopted). It consists of a set of criteria with an increasing level of accuracy for each stability failures. Moreover, the framework of the new criteria together with some fundamental definitions have been specified. At the 53rd Session of SLF in 2010, the excessive acceleration problem has been added to those stability failures addressed by the new generation criteria [21], [22] and the current name of the criteria has been proposed: SGISc.

In the following sessions, the working group handled the development of methodologies to assess the stability failures for each level of vulnerability, but soon it appeared that the work undertaken required long time to be completed. In particular, difficulties appeared when the results of the first and the second level were compared each other using the available version of the criteria at that period [23], [24], [25], [26], [27], [28], [29]. Therefore, the experts begin to deem that a top-bottom development of criteria would have been better in oreder to ensure a few cases of false positives by passing from a level to the higher one.The top-bottom procedure consists in design a realistic numerical model with several degrees of freedom that describes the stability failure considered and then, to gradually simplify it until the accuracy level desired is reached.

In 2013, the IMO Sub-Committee on Ship Design and Construction (SDC) has been established by IMO and it gathered the SLF Sub-Committee together with the IMO Sub-Committee on Ship Design and Equipment (DE) and the IMO Sub-Committee on Fire Protection (FP). The new Sub-Committee continued and enhanced the work on SGISc of the intersession correspondence group. Thanks the new impulse given, in 2012 the first draft text of Level 1 and Level 2 criteria for the phenomena has been presented to the Organization (Annex 1 and 2 of [30]). At the moment, the final draft text of criteria are those contained in Annex 1 to 3 of [31] and Annex 1 to 2 of [32] for all the stability failures. Concurrently, as an aid to the criteria application, a draft Explanatory Note for each stability problem has been drawn up by the working group. It includes a brief description of the physics of the phenomenon, a quick example of application of the criteria and some important definition about specific terms and quantity contained in the criteria formula (Annex 1 to 5 of [33]).

Once the vulnerability criteria have been defined, the working group began to set the basis of the third level, the so called Direct Stability Assessment (DSA). In 2012, the Sub Committee instructed the correspondence group to develop and verify the DSA procedures for all the stability failures. Due to lack of time the documents submitted have not been discussed until the 1st Session of SDC in 2014, when a working version of the Guidelines for direct stability assessment has been presented (Annex 27 of [27]). Nevertheless, to finalize this guidelines document, a dedicated discussion and more quantitative comparison data based on model experiments were indispensable. This happened at the 4th Session of SDC, where the working group addressed the item by using Annex 16 of [34] and [35] as base documents. At the end of this session, the current draft version of guidelines of direct stability assessment procedures have been issued in [36] with the purpose to finalize it in the next sessions. In 2018, during the intersession period subsequent to the 5th Session of SDC, hard work is underway in order to observe the deadline set in §6.15 of [37]: to present a complete draft version of the guidelines at the 6th Session and to publish the final report at the 7th Session.

2.1.1 Multi-Layered approach

The SGISc have been elaborated with reference to the vulnerability concept as explained in [21]. Three different levels are assumed: two levels are made of a

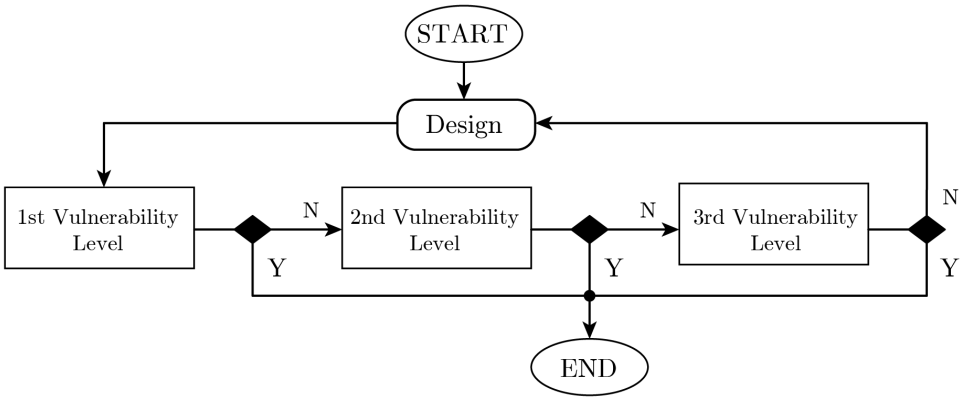

Figure 2.1: Operating principle of the multi-layred approach

vulnerability criterion with the objective to identify ships that could be vulnerable to the stability failures considered, while the last one is a performance based direct stability assessment. The First vulnerability level (L1) aims to roughly separate non-vulnerable ships, often referred to as *conventional* ships, from those which are supposed to be vulnerable, also referred to as *unconventional* ships. The criterion of first level has a procedure, algorithm or a formula as simple as the present Intact Stability code. The Second vulnerability level (L2) is more sophisticated than the first one and it employs physics based methods to consider the dynamic of the relevant phenomena. The outcome of second level assessment should confirm or retract the first level result. Finally, the third level is a direct stability assessment (DSA) procedure that should be as close to physics as practically possible. In Figure 2.1 the concept at the basis of the multi-tired approach is shown. The outcome of the DSA could be a change in the ship design or the development of an Operational Guidance (OG) or the definition of Operational Limitations (OL). The OG is a document containing the recommendation, information or advice to an operator during navigation aimed at decreasing the likelihood of failures (Annex 2 of [38]). The OG are ship-specific recommendations in terms of how to handle the vessel in particular environmental conditions in such a way to avoid potential stability failures. As regards the OL, a clear definition is still missing, although different viewpoint have been expressed so far regarding what they should look like ([39] and Annex 21 of [40]). It seems to be a common understanding that OL can be linked with either the outcome of L2 vulnerability criterion or DSA and it should be limitations on the overall operability of the ship in specific loading and environmental conditions. Currently, at the intersession correspondence group preceding the 6th session of SDC, it is under discussion the possibility to merge the operational limitation and operational guidance into an unique documents called Operational Measures (OM).

One of the objectives of this method, is to avoid unnecessary high costs for an assessment about ships not vulnerable to any specific failure mode. The lower level is based on quite simple formulations and procedures. On the other hand, as an inherent consequence, a very conservative level in term of safety is introduced. If the ship is not able to satisfy L1, the second level criteria is used. In this

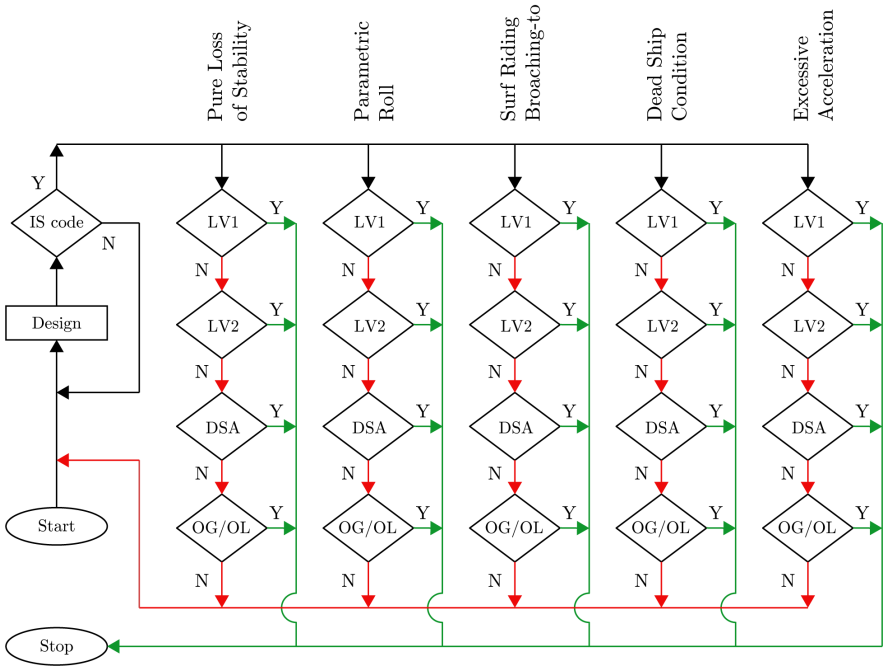

Figure 2.2: Complete structure of the multi-layred approach

case the procedure that has to be followed, is more complicated. Consistently, the safety margin is lower in comparison of L1, in fact, very often the most of merchant ships do not result to be vulnerable for L2. In Figure 2.2 the complete structure of the multilayered approach applied to the SGISc is given.

2.2 Significant accidents

The development of the SGISc have been triggered by a set of not ordinary incidents at sea registered in the latest years. They involve ship considered safe by the stability rule in effect at the time, therefore the concerns of administration and experts have been raised. These incidents have been selected as case studies to benchmark and validate the criteria developed. A selection of them is reported in the following sections. A brief description of the accidents and of the consequences of the events is given on the basis of the report drafted by the competent administrations. Other relevant investigations on similar accidents happened in the past years, not reported in the following sections, can be found in [41], [42], [43].

2.2.1 APL China

The information on the APL China accident given in this section refer to the investigation carried out in 2003 by France W.N. *et alii* [44].

The APL China belongs to the second generation of post-Panamax containership C11 and the overall dimensions are listed in Table 2.1.

The C11 class has been intensely studied by model test or numerical simulation for parametric rolling in following seas, but the head seas condition has never been

considered. This condition was not deemed to be of relevant concern until the APL China accident. The investigations on the accident [44] have shown, by means of numerical simulation with different tools, that the involved stability failure might have been parametric rolling in head seas.

The vessel put out to sea on 20th October 1998 from Kaohsiung (Taiwan), she was headed for Seattle (USA) with two way-point recommended by the weather routing service. Because of changes of weather condition, two forecast pressure lows merged into a meteorological *bomb* within about 120 nm far from the vessel. The storm encounter began on 26th at 00:00 and it lasted until about at 17:00. The worst condition occurred between about 13:00 and 14:30 during which extreme yaw angles, large pitch angles and heel angles up to 40 deg have been recorded. At the time of the accident, the mean draught was 12.34 m, with a freeboard of about 12 m. The transverse metacentric height was nearly 2 m making a natural roll period of around 26 sec. The deck log reported estimate winds of Beaufort force 11 and a sea state 9, the highest level on the International sea state scale, described as *phenomenal* and having average wave heights over 14 m. During the whole period, the master tried to maintain the vessel's head into the prevailing sea direction, as best as he could determine, since the sea was completely confused (Figure 2.3). At the arrival in Seattle, the accident of APL China has been defined as the largest container casualty in history: of the almost 1300 containers on-deck, about one-third has been lost overboard and another one-third has been damaged during the storm encounter (Figure 2.4); luckily no fatalities occurred.

2.2.2 Chicago Express

The information and pictures on the Chicago Express accident given in this section, refer to the investigation report 510/08 carried out by Federal Bureau of Maritime Casualty Investigation (BSU) in 2009 [45].

The Chicago Express is a containership sailing under German flag whose main particulars have been listed in Table 2.2.

The vessel put out to sea at about 17:30 on 23rd September 2008 from Hong Kong towards Ningbo (China) carefully following the instructions to shipping from the local port authority because of the approaching typhoon *Hagupit*. After heel angles up to 32 deg have been reached, at about 19:45, the intended north-easterly route to Ningbo was changed in order to avoid the upcoming thypoon and the course speed was reduced to about 3 to 5 knt due to the rough seas (Figure 2.5). In the first hours on 24th September the storm reached a wind of

Table 2.1: APL China - Overall dimension

Overall dimensions			
Length between perpendicular	L_{BP}	262.0	(m)
Maximum breadth	B	40.0	(m)
Height	D	24.45	(m)
Maximum summer draught	d_{max}	14.0	(m)

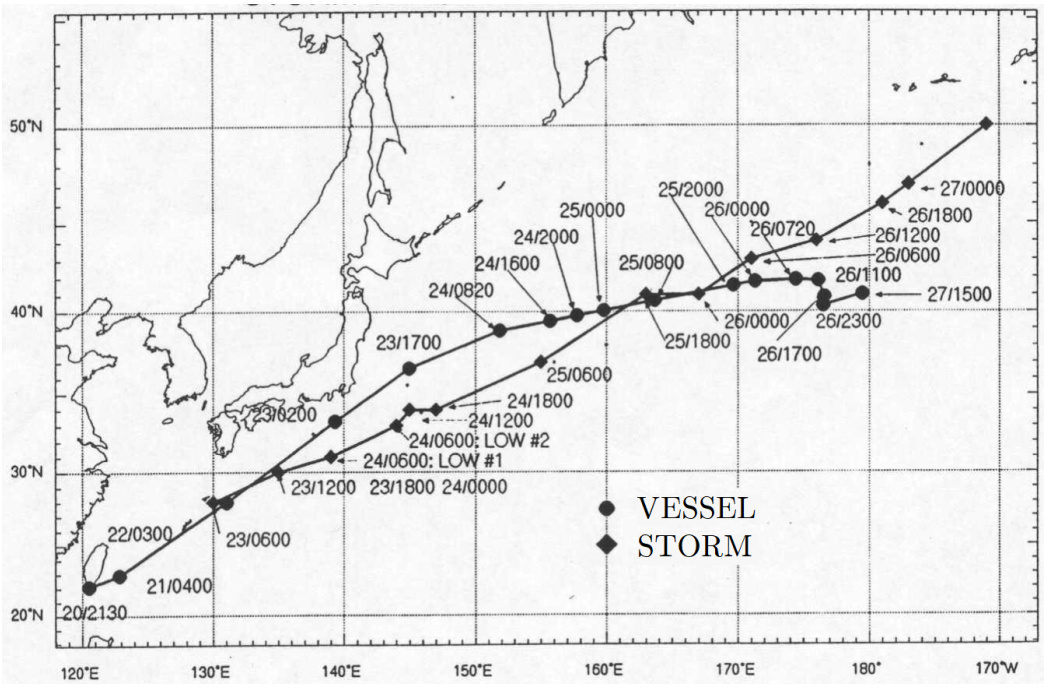

Figure 2.3: Storm track and APL China track [44]

(a) (b)

Figure 2.4: Container damages on APL China at the arrival

Beaufort force 10 with gusts up to 12; at 02:45 the vessel encountered a strong wave from starboard just as she rolled on that side. Because of this event, the Chicago Express heeled to portside and back in a period of about 10 sec reaching a maximum roll angle of about 44 deg and a transversal acceleration of about 9.81 m/sec^2. Due to the unexpected and sudden roll motion, the master, the helmsman and the lookout fell down, bumping into the furniture of the wheelhouse. The helmsman regained his composure well and stood up again very quickly, whereas the master and the lookout were still laying down unconscious. In Figure 2.6, a reconstruction of the path of the fall of the master and the lookout is reported. Immediately, the accident was notified to the competent inshore authority and first aids were given to the injured. Unfortunately, the lookout died on board a short time after the accident because of fatal head injuries, while the master suffered severe injuries to the spine and he was recovered into a hospital

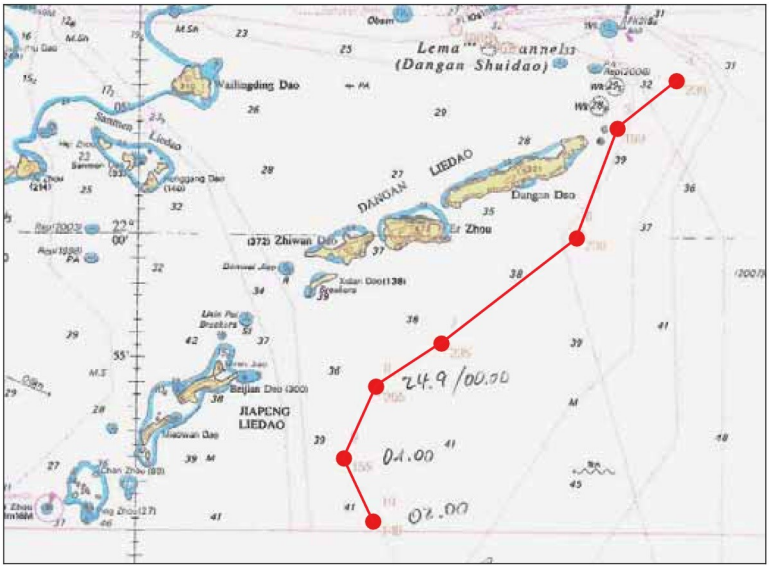

Figure 2.5: Reconstruction of the route of Chicago Express at the time of the accident

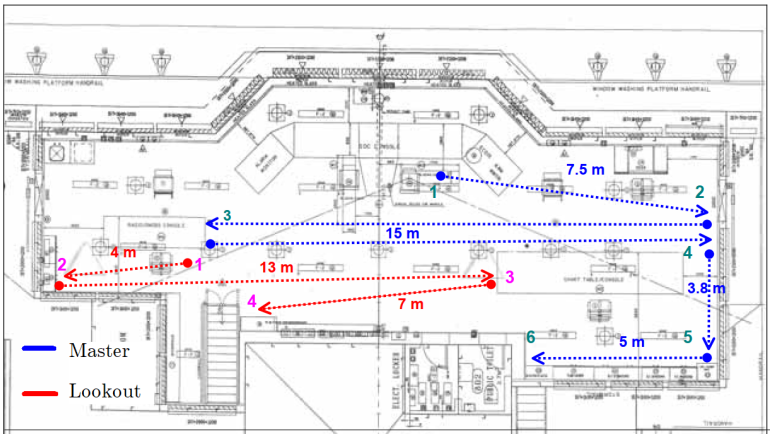

Figure 2.6: Path of the fall of the crew members onboard Chicago Express

Figure 2.7: Nautical chart of the area of the JRS Canis accident

in Hong Kong.

As a results of the investigation carried out by BSU, the experts point out that the simultaneously combination of a large stability value (GM = 7.72 m) and a low roll damping moment due to the low speed are the main responsible of the accidents. Since to drift abeam was not possible due to the proximity of islands, no guilts can be ascribed to the crew members.

2.2.3 JRS Canis

The information and pictures on the JRS Canis accident given in this section, refer to the investigation report 45/07 carried out by BSU in 2008 [46].

The JRS Canis is a container-ship sailing under Cyprus flag and the main particulars at the time of accident have been listed in Table 2.3. The ship departed from Bremerhave (Germany) on 11st January 2007 at 23:06 heading for St. Petersburg (Russia). After some adjustment, the route and the speed were set to 060 deg and 15.5 kts; the vessel was on her way to the Kiel Canal in a beam seas condition (Figure 2.7). The estimated wind force was about 10 on the Beaufort scale, the sea force was 7 to 8 with wave heights up to 5 m and the visibility was apparently good. At about 02:40 on 12nd January, the ship started to heel to each side several times, by up to 20 deg. At that moment, the crew members noticed that the containers on portside leaned inwards and ten of those on star-

Table 2.2: Chicago Express - Overall dimension

Overall dimensions			
Length overall	L_{OA}	336.19	(m)
Maximum breadth	B	42.80	(m)
Maximum draught	d_{max}	14.61	(m)
Maximum speed	V_{max}	25.2	(kts)
Deadweight	DWT	103'691	(tdw)

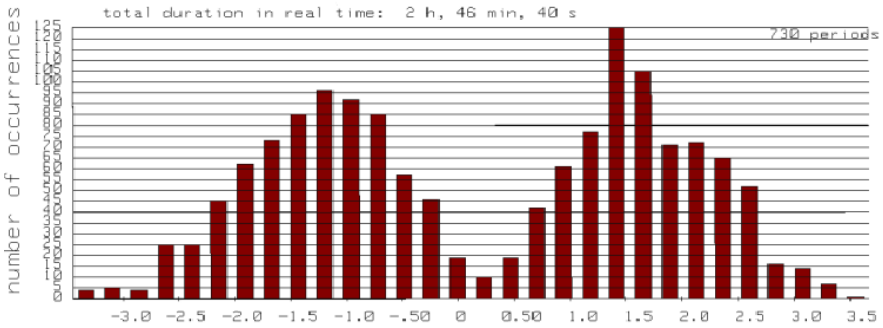

Figure 2.8: JRS Canis statistical distribution of the lateral acceleration in a simulation period of 10'000 sec and a significant wave height of 7 m

board side fell overboard. After a quick inspection on deck, it was decided to continue the voyage toward the Kiel Canal at a reduced speed, the next morning the JRS Canis moored at Brunsbüttel in order to complete investigations began onboard. The investigations report imputed the loss of cargo to a combination of the factors listed below:

- the container lashing experienced a prior wear;
- the unfavorably distribution of container weight in the considered stack;
- the transversal accelerations have been reproduced by a numerical simulation which pointed out values close to the design limit of 0.5 g (Figure 2.8);
- slamming pressures might be occurred leading to exceed a magnitude of 1 g.

Table 2.3: JRS Canis - Overall dimension

Overall dimensions			
Length overall	L_{OA}	129.20	(m)
Maximum breadth	B	20.60	(m)
Mean draught	d_{mean}	7.29	(m)
Service speed	V_s	17.5	(kts)
Deadweight	DWT	8'262	(t)

Chapter 3

Second Generation Intact Stability criteria

In the following sections an overview of each stability failure is given, addressing both the dynamics which govern the physics of the specific phenomenon and the criteria of each level. Furthermore, the background of the models adopted to develop the vulnerability levels has been described thoroughly, focussing on the relationship between the first and second level as well as the approximations embedded in the semplification process. Relevant publications addressed the fundamental of the physics of the phenomena within the SGISc framework, many of them have been submitted at IMO during the session of SLF and SDC of the latest years, but it is worth mentioning also the contribution of other papers and articles; in particular the milestones selected in this thesis addressing SGISc are [47], [48], [49], [50], [51].

3.1 Pure Loss of Stability

Many studies on transverse stability in regular following seas have been made in the past [52], [53] [54], [55]. Capsizing caused by pure loss of stability in following seas was observed by Paulling during experiments in San Francisco Bay [56], [57] (summary available from [58]) and the change of stability in seaway was evaluated with a series of model test [59] (available in English from [60]). They show how the pure loss of stability in regular seaway may be predicted by hydrostatic computations with a sufficient level of confidence. On the contrary, it is not easy to predict the behaviour of ships in irregular seas, especially when the relation between wave and ship stability is non-linear. Thus, to overcome this difficulties, approximated methodologies have been developed and validated, such as the effective wave concept proposed by Grim [61], [62] and [63] or assuming waves to be a narrow-banded stochastic process [64].

3.1.1 Physical background

The physical basis of pure loss of stability is the stability changes due to submerged hull changes because of the wave passage. The submerged hull shape modifications are significant when the wave length is equal to the ship length and the encounter angle is about 0° or 180°. An important factor that enhances the stability changes is a quick enlargement of hull between the deadwork and the quickwork. Vessels most vulnerable to stability changes due to wave profile are those with a relatively high speed and that need large volumes of space for the cargo or passengers. The first statement involves that the submerged hull forms should be very narrow to reduce the hull resistance; while the second one implies that the hull breadth increases swiftly once above the design waterline in order to maximize the available volumes reserved to the cargo or passengers. This description well fits with the operative condition of container-ships, for which large volumes are needed to store more container as possible, but also for some megayachts that require large decks to include the owner's facilities.

Hereunder, the influence of wave profile on the stability performance is described taking into account the most significant situations, i.e. both the wave crest and the wave trough located amidships considering a wave length equal to ship length:

The worst case happens when the wave crest is situated around amidships. While the midship sections are nearly wall-sided and the waterplane width changes little due to draught variations, in the bow and aft sections the decrease of draught involves a pronounced waterplane width reduction for the reasons described above. Therefore, when the wave crest is located amidships, the overall waterplane area is decreased. It is well known from ship hydrostatics that the waterplane area has a relevant effect on ship stability, so if the waterplane area is reduced also the righting moment effort is decreased (Figure 3.1).

On the contrary, when the wave trough is located midship, the effects of wave profile on ship stability are meliorative. For the same reason described above, the reduction of waterplane width amidships is negligible while in the bow and

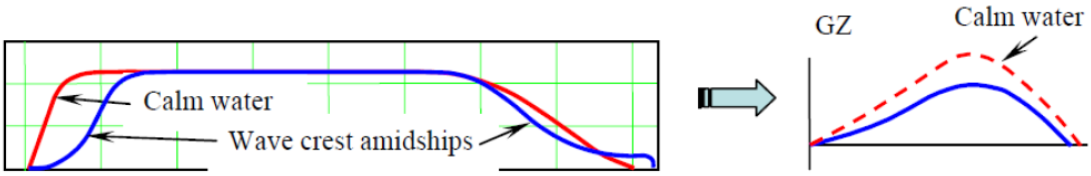

Figure 3.1: Effects of wave crest located amidships [48]

aft part of the hull the waterplane width increases significantly. Hence, when the wave trough is located around amidships the whole waterplane area is increased, as well as the righting arm curve (Figure 3.2).

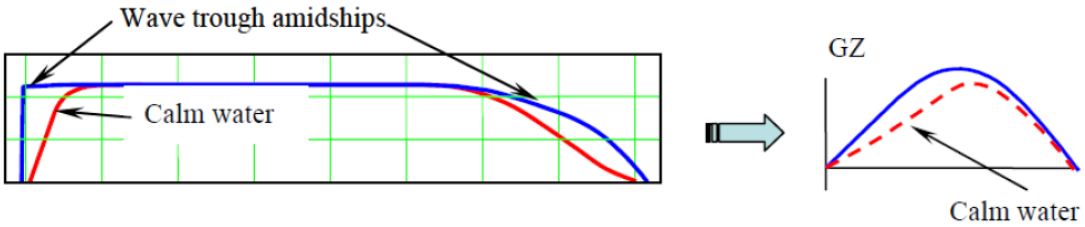

Figure 3.2: Effects of wave trough located amidships [48]

A typical scenario where the pure loss of stability phenomenon may occurs is the following: a wave with the wavelength comparable to the ship length reaches from the stern a ship sailing in following seas characterised by a relatively high speed and low metacentric height (Figure 3.3a). If the wave celerity of the approaching waves is just faster than the ship speed, it takes a long time to pass the ship (Figure 3.3b). Thus, the condition of wave crest amidships and the influence on stability can lasts enough time to be dangerous. This may lead to a large heel angle or even a capsize. Once the wave crest moves away from amidships (Figure 3.3c), the stability is regained and the ship returns to the upright position, only if she has not heeled too far.

3.1.2 Vulnerability Level 1

According to the fundamental of the physics of the phenomenon, both vulnerability Level 1 and Level 2 need not to be applied to all ships for which the Froude number (Fn) corresponding to the service speed, complies with the following formula:

$$Fn < 0.24$$

where:

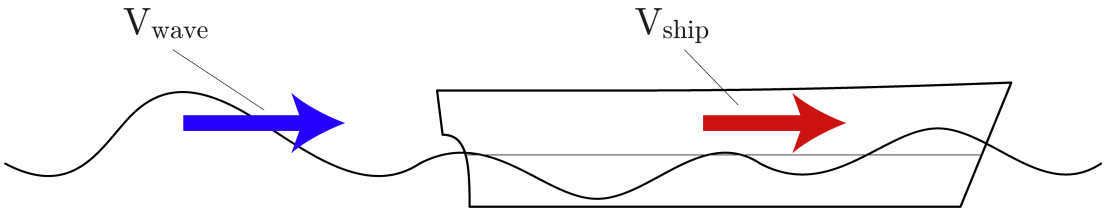

(a) Wave approaching from stern the ship

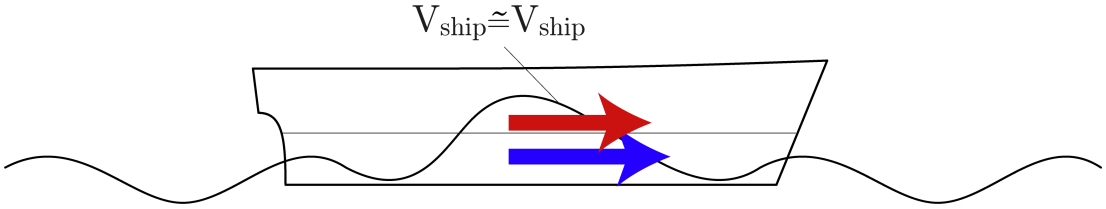

(b) Wave lasting amidship for a long time

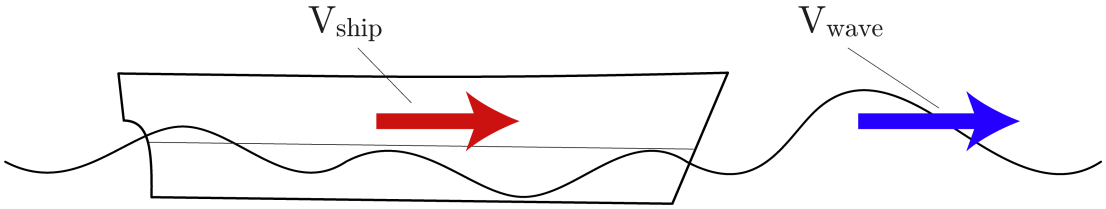

(c) Wave passing the ship

Figure 3.3: Typical scenario of pure loss of stability failure

Fn	=	Froude number,	
	=	$\sqrt{\frac{V_s}{g \cdot L}}$,	(-);
g	=	gravitational acceleration of 9.81,	(m/sec^2);
L	=	ship length,	(m);
V_s	=	service ship speed,	(m/sec).

The first level of vulnerability does not consider a ship to be vulnerable to the pure loss of stability failure mode if:

$$GM_{min} > R_{PLA} \tag{3.1}$$

where:

GM_{min}	=	the minimum value of the metacentric height in waves,	(m);
R_{PLA}	=	0.05,	(m).

Two different procedures are available to compute the amplitude of the metacentric height variation in waves, a description of them is given below. The first one is more precise and it takes into account directly a longitudinal wave while the second method is a simplified procedure applicable only under certain conditions.

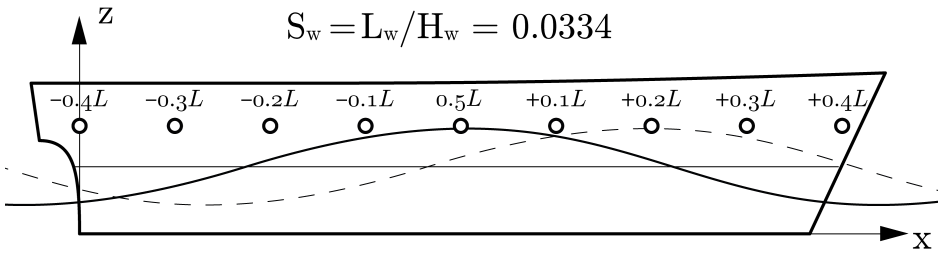

Figure 3.4: Application of direct procedure at pure loss of stability

Direct procedure

The minimum metacentric height (GM_{min}) may be determined considering the vessel balanced in sinkage and trim on a series of waves having a length equal to the ship length ($\lambda = L$) and a steepness coefficient equal to $S_W = 0.0334$. The wave crest should be centered amidships and moved forward and aftward from $0.1L$ to $0.5L$ in both directions with steps of $0.1L$ (Figure 3.4). The wave should be modeled by a sinusoidal wave without hydrodynamic disturbance due to the ship presence.

Simplified procedure

According to the simplified procedure, the minimum metacentric height is computed as follows:

$$GM_{min} = KB + \frac{I_L}{\nabla} - KG \qquad \text{only if} \qquad \frac{\nabla_D - \nabla}{A_w(D-d)} \geq 1.0 \tag{3.2}$$

where:

A_w	=	waterplane area at the draft equal to d,	(m^2);
D	=	molded depth at side to the weather deck,	(m);
d	=	draft amidships corresponding to the loading condition under consideration,	(m);
d_H	=	$d + \delta d_H$,	(m);
d_L	=	$d - \delta d_L$,	(m);
δd_L	=	$Min\big(d - 0.25 d_{full}, \frac{L \cdot S_W}{2}\big)$,	(m);
d_{full}	=	draft corresponding to the fully loaded departure condition,	(m);
I_L	=	moment of inertia of the waterplane at the draft d_L and at zero trim,	(m^4);
L	=	ship length,	(m);
S_W	=	wave steepness equal to 0.0334,	(-);

∇_D = volume of displacement at a waterline equal to D and at zero trim, (m^3);
∇ = volume of displacement corresponding to the loading condition under consideration, (m^3).

The aim of the simplified procedure is to avoid the calculation of *wavy waterlines*. They are simplified with straight lines to calculate the moment of inertia of water plane area: the equivalent metacentric height (GM_{eq}) is evaluated on the waterplane associated to the highest draught of the wave profile (Figure 3.5). Nevertheless, the results obtained by this procedure are more conservative than the Direct Procedure ([65], [66] and [67]).

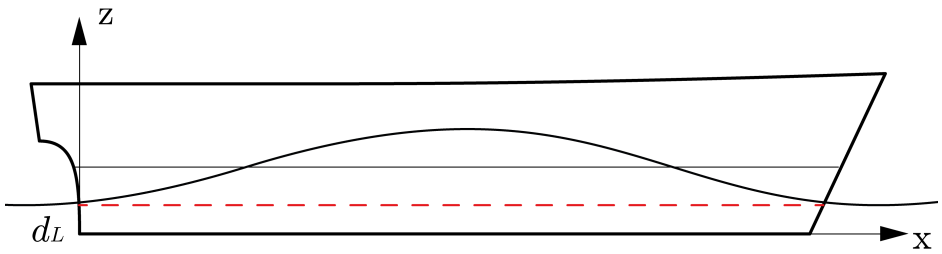

Figure 3.5: Application of simplified procedure at pure loss of stability

3.1.3 Vulnerability Level 2

The second level of vulnerability consists of two different checks: the first one judges the ship vulnerability on the basis of the vanishing angle while the second check takes into account the stable heel angle due to an external heeling lever, both considering the ship statically positioned in waves of defined height and length.

According to second level of vulnerability, a ship is considered not to be vulnerable at pure loss of stability if:

$$max\big(CR1; CR2\big) \leq R_{PL0} \tag{3.3}$$

where:

$CR1$ = criterion of the first check as defined in Eq. 3.4, (-);
$CR2$ = criterion of the second check Eq. 3.5, (-);
R_{PL0} = 0.06, (-).

The value of the standard R_{PL0} has been determined on the basis of the reports of major large heel incidents of RO-RO ships.

Criterion 1

The first criterion is defined as follows:

$$CR1 = \sum_{i=1}^{N} W_i C1_i; \tag{3.4}$$

where:

$CR1_i$	$= 1$	if $\phi_V < R_{PL1}$;	
	$= 0$	if not,	(-);
ϕ_V	$=$	minimum vanishing angle among all wave crest position for each wave defined by the code	(deg);
R_{PL1}	$=$	30 degrees,	(deg);
N	$=$	number of wave cases defined by the selected wave scatter diagram,	(-);
W_i	$=$	the weighting factor for the respective wave cases as specifed by the selected wave scatter diagram,	(-).

Criterion 2

The second criterion is defined as follows:

$$CR2 = \sum_{i=1}^{N} W_i C2_i; \tag{3.5}$$

where:

$CR2_i$	$= 1$	if $\phi_S > R_{PL2}$;	
	$= 0$	if not,	(-);
ϕ_S	$=$	stable heel angle considering the action of a constant heeling lever equal to R_{PL3}	(deg);
R_{PL2}	$=$	15 degrees for passenger ships,	
	$=$	25 degrees for other ships,	(deg);
R_{PL3}	$=$	$8 \cdot (H_i/\lambda) \cdot d \cdot Fn$	(m);
N	$=$	number of wave cases defined by the selected wave scatter diagram,	(-);
W_i	$=$	the weighting factor for the respective wave cases as specifed by the selected wave scatter diagram,	(-).

The calculation of stability in waves should assume the ship balanced in sinkage and trim on a series of waves with a length equal to the ship length and the following wave heights:

$$h = 0.01 \cdot jL \qquad \text{where} \qquad \text{j} = 0, 1, \ldots, 10.$$

For each studied wave, the wave crest is to be centered amidships and shifted aftward and forward, with steps of $0.1L$, from $0.1L$ to $0.5L$.

The stability analysis should be carried out for each value of h_j. Thereafter, for each sea state defined by the wave scatter diagram, a 3% largest effective wave height (H_i) should be evaluated according to the procedure defined in [33]. Both the vanishing angle and the stable heel angle associated to the representative wave height are obtained by linear interpolation among the corresponding indexes computed for the different wave heights (h).

For the evaluation of the above requirement, the wave scatter diagram should be selected to the satisfaction of the Administration. In case of no specific data, the rule text suggests the wave scatter diagram provided by International Association of Classification Societies (IACS) Recommendation No.34 (Appendix A).

3.1.4 Background and relationship between Level 1 and Level 2

As it is in the general philosophy of SGISc, the Vulnerability Level 1 is modeled as a simplified version of the second level. The righting arm curve and the maximum heeling angle achieved in specific wave conditions are considered by the second level of vulnerability, while, in the first level, only the minimum metacentric height is judged. Small metacentric heights does not always lead to weak values of righting arm in waves. Therefore, the first level of vulnerability is more conservative than the second one because it considers only the metacentric height instead of the whole righting arm diagram. In order that a critical situations happens, besides the restoring moment reduction due to hull and wave profile interaction, a heeling moment is required. This is because if no heeling moment exists, the upright position can be kept. Therefore, a relevant external moment is required such as a wave exciting roll moment due to oblique wave heading or a transversal moment induced by a centrifugal force due to ship manoeuvring motions. Thanks to the cross comparison of tank test and numerical simulations (Annex 2 and 4 of [68], [69], [70]), both the restoring reduction due to a wave crest and the centrifugal force due to large yaw angular velocity should be considered to register large roll angle with the wave crest amidship. In view of this, the current formulation of the standard at the second level of vulnerability considers an heeling lever due to the centrifugal force (Annex 12 of [71]).

Environmental condition selection to assess the pure loss of stability (as well as for parametric roll) has been a crucial part of the development of the relevant criteria. Two main proposals have been submitted during the SLF 55 meeting, in order to define the wave characteristics (i.e. wave length and wave height). The first one is a probabilistic-based method (Annex 2 of [71]), which takes into account the ship length and, by means of some probabilistic assumption, it computes a wave height as function of a selected wave length. The second method defines a set of waves evaluated according to the procedure in Annex 1 of [71]: considered the wave scatter diagram provided by IACS Recommendation No.34 (Appendix A), for each zero crossing period T_Z the wave length is directly calculated as follows:

$$\lambda = \frac{g \cdot T_Z^2}{2 \cdot \pi} \tag{3.6}$$

while, the wave height is obtained by the following formula:

$$H_i = k \cdot H_{ref,i} \tag{3.7}$$

where k is a specific constant factor for the stability failure considered (pure loss of stability or parametric roll) and $H_{ref,i}$ is the reference significant wave height selected as the conditional mean significant wave height from the wave scatter

diagram. This method does not take into account the ship length, therefore, minor revisions have been proposed during the intersession correspondence group (Annex 3 of [71]). In this way, the ship length has been taken into account by means the Grim's effective wave concept [61] while the reference significant wave height is selected as the conditional maximum significant wave height, in order to be more conservative than the first proposal.

3.2 Parametric Roll

The fundamentals that characterize the parametric roll failure mode within the SGISc framework are faced in this section, including some background information on the physics of this phenomenon and a brief description of the main mathematical model used to study it. Moreover, an analytical and commented description of the vulnerability Level 1 and Level 2 is provided.

This phenomenon was well known at naval architects in the past as discussed by Froude [72], by Pollard and Dudebout [73] and by Paulling in 1930s [74], [75]. At the beginning, it was considered only a following seas failure [76] limited to smaller high-speed displacement vessels, but successively, Dallinga [77] has observed that parametric roll may affect also longer ship in heading seas, in particular large container-ships.

3.2.1 Physical background

The phenomenon of parametric rolling is based on the variation of restoring moment due to waves encounter, previously described in Section 3.1.1. Three important factors characterize the development of parametric roll resonance: the wavelength, the ship roll damping and the encounter period between the ship and the waves train. As regards the wavelength, the worst case is represented by a wavelength equal or nearly the ship length. This condition involves the maximum waterplane area change and immersed volume distribution variation, thus, the maximum change of the righting moment. In order that parametric roll starts and persists for a sufficient time to develop large angles of heel, the ship roll damping should be insufficient to dissipate additional energy accumulated because of parametric resonance. The third important factor is the relationship between the ship natural roll frequency and the encounter frequency, it characterizes the type of parametric roll. If the encounter frequency is about twice the roll frequency, the roll motion will start growing more and more. This condition is called principal parametric roll and it is the most common phenomenon. The other condition for which parametric roll may still exist is unusual and it is called fundamental parametric resonance. It happens when the encounter frequency is nearly the same of the ship natural frequency even if the likelihood to encounter such a condition is relatively small.

The development of principal parametric roll is a combination of factor that lead the ship to roll angle larger and larger. Considering the ship transversally far away from the upright position, a wave with a length equal to ship length moves its crest to amidships (Figure 3.6a). Due to the wave profile on the hull, the increased righting moment roughly pushbacks the ship towards her upright position with a higher rate. Because of the particular encounter frequency, when the ship is nearly to reach the upright point, the wave trough gets to amidships section. In this condition, stability is decreased and the ship will roll to the opposite side with less resistance to heeling and greater speed (Figure 3.6b). Then, once the ship comes at her maximum roll amplitude and the wave trough reaches again the amidships section, the stability increases again and the cycle

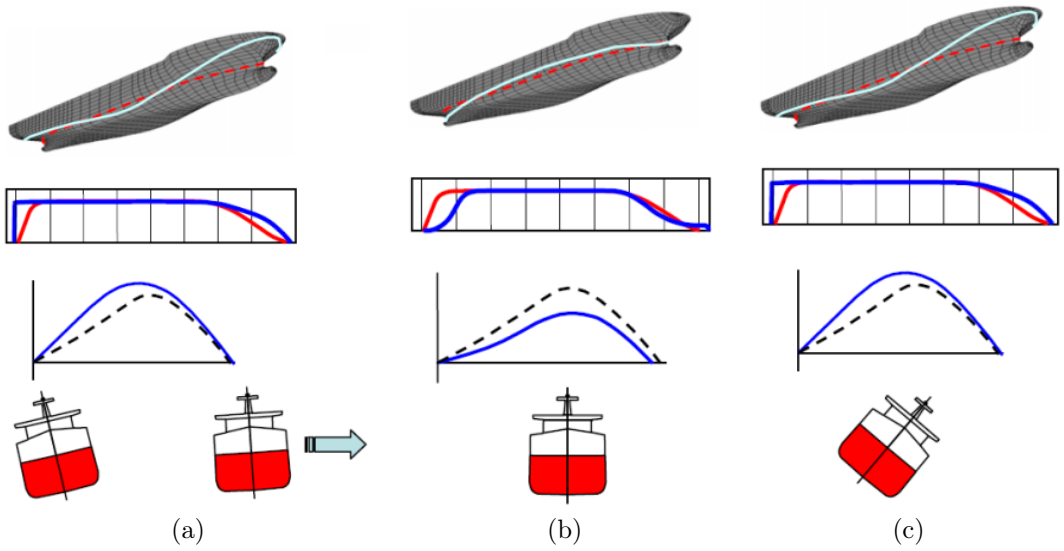

Figure 3.6: Development of parametric roll phenomenon [48]

starts with heel angle larger and larger (Figure 3.6c). In order that principal parametric roll develops, two waves should pass trought the hull during each period. That means the encounter period is about half the natural roll period (Figure 3.7).

$$T_{enc} \simeq \frac{1}{2} \cdot T_{\phi}$$

Frequency influence on Paramentric Roll

Sometime, due to the similar ship rolling behaviour, parametric roll is confused with the synchronous roll resonance. Parametric roll may exist only within a limited field of encounter frequencies outside them its amplitude is zero (Figure 3.8a), on the contrary, roll resonance phenomenon exists for all frequencies even if with lower effects on the amplitude for frequencies away from that of res-

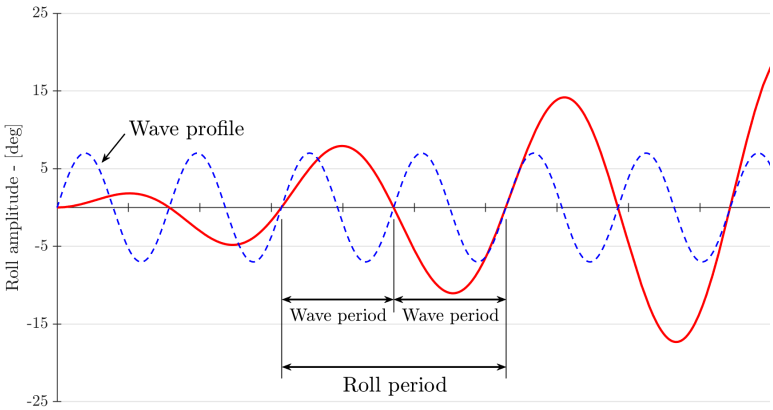

Figure 3.7: Relationship between the wave period and natural roll period in parametric roll

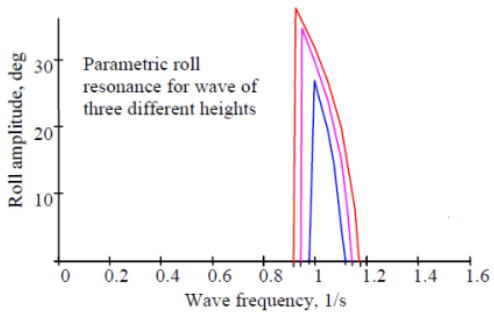

(a) Roll amplitude of parametric roll

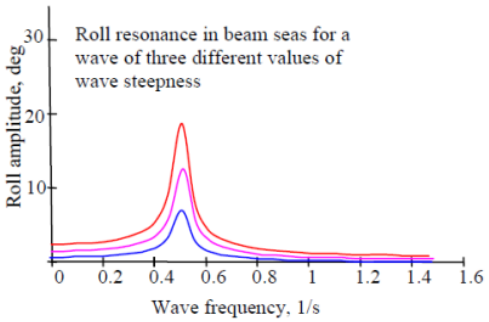

(b) Synchronous roll

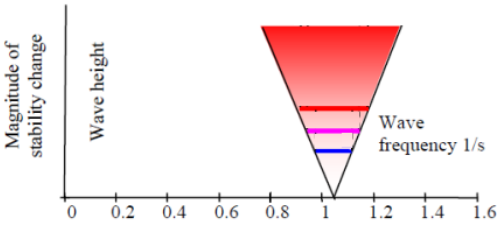

(c) Magnitude of stability change of parametric roll

Figure 3.8: Range of frequencies of parametric roll phenomenon and synchronous roll [33]

onance (Figure 3.8b). Both these two phenomena depend on the wave steepness but for different reason: for parametric roll the amplitude of roll motions depends on the magnitude of stability changes (Figure 3.8c), while in roll resonance the roll motion amplitude depends on the wave height. Should be taken into account that parametric roll develops in longitudinal seas while synchronous roll resonance happens in beam seas.

3.2.2 Vulnerability Level 1

The first level of vulnerability does not consider a ship to be vulnerable to the parametric rolling failure mode if:

$$\frac{\delta GM}{GM_C} \leq R_{PR} \tag{3.8}$$

where:

$$\begin{aligned}
R_{PR} &= 1.87, \text{ if the ship has a sharp bilge;} && \text{otherwise,} \\
&= 0.17 + 0.425 \cdot \left(\tfrac{100 \cdot A_k}{LB}\right), && \text{if } C_m > 0.96; \\
&= 0.17 + (10.625 \cdot C_m - 9.775) \cdot \left(\tfrac{100 \cdot A_k}{LB}\right), && \text{if } 0.94 < C_m < 0.96; \\
&= 0.17 + 0.2125 \cdot \left(\tfrac{100 \cdot A_k}{LB}\right), && \text{if } C_m < 0.94; \\
&\text{and } \left(\tfrac{100 \cdot A_k}{LB}\right) \text{ should not exceed 4.}
\end{aligned}$$

A_k	=	total overall projected area of the bilge keels,	(m^2);
B	=	moulded breadth of the ship,	(m);
C_m	=	midship section coefficient of the fully loaded condition in calm water,	(-);
δGM	=	amplitude of the variation of metacentric height in wave,	(m);
GM_C	=	metacentric height in calm water for the assessed loading condition,	(m);
L	=	ship length,	(m).

Also in this failure mode, two procedures to compute the minimum metacentric height in waves are provided in the rule text. The first one is more accurate and it considers the vessel balanced on a prescribed wave; the second procedure is a simplified formulation applicable only under certain conditions.

Direct procedure

The amplitude of metacentric height variation (δGM) may be determined as one-half the difference between the maximum and minimum values of the metacentric height calculated for the ship, in the assessed loading condition.

$$\delta GM = \frac{GM_{max} - GM_{min}}{2} \tag{3.9}$$

The vessel should be considered to be balanced in sinkage and trim on a series of waves having a length equal to the ship length ($\lambda = L$) and a steepness coefficient equal to $S_W = 0.0167$. The wave crest should be centered amidships and moved forward and aftward from $0.1L$ to $0.5L$ in both directions with steps of $0.1L$ (Figure 3.9). A computational tool able to balance the equilibrium position of a ship in waves is required by this procedure.

Simplified procedure

According to the simplified procedure, the amplitude of metacentric height variation is computed as follows:

$$\delta GM = \frac{I_H - I_L}{2\nabla} \qquad \text{only if} \qquad \frac{\nabla_D - \nabla}{A_w(D-d)} \geq 1.0 \tag{3.10}$$

where:

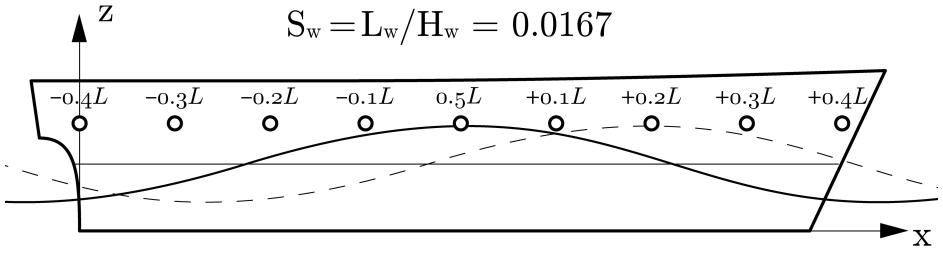

Figure 3.9: Application of direct procedure at parametric roll

A_w	=	waterplane area at the draft equal to d,	(m^2);
D	=	moulded depth at side to the weather deck,	(m);
d	=	draft amidships corresponding to the loading condition under consideration,	(m);
d_H	=	$d + \delta d_H$,	(m);
d_L	=	$d - \delta d_L$,	(m);
δd_H	=	$Min\big(D - d, \frac{L \cdot S_W}{2}\big)$,	(m);
δd_L	=	$Min\big(d - 0.25 d_{full}, \frac{L \cdot S_W}{2}\big)$,	(m);
d_{full}	=	draft corresponding to the fully loaded departure condition,	(m);
I_H	=	moment of inertia of the waterplane at the draft d_H and at zero trim,	(m^4);
I_L	=	moment of inertia of the waterplane at the draft d_L and at zero trim,	(m^4);
L	=	ship length,	(m);
S_W	=	wave steepness equal to 0.0167,	(-);
∇_D	=	volume of displacement at a waterline equal to D and at zero trim,	(m^3);
∇	=	volume of displacement corresponding to the loading condition under consideration,	(m^3).

The aim of the simplified procedure is to simplify the calculation of metacentric height in waves by means of an equivalent straight waterline, as mentioned in Sec. 3.1.2 (Figure 3.10). In this case, the variation of metacentric height is computed by the difference between the maximum equivalent GM and the minimum equivalent GM, respectively evaluated on the highest and the lowest waterplane in relation to the wave profile.

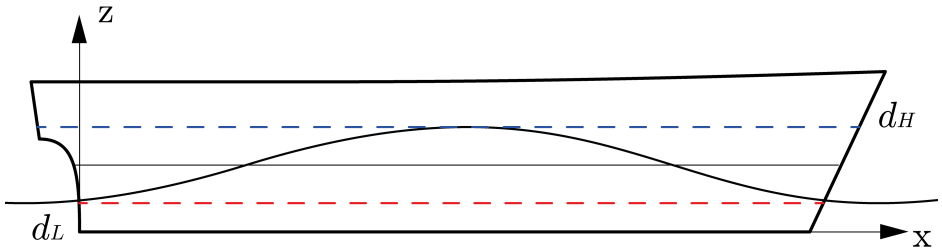

Figure 3.10: Application of simplified procedure at parametric rolling

3.2.3 Vulnerability Level 2

The second level of vulnerability consists of two different checks. While the first judges the ship vulnerable or not on the basis of the occurrence of parametric roll

$C1$	=	criterion of the first check (Eq. 3.12),	(-);
$C2$	=	criterion of the second check (Eq. 3.15),	(-);
R_{PR0}	=	0.06,	(-).

failure, the second check takes into account the magnitude of roll angle achieved during the parametric rolling.

According to second level of vulnerability, a ship is considered not to be vulnerable at parametric rolling if:

$$max\big(C1; C2\big) \leq R_{PR0} \tag{3.11}$$

where:

The value of the standard R_{PR0} has been determined on the basis of the reports of major large heel incidents of a container-ship.

First check

The criterion of first check is defined as follows:

$$C1 = \sum_{i=1}^{N} W_i C_i; \tag{3.12}$$

where:

C_i	$= 0$	if the requirements of either the variation of GM in waves (Eq. 3.13) or the ship speed in waves (Eq. 3.14) are satisfied;	
	$= 1$	if not satisfied,	(-);
N	=	number of wave cases defined by the selected wave scatter diagram,	(-);
W_i	=	the weighting factor for the respective wave cases as specified by the selected wave scatter diagram,	(-).

The requirements of the variation of GM in waves is considered satisfied if, for waves defined by the code, the assessed loading condition agrees with the following equations:

$$GM\big(H_i, \lambda_i\big) > 0 \quad \text{and} \quad \frac{\Delta GM\big(H_i, \lambda_i\big)}{GM\big(H_i, \lambda_i\big)} < R_{PR} \tag{3.13}$$

where:

$GM\big(H_i, \lambda_i\big)$	=	the average value of GM considering the ship to be balanced in sinkage and trim on a series of wave characterized by H_i and λ_i,	(m);
$\Delta GM\big(H_i, \lambda_i\big)$	=	the amplitude of the variation of GM, considering the ship to be balanced in sinkage and trim on a series of wave characterized by H_i and λ_i,	(m);

H_i	=	wave height of wave-i defined by the code,	(m);
λ_i	=	wave length of wave-i defined by the code,	(m);
R_{PR}	=	standard as defined in Sec. 3.4.2,	(-).

The requirements of ship speed in waves is considered satisfied if, for waves defined by the code, the vessel agrees with the following equations:

$$V_{PR_i} > V_S \tag{3.14}$$

where:

V_S	=	service ship speed,	(m/sec);
V_{PR_i}	=	reference ship speed corresponding to parametric resonance conditions,	
	=	$\left\lvert\left(\frac{2\lambda_i}{T_\phi}\cdot\sqrt{\frac{GM(H_i,\lambda_i)}{GM_C}}\right)-\sqrt{\frac{g\lambda_i}{2\pi}}\right\rvert$	(m/sec);
GM_C	=	as defined in Eq. 3.8,	(m);
$GM(H_i,\lambda_i)$	=	as defined in Eq. 3.13,	(m);
g	=	gravitational acceleration of 9.81,	(m/sec^2);
H_i	=	wave height of wave-i defined by the code,	(m);
λ_i	=	wave length of wave-i defined by the code,	(m);
T_ϕ	=	roll natural period in calm water,	(sec).

The 16 wave cases to be analysed in the previous requirements, are obtained from the wave scatter diagram provided by IACS Recomendation No. 34 (Appendix A). If an other wave scatter diagram is selected, the procedure to extrapolate the new wave cases is defined in the Explanatory Notes of the rule text, as proposed for the first time in Annex 1 of [71].

Second check

The criterion of second check is defined as follows:

$$C2 = \left(\sum_{i=1}^{3} C2_h(Fn_i) + C2_h(Fn=0) + \sum_{i=1}^{3} C2_f(Fn_i)\right)/7; \tag{3.15}$$

where:

$C2_h(Fn_i)$	=	calculated according to Eq. 3.16 with the ship sailing in heading seas with a Froude number equal to Fn_i,	(-);
$C2_f(Fn_i)$	=	calculated according to Eq. 3.17 with the ship sailing in following seas with a Froude number equal to Fn_i,	(-);
Fn_i	=	Froude number corresponding to considered ship speed,	
	=	$V_i/\sqrt{L\cdot g}$,	(-);

g	=	gravitational acceleration of 9.81,	(m/sec^2);
L	=	length of the ship,	(m);
V_i	=	$V_S \cdot K_i$,	(m/sec);
V_S	=	ship service speed,	(m/sec);
K_i	=	as defined in Table 3.1,	(-).

Table 3.1: Corresponding speed factor - K_i

i	$\mathbf{K}_i$
1	1.00
2	0.866
3	0.50

The value of $C2(Fn)$ is calculated as a weighted average from the set of waves described by a selected scatter diagram prescribed by the text.

$$C2_h(Fn) = \sum_{i=1}^{N} W_i \cdot C_i \tag{3.16}$$

$$C2_f(Fn) = \sum_{i=1}^{N} W_i \cdot C_i \tag{3.17}$$

where:

C_i	= 0	if the maximum roll angle evaluated according to the procedure described below, is lower than 25 degrees,	
	= 1	otherwise,	(-);
W_i	=	the weighting factor for the respective wave cases as defined by the selected scatter diagram,	(-);
N	=	total number of wave cases defined by the selected scatter diagram,	(-).

The calculation of stability in waves should assume the ship balanced in sinkage and trim on a series of waves with a length equal to the ship length and the following wave heights:

$$h_j = 0.01 \cdot jL \qquad \text{where} \qquad \text{j} = 0, 1, \ldots, 10.$$

The model simulation should be carried out for each value of h_j. Thereafter, for each sea state defined by the selected wave scatter diagram, a representative wave height H_{r_i} should be evaluated according to the procedure defined in the Explanatory Notes of the rule text. The maximum roll angle associated to the representative wave height is obtained by linear interpolation among the maximum roll angles computed for different wave heights h_j.

The simplest mathematical model capable to carry out this simulation is the one degree-of-freedom model:

$$\hat{I}_{44} \cdot \ddot{\phi} + B_{44} \cdot \dot{\phi} + C_{44} \cdot \phi = M_{44}(\phi) \tag{3.18}$$

The model includes four different moments, represented by the following coefficients:

- $\hat{I}_{44}$: Moment of Inertia coefficient considering also the added inertia due to hydrodynamic forces, $\hat{I}_{44} = I_{44} + A_{44}$. In the absence of specific data, the added mass term can be assumed $A_{44} = 0.25 I_{44}$;

- B_{44}: Roll damping moment coefficient, which represents the dissipated energy by the roll motion. The roll damping component represented by linear and cubic coefficients is suggested by the rule. An in-depth analysis of roll damping is given in § 7.1;

- C_{44}: Roll restoring moment coefficient taking into account the variation of stability in waves. A quasi-static approach can be used to define the righting arms for each crest and computing the values of intermediate wave crest positions by a bilinear or bi-cubic spline interpolation. Otherwise, an averaging method for determining roll amplitude is proposed in the Explanatory Notes of the rule text;

- M_{44}: Transverse external moments which are considered null in following or heading long crested seas.

For the evaluation of the above requirement, the wave scatter diagram should be selected to the satisfaction of the Administration. In case of no specific data, the rule text suggests the wave scatter diagram provided by IACS Recommendation No.34 (Appendix A)

3.2.4 Background of Level 1 and Level 2

The criterion of the first level of vulnerability and the first check of the second level have been developed by simplifying the second check of the second level of vulnerability. As explained in [78], Eq. 3.18 can be rewritten as follows:

$$\ddot{\phi} + \frac{B_{44}(\phi)}{\hat{I}_{44}} \cdot \dot{\phi} + \frac{C_{44}}{\hat{I}_{44}} \cdot \phi = 0 \tag{3.19}$$

The roll damping component and the restoring moment in waves can be expressed in the following linear formulation:

$$\frac{B_{44}(\phi)}{\hat{I}_{44}} \cdot \dot{\phi} = 2\delta\dot{\phi} \tag{3.20}$$

$$\frac{C_{44}}{\hat{I}_{44}} \cdot \phi = {\omega_\phi}^2 \cdot f_L(\phi, t) \tag{3.21}$$

Replacing Eq. 3.20 and Eq. 3.21 in Eq. 3.19, an equivalent form of Mathieu equation is obtained:

$$\ddot{\phi} + 2\delta\dot{\phi} + {\omega_\phi}^2 \cdot f_L(\phi, t) = 0 \tag{3.22}$$

Due to strong non-linearity of the righting arm curve and of the ship roll damping, as proposed in [68], the following equation of the parametric roll model is obtained:

$$\ddot{\phi} + \left(2\alpha\dot{\phi} + \gamma\dot{\phi}^3\right) + {\omega_\phi}^2 \cdot f_N(\phi, t) = 0 \tag{3.23}$$

where the non-linear function which described the restoring moment is expressed as follows:

$$f_N(\phi, t) = \phi + l_3\,\phi^3 + l_5\,\phi^5 + \\ + \left\{GM_{mean} + GM_{amp}\cos(\omega_{enc}t)\right\}\left\{1 - \left(\frac{\phi}{\pi}\right)^2\right\} \cdot \frac{\phi}{GM} \tag{3.24}$$

with:

α, γ	=	respective the linear and cubic coefficient of the roll damping;
ω_ϕ	=	natural roll frequency;
ω_{enc}	=	encounter frequency;
l_3, l_5	=	constants coefficients of restoring moment in calm water;
GM_{mean}	=	mean of the variation of metacentric height in waves;
GM_{amp}	=	amplitude of variation of metacentric height in waves;
GM	=	metacentric height in calm water.

To develop the criterion of the first level of vulnerability and the first check of the second level, the roll damping term and the restoring moment are linearized as follows:

$$\alpha_e \approx \alpha, \quad \gamma = 0, \quad GM \approx GM_E, \quad GM\omega_\phi \approx \omega_{\phi E} \quad \text{and} \quad \mathrm{l}_3 = \mathrm{l}_5 = 0 \tag{3.25}$$

where the suffix E means the equivalently linearized value. In addition, assuming that the mean of metacentric height variation due to waves is small, the following approximation formula can be applied:

$$GM_{mean} = 0 \tag{3.26}$$

when equations 3.25 and 3.26 are substituted into Eq. 3.23, the following formula is obtained:

$$\frac{GM_{amp}}{GM_E} = \frac{8\pi^2\alpha_E}{(2\pi^2 - \theta^2)\omega_{\phi E}} \tag{3.27}$$

where θ is the limiting amplitude of roll angle. Selecting the limiting roll angle in radians equal to 25°, the Eq. 3.27 can be rewritten as follows:

$$\frac{GM_{amp}}{GM_E} \simeq \frac{4\alpha_E}{\omega_{\phi E}} = \frac{4a}{\pi} \tag{3.28}$$

where a is the linear coefficient of roll extinction curve, obtained by the well known energy relationship:

$$a = \frac{\alpha\pi}{\omega_{\phi E}} \tag{3.29}$$

Therefore, a ship may be considered susceptible to parametric roll if the variation of GM in waves to GM in calm water ratio is greater than the right-hand

side of the equations above. The final proposal and other proposals, which are overlooked after wide discussion among the members, are submitted to the inter-session Correspondence Group between the session of SLF 52 and SLF 54. The early stages of such formulation are summarized in [68], [79], [80].

The first check of second level considers a set of 16 typical waves with different heights and lengths. The set of waves is obtained filtering the selected wave scatter diagram and defining a reference significant wave height $H_{1/3,ref}$ for each listed wave period. The detailed procedure is described in Add.1 of [33]. The worst wave length (i.e. the wave as long as the ship) and the maximum wave steepness calculated from the selected wave scatter diagram ($S_W = 0.0167$) are chosen for the first level of vulnerability. Thus the first level is expected to be more conservative than the first check of second level of vulnerability.

While Level 1 and check 1 of Level 2 assess the occurrence of parametric roll condition, the second check of Level 2 criterion evaluates the magnitude of parametric rolling. Hence, if the phenomenon happens with small angle of roll, the procedure of check 2 of second level concludes that the ship is not vulnerable to stability failure due to parametric roll.

3.3 Broaching-to and Surf-Riding

The broaching-to, usually shortened in broaching, is a typical phenomenon occurring in astern seas, where different aspect of stability, manoeuvring and seakeeping are involved. Ship motion in both following and quartering seas has been an important subject for research activity and model test experiment since the 1960s [81], [82], [83], [84], [85]. Thanks to an intensive problem analysis by towing tank tests and numerical simulations, the investigation of the dynamic of this non-linear phenomenon has been very productive and it has involved researchers both from the stability issues community and from the seakeeping experts [86], [87],[88],[89]. The outcomes achieved shown how the broaching phenomenon is preceded by an other one, called surf-riding [90], [91]. The two phenomena characterize mainly medium-sized and relatively fast boats, such as fishing vessels [67], but also some particular navy vessels [92], [93], [94].

For this reasons, the development of a stability criterion for broaching focused on surf-riding, considered as an initial situation very likely capable to evolve in broaching. Hereinafter a description of physics leading to surf-riding and broaching is given.

3.3.1 Physical background

Broaching is identified as a sudden uncontrollable turn of a sailing ship, despite the effort of the rudder to counteract it by manoeuvring in the opposite direction. As common for any other turn in speed, broaching is followed by a large heel angle or even capsizing. The phenomenon that leads to broaching is called surf-riding, for this resons the likelihood of surf-riding occurrence has been selected as a criterion to evaluate the vulnerability to the broaching failure. Surf-riding occurs when a wave, approaching from the stern, engages a ship and accelerates her to the wave celerity keeping constant the wave profile position relative to the ship. Usually, most of ships are directionally unstable in this situation, so any small disturbance may lead the ship to the broaching failure. In order for surf-riding to develop, the following main conditions shall occur:

- *Condition on wave length and ship speed*: The wave length should be between one and three times the ship length, and besides, the ship speed should be comparable to the wave celerity. The combination of these two requisites excludes longer ship because of the relationship between wave length and wave celerity. In light of the fundamental relation $c^2 = g \cdot \lambda/(2\pi)$, long waves are associated to fast celerity which are not achievable for large ships.

- *Condition on wave steepness*: The wave steepness should be great enough to produce a sufficient wave surge force initiating the surf-riding phenomenon. Also for this condition, long ships are unlikely to be vulnerable at surf-riding, since long and steep waves are very rare to occur.

When a ship is sailing in a following seas, three main forces act along the longitudinal axis: propeller thrust, hull resistance and surging wave force. The

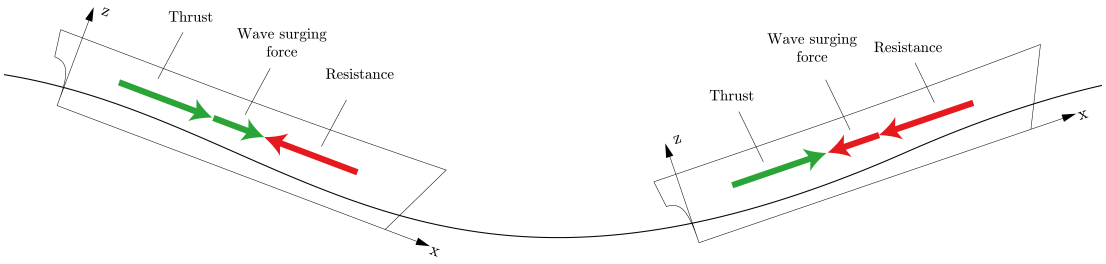

Figure 3.11: Forces acting along the longitudinal axis in following seas

latter is a force applied by the wave, pushing the ship either forward or backward, depending on the relative position of the ship and the wave crest (Figure 3.11).

In order that the ship equilibrium is respected, the following equation must be verified.

$$R_{\text{hull}} - F_{\text{prop}} + F_{\text{surge}} = 0 \tag{3.30}$$

where:

R_{hull}	=	hull resistance as a function of ship speed,	(N);
F_{prop}	=	propeller thrust as a function of ship speed and the commanded number of revolutions of the propulsor,	(N);
F_{surge}	=	surging force generated by the wave, it can be approximated by the following equation:	
	=	$f_x \cdot \sin(-k\, x_G)$	(N);
f_x	=	wave surging factor defined in Ch.6 of [60]	(N);
x_G	=	longitudinal position of the centre of gravity of the ship	(m).

thus, introducing $\delta_x(Fn)$ as the difference between thrust and hull resistance, the surging equation can be rewritten as follows:

$$\delta_x(Fn) = f_x \cdot \sin(-k\, x_G) \tag{3.31}$$

As a result, the only possible solution is verified when the difference between thrust and resistance as a function of wave celerity is equal or less than the amplitude of the sinusoidal surging force. Therefore, two different scenario can develop: surging motion if no equilibrium is possible, surf-riding if it is.

Surging motion

The condition of surging motion occurs when the difference, measured at wave celerity, between hull resistance and propeller thrust $\delta_x(Fn_{textwave})$ is always larger than the magnitude of the wave surge force F_{wave} (Figure 3.12). In this case, wave force is not enough to overcome the difference δ_x and it is insufficient to keep accelerated the ship at the wave celerity, hence no equilibrium points exist.

To better describe the dynamic of surging motion, an example of the resistance and thrust curves around the self-propulsion point are shown in Figure 3.13.

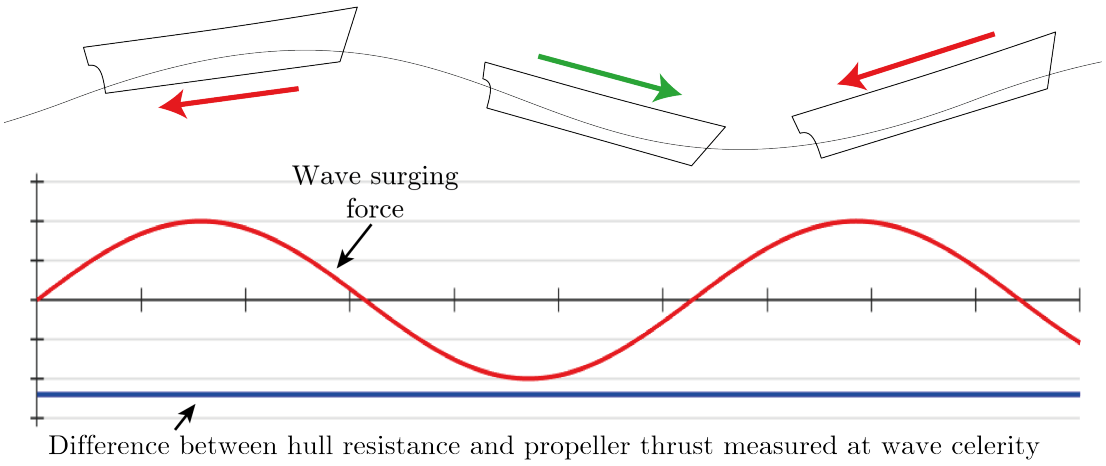

Figure 3.12: Motion of surge in following seas

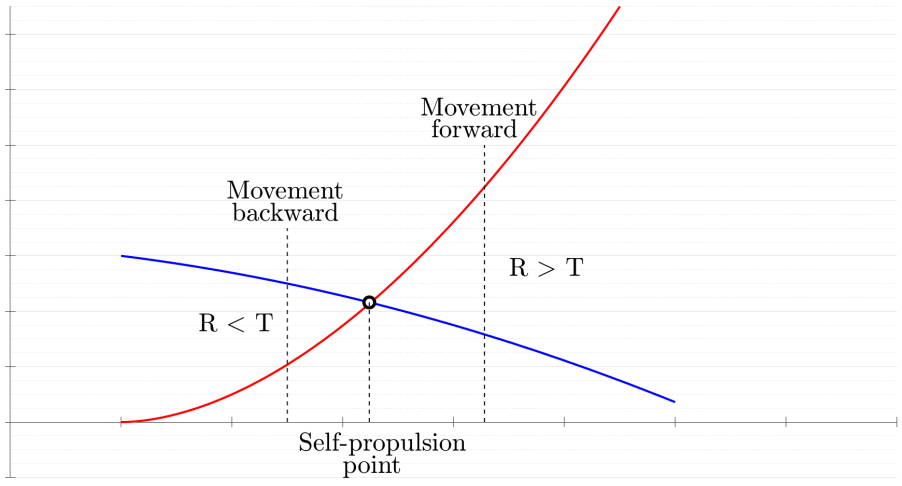

Figure 3.13: Resistance and thrust curves around the self-propulsion point

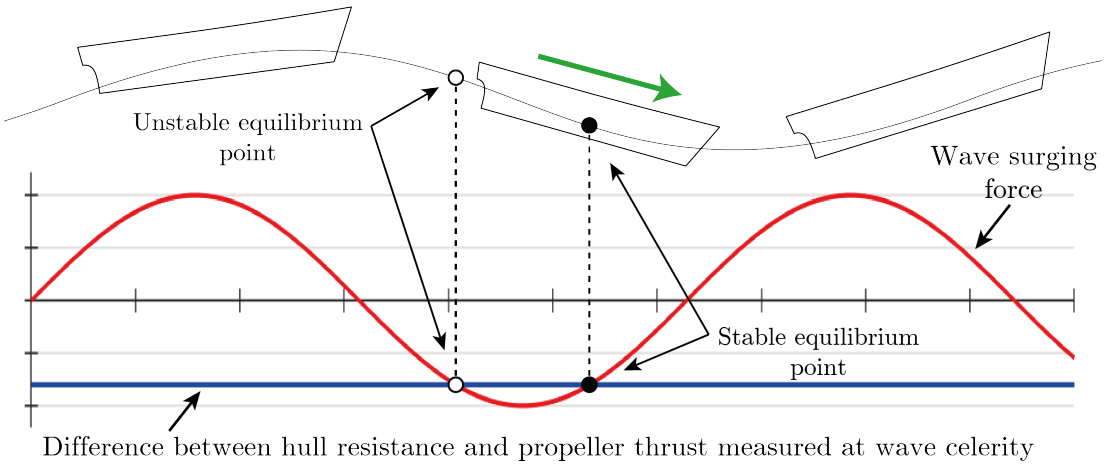

Figure 3.14: Motion of surf-riding in following seas

When the ship moves on the front side of the wave, the increased wave surging force accelerates the ship; so that the istantaneous speed increases and the resistance becomes greater than the thrust. The new difference between resistance and thrust, directed backward, is greater than the wave surge force, therefore the vessel slows down. On the contrary, when the back side of the wave approaches the vessel, the surging force decreases and the ship reduces in speed. As a consequence, the difference between resistance and thrust is greater than wave force but it is directed forward, so the vessel increases her speed. This oscillating motion starts again when the wave overcomes the ship.

Surf-riding condition

The surf-riding condition may occur when at least a solution to Eq. 3.31 exists. Since the sinusoidal shape of wave force, an infinite number of solutions appear when the difference between resistance and thrust at wave celerity is lower than the magnitude of wave force. On the equilibrium points the sum of longitudinal forces is zero, indeed on the other points the resultant force pushes the vessel either forward if the vessel is in the front side of the wave or backward if she is located behind the wave crest.

Since the equilibrium is possible on each wave, when the threshold is crossed an infinite number of solutions appear (Figure 3.14). To get rid of infinity it is possible to limit the observation to only one wave, otherwise it is possible as well to introduce the surging displacement in the form of $\cos(2\pi x/\lambda)$ as Spyrou did in [95], where x is the relative position between the ship and the wave. At this point, two possibile equilibrium points exist where the ship speed is equal to the wave celerity: a stable equilibrium point, located near the wave trough, and an unstable position located a little further on the wave crest (Figure 3.14).

When the ship is under the stable equilibrium condition, despite an external disturbance forward or backward, she returns to the initial condition. If the vessel is pushed ahead along the wave profile, the wave force decreases and she slows down regaing her initial position. On the contrary, if the ship is moved backward,

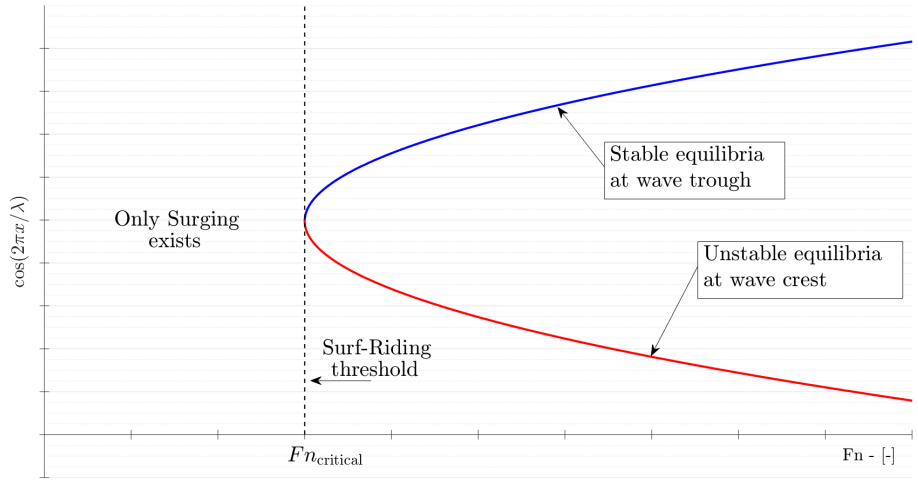

Figure 3.15: Threshold of surf-riding as a function of ship speed

the wave surging force increases pushing the vessel towards the equilibrium point.

The same consideration cannot be taken for the unstable equilibrium. In this case, if the ship is pushed not far from the equilibrium point, she will move away from the initial position. When the disturbance pushes the ship forward, the wave force increases moving the hull along the wave profile until the stable equilibrium point is reached. On the other hand, a disturbance to backward causes a decrease of wave force getting the ship slower, so she will move away from the equilibrium position. Several scenario concerning what may happen next exist, but there are not cases where she returns back to the unstable equilibrium point.

3.3.2 Phase plan analysis

The surf-riding is a phenomenon that can be simulated by a non linear dynamic system, as done in Eq. 3.31. As mentioned above, the solutions of the system correspond to the surf-riding equilibrium points, which can be stable or unstable. In Figure 3.15, the dependence of surf-riding threshold on ship Froude number is represented, moreover the location of stable and unstable equilibria can be appreciated.

Due to the non linearity of the model, an useful tool to represent the changes of system state is the phase plan analysis. The phase plan represents the relationship between a set of variables and parameters with the corresponding time derivatives. In surf-riding case, the plot of speed and surge displacement have been used to develop the criteria setting the Froude number as parameter. A precursor study on surf-riding using phase plan analysis has been done by Makov in [96] and subsequently it has been enhanced by Spyrou in [97], [98]. The outcome of studies on surf-riding shown how two different thresholds as a function of Froude number exist. Representing the system as a dynamic model and setting the ship speed parameter slower than the first surf-riding threshold, for every positions of ship along wave profile the periodic surging motion occurs, as described in § 3.3.1. In the phase plan, such condition means that for each couple of relative

speed and position $(x, \dot{x})$ the ship will be attracted toward the periodic surging curve (Figure 3.16). Increasing the Froude number, the behaviour of the dynamic

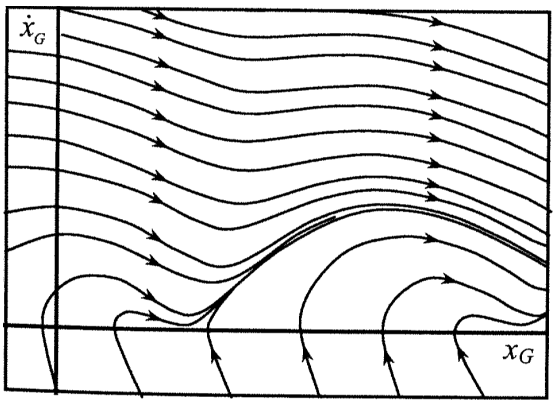

Figure 3.16: Phase plan - Fn $<$ $\mathrm{Fn}_{1^{\mathrm{st}}\mathrm{threshold}}$ [60]

system changes and a global bifurcation occurs, corresponding to the condition when the ship speed overcomes the first surf-riding threshold. A huge change of the phase plan topology occurs and it becomes impossible to map the correspondence of each point before and after bifurcation. Figure 3.17 shows the phase plan after the global bifurcation, in the case when it is possible to identify two equilibrium points (stable and unstable), as defined in § 3.3.1, while the periodic surging motion still exists. An initial condition $(x,\ \dot{x})$ within the attraction area of the stable equilibrium will lead the ship to the surf-riding phenomenon; at the same time, all the points outside this area will lead the ship to the periodic surging motion; this condition is called as surf-riding under certain initial conditions. Setting the initial condition on the unstable equilibrium point, it is possible to understand how, after a small disturbance, the ship will move towards either the stable equilibrium point or the surging motion condition (Figure 3.17a).

Approaching the second speed threshold, again a dramatic change of the phase plan topology happens: a global bifurcation called *homoclinic connection* occurs (Figure 3.18a). When Froude number overcomes the second Froude number threshold, each point of the phase plan $(x,\ \dot{x})$ leads to the stable equilibrium point implying surf-riding phenomenon (Figure 3.18b) that it is called surf-riding under any initial condition. The second threshold is what the criterion takes into account to consider a ship vulnerable or not to the surf-riding phenomenon. The whole behaviour of the dynamic system as a function of the Froude number parameter is shown in Figure 3.19, it is possible also to identify the two thresholds and the corresponding phase plans before and after the global bifurcations.

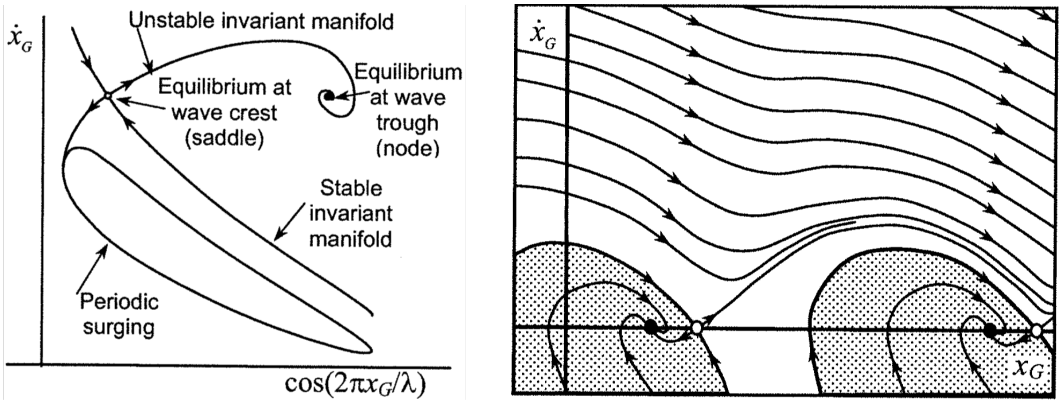

(a) Surge displacement expressed as $\cos(2\pi x/\lambda)$

(b) Surge displacement expressed as x

Figure 3.17: Phase plan - $\mathrm{Fn}_{1^{\mathrm{st}}\mathrm{threshold}} < \mathrm{Fn} < \mathrm{Fn}_{2^{\mathrm{nd}}\mathrm{threshold}}$ [60]

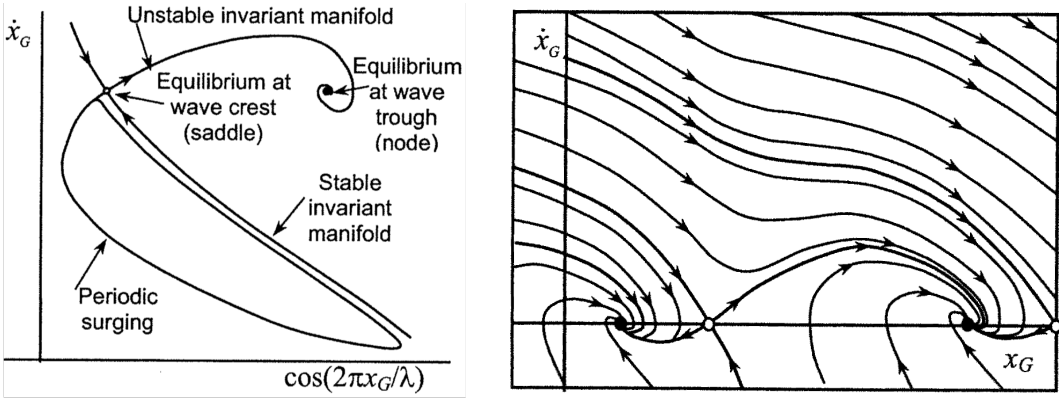

(a) Surge displacement expressed as $\cos(2\pi x/\lambda)$ - $\mathrm{Fn} \simeq \mathrm{Fn}_{2^{\mathrm{nd}}\mathrm{threshold}}$

(b) Surge displacement expressed as x - $\mathrm{Fn} > \mathrm{Fn}_{2^{\mathrm{nd}}\mathrm{threshold}}$

Figure 3.18: Phase plan approaching the second threshold [60]

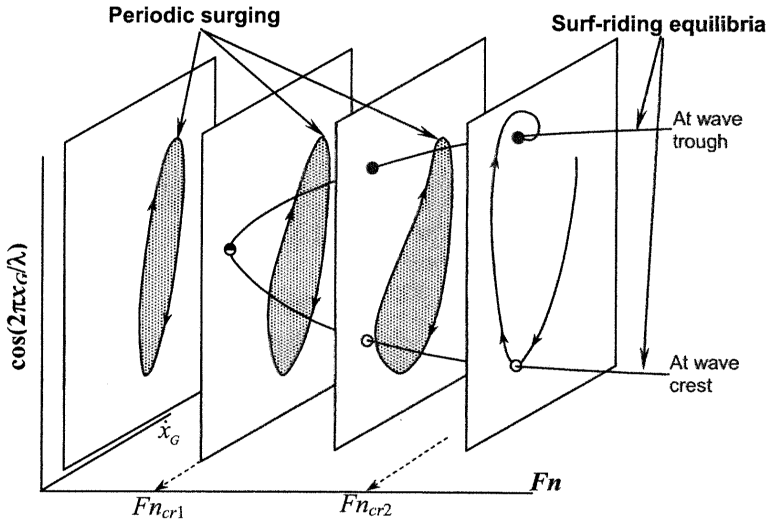

Figure 3.19: Changing of phase plan as a function of Froude number [60]

3.3.3 Vulnerability Level 1

The first level of vulnerability does not consider a ship to be vulnerable to the surf-riding failure mode if:

$$\begin{cases} L > 200 & (m) \\ Fn \leq 0.3 & (-) \end{cases} \tag{3.32}$$

where:

L	=	ship length,	(m);
Fn	=	Froude number,	(-).

3.3.4 Vulnerability Level 2

According to the second level of vulnerability, a ship is considered not to be vulnerable to surf-riding if:

$$C = \sum_{H_S} \sum_{T_Z} \Big(W(H_S; T_Z) \cdot \sum_{i=1}^{N_\lambda} \sum_{j=1}^{N_a} \big(W2_{ij} \cdot C2_{ij} \big) \Big) < R_{SR} \tag{3.33}$$

where:

$C2$	$= 0$	if the requirement of Froude number (Eq. 3.35) is satisfied,	
	$= 1$	if not satisfied,	(-);
R_{SR}	=	0.005,	(-);
$W2_{ij}$	=	statistical weight of wave calculated according to Eq. 3.34,	(-);
$W(H_S; T_Z)$	=	weighting factor for the respective wave cases as specifed by the selected wave scatter diagram,	(-).

The value of the standard R_{SR} has been determined on the basis of the reports of major large heel incidents of a container-ship.

Statistical weight of wave

The value of W_{ij} should be calculated with the following formula:

$$W2_{ij} = \frac{4\sqrt{g}}{\pi\nu} \cdot \frac{L^{5/2} T_{01}}{H_S^3} \cdot s_j^2 r_i^{3/2} \cdot \Big(\frac{\sqrt{1+\nu^2}}{1+\sqrt{1+\nu^2}} \Delta s \cdot \Delta r \Big) \cdot \exp\Big[-2 \Big(\frac{L \cdot r_i \cdot s_j}{H_S} \Big)^2 \cdot \Big(1 + \frac{1}{\nu^2} \big(1 - \sqrt{\frac{g T_{01}^2}{2\pi r_i L}} \big)^2 \Big) \Big] \tag{3.34}$$

where:

g	=	gravitational acceleration of 9.81 ,	(m/sec^2);
H_S	=	significant wave height defined from the wave scatter diagram,	(m);
L	=	ship length,	(m);
ν	=	0.4256,	(-);
r_i	=	wavelength to ship length ratio varies from 1.0 to 3.0,	(-);
Δr_i	=	variation step of r_i equal to 0.025,	(-);
s_j	=	wavelength to ship length ratio varies from 0.03 to 0.15,	(-);
Δs_j	=	variation step of s_i equal to 0.0012,	(-);
T_{01}	=	average wave period,	
	=	$1.088 \cdot T_Z$,	(sec);
T_Z	=	zero-crossing period defined from the wave scatter diagram,	(sec).

Vulnerability criterion

The requirement of Froude number is considered satisfied if, for each wave of the selected wave scatter diagram, the assessed loading condition agrees with the following equation:

$$Fn \leq Fn_{cr} \tag{3.35}$$

where:

Fn	=	Froude number of the ship,	(-);
Fn_{cr}	=	critical Froude number corresponding to the threshold of surf-riding,	(-).

The critical Froude number is calculated using the critical ship speed u_{cr} (m/sec) determined by solving the Eq 3.36.

$$T_e(u_{cr}; n_{cr}) - R(u_{cr}) = 0 \tag{3.36}$$

where:

$R(u_{cr})$	=	calm water resistance of the ship at the critical ship speed,	(N);
$T_e(u_{cr}; n_{cr})$	=	thrust delivered by the ship's propulsors in calm water at the critical ship speed and critical number of revolutions of the propeller,	(N);
n_{cr}	=	critical commanded number of revolutions of propulsors corresponding to the first threshold of surf-riding computed according to Eq. 3.39,	(1/sec).

The calm water ship resistance $R(u)$ can be estimated either by model tank tests or using a numerical method. The resistance curve should be approximated with a polynomial form up to the fifth degree, based on the available resistance data.

$$R(u) \approx r_0 + r_1 u + r_2 u^2 + r_3 u^3 + r_4 u^4 + r_5 u^5 \tag{3.37}$$

The polynomial fit should be appropriate to ensure the resistance is always increasing as function of speed in the appropriate range of application.

The propeller thrust can be estimated by scaled model test or using a numerical method. For one propeller, the ship thrust can be approximated by using a second order polynomial approximation covering the whole positive range of propeller thrust coefficient:

$$T_e(u;n) = (1-t_p)\rho\, n^2 D_P^4 \cdot \left(k_0 + k_1 J + k_2 J^2\right) \tag{3.38}$$

where:

D_P	=	propeller diameter,	(m);
J	=	advanced ratio,	
	=	$\frac{u(1-w_p)}{n \cdot D_P}$	(-);
k_0, k_1, k_2	=	approximated coefficients for the propeller thrust coefficient in calm water	;
n	=	commanded number of revolutions of propulsor,	(1/sec);
ρ	=	density of sea water, equal to 1025	(kg/m^3);
t_p	=	thrust deduction,	(-);
w_p	=	wake fraction,	(-).

The effort of more than one propeller having the same characteristics can be evaluated by summing the effect of each individual propeller.

The critical commanded number of revolutions of the propeller corresponding to the first threshold of surf-riding should be calculated by means of an iterative method. In Annex 3 of [33], a recommended numerical iteration method for this calculation is proposed based on the following equation:

$$2\pi \frac{T_e(c_i;n_{cr}) - R(c_i)}{f_{ij}} + 8a_0 n_{cr} + 8a_1 - 4\pi a_2 + \frac{64}{3}a_3 - 12\pi a_4 + \frac{1024}{15}a_5 = 0 \tag{3.39}$$

where:

$a_{k_{ij}}$	=	numerical coefficients as function of ship and wave properties (see Section 3.3.1 of Annex 3 in [33])	;
c_i	=	wave celerity,	
	=	$\sqrt{g/k_i}$,	(m/sec);
f_{ij}	=	amplitude of wave surging force according to Eq. 3.41,	(N);
k_i	=	wave number,	
	=	$2\pi/\lambda_i = 2\pi/r_i L$,	(1/m);
n_{cr}	=	critical commanded number of revolutions propulsors corresponding to the first threshold of surf-riding,	(1/sec);
$R(c_i)$	=	calm water ship resistance evaluated at wave celerity,	(N);

$$
\begin{array}{lcll}
T_e(c_i; n_{cr}) & = & \text{ship thrust at wave celerity,} & \\
 & = & \tau_0 n_{cr}^2 + \tau_1 c_i n_{cr} + \tau_2 c_i^2, & \text{(N);} \\
\tau_0, \tau_1, \tau_2 & = & \text{thrust approximation coefficient according to Eq. 3.40} & .
\end{array}
$$

This proposal is applicable only if the calm water resistance is approximated with the 5^{th} power polynomial.

The thrust approximation coefficient are defined in the following formula:

$$\tau_0 = k_0 \cdot (1 - t_p)\rho D_P^4 \tag{3.40a}$$
$$\tau_1 = k_1 \cdot (1 - t_p)(1 - w_p)\rho D_P^3 \tag{3.40b}$$
$$\tau_2 = k_2 \cdot (1 - t_p)(1 - w_p)^2 \rho D_P^2 \tag{3.40c}$$

while the amplitude of wave surging force is evaluated with the following formula:

$$f_{ij} = \rho g k_i \cdot \frac{H_{ij}}{2} \cdot \sqrt{F_{Ci}^2 + F_{Si}^2} \tag{3.41}$$

with the Froude-Krylov component of the wave surging force defined as:

$$F_{Ci} = \sum_{m=1}^{N} \Big(\Delta x_m \cdot S(x_m) \sin(k x_m) \cdot \exp\big(-\frac{1}{2} k_i \cdot d(x_m)\big) \Big), \quad (\text{m}^3); \tag{3.42a}$$

$$F_{Si} = \sum_{m=1}^{N} \Big(\Delta x_m \cdot S(x_m) \cos(k x_m) \cdot \exp\big(-\frac{1}{2} k_i \cdot d(x_m)\big) \Big), \quad (\text{m}^3). \tag{3.42b}$$

where:

$$
\begin{array}{lcll}
H_{ij} & = & \text{wave height,} & \\
 & = & s_j \lambda_i = s_j r_i L, & \text{(m);} \\
k_i & = & \text{wave number,} & \\
 & = & 2\pi/\lambda_i = 2\pi/r_i L, & \text{(1/m);} \\
d(x_m) & = & \text{calm water draft of } m\text{-station} & \text{(m);} \\
S(x_m) & = & \text{calm water area of submerged portion of the ship of } m\text{-station} & (\text{m}^2); \\
x_m & = & \text{longitudinal distance from amidships to a } m\text{-station (positive forward),} & \text{(m).}
\end{array}
$$

3.4 Dead ship condition

The physical fundamentals that characterize the dead ship condition failure mode within the SGISc framework are addressed in this section. Moreover, the first two levels of vulnerability are explained, together with some brief hints on their development process.

This criterion defines the minimum requirement to guarantee safety against stability failure when a ship is not able to steer and to manoeuvre, namely the dead ship condition. Since all operational means such as rudders control and propeller thrust are lost, a vessel in dead ship condition cannot sail away from a severe sea state by herself, thus she should preserve her stability for a sufficiently long period of survivability. The severe wind and rolling criterion, known as weather criterion, is the most used assessment tool to evaluate stability performance of a vessel in dead ship condition. It has been developed to overcome the limitation of criteria based only GZ curve and it firstly appeared as attachment to final act of Torremolinos international convention for the Safety of Fishing Vessels (SFV) in 1977. That version of weather criterion was based on the Japanese proposal [99] which was developed from the Japanese stability standard for passenger ships [100],[101]. Similar criticism to the GZ curve criterion standing alone were raised by other nations which developed their own version of the criterion such as Russia [102], US Navy [103], Poland, Australia, China and others [104]. The present weather criterion was obtained using the Japanese criterion as the backbone structure and implementing the standard adopted by Russia, in particular as concern the evaluation of roll-back angle and the effect of appendages on roll damping.

The weather criterion has always worked well for the conventional ship on which it has been designed and calibrated. Recently, new vessels have shown some inconsistencies with the weather criterion in relation with new characteristics. The formulation of the roll-back angle seems to be not realistic anymore for certain ship, as well as the factor taking into account gustiness does not consider the actual shape and dimensions of the ship. Furthermore, the environmental condition assumed is basically a deterministic one. For these reasons, during the revision of Intact Stability code, an alternative assessment of the weather criterion through model test experiments has been allowed and the relative guidelines were issued via Maritime Safety Committee (MSC) Circular [105]. The same motivation are the driver of the needs to develop a stability criterion to regulate the dead ship condition within the SGISc.

3.4.1 Physical background

At the basis of this phenomenon there is the assumption that a vessel loses power and cannot move away or avoid an incoming rough weather. Because of the action of wind and waves, ships usually turn in beam seas. In this position, the exposed longitudinal area is maximum, so the heeling effect due to the action of wind and waves is maximized.

It is assumed that the ship is rolling under the action of waves as well as

heeling and drifting under the action of a steady wind. Drift-related heel is the result of the coupling between the wind aerodynamic force the hydrodynamic reaction caused by the transverse motion of the ship (Figure 3.20a). Next a sudden and long gust of wind occurs exactly when the ship is rolled at the maximum windward angle (Figure 3.20b), this is the worst condition because, in this case, the action of wind is added to the waves one. The strengthening wind increases drift velocity thus leading to an increase of the hydrodynamic drift reaction. The latter force enhances the heeling moment generated by the wind-wave coupling pushing the ship to roll even farther (Figure 3.20c). The wind's gust is assumed to last long enough for the ship to completely roll to the other side, the achieved leeward roll angle due to the increased pushback is the key point of the criterion (Figure 3.20d).

This angle is seen as a new stable condition reached by the ship reacting to the wind's blowing, so the roll motion equation and variables must be expressed according to this new condition. If the achieved angle is too large some openings may get flooded or even the ship may capsize.

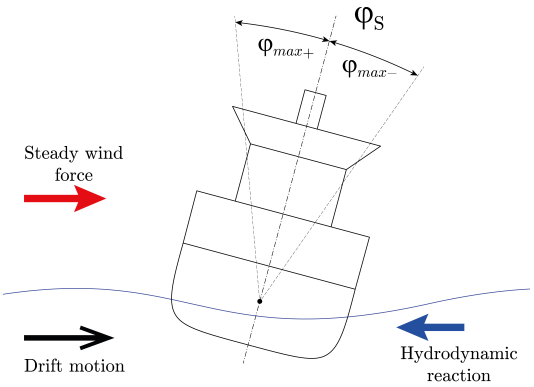

(a) Steady wind and waves action around the stable heel angle φ_s

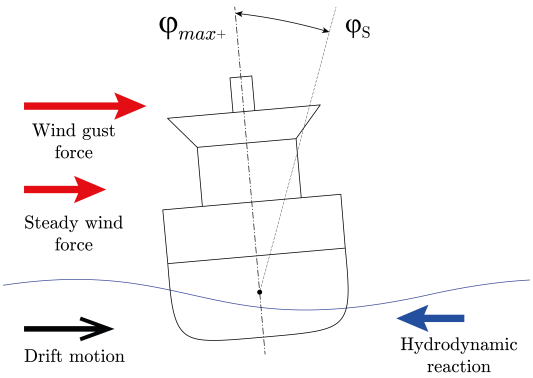

(b) Sudden gust at the maximum windward roll angle φ_{max+}

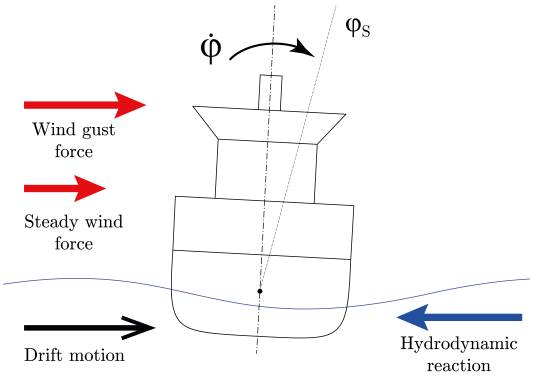

(c) Gust lasts long enough to heel leeward the vessel

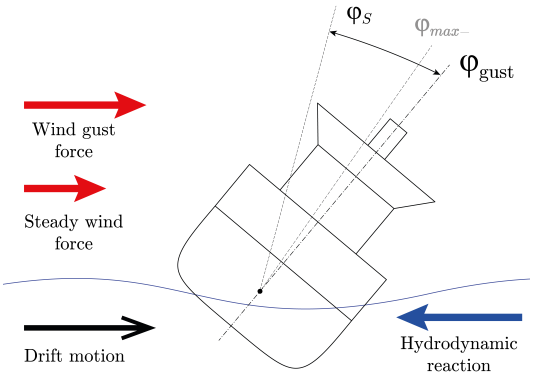

(d) Maximum leeward heel angle due to gust effect φ_{gust}

Figure 3.20: Typical scenario of dead ship condition stability failure

3.4.2 Vulnerability Level 1

A ship is not vulnerable at dead ship condition failure mode if she complys with the requirements defined in the severe wind and rolling criterion (*weather criterion*) [8], but using the wave steepness factor values defined in Table 3.2 instead of those contained in Table 2.3.4-4 of Section 2.3 - Part A of the Intact Stability code.

Table 3.2: Values of wave steepness factor

Roll period, T_ϕ (sec)	Wave steepness, s (-)
$\leq$6	0.100
7	0.098
8	0.093
12	0.065
14	0.053
16	0.044
18	0.038
20	0.032
22	0.028
24	0.025
26	0.023
28	0.021
$\geq$30	0.020

3.4.3 Vulnerability Level 2

In order to assess the vulnerability of a ship to the second level of dead ship condition, a long term probabilistic analysis is carried out, taking into account the occurrences of sea states in the considered geographical area. A ship is not vulnerable to dead ship condition if:

$$C \leq R_{DS0} \tag{3.43}$$

where:

C = long term probability index, as calculated in Eq. 3.44, (-);
R_{DS0} = 0.06, (-).

The long term probability index C is computed as the weighted sum of the sea states occurrences evaluated:

$$C = \sum_{i=1}^{N} W_i C_{S,i} \tag{3.44}$$

where:

$C_{S,i}$	=	short term probability index, as defined in Eq. 3.45,	(-);
N	=	number of wave cases as specified by the selected wave scatter diagram,	(-);
W_i	=	weighting factor of the respective wave cases as specified by the selected wave scatter diagram,	(-).

The short term probability index $C_{S,i}$ measures the likelihood that, at least one time, a heel angle threshold is achieved by the ship in an exposure time period of 1 hour. The threshold angle is defined by the criterion for each wave cases and it takes into account the effective heel angle between the ship and waves. The short term index should be chosen equal to 1 if one of the following condition happens:

1. the inclining lever due to wind effects $\bar{l}_{wind,tot}$ (m), as defined in Eq. 3.46, is greater than the righting moment GZ (m) for each heel angle;

2. the stable heel angle ϕ_S (rad) due to the steady wind effect is greater than the failure angle to leeward $\phi_{fail,+}$ (rad).

otherwise, the short term index is calculated according to the following formula:

$$C_{S,i} = 1 - \exp\left(-\lambda_{EA} \cdot T_{exp}\right) \tag{3.45}$$

where:

T_{exp}	=	exposure time, equal to 3600	(sec);
λ_{EA}	=	failure rate, defined as follows:	
	=	$\frac{1}{T_{z,C_S}} \cdot \Big(\exp\big(\frac{-1}{2 \cdot RI_{EA+}^2}\big) + \exp\big(\frac{-1}{2 \cdot RI_{EA-}^2}\big)\Big)$,	(1/sec);
RI_{EA+}	=	$\frac{\sigma_{c_S}}{\Delta\phi_{res,EA+}}$,	(-);
RI_{EA-}	=	$\frac{\sigma_{C_S}}{\Delta\phi_{res,EA-}}$,	(-);
T_{z,C_S}	=	roll motion zero crossing period due to the action of wind and waves, as defined in Eq. 3.47,	(sec);
σ_{C_S}	=	effective roll motion standard deviation due to the action of wind and waves, as defined in Eq. 3.48,	(rad);
$\Delta\phi_{res,EA+}$	=	range of residual stability to the leeward equivalent area limit angle, defined as follows:	
	=	$\phi_{EA+} - \phi_S$,	(rad);
$\Delta\phi_{res,EA-}$	=	range of residual stability to the windward equivalent area limit angle, defined as follows:	
	=	$\phi_S - \phi_{EA-}$,	(rad);

ϕ_{EA+} = limit angle of the leeward equivalent virtual area, calculated as follows:

$$= \phi_S + \sqrt{\frac{2A_{res,+}}{GM_{res}}}, \quad \text{(rad)};$$

ϕ_{EA-} = limit angle of the windward equivalent virtual area, calculated as follows:

$$= \phi_S - \sqrt{\frac{2A_{res,-}}{GM_{res}}}, \quad \text{(rad)};$$

ϕ_S = stable heel angle obtained as the first intersection between the righting lever GZ and the mean wind inclining lever $\bar{l}_{wind,tot}$ determined in Eq. 3.46, (rad);

$A_{res,+}$ = area under the residual righting lever (i.e. $GZ - \bar{l}_{wind,tot}$) between ϕ_S and $\phi_{fail,+}$, (m·rad);

$A_{res,-}$ = area under the residual righting lever (i.e. $GZ - \bar{l}_{wind,tot}$) between $\phi_{fail,-}$ and ϕ_S, (m·rad);

GM_{res} = residual metacentric height, defined as the slope of the residual righting lever (i.e. $GZ - \bar{l}_{wind,tot}$) evaluated in ϕ_S, (m);

$\phi_{fail,+}$ = leeward failure angle, defined as

$$= \min\left(\phi_{VW,+}; \phi_{crit,+}\right), \quad \text{(rad)};$$

$\phi_{fail,-}$ = windward failure angle, defined as

$$= \max\left(\phi_{VW,-}; \phi_{crit,-}\right), \quad \text{(rad)};$$

$\phi_{VW,+}$ = angle of second intercept to leeward between the righting lever GZ and the mean wind heeling lever $\bar{l}_{wind,tot}$, (rad);

$\phi_{VW,-}$ = angle of second intercept to windward between the righting lever GZ and the mean wind heeling lever $\bar{l}_{wind,tot}$, (rad);

$\phi_{crit,+}$ = critical angle to leeward, defined as

$$= \min\left(\phi_{f,+}; 50\right), \quad \text{(rad)};$$

$\phi_{crit,-}$ = critical angle to windward, defined as

$$= \max\left(\phi_{f,-}; -50\right), \quad \text{(rad)};$$

$\phi_{f,+}$,$\phi_{f,-}$ = downflooding angles to leeward and windward, according to the definition in the Intact Stability code Section 2.3.1.4 - Part A [8], (rad).

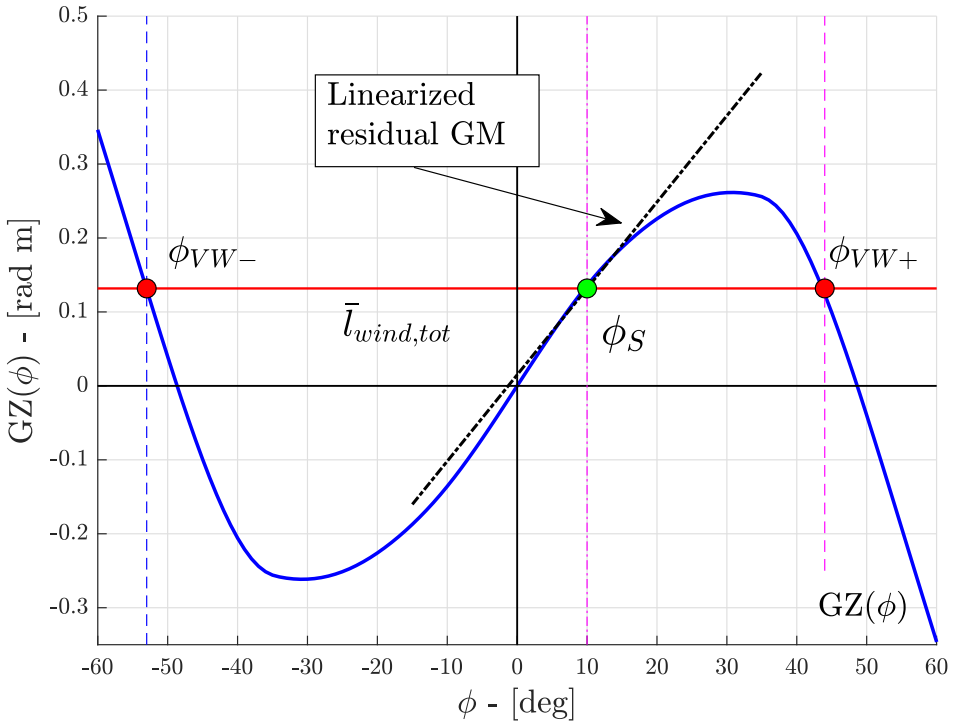

Figure 3.21: Representation of the residual metacentric height GM_{res} and the stable heel angle ϕ_S

As an example, in Figure 3.21 the righting lever $GZ(\varphi)$ (blue curve), the mean wind heeling lever $\bar{l}_{wind,tot}$ (red horizontal line), the stable heel angle ϕ_S (green dot) and the residual metacentric height GM_{res} (dashed black line) are reported.

The inclining lever due to the action of wind

The inclining lever due to wind is constant at all heel angles. It is calculated according to the following formula:

$$\bar{l}_{wind,tot} = \frac{\bar{M}_{wind,tot}}{W} \tag{3.46}$$

where:

W	=	ship weight,	(N);
$\bar{M}_{wind,tot}$	=	inclining moment due to the action of wind, defined as follows:	
	=	$\frac{1}{2} \cdot \rho_{air} \cdot U_w^2 \cdot C_m \cdot A_L \cdot Z$	(N·m);
ρ_{air}	=	air density, equal to 1.222	(kg/m^3);
C_m	=	wind heeling moment coefficient, to be chosen equal to 1.22	(-);
A_L	=	lateral exposed area of the ship above the waterline,	(m^2);

Z = vertical distance from the centre of A_L to centre of the submerged lateral area, in alternatively the distance to half draught d, (m);

U_w = mean wind speed, calculated as follows:

= $\left(\frac{H_S}{0.06717}\right)^{2/3}$ (m/sec);

H_S = significant wave height of the selected wave cases, (m).

Roll motion response spectrum

The zero-crossing period of the effective relative roll motion T_{z,C_S} and the corresponding standard deviation σ_{C_S} are determined by means the response spectrum of the roll motion under the action of wind and waves:

$$T_{z,C_S} = 2\pi \cdot \sqrt{m_0/m_2} \tag{3.47}$$

$$\sigma_{C_S} = \sqrt{m_0} \tag{3.48}$$

where:

m_0 = area under the roll motion response spectrum $S(\omega)$, (rad^2);

m_2 = area under the roll rate response spectrum $\omega^2 \cdot S(\omega)$, ($\text{rad}^4/\text{sec}^2$);

ω = circular frequency, (rad/sec);

$S(\omega)$ = roll motion response spectrum, calculated as follows:

= $H^2_{rel}(\omega) \cdot S_{\alpha\alpha,c}(\omega) + H^2(\omega) \cdot \frac{S_{\delta M_{wind,tot}}(\omega)}{(W \cdot GM)^2}$ ($\text{rad}^2/(\text{rad(sec)})$.

It is possible to separate the total roll motion in two components: the first one identifies the contribution of waves, the latter the effects due to wind action.

— *Wave effects component on roll motion:*

The ship roll Response Amplitude Operator (RAO) due to the wave action is defined by the following formula:

$$H^2_{rel} = \frac{\omega^4 + \left(2\mu_e \cdot \omega\right)^2}{\left(\omega^2_{\phi,e}(\phi_S) - \omega^2\right)^2 + \left(2\mu_e \cdot \omega\right)^2} \tag{3.49}$$

where:

μ_e = equivalent linear roll damping coefficient calculated according to the stochastic linearization method as described in § 3.4.3, (1/sec);

$\omega_{\phi,e}$ = modified natural roll frequency close to the stable heel angle ϕ_S, defined as follows:

$$= \omega_\phi \cdot \sqrt{\frac{GM_{res}}{GM}}, \quad \text{(rad/sec)};$$

The environmental conditions relative to sea states are modeled by the Bretschneider spectrum, taking into account the effective wave slope:

$$S_{zz}(\omega) = \frac{4\pi^3 \cdot H_S^2}{T_Z^4} \cdot \omega^{-5} \cdot \exp\left(-\frac{16\pi^3}{T_Z^4} \cdot \omega^{-4}\right) \quad (\mathrm{m}^2/(\mathrm{rad/sec})); \tag{3.50}$$

$$S_{\alpha\alpha}(\omega) = \frac{\omega^4}{g^2} \cdot S_{zz}(\omega) \quad (\mathrm{rad}^2/(\mathrm{rad/sec})); \tag{3.51}$$

$$S_{\alpha\alpha,c}(\omega) = r^2(\omega) \cdot S_{\alpha\alpha}(\omega) \quad (\mathrm{rad}^2/(\mathrm{rad/sec})). \tag{3.52}$$

where:

$r(\omega)$ = effective wave slope correction, as defined in § 3.4.3, (-);

T_Z = zero-crossing period of the sea state considered, (sec);

— *Wind effects component on roll motion:*

The ship roll RAO referred to action of gust is evaluated by the following formula:

$$H^2 = \frac{\omega_\phi^4}{\left(\omega_{\phi,e}^2(\phi_S) - \omega^2\right)^2 + \left(2\mu_e \cdot \omega\right)^2} \tag{3.53}$$

The action of gust is modeled with the Davenport spectrum [106] with the following expression:

$$S_v(\omega) = 4K \cdot \frac{U_w^2}{\omega} \cdot \frac{X_D^2}{\left(1 + X_D^2\right)^{4/3}} \qquad ((m/sec)^2/(rad/sec)) \tag{3.54}$$

where:

K = 0.003 (-);

X_D = $600 \cdot \dfrac{\omega}{\pi \cdot U_w}$, (-);

— *Spectrum of total roll moment:* The spectrum of total roll moment is defined as the sum of the contributions of waves and wind gust:

$$S_M(\omega) = S_{M_{waves}}(\omega) + S_{\delta M_{wind,tot}}(\omega) \qquad ((N \cdot m)^2/(rad/sec)) \tag{3.55}$$

To sum the contributions of gust and wave, the corresponding spectrum of roll moment acting on ship should be computed. The roll moment spectrum due to the action of waves is obtained by the following equation:

$$S_{M_{waves}}(\omega) = \left(W \cdot GM_{res}(\phi_S)\right)^2 \cdot S_{\alpha\alpha,c} \quad ((N \cdot m)^2/(rad/sec)) \tag{3.56}$$

while the roll moment spectrum due to the wind gust effects is defined by the following equation:

$$S_{\delta M_{wind,tot}}(\omega) = \left(\rho_{air} \cdot U_w \cdot C_m \cdot A_L \cdot Z\right)^2 \cdot \chi^2(\omega) \cdot S_v(\omega) \tag{3.57}$$
$$((N \cdot m)^2/(rad/sec))$$

where $\chi(\omega)$ is the standard aerodynamic admittance function, as first attempt it can be assumed equal to 1 .

Effective wave slope coefficient

In absence of any specific information and only for mono-hull vessel, to calculate the effective wave slope coefficient $r(\omega)$ a simplified standard methodology is suggested by the criteria. It is based on the following assumptions:

1. the submerged part of transversal sections are substituted by equivalent underwater section having the same breadth at waterline and the same underwater area of the original transversal section, moreover:
   (a) sections having a zero breadth at waterline are neglected (i.e. bulbous bow sections);
   (b) the draught of the equivalent underwater section is limited to the ship sectional draught;
2. only the undisturbed linear wave pressure is considered to determine the effective wave slope coefficient for each frequency;
3. the applied formula is exact for rectangular shapes.

Every underwater section is replaced by an equivalent underwater section characterized by an equivalent breadth at waterline B_{eq}, an equivalent draught T_{eq} and an equivalent submerged area A_{eq} obtained from the following relationship:

$$\begin{cases} \text{if } A(x) > 0 \text{ and } B(x) > 0, \begin{cases} \text{if } \dfrac{A(x)}{B(x)} \leq T(x) \text{ then } \begin{cases} A_{eq}(x) = A(x) \\ B_{eq}(x) = B(x) \\ T_{eq}(x) = \dfrac{A(x)}{B(x)} \end{cases} \\ \text{else } \begin{cases} T_{eq}(x) = T(x) \\ B_{eq}(x) = B(x) \\ A_{eq}(x) = B_{eq}(x) \cdot T_{eq} \end{cases} \end{cases} \\ \text{otherwise, } \begin{cases} A_{eq}(x) = 0 \\ B_{eq}(x) = 0 \\ T_{eq}(x) = 0 \end{cases} \end{cases}$$

The equivalent hull is made up of transversal equivalent sections having the following geometrical properties:

$$\nabla_{eq} = \int_L A_{eq}(x)dx\,; \tag{3.58a}$$

$$BMT_{eq} = \frac{1}{\nabla_{eq}} \int_L \frac{1}{12} \cdot B_{eq}^3(x)dx\,; \tag{3.58b}$$

$$KB_{eq} = T + \frac{1}{\nabla_{eq}} \cdot \int_L \frac{-T_{eq}(x)}{2} \cdot A_{eq}(x)dx\,; \tag{3.58c}$$

$$KG_{eq} = KB_{eq} + BMT_{eq} - GM \tag{3.58d}$$

from which it is possible to derive the needed parameters:

$$k_w = \omega^2/g\,; \qquad OG_{eq} = KG_{eq} - T\,; \tag{3.59a}$$

$$F_1 = -\frac{1 - e^{-k_w T_{eq}(x)}}{k_w \cdot T_{eq}(x)} \cdot \frac{\sin\left(k_w \frac{B_{eq}(x)}{2}\right)}{\left(\frac{k_w \cdot B_{eq}(x)}{2}\right)}\,; \tag{3.59b}$$

$$K_1(x) = \frac{\sin\left(k_w \frac{B_{eq}(x)}{2}\right)}{\left(\frac{k_w \cdot B_{eq}(x)}{2}\right)} \cdot \frac{\left(\left(1 + k_w \cdot T_{eq}(x)\right) \cdot e^{-k_w T_{eq}(x)}\right) - 1}{k_w^2 \cdot T_{eq}(x)}\,; \tag{3.59c}$$

$$K_2(x) = -\frac{e^{-k_w T_{eq}(x)}}{k_w^2 \cdot T_{eq}(x)} \cdot \left(\cos\left(k_w \cdot \frac{B_{eq}(x)}{2}\right) - \frac{\sin\left(k_w \frac{B_{eq}(x)}{2}\right)}{\left(\frac{k_w \cdot B_{eq}(x)}{2}\right)}\right) \tag{3.59d}$$

and

$$C(x) = \begin{cases} \text{if } A_{eq}(x) = 0 \text{ e } B_{eq}(x) = 0 & 0; \\ \text{otherwise.} & A_{eq}(x) \cdot \left(K_1(x) + K_2(x) + F_1(x) \cdot OG_{eq}\right) \end{cases} \tag{3.60}$$

Finally, the effective wave slope coefficient is obtained with the following formula:

$$r(\omega) = \left| \frac{\int_L C(x)dx}{\nabla_{eq} \cdot GM} \right| \tag{3.61}$$

Equivalent linear roll damping coefficient

In the calculation of the ship roll response amplitude operator (Eq. 3.49), the damping coefficient for the analysed loading condition is requested. If sufficient information are not available, it is possible to apply the standard methodology suggested by the criteria based on the simplified Ikeda's method [107].

The standard methodology to compute the roll damping coefficient is constituted of two important steps:

1. At the beginning, the equivalent linear roll damping coefficient is calculated as a function of the roll motion amplitude;

2. As second step, starting from the previously data, the roll damping coefficient is obtained by a least square fitting.

The equivalent linear roll damping coefficient $B_{44}(\phi_a)$ as a function of the rolling amplitude is evaluated according to the simplified Ikeda's method.

Thereafter, the damping coefficients μ, β and δ are calculated by the following least square fitting:

$$\frac{B_{44}(\phi_a)\cdot\omega_\phi^2}{2W\cdot GM} \quad \mapsto \quad \mu+\frac{4}{3\pi}\cdot\beta\cdot\omega_\phi\cdot\phi_a+\frac{3}{8}\cdot\delta\cdot\omega_\phi^2\cdot\phi_a^2 \tag{3.62}$$

Once the damping coefficients have been defined, it is possible to compute the equivalent linear roll damping coefficient μ_e by numerically solving for the roll velocity standard deviation described in Eq. 3.63.

$$F(\sigma_{\dot{x}})=0 \tag{3.63}$$

where:

$$F(\sigma_{\dot{x}})=\sigma_{\dot{x}}^2-\int_0^{+\infty}\frac{\omega^2\cdot\omega_\phi^4}{\left(\omega_{\phi,e}^2(\phi_S)-\omega^2\right)^2+\left(2\mu_e(\sigma_{\dot{x}})\cdot\omega\right)^2}\cdot\frac{S_M(\omega)}{\left(W\cdot GM\right)^2}\cdot d\omega\,; \tag{3.64}$$

$$\mu_e(\sigma_{\dot{x}})=\mu+\sqrt{\frac{2}{\pi}}\cdot\beta\cdot\sigma_{\dot{x}}+\frac{3}{2}\cdot\delta\cdot\sigma_{\dot{x}}^2 \tag{3.65}$$

while $S_M(\omega)$ is the ship roll moment spectrum due to wind and wave effects, as defined in § 3.4.3.

3.4.4 Background on the vulnerability levels

The dead ship condition criterion differs from others because no direct relationship exists between the first level assessment model and the second one. The first level adopts the same model of the weather criterion, except for some adjustment as regards the environmental characteristics. The calculation methodology of the second vulnerability level is based upon a dynamic model from which a probabilistic stability failure index is derived. Hereinafter a brief description of the two methodologies is given.

Energy based model

The energy balance between wind heeling and righting moments is the basic principle of the weather criterion. One of the most important contribution to the method has been the pioneering works done by Pierrottet in 1935 [108]. In that methodology no roll motion was taken into account, therefore the vessel was assumed to suffer wind heeling moment starting from the upright position. Subsequently, the method has been revised introducing the roll motion oscillations around a stable heel angle caused by a steady wind heeling lever, moreover the energy balance is evaluated taking into account a sudden increment of inclining lever when the ship is at the maximum windward angle. A detailed description of this well known model can be find in the explanatory notes to the Intact Stability code [109].

Table 3.2, which defines the relationship between wave steepness s_w and the ship natural roll period T_ϕ, derives from Table 4.5.1 defined in the Interim Guidelines for alternative assessment of the weather criterion [105].

Dynamic based model

The methodology at the basis of the dynamic based model for dead ship condition has been proposed by Italy in [110] with reference to [111]. Starting from a one degree of freedom roll motion non-linear system, the effects of waves and wind of a realistic stochastic environment are considered; the relation between sea elevation spectrum and the gust spectrum is represented by the mean wind speed and the roll spectrum is evaluated by a simplified stochastic linearization approach where damping and restoring moment are non-linearly modeled. Thanks to its modularity, this method can be easily updated and customised on the basis of particuar environmental conditions or ship properties. In Figure 3.22, the methodology of the proposed dynamic based model is represented by a block diagram . It is possible to evaluate a specific block with sophisticated simulations tool or by using experimental results instead of the analytical and approximated formula proposed.

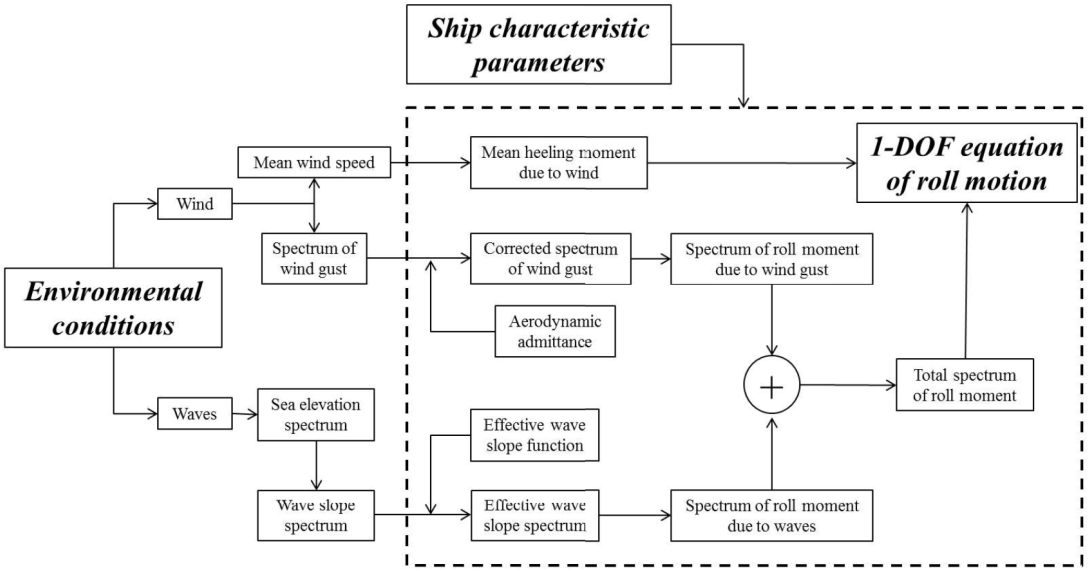

Figure 3.22: Conceptual scheme of the assumed simplified physical model [110]

At the basis the model there are several assumptions and approximations, most of them are the same adopted for the weather criterion, such as that the ship is considered to be in dead ship condition in irregular waves and gusty wind, the wind and waves propagate in the same direction as well as the ship is assumed to remain beam wind and waves during the whole exposure time. Other specific assumptions for the dynamic based model are that the wind state is characterized by a mean wind speed and a gustiness spectrum as well as that the sea state is represented by a long crested wave elevation spectrum as well. The one degree of freedom equation (Eq. 3.66) adopted considers the non linearity of both restoring

term and damping term, while the external moment taken into account is obtained by the sum of wind and wave effects.

$$\hat{I}_{44} \cdot \ddot{\phi} + B(\phi) + \Delta \cdot GZ(\phi) = M_{wind}(t) + M_{wave}(t) \tag{3.66}$$

where:

$\hat{I}_{44}$	=	moment of inertia including the added moment of inertia,	(N m sec^2);
$B(\phi)$	=	non linear damping moment,	(N m sec);
$GZ(\phi)$	=	non linear restoring lever,	(m);
$M_{wind}(t)$	=	total instantaneous moment due to wind,	(N m);
$M_{wave}(t)$	=	total instantaneous moment due to waves,	(N m).

The equation of motion is then divided by the first term leading to the following equation:

$$\ddot{\phi} + \frac{B(\phi)}{\hat{I}_{44}} + \frac{\Delta \cdot GZ(\phi)}{\hat{I}_{44}} = \frac{M_{wind}(t)}{\hat{I}_{44}} + \frac{M_{wave}(t)}{\hat{I}_{44}} \, ;$$

$$\ddot{\phi} + b(\phi) + \omega_0 \cdot gz(\phi) = \omega_0 \cdot \big(m_{wind}(t) + m_{wave}(t)\big) \tag{3.67}$$

where:

$gz(\phi)$	=	non dimensional righting lever,	(-);
$m_{wind}(t)$	=	non dimensional total moment due to wind,	
	=	$M_{wind}(t)/(\Delta \cdot GM)$	(-);
$m_{wave}(t)$	=	non dimensional total moment due to wind,	
	=	$M_{wave}(t)/(\Delta \cdot GM)$	(-).

Damping term As proposed in [112], the non dimensional damping moment may be described adopting a cubic equation:

$$b(\phi) = 2 \cdot \mu \cdot \dot{\phi} + \beta \cdot \dot{\phi}|\dot{\phi}| + \delta \cdot \dot{\phi}^3 \tag{3.68}$$

Wave effects The wave moment acting on the ship is analysed through the assumption of linear hydrodynamic theory. The total excitation moment due to waves M_{wave} is supposed to be a Gaussian process and it is taken into account by means of its spectrum $S_{M_{waves}}$ obtained starting from the wave slope spectrum $S_{\alpha\alpha}$:

$$S_{M_{waves}}(\omega) = S_{\alpha\alpha}(\omega) \cdot \big(\Delta \cdot GM \cdot r(\omega)\big)^2 \tag{3.69}$$

where $r(\omega)$ is the effective wave slope function. Its values for low frequencies are usually larger than the respective values at high frequencies, it means that long waves are more effective on ship roll motion than short waves.

Wind effects The action of wind has been divided in two components, one representing the steady wind action and the other one modeling the wind speed fluctuation. The concept at the basis of this separation is that:

- the steady action of wind leads the ship to a constant drift motion in order to develop a hydrodynamic sway opposite force;
- this moment inclines the ship to a stable heel angle ϕ_S;
- the fluctuating force due to gust effect does not last enough time to fully develop the added hydrodynamic reactions;
- the ship rolls around the achieved stable heel angle.

The mean wind speed is fully correlated to the significant wave height selected, as can be found in [113]. Considering the data in [114], a regression analysis has been done and the following relation between the significant wave height and the mean wind speed is obtained:

$$U_{wind} = \frac{H_S}{0.06717}^{2/3} \tag{3.70}$$

Short Term prediction of capsize probability In light of the approximation and linearization introduced above, the roll motion process is assumed to be Gaussian, stationary and ergodic. The next steps analyse the methodology which estimates the probability that a heel angle leading to a stability failure is achieved. The failure heel angle has been assumed as the minimum value among the vanishing stability angle ϕ_{VW} for the residual righting moment due to steady wind effect, flooding angle ϕ_f or a limit angle equal to 50°. To do that, the hypothesis of Poisson process is assumed for the failure event and the probability of fail will depends on the exposure time T_{exp} at the given environmental conditions. To better explain the final relation for the probability of failure, it is worthwhile to introduce some relevant intermediate steps:

$$P\{\text{failure in } T_{exp}\} = 1 - P\{\text{no failure in } T_{exp}\} \tag{3.71}$$

but, the probability of not fail in a fixed time T_{exp} can be expressed in relation to the occurence of the fail event as

$$P\{\text{no failure in } T_{exp}\} = P\{\text{having zero failure events in } T_{exp}\} \tag{3.72}$$

Therefore, modelling the failure event as a Poisson process, the probability to have a specified number of events n in a fixed time period is given by the probability mass function [115], [116].

$$P\{n \text{ failure in } T_{exp}\} = \frac{1}{n!}\Big(\frac{T_{exp}}{T_{fail}}\Big)^n \cdot \exp\Big(-\frac{T_{exp}}{T_{fail}}\Big) \tag{3.73}$$

where T_{fail} is a characteristic parameter of the distribution and it is the mean time to fail. Thus, combining equations Eq 3.73 to Eq. 3.72 the probability of fail in a time T_{exp} becomes:

$$P\{\text{fail in } T_{exp}\} = 1 - \exp\left(-\frac{T_{exp}}{T_{fail}}\right) \tag{3.74}$$

Before estimating the probability failure index, the formulation of T_{fail} must be obtained. In order to do that is useful to introduce the failure rate coefficient defined as follows:

$$\lambda_{fail} = \frac{1}{T_{fail}} \tag{3.75}$$

After which, considering reference [117], it is possible to evaluate the failure rate index for a Gaussian process using the following expression:

$$\lambda_{fail} = \frac{1}{2\pi} \cdot \frac{\sigma_{\dot{\phi}}}{\sigma_{\phi}} \cdot \exp\left(-\frac{1}{2}\Big(\frac{\phi_{fail} - \phi_S}{\sigma_{\phi}}\Big)^2\right) \tag{3.76}$$

Combining Eq. 3.75 and 3.76 to Eq. 3.74 the probability of failure in a fixed exposure time is given by:

$$\begin{aligned} P\{\text{fail in } T_{exp}\} &= 1 - \exp\left(-\lambda_{fail} \cdot T_{exp}\right); \\ &= 1 - \exp\left(-\frac{T_{exp}}{2\pi} \cdot \frac{\sigma_{\dot{\phi}}}{\sigma_{\phi}} \cdot \exp\left(-\frac{1}{2}\Big(\frac{\phi_{fail} - \phi_S}{\sigma_{\phi}}\Big)^2\right)\right) \end{aligned} \tag{3.77}$$

It is to be noted that the formulation obtained is referred only to the probability to achieve a stability failure angle only towards the leeward side, neglecting the probability to capsize on the windward side. This assumption is acceptable if the heel angle due to steady wind lever is sufficiently large, but the smaller the stable heel angle, the higher the probability to reach a stability failure on the windward side. For this reason, some correction at Eq. 3.78 should be introduced to take into account of what above as discussed in [114]. Considering the two events as independent Poisson processes, it is possible to obtain the total probability of failure adding up the probabilities to reach the failure angle leeward and windward.

$$\begin{aligned} P\{\text{fail in } T_{exp}\} = 1 - \exp\Bigg(-\frac{T_{exp}}{2\pi} \cdot \frac{\sigma_{\dot{\phi}}}{\sigma_{\phi}} \cdot \Bigg(&\exp\left(-\frac{1}{2}\big(\frac{\phi_{fail+} - \phi_S}{\sigma_{\phi}}\big)^2\right) \\ &+ \exp\left(-\frac{1}{2}\big(\frac{\phi_S - \phi_{fail-}}{\sigma_{\phi}}\big)^2\right)\Bigg)\Bigg) \end{aligned} \tag{3.78}$$

where the subscript "+" means the leeward failure angle, while the subscript "−" the windward failure angle.

Subsequently, a linearized residual restoring lever is introduced considering the residual metacentric height GM_{res} defined as the slope of GZ evaluated in correspondence of the stable heel angle ϕ_S.

$$GM_{res} = \left.\frac{dGZ(\phi)}{d\phi}\right|_{\phi=\phi_S} \tag{3.79}$$

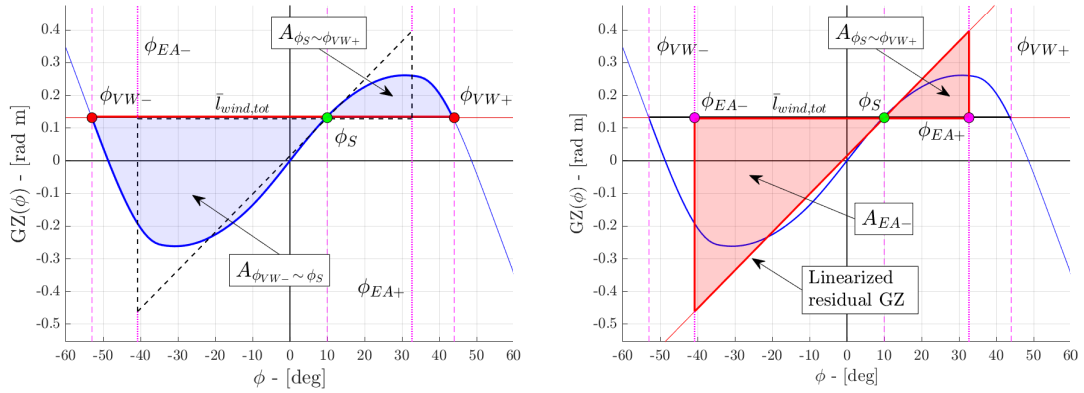

(a) Area between the actual residual GZ and the steady wind lever $\hat{l}_{wind,tot}$

(b) Equivalent Area between the linearized GZ and the steady wind lever $\hat{l}_{wind,tot}$

Figure 3.23: The *equivalent area approach* to determine the virtual limit angles

To take into account the actual shape of the GZ curve, two virtual limit angles to leeward ϕ_{EA+} and windward ϕ_{EA-} are defined on the basis of the *equivalent area concept* [118],[119]. The virtual limit angles are computed in order to keep the area under the linearized righting lever equivalent to the actual residual righting lever (Figure 3.23). The area under the linearized righting lever A_{EA} is the area of a triangle as defined below:

$$A_{EA+} = \frac{GM_{res} \cdot (\phi_{EA+} - \phi_S)^2}{2} \tag{3.80a}$$

$$A_{EA-} = \frac{GM_{res} \cdot (\phi_S - \phi_{EA-})^2}{2} \tag{3.80b}$$

The value of the area under the actual residual righting moment is defined as follows:

$$A_{\phi_S \sim \phi_{EA}} = \int_{\phi_S}^{\phi_{EA}} GZ(\phi) d\phi \tag{3.81}$$

Thus, the equivalence between the area under the actual residual righting lever GZ_{res} and that under the linearized righting arm is set combining Eq. 3.81 to Eq. 3.80.

$$\frac{GM_{res} \cdot (\phi_{EA+} - \phi_S)^2}{2} = \int_{\phi_S}^{\phi_{EA+}} GZ_{res}(\phi) d\phi \tag{3.82a}$$

$$\frac{GM_{res} \cdot (\phi_S - \phi_{EA-})^2}{2} = \int_{\phi_{EA-}}^{\phi_S} GZ_{res}(\phi) d\phi \tag{3.82b}$$

Solving Eq 3.82, it is possible to extract the formulation of the virtual limit angles for both leeward and windward side.

$$\phi_{EA+} = \phi_S + \sqrt{\frac{2 \cdot A_{\phi_S \sim \phi_{EA+}}}{GM_{res}}} \tag{3.83a}$$

$$\phi_{EA-} = \phi_S - \sqrt{\frac{2 \cdot A_{\phi_{EA-} \sim \phi_S}}{GM_{res}}} \tag{3.83b}$$

At this point, the zero-crossing period of roll motion $T_{Z,\phi}$, the residual margins $\Delta\phi_{res,EA\pm}$ and the risk indexes $RI_{EA\pm}$ are introduced:

$$T_{Z,\phi} = \frac{2\pi \cdot \sigma_\phi}{\sigma_{\dot{\phi}}}\,; \tag{3.84a}$$

$$\Delta\phi_{res,EA+} = \phi_{EA+} - \phi_S\,; \tag{3.84b}$$

$$\Delta\phi_{res,EA-} = \phi_S - \phi_{EA-}\,; \tag{3.84c}$$

$$RI_{EA\pm} = \frac{\sigma_\phi}{\Delta\phi_{res,EA\pm}} \tag{3.84d}$$

Finally, as a consequence of the high number of assumptions made up to here, it has been chosen to rename the probability of stability failure as a more general short term stability failure index C_S, obtaining the final formulation reported in the criteria (§ 3.4.3), taking into account Eq. 3.84

$$C_S = 1 - \exp\left(-\frac{T_{exp}}{T_{Z,\phi}} \cdot \left(\exp\left(-\frac{1}{2\,RI_{EA+}^2}\right) + \exp\left(-\frac{1}{2\,RI_{EA-}^2}\right)\right)\right) \tag{3.85}$$

3.5 Excessive Acceleration

As reported in Chapter 2, the excessive acceleration stability failure was introduced later than the other phenomena, when the delegation of Germany submitted at IMO a list of casualties due to the effects of large stability parameters [120]. The report about some worth mentioning incidents have been carried out by BSU and a brief summary is given in § 2.2 of this thesis. The investigations show how the casualties happened were strictly related to the loading condition. At the moment of the accidents, the ships were sailing in ballast condition, with a large stability caused by high values of metacentric height and when adverse environmental conditions have been encountered, large and sudden ship roll motions occurred leading to damages to the cargo and injuries to the crew. Another marine incident related to excessive acceleration phenomena was analysed at TUHH and submitted at IMO in [42]. In that report a numerical simulation of the accident has been carried out and it strengthened the need of an improved and comprehensive analysis of stability in waves. Hereinafter, a brief description of the physics of the excessive acceleration phenomenon is given, moreover, the vulnerability levels concerning this stability failure are described and analysed.

3.5.1 Physical background

The stability failure addressed by this vulnerability criterion is the lateral acceleration due to ship motions. Considering fixed positions on board, the higher is the quote the longer is the distance to be covered in a half roll period. Since the roll velocity is constant along the whole ship, in order to cover in the same time a longer distance, the highest point has a large lateral linear velocity (Figure 3.24). Every half roll period the roll motion changes its direction, therefore the linear velocity changes leading to a linear acceleration. Hence, higher lateral velocities cause large lateral accelerations, that means large inertial forces.

Since the roll period is strictly related to the transversal metacentric height, it has a relevant impact on this stability failure. Lowering the GM, the roll period gets shorter so, for the same roll amplitude, the rate of velocity change is higher with larger lateral accelerations. The inertial forces on the horizontal plane are more dangerous than those acting in the vertical plane. The latter causes short overloading on the human body, while horizontal inertial forces may cause lose of balance, fall or even being thrown against bulkheads or furnitures.

Several studies have been carried out on the influence of lateral acceleration on crew efficiency or passengers wellness [121],[122],[123]. As outcome of these studies, indexes to evaluate the effect of ship motion on crew or passenger have been formulated. The Motion Induced Interruptions (MII) and the Motion Induced Fatigue (MIF) indexes are defined to describe the crew effectiveness. Both indexes take into account the effect of ship motion on crew tasks and operations. The first one measures the occurrences of balance losses in a fixed time period, the index has been introduced in [124] and fully described in [125], [126]. The MIF index quantifies the additional energy losses of crew operating in moving environments such as vessels in rough seas, this effect has been observed since 1969

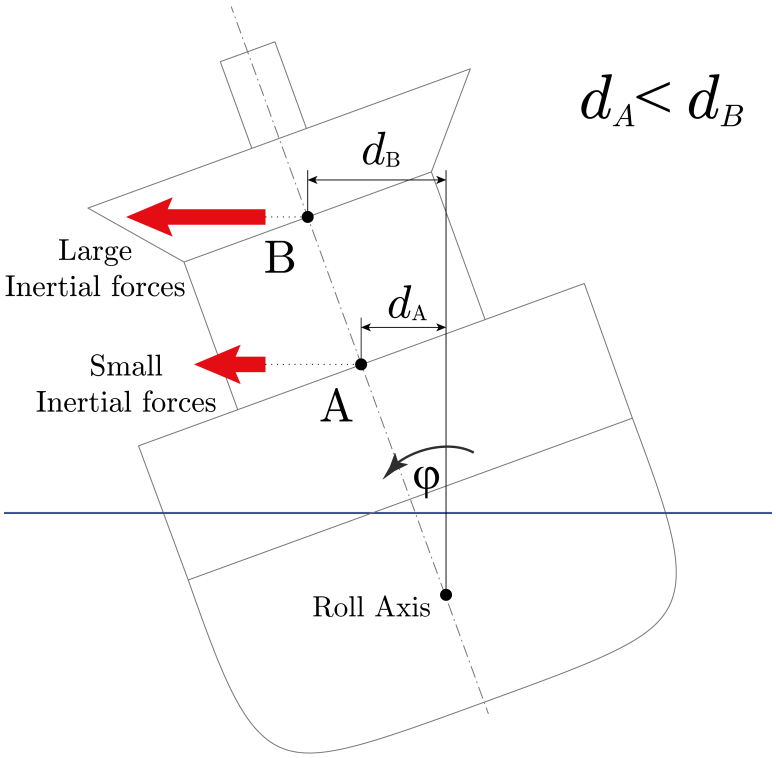

Figure 3.24: Typical scenario of excessive acceleration failure

[127], [128]. It is worth mentioning the Motion Sickness Incidence (MSI) index too. It evaluates the percentage of passengers or crew on board which has been sick after a specified exposure time. This index is more considerable for cruise ships or Ro-Ro ferries, where the comfort of passenger is an important aspect [129], [130].

Motions causing large roll angle

Large transversal accelerations are mainly related to large roll motions. There are different physical mechanisms inducing relevant roll motion on board. Among those tackled within the SGISc framework, parametric rolling is known also to cause excessive accelerations, in particular for head seas condition. Another of the main responsible sources of roll motion and also large transversal accelerations is the synchronous resonance. Synchronous resonance consists of a fast and huge amplification of ship motion response. It happens when the external roll excitation has a frequency close to the ship natural roll frequency. The higher is the amplitude of excitation, such as angle of wave slope, the greater are the effects of resonance at all frequencies with a peak near the natural roll frequency (Figure 3.25a). A similar effect but with opposite results is caused by roll damping (Figure 3.25b), where the amplitude of motions decreases at all frequencies with an increment of roll damping.

Since this phenomenon is very well known in literature, only a brief description on its physics is shown below. More detailed studies and definition on synchronous

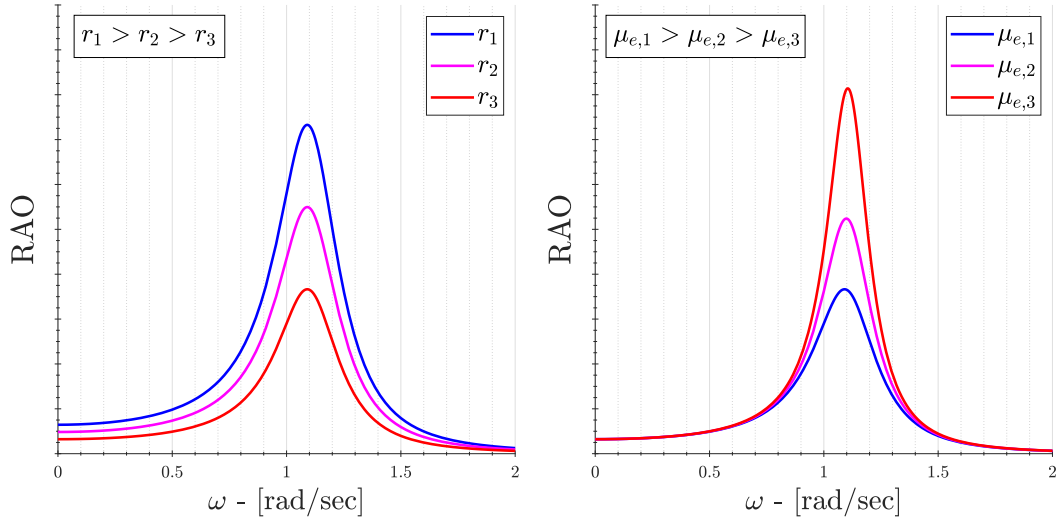

(a) Changes of the angle of wave slope (b) Changes of the roll damping coefficient

Figure 3.25: Influence of the wave slope and damping coefficient on the roll motion response amplitude operator

resonance may be found in the milestone books of naval architecture such as [131], [132], [133]. Basically, a part of the work of an external excitation on a dynamic system is spent on making the system oscillating with the excitation frequency instead of the natural frequency. The remaining energy is used to counteract the damping property of the system. When the equivalence between exciting frequency and natural frequency occurs, the whole work of the external force is spent on overcoming damping, hence more energy is left available to increase roll motion. Referring to vessels, this condition happens when the position of the sea spectrum peak, comparable to the exciting force of a generic dynamic system, falls on the maximum value of the RAO of the ship. In Figure 3.26 the variation of the roll response spectrum due to the position of the sea spectrum peak is depicted. The maximum roll response value occurs when the peak of RAO and sea spectrum correspond (Figure 3.26a), on the contrary shifting the sea spectrum peak frequency away from the natural roll frequency, the roll response decreases substantially (Figure 3.26b)

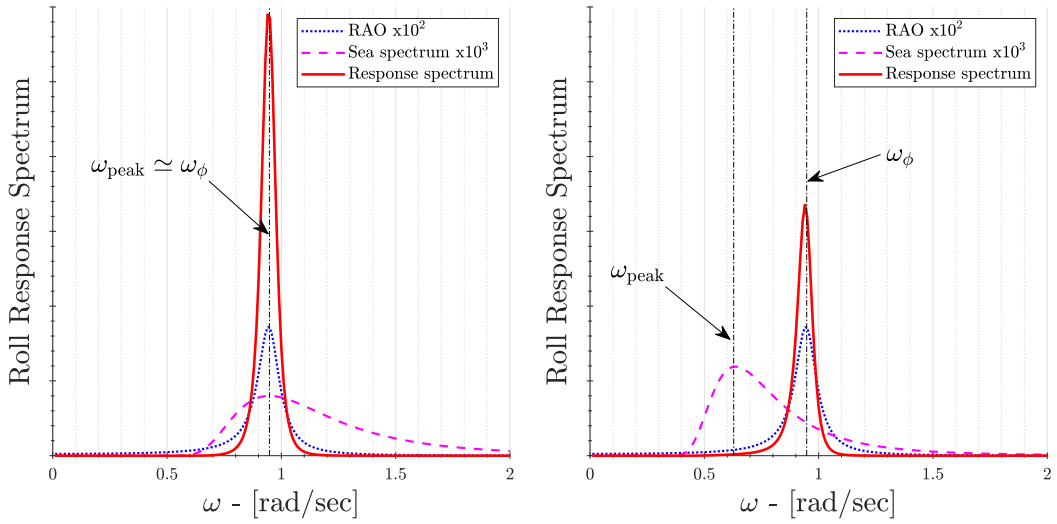

(a) $\omega_{\text{peak}} \simeq \omega_\phi$ (b) $\omega_{\text{peak}} < \omega_\phi$

Figure 3.26: Superimposition of the elevation sea spectrum and the roll response operator

3.5.2 Vulnerability Level 1

It is to be noted that the assessment for excessive acceleration vulnerability should be done only if:

- The distance from the waterline to the highest position where the crew or passenger may be present exceeds 70% of the ship breadth;
- The metacentric height exceeds 8% of ship breadth.

If the previous statements apply to the loading condition under consideration, the stability failure should be addressed by the vulnerability criteria.

The first level of vulnerability does not consider a ship to be vulnerable to the excessive acceleration failure mode if, for each loading condition and location along the ship where crew or passenger may be present, the following equation is verified:

$$\varphi \cdot k_L \cdot \left(g + \frac{4\pi^2 \cdot h}{T_\phi^2}\right) < R_{EA} \tag{3.86}$$

where:

R_{EA}	=	4.64 or 5.88,	(m/sec^2);
g	=	gravitational acceleration of 9.81,	(m/sec^2);
h	=	height of the assessed point above the roll axis,	(m);
k_L	=	coupling factor of the action of roll, pitch and yaw motions (Eq. 3.89),	(-);

φ = characteristic roll amplitude,
= $4.43rs/\sqrt{\delta_\phi}$ (rad);

δ_ϕ = non-dimensional logarithimic decrement of roll decay test (Eq 3.87), (-);
r = non-dimensional effective wave-slope correction (Eq 3.88), (-);
s = non-dimensional wave steepness, (-);
T_ϕ = natural roll period of the ship, (sec).

In this vulnerability level, the roll axis may be assumed to be located at the midpoint between the waterline and the vertical center of gravity. The logarithmic decrement of roll decay is defined by the following formula:

$$\delta_\phi = 0.5\pi \cdot R_{PR} \tag{3.87}$$

where:

R_{PR} = standard value evaluated according to Eq. 3.8, (-);

while the non-dimensional effective wave slope correction is evaluated according the following equation:

$$r = \frac{K_1 + K_2 - (OG \cdot F)}{\frac{B^2}{12 \cdot C_B d} - \frac{C_B d}{2} - OG} \tag{3.88}$$

where:

K_1 = $g\beta {T_\phi}^2 \cdot (\tau + \tau\tilde{T} - 1/\tilde{T})/(4\pi^2)$, (-);
K_2 = $g\tau {T_\phi}^2 \cdot \big(\beta - \cos(\beta)\big)/(4\pi^2)$, (-);
β = $\sin(\tilde{B})/\tilde{B}$, (-);
$\tilde{B}$ = $2\pi^2 B/(g{T_\phi}^2)$, (-);
B = ship moulded breadth, (m);
τ = $\exp(\tilde{T})/\tilde{T}$, (-);
$\tilde{T}$ = $4\pi^2 C_B d/(g{T_\phi}^2)$, (-);
d = draught at midship, (m);
C_B = block coefficient of the ship, (-);
F = $\beta \cdot (\tau - 1/\tilde{T})$, (-);
OG = $KG - d$, (m).

The factor taking into account simultaneous action of roll, yaw and pitch motion k_L, is defined by the following relationship:

$$k_L = \begin{cases} 1.125 - 0.625x/L & \text{if } x < 0.2L; \\ 1.0 & \text{if } 0.2L < x < 0.65L; \\ 0.527 + 0.727x/L & \text{if } x > 0.65L. \end{cases} \tag{3.89}$$

3.5.3 Vulnerability Level 2

According to second level of vulnerability, a ship is considered not to be vulnerable at the excessive acceleration failure mode if:

$$C < R_{EA\ 2} \tag{3.90}$$

where:

C	=	criterion according to Eq. 3.91,	(-);
R_{SR}	=	0.00039,	(-).

The criterion C is a long-term probability index that measures the vulnerability to excessive acceleration. It is based on the probability of occurrence of short-term environmental conditions.

$$C = \sum_{i=1}^{N} W_i C_i \tag{3.91}$$

where:

C_i	=	short-term index calculated as indicated in Eq. 3.92,	(-);
N	=	number of wave cases as specified by the selected wave scatter diagram,	(-);
W_i	=	weighting factor for the respective wave cases as specifed by the selected wave scatter diagram,	(-).

The short-term excessive acceleration failure index is a measure of the probability that the ship will exceed a specified acceleration at least once in the exposure time considered.

$$C_i = \exp\left(\frac{-{R_2}^2}{2\sigma_{LAi}^2}\right) \tag{3.92}$$

where:

R_2	=	9.81	(m/sec^2);
σ_{LA}	=	standard deviation of lateral acceleration (Eq. 3.93)	(m/sec^2).

The standard deviation of lateral acceleration is calculated at zero speed in a beam seaway. It is determined using the spectrum of roll motions due to the action of waves.

$$\sigma_{LAi}^2 = \frac{3}{4} \sum_{j=1}^{N} a_y(\omega_j)^2 \cdot S_{ZZ}(\omega_j) \cdot \Delta\omega \tag{3.93}$$

where:

a_y	=	unit amplitude response amplitude operator of lateral accelerations,	
	=	$k_L \cdot \big(g + h \cdot \omega_j^2\big) \cdot \varphi_a(\omega_j)$	((m/sec^2)/m);
g	=	gravitational acceleration of 9.81	(m/sec^2)
h	=	height of the assessed point from the roll axis,	(m);
k_L	=	coupling factor of the action of roll, pitch and yaw motions (Eq. 3.89),	(-);
φ_a	=	roll amplitude in regular beam waves of unit amplitude at zero speed (Eq. 3.102),	(rad/m);
$\Delta\omega$	=	the interval of wave frequency,	
	=	$(\omega_2 - \omega_1)/N$	(rad/sec);
ω_1	=	the lower limit of the wave frequency spectrum,	
	=	$\max\big((0.5/T_\phi); 0.2\big)$	(rad/sec);
ω_2	=	the upper limit of the wave frequency spectrum,	
	=	$\min\big((25/T_\phi); 2.0\big)$	(rad/sec);
ω_j	=	wave frequency at the midpoint of the interval considered,	
	=	$\omega_1 + \big((2j-1)/2\big) \cdot \Delta\omega$	(rad/sec);
N	=	the number of intervals in the frequency spectrum evaluation range, not to be taken less than 100	(-) ;
S_{ZZ}	=	wave frequency spectrum,	(m^{2}sec/rad).

The response amplitude operator of roll motions is divided in two component: the real part and the imaginary part of the roll motion.

$$\varphi_a = \sqrt{\Re(\varphi)^2 + \Im(\varphi)^2} \tag{3.94}$$

with the two component defined as follows:

$$\Re(\varphi) = \frac{a(\Delta \cdot g \cdot GMc - I_{xx} \cdot \omega_j^2) + b(B_e^2 \cdot \omega_j)}{(\Delta \cdot g \cdot GMc - I_{xx} \cdot \omega_j^2)^2 + (B_e^2 \cdot \omega_j)^2} \tag{3.95a}$$

$$\Im(\varphi) = \frac{b(\Delta \cdot g \cdot GMc - I_{xx} \cdot \omega_j^2) - a(B_e^2 \cdot \omega_j)}{(\Delta \cdot g \cdot GMc - I_{xx} \cdot \omega_j^2)^2 + (B_e^2 \cdot \omega_j)^2} \tag{3.95b}$$

where:

a, b	=	respectively the cosine and sine component of Froude Krylov roll moment (Eq. 3.96 or Eq. 3.97),	(N m);
Δ	=	ship displacement	(t);
GMc	=	metacentric height not corrected for free surface effect	(m);
I_{xx}	=	roll moment of inertia,	
	=	$\Delta \cdot g \cdot GMc \,/\, {\omega_\phi}^2$	(N m sec^2);
ω_ϕ	=	natural roll frequency of the ship,	(rad/sec);

B_e	=	equivalent linear roll damping,	
	=	$2 \cdot I_{xx} \cdot \mu_e$	(N m sec)
μ_e	=	equivalent linear roll damping coefficient, as defined in § 3.4.3,	(1/sec).

Froude-Krylov moment

The Froude-Krylov roll moment in regular beam waves should be calculated directly, otherwise, it is possible to use the following formulation:

$$a = \rho g \iint_{S_H} e^{kz} \cos(ky) \cdot n_4 \, dS \tag{3.96a}$$

$$b = -\rho g \iint_{S_H} e^{kz} \sin(ky) \cdot n_4 \, dS \tag{3.96b}$$

but, for laterally symmetric hulls, the previous formula can be simplified as follows:

$$a = 0 \tag{3.97a}$$

$$b = \Delta \cdot GMc \cdot r \cdot \left(\frac{\omega^2}{g}\right) \tag{3.97b}$$

where:

Δ	=	ship displacement,	(t);
GMc	=	metacentric height in calm water,	(m);
k	=	wave number,	
	=	${\omega_{\text{wave}}}^2/g$	(1/m);
n_4	=	normal vector of roll,	(-);
ρ	=	sea water density equal to 1.025,	(t/m^3);
r	=	effective wave slope, as defined in § 3.4.3,	(-);
S_H	=	mean wetted hull surface,	(m^2);
x, y, z	=	coordinates of mean wetted hull surface,	(m).

3.5.4 Relationship between the vulnerability levels

According to the philosophy of the SGISc, the first level of vulnerability is modeled by a simplification of the second level. The latter one, in turn, is obtained thanks to a simplified one-degree of freedom motion model without taking into consideration the coupling effect of other motions. The general formula of this model is shown in Eq. 3.98.

$$\hat{I}_{44} \cdot \ddot{\varphi} + B_{44} \cdot \dot{\varphi} + C_{44} \cdot \varphi = M_{FK} \tag{3.98}$$

where:

$\hat{I}_{44}$ = moment of inertia including the added roll moment of inertia, (N m sec^2);

B_{44} = linear roll damping coefficient, (N m sec);
C_{44} = roll restoring moment, (N m);
M_{FK} = external exciting moment (N m);
φ = roll angle, (rad);
$\dot{\varphi}$ = roll velocity, (rad/sec);
$\ddot{\varphi}$ = roll acceleration, (rad/sec^2).

At this point, it is introduced the first simplifications at the model: the Froude-Krylov assumption is assumed and the diffraction moment is neglected. The external moment is break up into a real and an imaginary component calculated by direct integration of pressure including hydrostatic pressure and pressure do to particle velocity in beam waves over the mean wetted hull surface of the ship, known as Smith effect. In this way, the exciting moment can be written as follows:

$$M_{FK} = (a + ib)e^{i\omega_e t} \tag{3.99}$$

where a and b are the real and imaginary part of th external moment while ω_e is the encounter frequency. The solution of Eq. 3.98 can be expressed by the following formula:

$$\varphi = \varphi_a \cdot e^{i\omega_e t} \tag{3.100}$$

The considered accidents occurred at very low forward speed (2 to 4 knots) and in beam seas as it shown in the investigation outcome in Sec. 2.2, therefore it is reasonable and not too conservative, to consider zero-speed condition in a beam seas. Hence, the following assumption are assumed:

$$Fn = 0 \qquad \text{and} \qquad \omega_e = \omega_{wave}$$

Substituting Eq. 3.100 and Eq. 3.99 in Eq. 3.98, the following formulation is obtained:

$$\hat{I}_{44}\cdot(-\omega_{wave}^2\cdot\varphi_a)\cdot e^{i\omega_{wave}t}+B_{44}\cdot(i\omega_{wave}\cdot\varphi_a)\cdot e^{i\omega_{wave}t}+C_{44}\cdot\varphi_a\cdot e^{i\omega_{wave}t} = (a+ib)\cdot e^{i\omega_{wave}t} \tag{3.101}$$

where the complex form of the roll amplitude φ_a is shown in the following formula:

$$\varphi_a = \frac{a + ib}{(C_{44} - \hat{I}_{44} \cdot \omega_{wave}^2) + (iB_{44} \cdot \omega_{wave})} =$$

$$= \frac{(a + ib) \cdot \big((C_{44} - \hat{I}_{44} \cdot \omega_{wave}^2) - (iB_{44} \cdot \omega_{wave})\big)}{(C_{44} - \hat{I}_{44} \cdot \omega_{wave}^2)^2 - (B_{44} \cdot \omega_{wave})^2} \tag{3.102}$$

After this operation, it is possible to separate the real component from the

imaginary component of the roll amplitude φ_a, as shown below:

$$\Re(\varphi_a) = \frac{a(C_{44} - \hat{I}_{44} \cdot \omega_{wave}^2) + b(B_{44} \cdot \omega_{wave})}{(C_{44} - \hat{I}_{44} \cdot \omega_{wave}^2)^2 - (B_{44} \cdot \omega_{wave})^2} \tag{3.103a}$$

$$\Im(\varphi_a) = \frac{b(C_{44} - \hat{I}_{44} \cdot \omega_{wave}^2) - a(B_{44} \cdot \omega_{wave})}{(C_{44} - \hat{I}_{44} \cdot \omega_{wave}^2)^2 - (B_{44} \cdot \omega_{wave})^2} \tag{3.103b}$$

Then, the magnitude of the roll amplitude is calculated as follows:

$$||\varphi_a|| = \sqrt{\Re(\varphi_a)^2 + \Im(\varphi_a)^2} \tag{3.104}$$

Once the roll amplitude is computed, the equation of lateral motion should be formulated. As shown in Figure 3.27a, the accelerations acting on a fixed reference point are the following:

- vertical acceleration a_V due to pitch and heave motions;
- horizontal acceleration a_H due to yaw motion;
- gravitational acceleration g;
- acceleration $\ddot{\varphi}$ due to roll motion.

The acceleration due to an harmonic roll motion for a point far from the roll axis, can be written in the frequency domain by following expression:

$$\vec{a}_{roll} = \vec{d} \cdot \omega^2 \, \varphi$$

Therefore, considering an harmonic roll motion in a ship based reference system, the components of the maximum acceleration (Figure 3.27b) are:

$$a_y = (g + a_V) \cdot \sin(\varphi_a) + a_H \cdot \cos(\varphi_a) + h \cdot \omega^2 \cdot \varphi_a \tag{3.105a}$$

$$a_z = (g + a_V) \cdot \cos(\varphi_a) - a_H \cdot \sin(\varphi_a) - y \cdot \omega^2 \cdot \varphi_a \tag{3.105b}$$

where:

h	=	height of the fixed reference point above the roll axis	
	=	$z - z_R$,	(m);
z	=	height of the fixed reference point above base line,	(m);
z_R	=	height of the roll axis above base line,	(m);
y	=	lateral distance from the roll axis,	(rad);

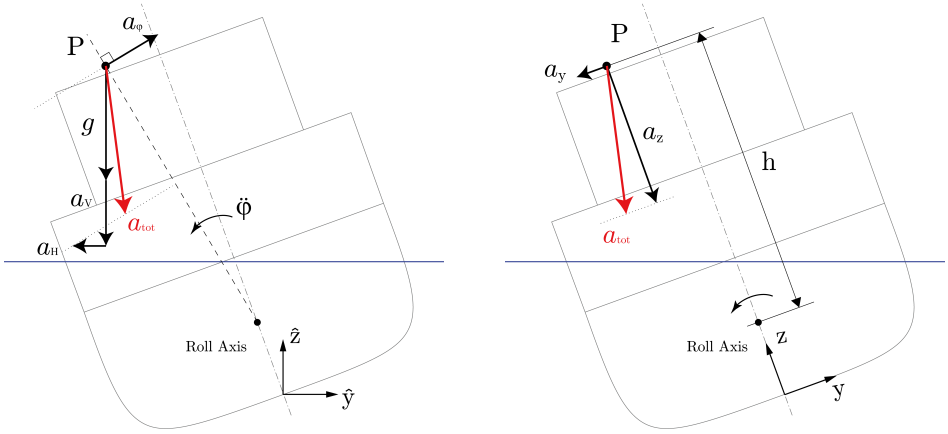

(a) Earth based reference system $(\hat{x}, \hat{y}, \hat{z})$

(b) Ship based reference system (x, y, z)

Figure 3.27: Accelerations acting on a fixed point respect different reference coordinate systems

Simplification within the 2nd vulnerability level

Since the second level of vulnerability for excessive acceleration is based on a one degree of freedom model, it is not possible to evaluate the contribution of motions other than roll to the lateral acceleration acting on board (i.e. a_V and a_H). In light of this, a coupling factor k_L is introduced as a function of longitudinal position along the ship. Thus, (3.105a) can be rewritten as:

$$a_y = k_L \cdot \left(g \cdot \sin\left(\varphi_a\right) + h \cdot \omega^2 \cdot \varphi_a\right) \tag{3.106}$$

Furthermore, for angle up to 30°, it is possible to replace φ_a instead of $\sin\left(\varphi_a\right)$, with acceptable conservative errors for vulnerability criterion.

$$a_y = k_L \cdot \left(g \cdot \varphi_a + h \cdot \omega^2 \cdot \varphi_a\right) \tag{3.107}$$

Another simplification involves the calculation of the lateral acceleration response spectrum in irregular short-crested seas. According to the linearity hypothesis, the lateral acceleration response spectrum $S_{acc,LC}(\omega)$ for a mono-directional irregular sea, namely long-crested sea, is evaluated with the following formula:

$$S_{Acc,\mathrm{Long}}(\omega) = a_y(\omega)^2 \cdot S_{ZZ}(\omega) \tag{3.108}$$

where $S_{ZZ}(\omega)$ is the sea elevation spectrum. Actually, waves come from more than one direction therefore, a spreading function $D(\beta)$ is introduced to take into account this effect. A spreading function depends on the provenience angle of waves respect to the main direction β and its integral should be unitary.

$$S_{Acc,\mathrm{Short}}(\omega, \beta) = a_y(\omega)^2 \cdot S_{ZZ}(\omega) \cdot D(\beta) \tag{3.109}$$

At this point, within the second vulnerability level, a conservative simplification on the influence of short crestedness is introduced. The calculation should be done

for a long crested sea and the short crested effects for a beam sea are considered by means of a reduction factor, as follows:

$$\begin{aligned} S_{Acc}(\omega) &= 0.75 \cdot S_{Acc,\text{Long}}(\omega) = \\ &= 0.75 \cdot a_y(\omega)^2 \cdot S_{ZZ}(\omega) \end{aligned} \tag{3.110}$$

Thereafter, the integral of the response spectrum should be computed in the range of wave frequency defined by the criterion, to obtain the variance value of lateral acceleration, which should be used within the second vulnerability level.

$$\sigma_\varphi^2 = 0.75 \int_{\omega_1}^{\omega_2} a_y(\omega)^2 \cdot S_{ZZ}(\omega) \tag{3.111}$$

Simplification within the 1st vulnerability level

The criterion of first vulnerability level is drawn up beginning from the assumptions of the second level and reducing its complexity. In this way, the criterion results to be more simple and conservative than the criterion of second vulnerability level and at the same time the consistency between levels is ensured.

Substituting Eq. 3.99 and Eq. 3.102 in Eq. 3.111, it is possible to obtain the following formula:

$$\sigma_\varphi^2 = \frac{0.75 \cdot {M_{FK}}^2}{{C_{44}}^2} \int_{\omega_1}^{\omega_2} \frac{\omega_\phi^4 \cdot S_{ZZ}(\omega)}{(\omega_\phi^2 - \omega^2)^2 + (2 \cdot \mu_e \cdot \omega)^2} d\omega \tag{3.112}$$

where $\mu_e = 2 \cdot I_{44} \cdot B_{44}$ is the equivalent linear roll damping coefficient (1/sec).

The damping coefficient may be expressed as function of the logarithmic decrement of roll decay δ_ϕ as follows:

$$\mu_e = \delta_\phi \cdot \omega_\phi / 2\pi \tag{3.113}$$

and the effective wave slope is introduced by the following formula:

$$r(\omega) = g \cdot \frac{M_{FK}}{\omega^2 \cdot C_{44}} \tag{3.114}$$

Hence, by substituting Eq. 3.113 and Eq. 3.114 in Eq. 3.112, the variance of roll motion becomes:

$$\sigma_\varphi^2 = \frac{0.75 \cdot \omega_\phi^4}{g^2} \int_{\omega_1}^{\omega_2} \frac{r(\omega)^2 \cdot \omega^4 \cdot S_{ZZ}(\omega)}{(\omega_\phi - \omega)^2 + (\omega \cdot \omega_\phi \cdot \delta_\phi / \pi)^2} d\omega \tag{3.115}$$

Focusing on the integral of the right-hand-side in Eq. 3.115, it is possible to demonstrate that the dominating contribution comes from the region of frequencies close to the natural frequency. For this reason, the main approximation of first level of vulnerability is introduced when the roll motion variance is computed at the natural roll frequency ω_ϕ. Therefore, the integral on the right-hand-side may be approximated with the following expression:

$$\int_{\omega_1}^{\omega_2} \frac{r(\omega)^2 \cdot \omega^4 \cdot S_{ZZ}(\omega)}{(\omega_\phi - \omega)^2 + (\omega \cdot \omega_\phi \cdot \delta_\phi / \pi)^2} d\omega \approx \omega_\phi \cdot \frac{\pi^2}{2\delta_\phi} \cdot r(\omega_\phi)^2 \cdot S_{ZZ}(\omega_\phi) \tag{3.116}$$

where $r(\omega_\phi)$ and $S_{ZZ}(\omega_\phi)$ are respectively the effective wave slope and the Bretschneider sea spectrum evaluated at the natural roll frequency ω_ϕ.

Substituting Eq. 3.116 into Eq. 3.115, the variance of the roll angle becomes:

$$\sigma_\varphi{}^2 = 0.0384 \cdot \omega_\phi^5 \cdot r(\omega)^2 S_{ZZ}(\omega_\phi)/\delta_\phi \tag{3.117}$$

According to the International Towing Tank Conference (ITTC) procedure in [134], the sea elevation spectrum $S_{ZZ}(\omega)$ is calculated and it is assumed that the modal frequency is equal to the natural roll frequency:

$$\omega_m = \omega_\phi$$

Thus the simplified variance of the roll motion is obtained as follows:

$$\begin{aligned} \sigma_\varphi^2 &= 19.625 \cdot \frac{r^2 \cdot s^2}{\delta_\phi}; \\ \sigma_\varphi &= 4.43 \cdot r \cdot s/\sqrt{\delta_\phi} \end{aligned} \tag{3.118}$$

where $s = H_s\,\omega_\phi/g$ is the seaway steepness and H_s is the significant wave height.

Finally, it is possible to evaluate the standard deviation of lateral acceleration with the following formula:

$$\sigma_a = \sigma_\varphi \cdot (g + \omega_\phi^2 \cdot h) \tag{3.119}$$

Chapter 4

Development of computational tools

4.1 Stability code available at UNIGE

At the beginning of my Ph.D., a computational code developed in-house, dealing with intact stability, was already available at UNIGE, namely *Nautilus*. *Nautilus* is written in Matlab® language and it is able to perform traditional hydrostatics calculations as well as stability performance assessment considering a wave profile along the hull. The working principle of *Nautilus* can be summarized in three steps:

- Definition of input data and hull surface;
- Calculation of geometric data, such as volume and centre of buoyancy;
- Calculation of ship stability parameters.

The code works considering the hull made up of 2D sections defined by points. To take into account the wave profile effect, each section is shifted above or below the still waterline according to a sinusoidal law, after that the main geometrical parameters are computed. In the *structure* variable, (built-in Matlab® variable type) named CONDeq, the evaluated output data are stored (see Table 4.1 for more details). The flow chart representing the code main process is given in Figure 4.1 while, a more detailed description about *Nautilus* computational tool can be find in [135], [136].

4.2 Flow chart and significant comments

As mentioned in the scope of this thesis, a part of my work has been focused on the development of a comprehensive set of tools able to assess the compliance with the SGISc. The computational tools have been developed for academic and research purposes within UNIGE, therefore the Matlab® programming language has been the first choice since it is widely adopted among UNIGE researchers and students. Moreover, the stability code, already available and used as a starting point to build the comprehensive set of SGISc tools, was written in this programming language.

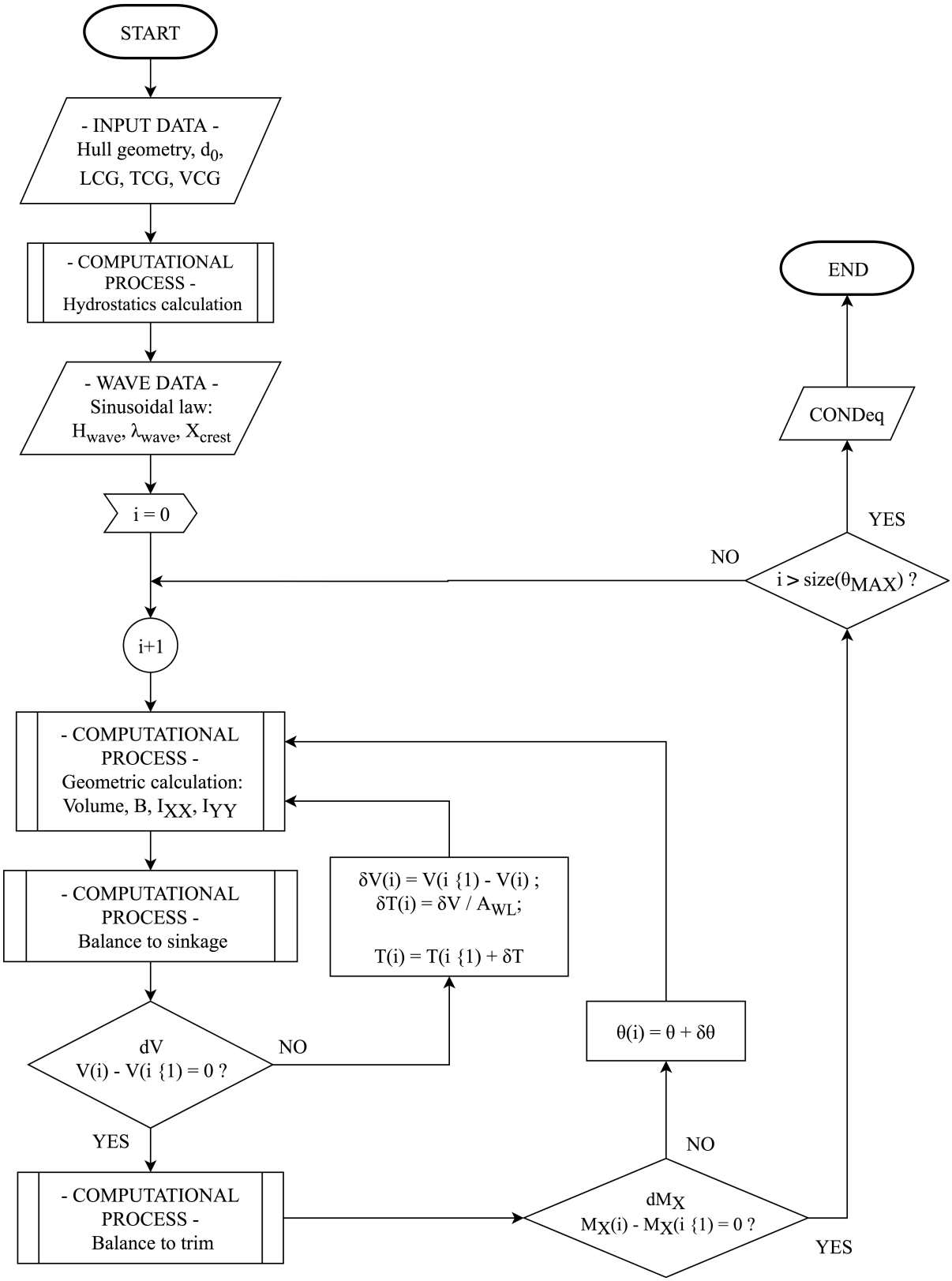

Figure 4.1: Flow chart of the UNIGE *Nautilus* computational tool

Table 4.1: Geometric information collected within CONDeq output variable

CONDeq structure			
V	=	Submerged hull volume,	(m^3);
T	=	Mean draught,	(m);
B	=	Center of buoyancy coordinates (x,y,z),	(m);
G	=	Center of gravity coordinates (x,y,z),	(m);
F	=	Center of waterplane coordinates (x,y),	(m);
A_{wl}	=	Waterplane area,	(m^2);
I_{XX}	=	Waterplane moment of inertia around X-axis,	(m^4);
I_{YY}	=	Waterplane moment of inertia around Y-axis,	(m^4);
L_{wl}	=	Waterplane length,	(m);
B_{wl}	=	Waterplane breadth,	(m);
ϑ_T	=	Heel angle,	(m);
τ	=	Trim angle,	(m);
GZ	=	Righting arm calculated at ϑ_T,	(m·rad);
λ	=	Wave length,	(m);
H_{wave}	=	Wave height,	(m);
X_{crest}	=	Wave crest longitudinal position,	(m).

For the first vulnerability levels for each stability failures a script has been written and in every computational code a similar structure made up of three main steps can be found:

- Input data collection: all the requested data are loaded by the script and elaborated if necessary. In this step, it is usually called the developed function *computeGZ* to extract the righting arm from CONDeq variable and to calculate the value of the transverse metacentric height. GM is evaluated computing the finite derivative between the first two point of GZ ($\vartheta_0 = 0°$ and ϑ_1);

- Main computational process: specific procedures requested by each stability failure mode are computed. Sometimes, in this step functions developed to evaluate some specific parameter such as damping coefficient or wave slope coefficient (a brief summary of all the developed functions, not described by the flow charts, is given in Table 4.2) are called;

- Assessment phase: after the criterion value calculation,a comparison is carried out with the respective standard in order to judge the vessel vulnerabillty or not with reference to the stability failure under investigation.

As concern the second vulnerability levels, the backbone structure is nearly the same of previous one, nevertheless the flow charts are more elaborated in order to reflect the higher level of complexity. With respect to the first levels a principal difference, common to every script, is the *for* – cycle among each cell of the wave scatter diagram, which is not present in the first levels. Since second vulnerability level of parametric roll failure requires a one degree of freedom dynamic model, only for this stability failure, it has been implemented a Simulink® model. The structure of the dynamic model is given in § 4.2.2.

To verify and validate the codes, an application to a set of different vessel typologies has been carried out: to quickly apply each script to different loading conditions, changing whether the draught or the center of gravity, an iterative process has been implemented in each computational code.

In the following sections, the flow charts for each computational code developed are given. Where the representation is on more than one page, the flow chart has been separeted and a triangular marker with a capital letter has been put to show the respective connection point. Moreover, to make easier the undestanding of each flow chart, some basic Matlab® built-in functions, such as interpolation or integration processes, have been summed up in a single rectangular box identifiable by two parallel vertical line on the side. The same depiction has been applied also for the in-house developed functions.

Table 4.2: Geometric information collected within CONDeq output variable

Summary of developed functions		
Function name	Scope	Stability failure
Bretschneider	To compute the analytical elevation sea spectrum of Bretschneider as a function of circular frequency $S_{ZZ}(\omega)$.	DS, EA
computeGZ	To extract the values of righting arm $GZ(\vartheta)$ and respective heel angle ϑ from the CONDeq variable and to compute the transverse metacentric height GM.	PR,PLS,DS,EA
EqLinDamping	To compute the equivalent linear roll damping coefficient μ_e, according to the procedure described in the explanatory notes of the dead ship condition criterion.	DS, EA
Ikeda	To compute the linear roll damping coefficient B_{44}, according to the simplified Ikeda's method [107].	PR, DS, EA
ITTCdamping	To compute the linear roll damping coefficient corrected according to the ITTC recommended procedure [137]	PR
RelazioneHeff	To compute the 3% largest effective wave height H_i, according to the procedure described in the explanatory notes of the pure loss of stability criterion.	PLS
RelazioneHr	To compute the representative wave height H_r, according to the procedure described in the explanatory notes of the parametric roll criterion.	PR
WaveSlope	To compute the effective wave slope coefficient as a function of circular roll frequency $r(\omega)$, according to the procedure described in the explanatory notes of the dead ship condition criterion.	DS, EA

4.2.1 Pure loss of stability

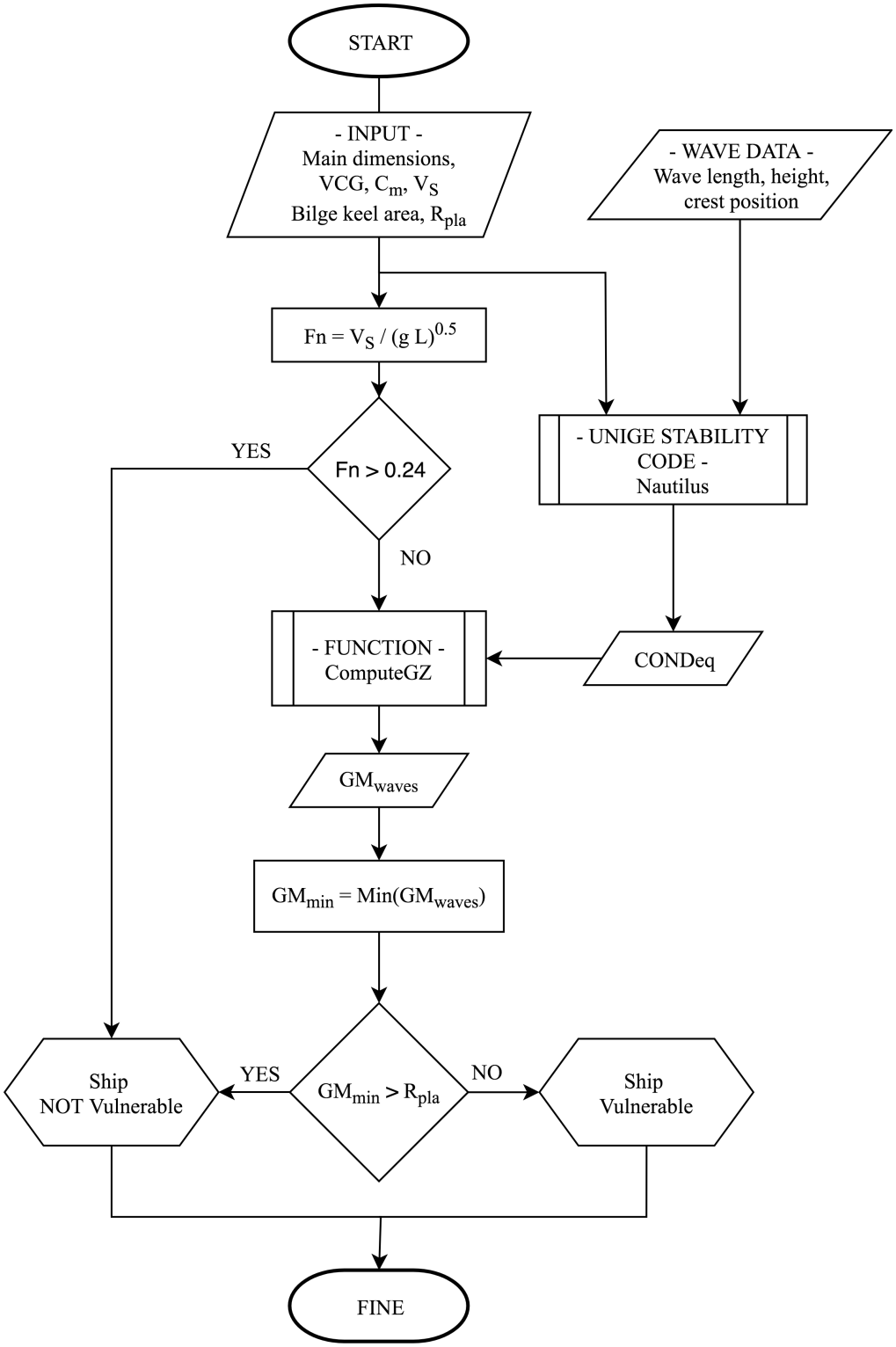

Figure 4.2: Pure loss of stability - Level 1

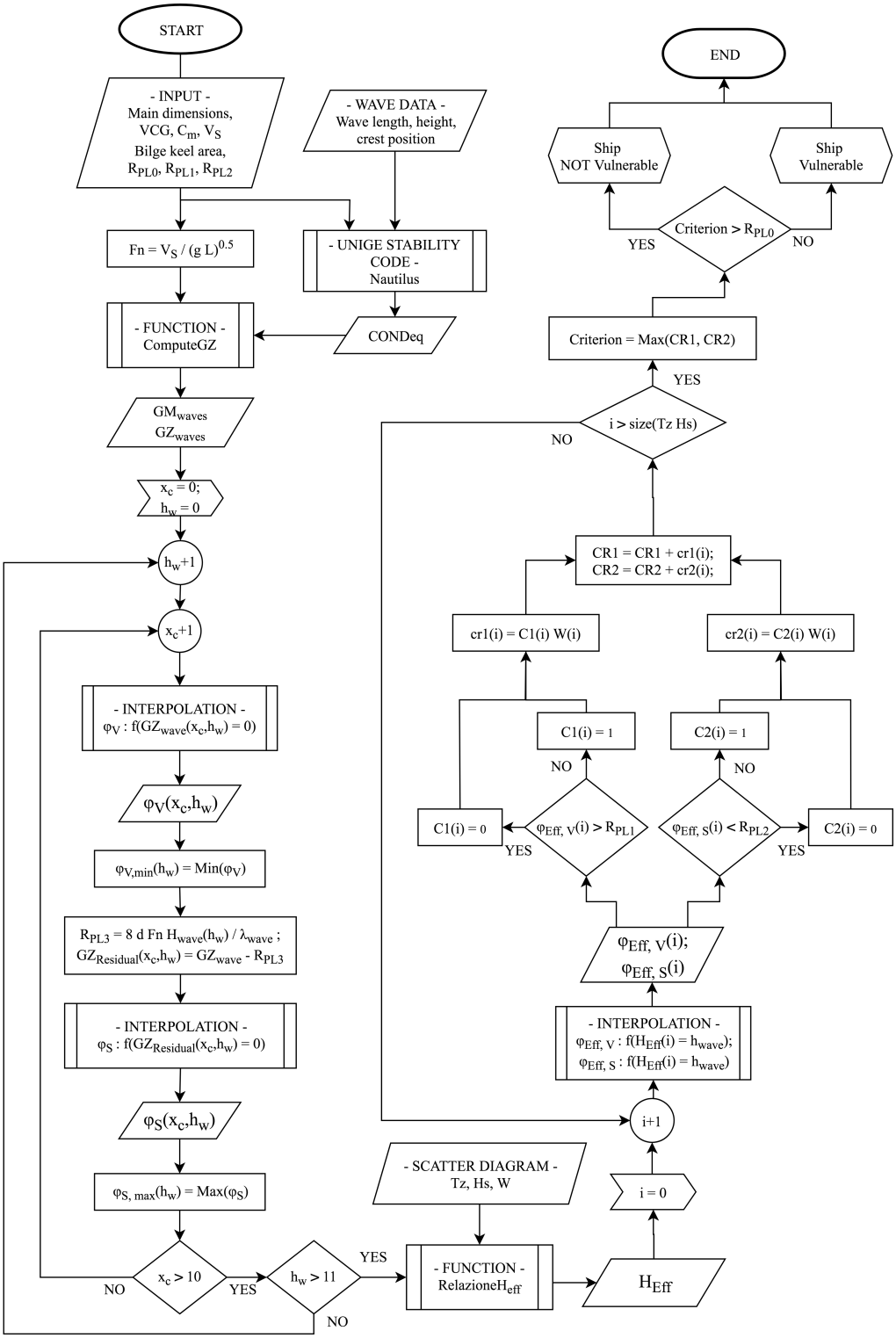

Figure 4.3: Pure loss of stability - Level 2

4.2.2 Parametric roll

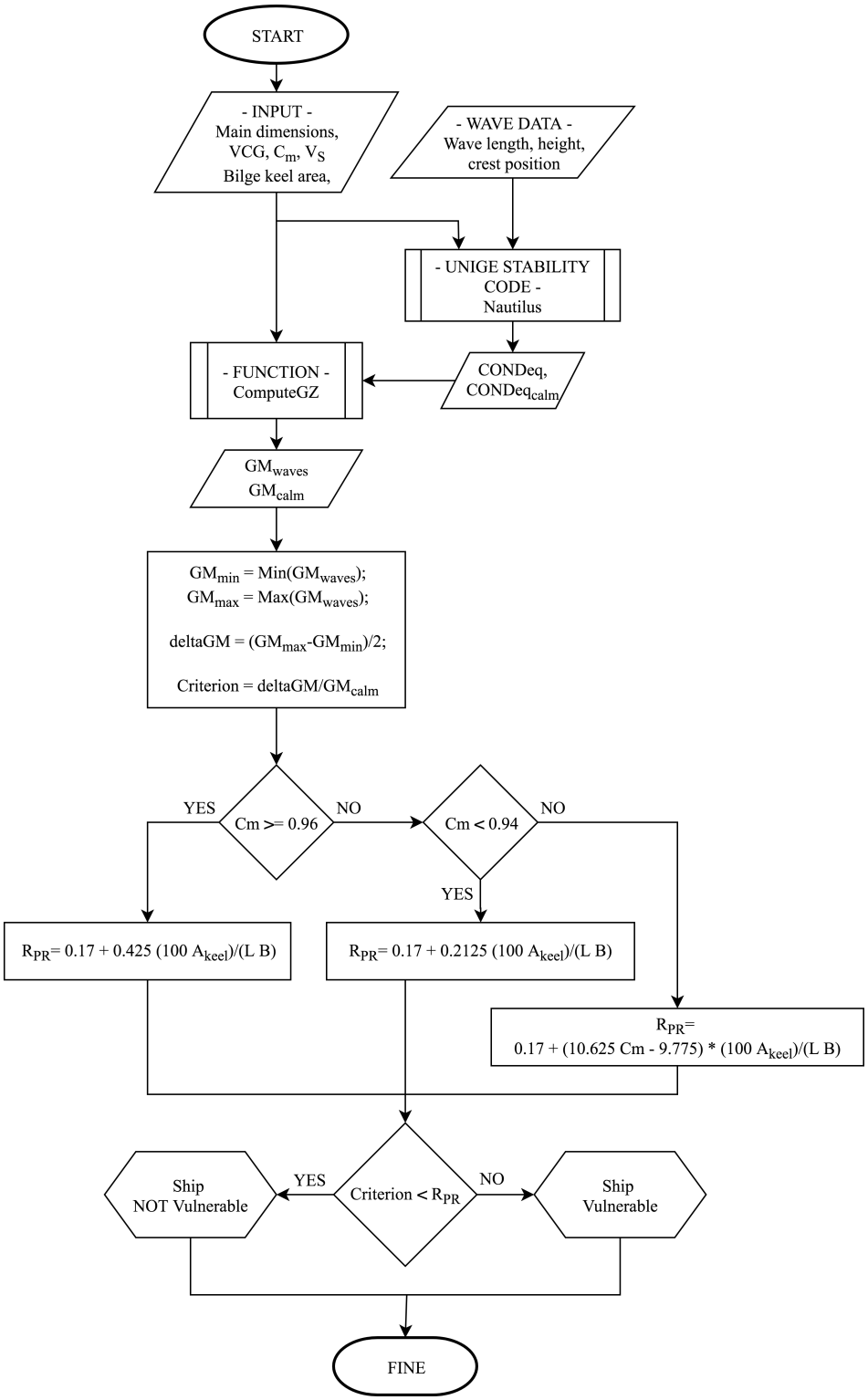

Figure 4.4: Parametric rolling - Level 1

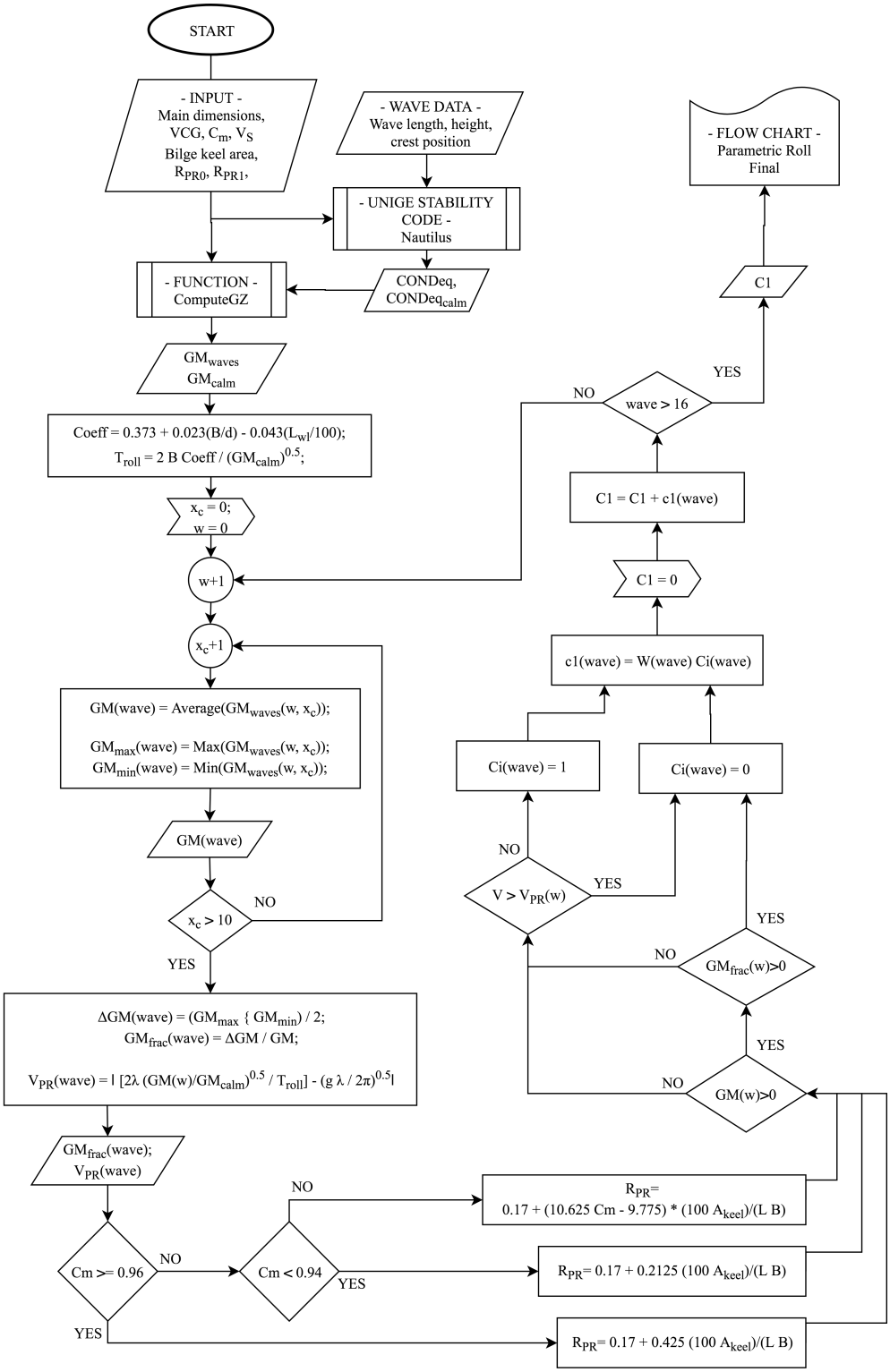

Figure 4.5: Parametric rolling - Level 2 - Check 1

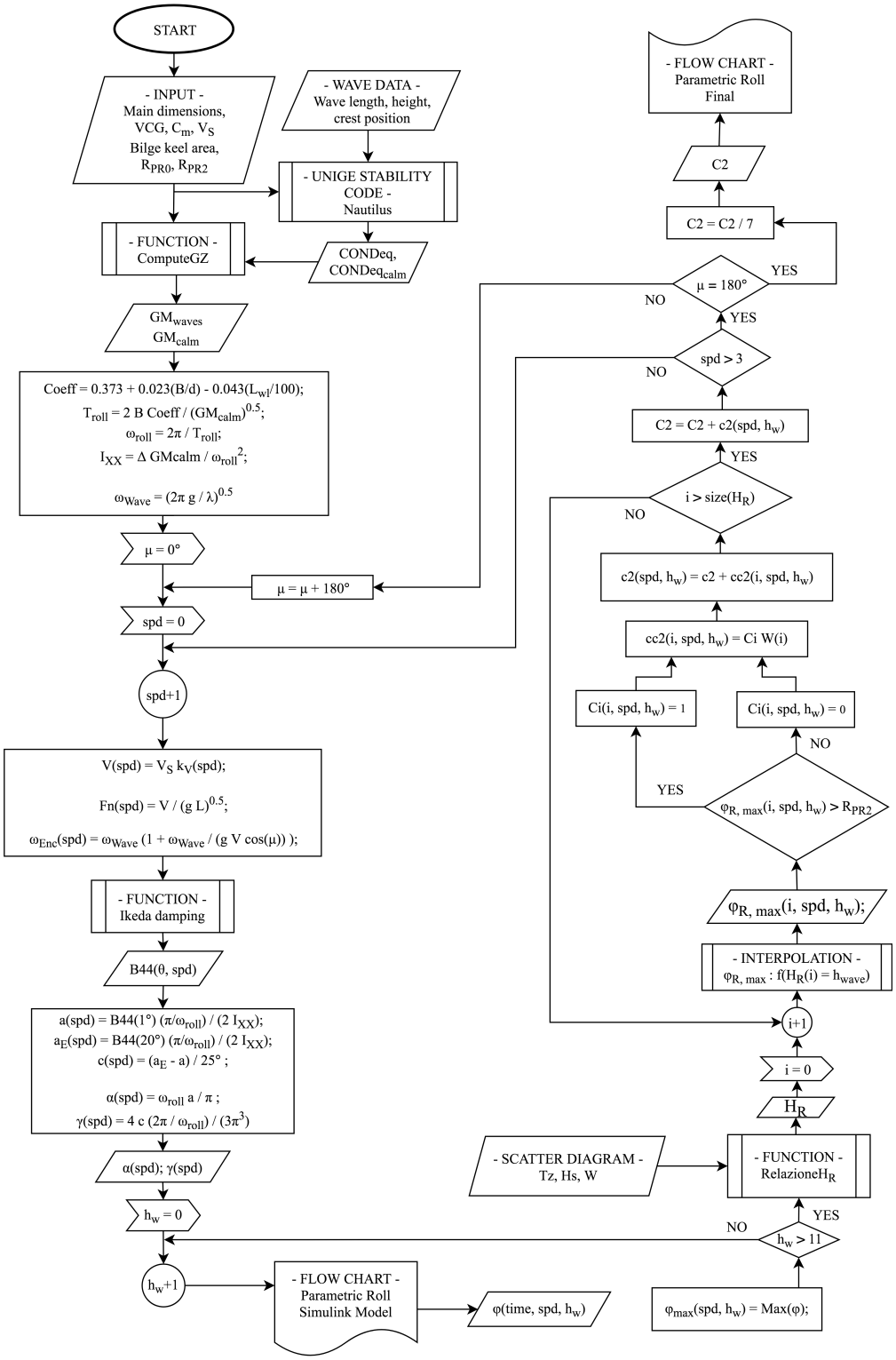

Figure 4.6: Parametric rolling - Level 2 - Check 2

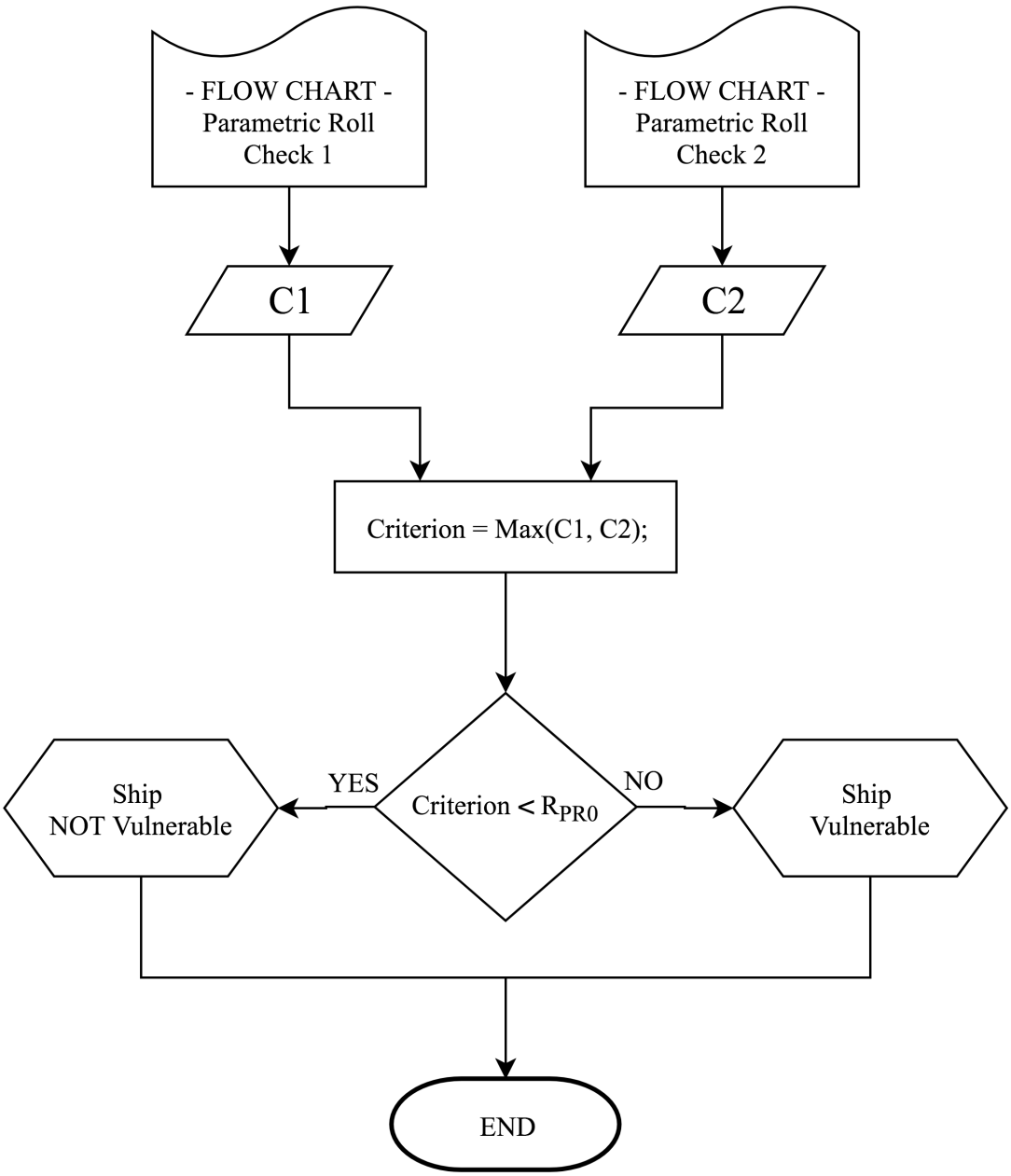

Figure 4.7: Parametric rolling - Level 2 - Final

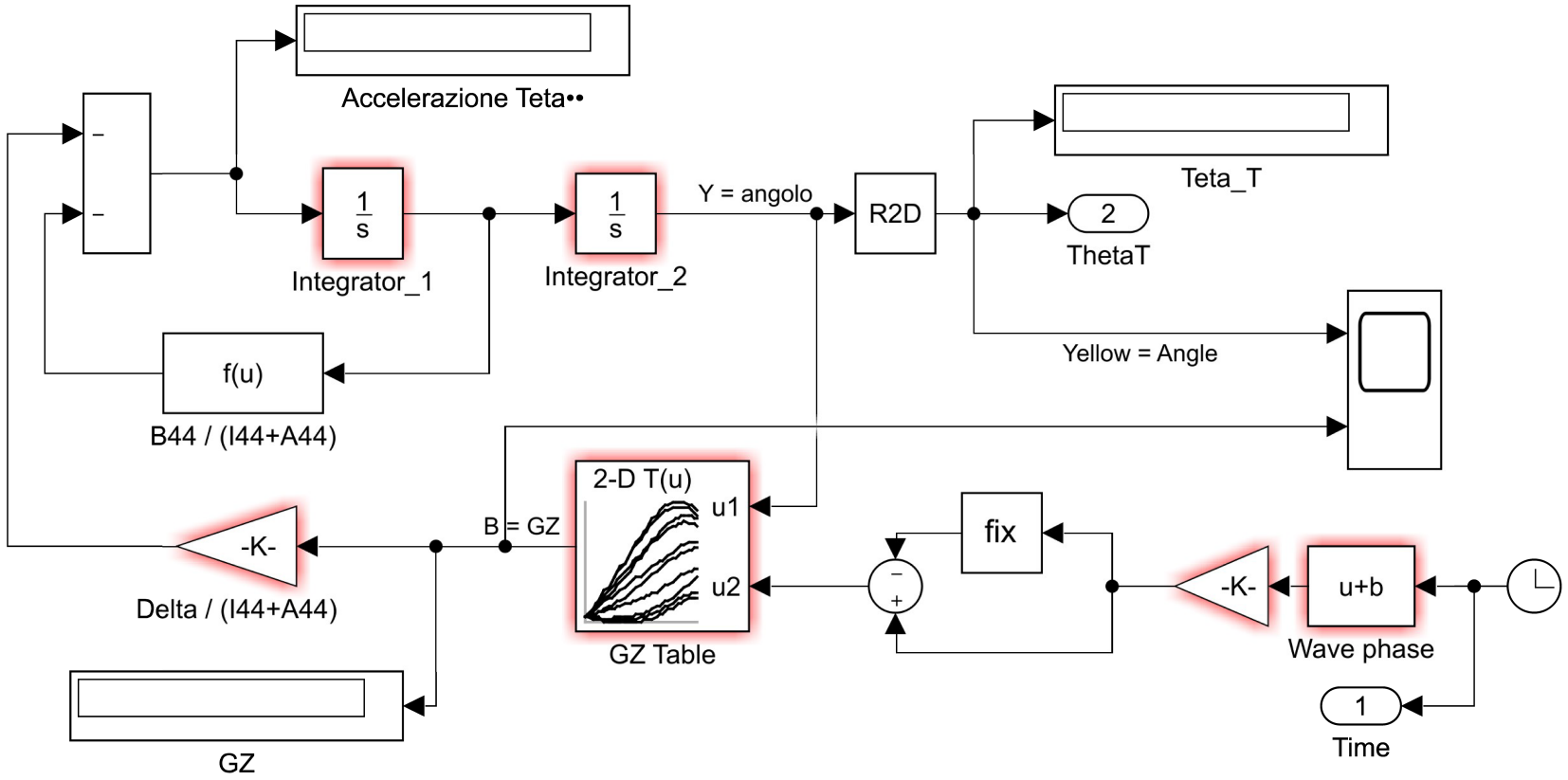

Figure 4.8: Parametric rolling - Simulink® model

4.2.3 Surf-riding

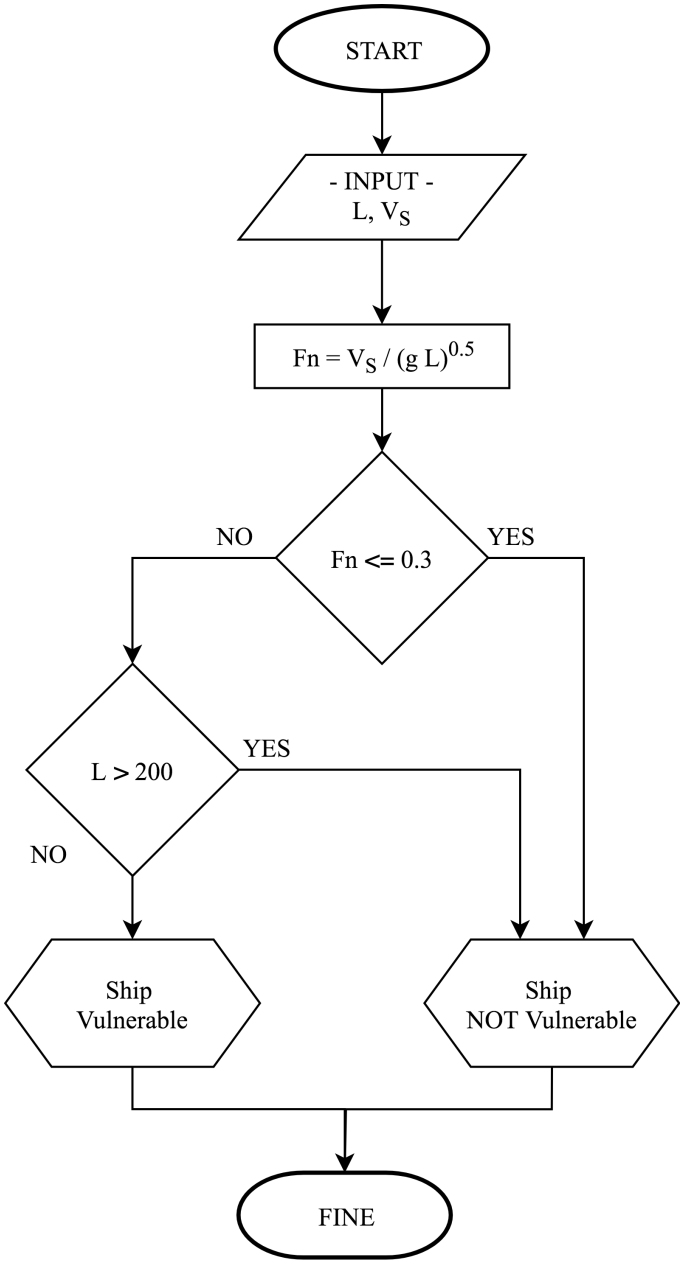

Figure 4.9: Surf-riding - Level 1

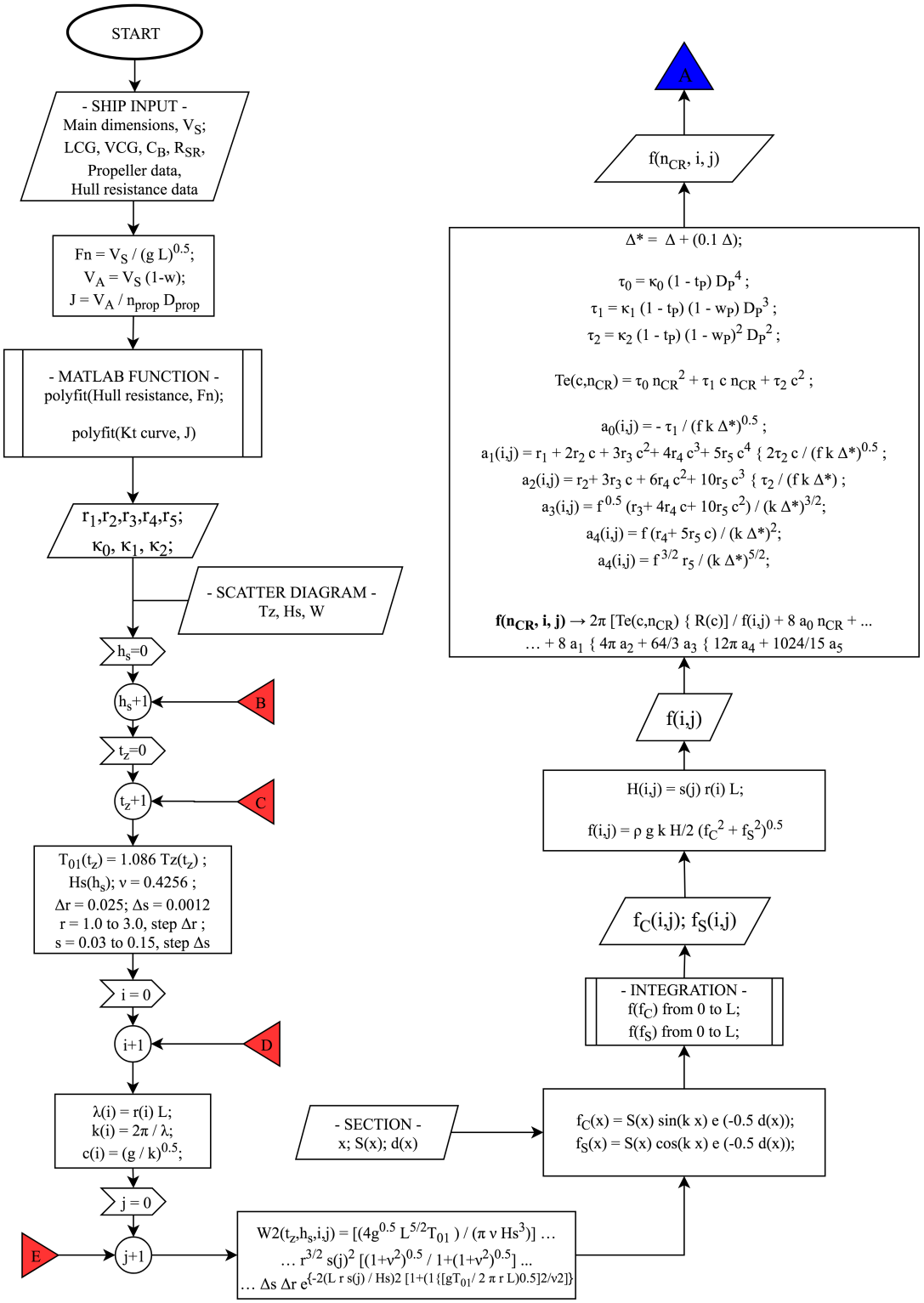

Figure 4.10: Surf-riding - Level 2 - continue. . .

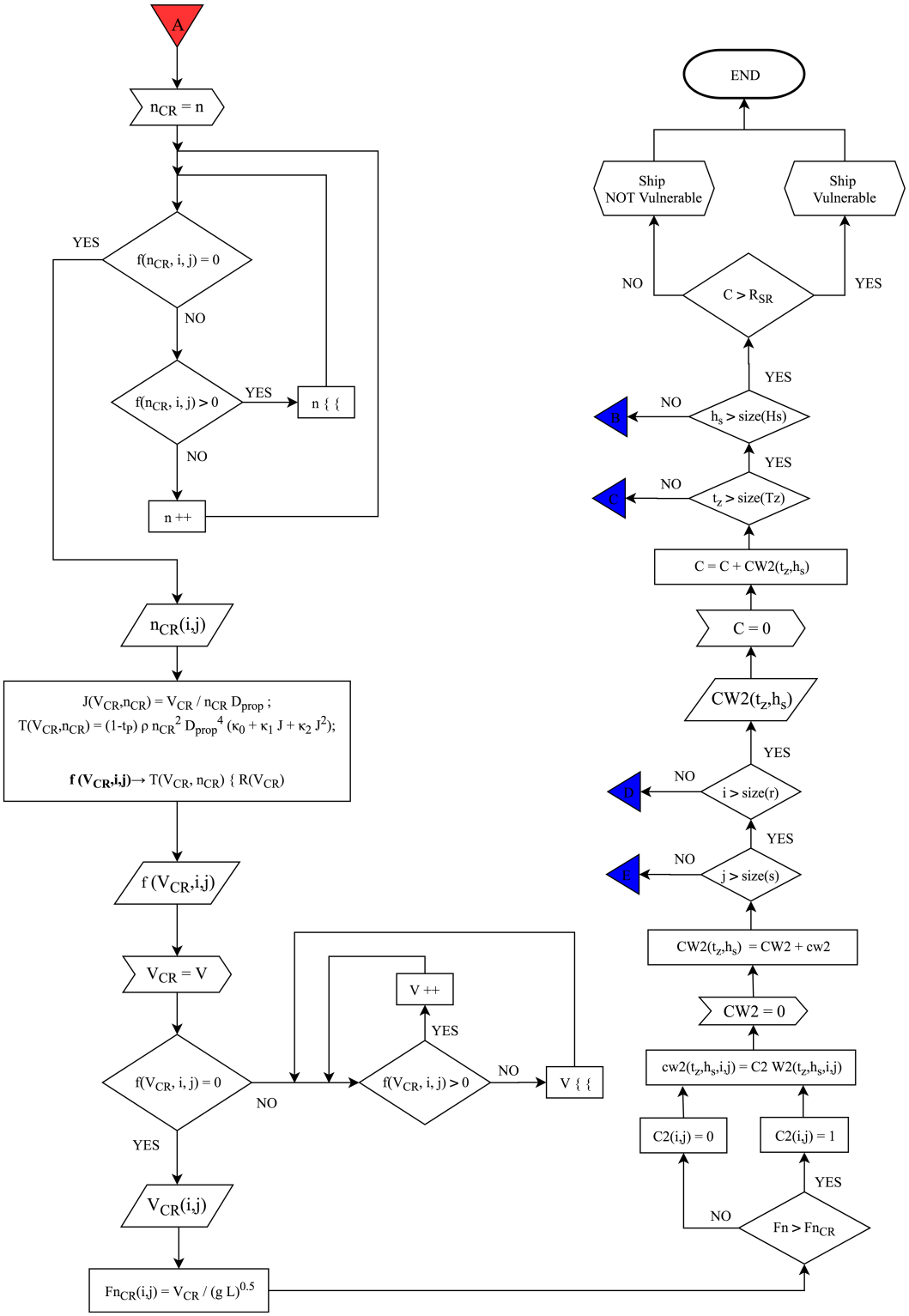

Figure 4.11: Surf-riding - Level 2

4.2.4 Dead ship condition

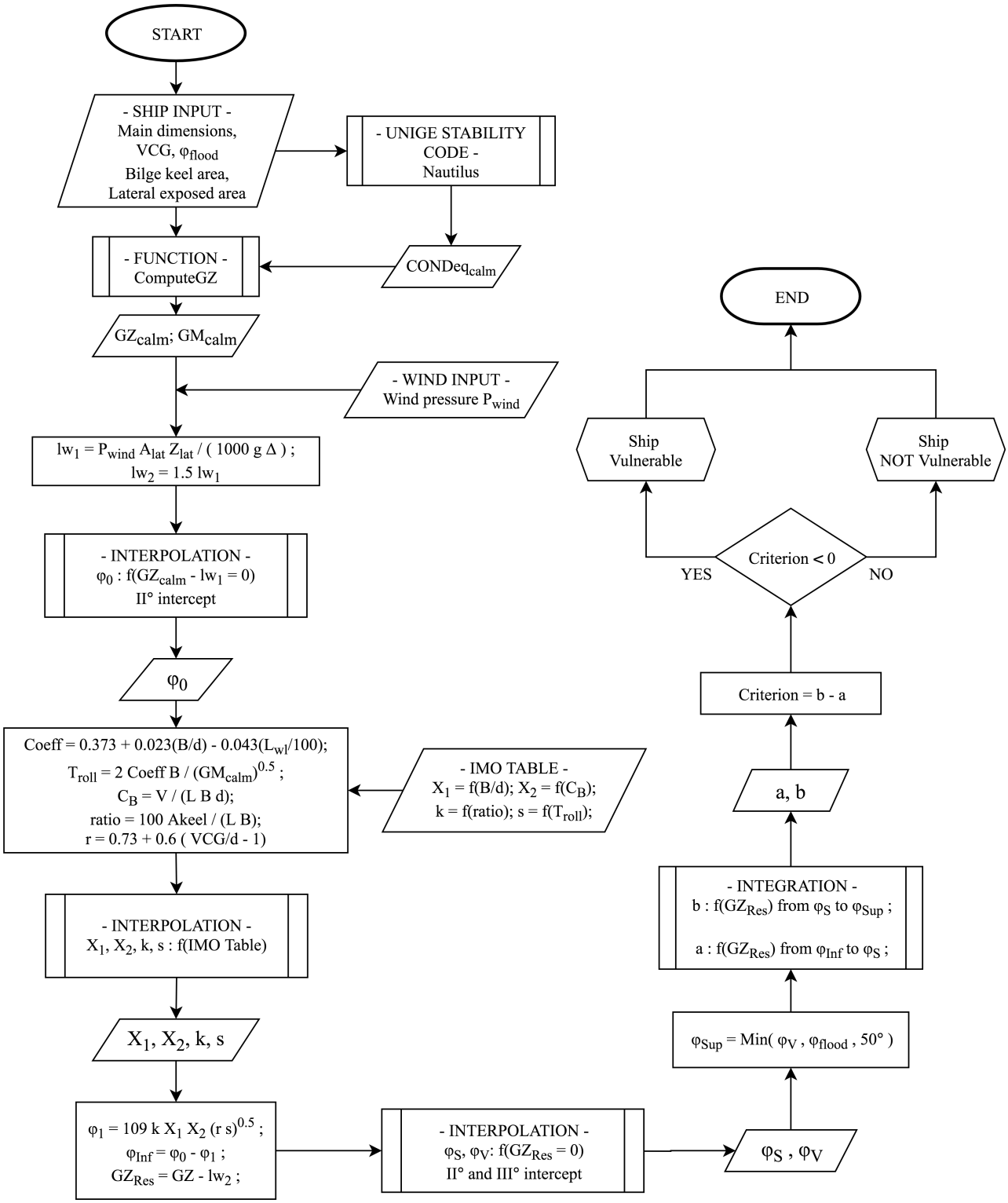

Figure 4.12: Dead ship condition - Level 1

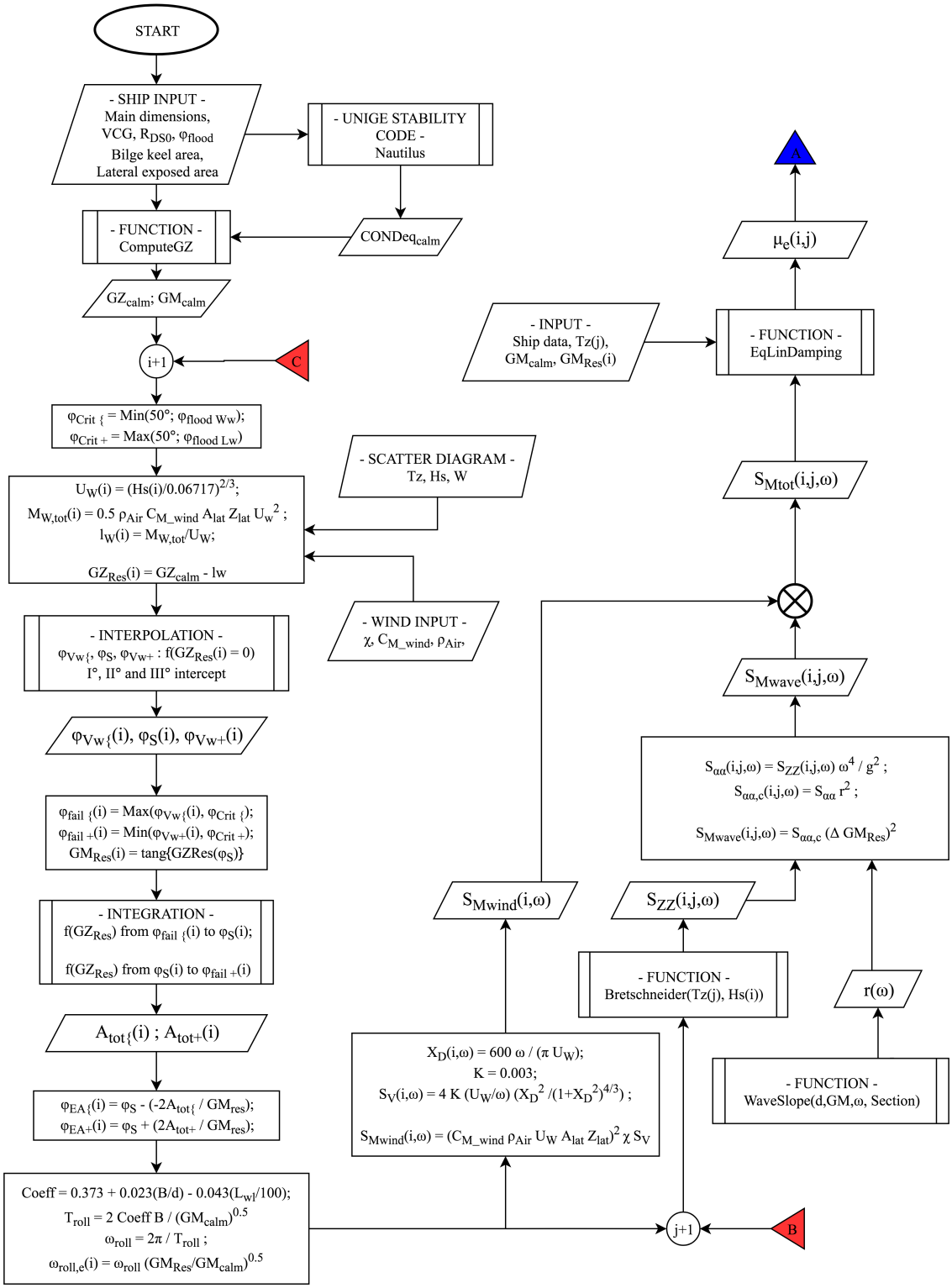

Figure 4.13: Dead ship condition - Level 2 - continue...

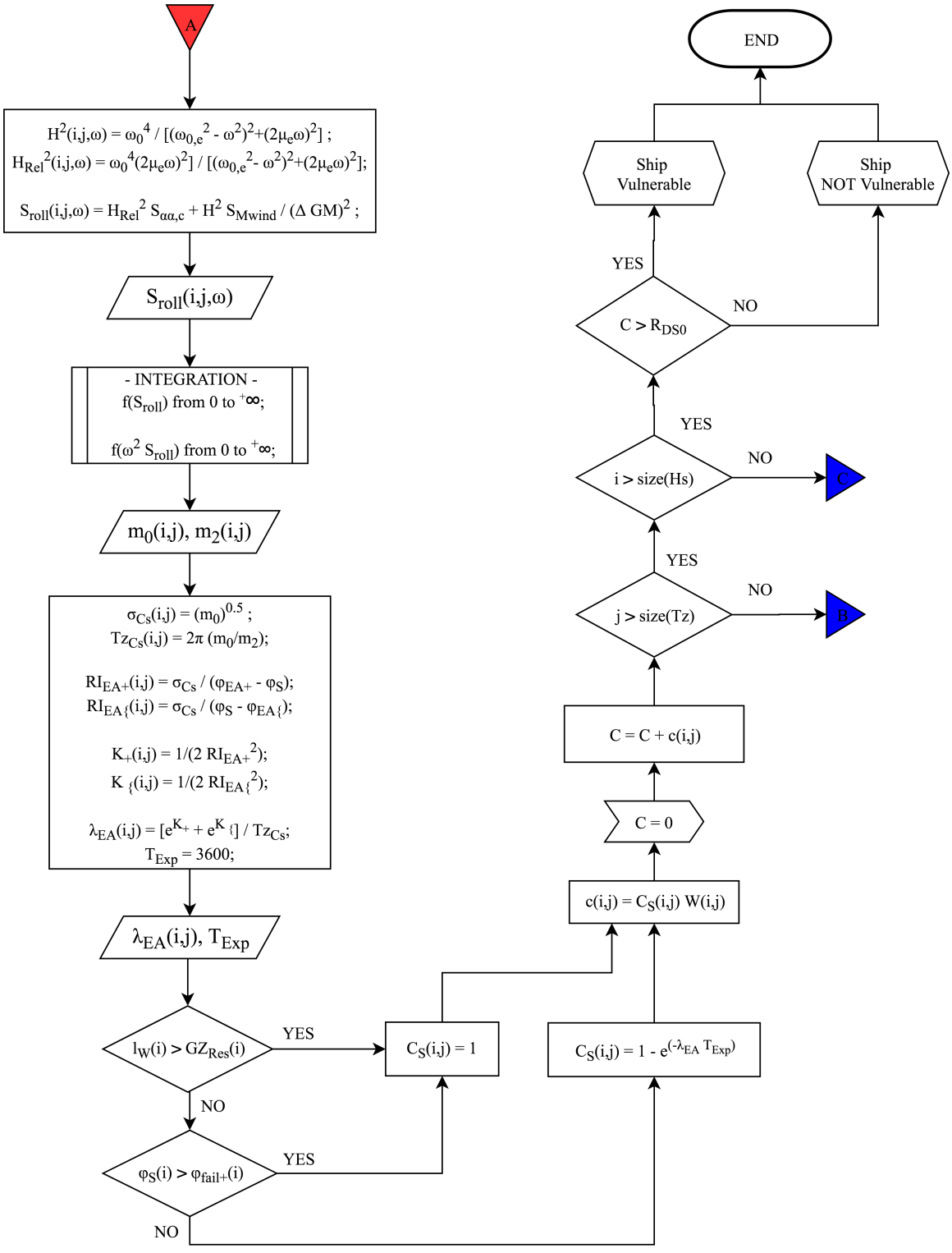

Figure 4.14: Dead ship condition - Level 2

4.2.5 Excessive acceleration

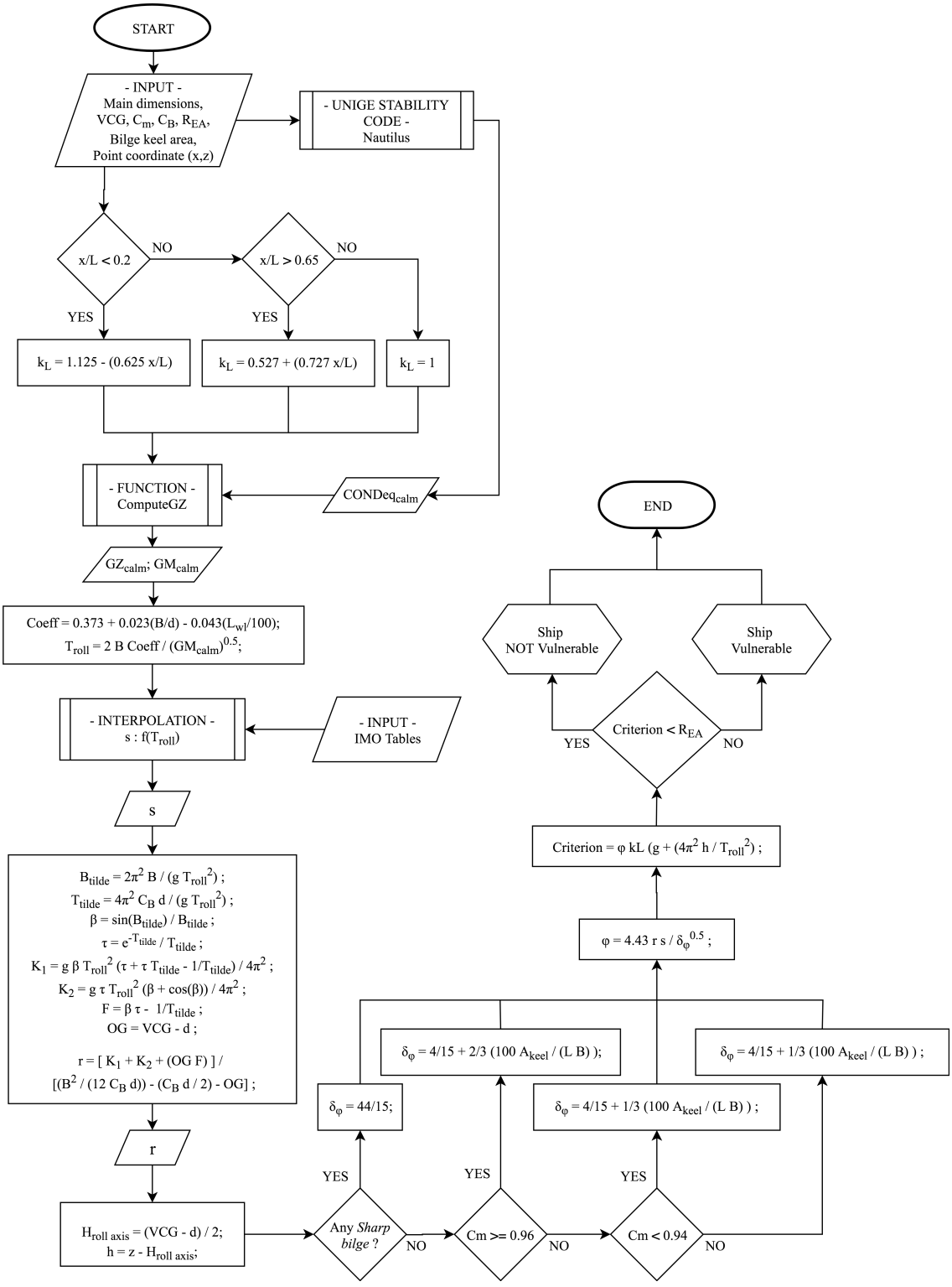

Figure 4.15: Excessive acceleration - Level 1

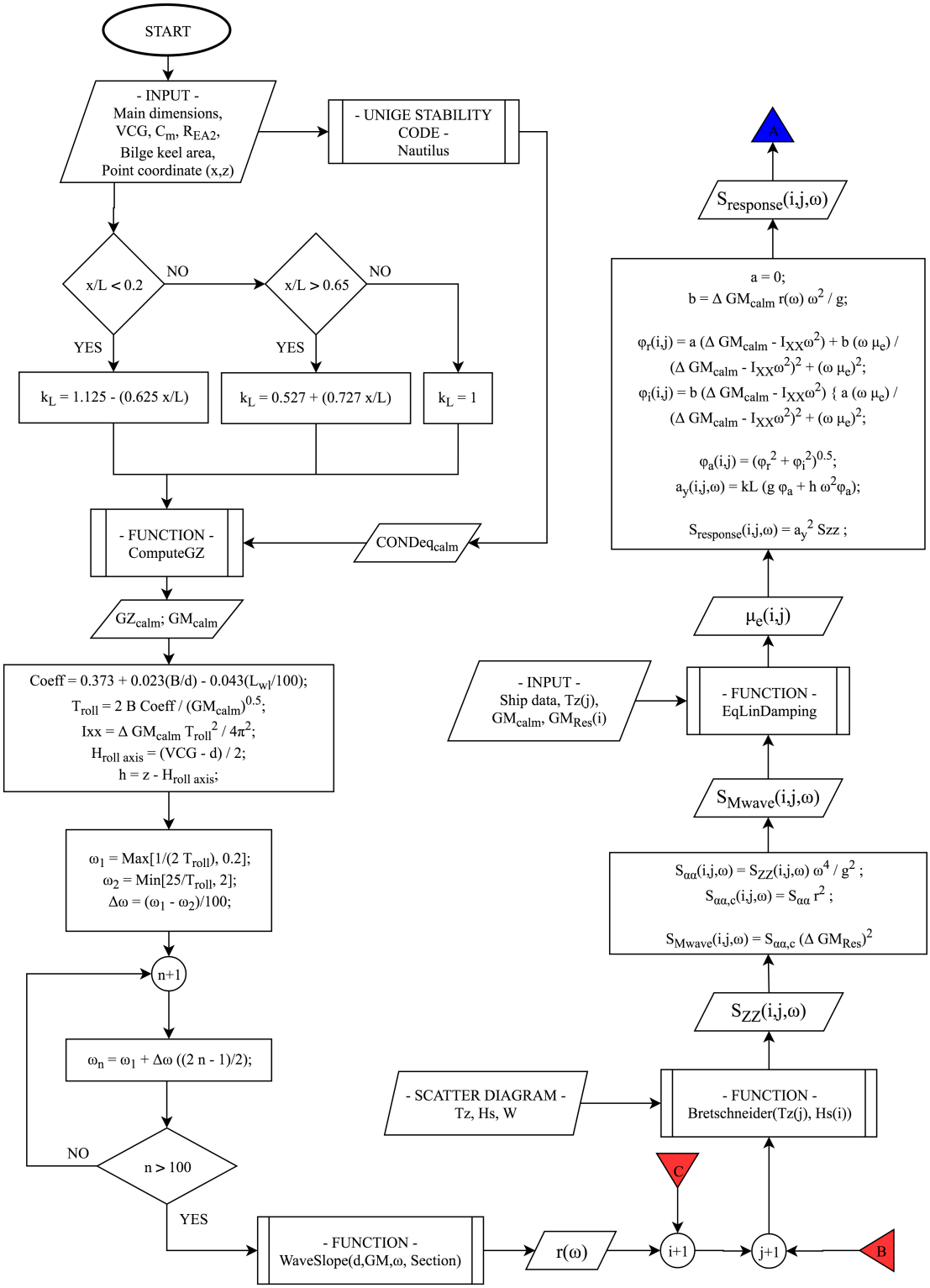

Figure 4.16: Excessive acceleration - Level 2 - continue...

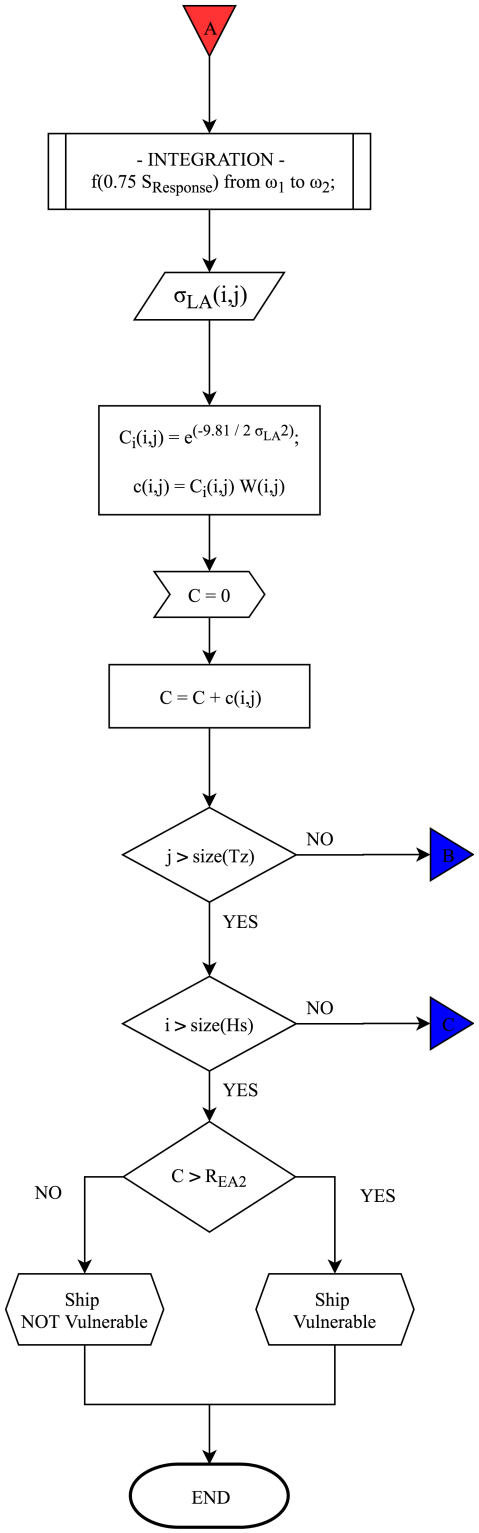

Figure 4.17: Excessive acceleration - Level 2

Chapter 5

Design Structured Matrix

5.1 The need for an holistic approach

After describing the criteria structure, it appears that the topics addressed are influenced by a lot of different parameters and the relationship among them are not always fair to understand. Moreover, the differences of the approaching methodology of each stability failure are rather relevant, therefore a specific knowledge is requested. The five stability failures are based on rather different physical phenomena, e.g. pure loss of stability and parametric roll address mainly the geometrical interaction between the hull and the wave profile, on the contrary, surf-riding is characterized by the relationship among longitudinal forces acting on the vessel, such as wave surging force, propeller thrust and hull resistance.

Keeping in mind that the aim of SGISc is to improve the safety of vessels under every aspects, it is necessary to adopt a comprehensive point of view on the whole design process. Thus, the five stability failures should be applied together giving a complete framework on the stability performance of the vessel.

In light of what above, it seems useful to identify which parameters are the most relevant and how they influence every single criterion. Since their complex structure, there is the need to adopt a tool able to carry out a clear and straightforward analysis on the procedure defined in the criterion. A possible interesting outcome is the selection of restricted number of parameters which most influence the whole process. Thank to its properties the Design Structure Matrix (DSM) well fits the requirements identified until now.

5.2 DSM: what it is and how it works

A DSM is a simple technique that describes in a compact and efficient way a set of design activities or a flow of information. The use of DSM in both industrial and research practice increased greatly in 90's. The tool has been applied in the real estate development, aerospace industries [138], small-scale manufacturing, automotive [139] and building construction [140]. Two strong points of this kind of approach are:

– Strong visual asset is provided, by means of matrices. They show clearly

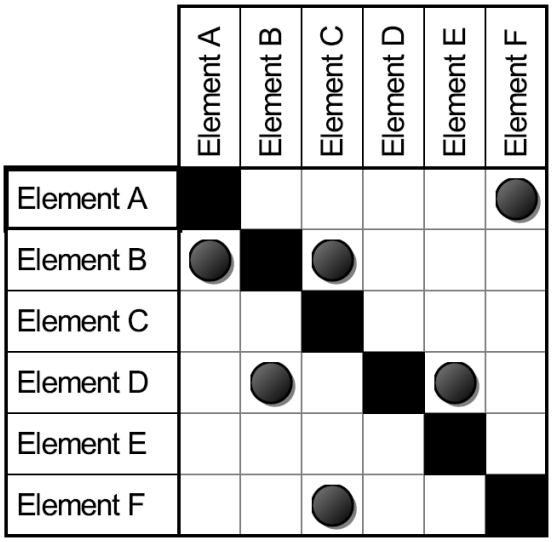

Figure 5.1: Example of a generic Design Structure Matrix

the relationships among each activity and they also may reveal possible interactions, i.e. how a parameter influences or may be influenced by another one in a clear and rapid way;

– Possibility to represent a huge amount of activities, data or parameters and their relationships in a compact way, to be read easily.

DSM is a square matrix with the same number of rows and columns. The cells on the main diagonal represent the elements or activities selected to model the system, while the off-diagonal cells depict the dependency among these elements. Exactly this last concept is the useful feature that makes different DSM from the previous project management tools such as Program Evaluation and Review Technique (PERT) or Critical Path Method (CPM), which lack in the representation of interdependency between tasks or activities. In Figure 5.1 an example of a generic DSM is given. A dot in a cell means that the output of that column is required to process/elaborate the element identified by that specific row. On the contrary, reading by column, marked (by dots) rows means that are influenced by the parameter selected in the considered column. According to Eppinger & Browning in [141], this kind of reading is conventionally called IC/FBD where IC means *Input in Column* and FBD means *Feedback Below Diagonal*. It is worthwhile to mention that there is also the other convention that reads DSMs in the reverse order and it is called Input in Row - Feedback Above Diagonal (IR/FAD).

Three different type of representation exist to describe the relationship between two tasks of the system: sequential (or dependent), parallel (or concurrent) and coupled (or interdependent). In the first configuration, the main element influences the outcome of the following task in a unidirectional flow, the dependent element may be performed only after the previous one. A sequential representation expressed by a DSM is given in Figure 5.2a. In the concurrency configuration, the elements do not interact each other, so it is possible to perform the two task in parallel (Figure 5.2b). In the last one, the elements depend on each other, there-

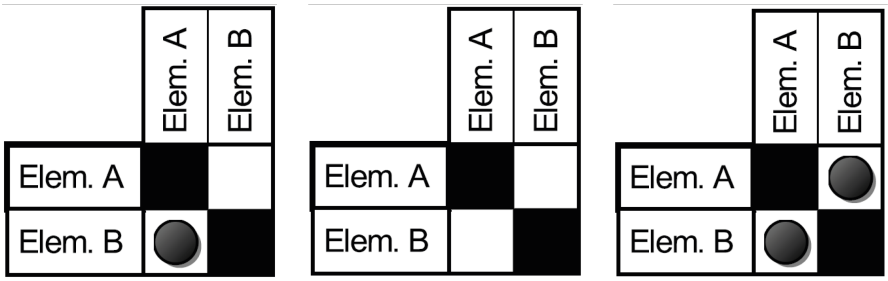

(a) Sequential process (b) Parallel process (c) Coupled process

Figure 5.2: Representation method of the relationships between elements

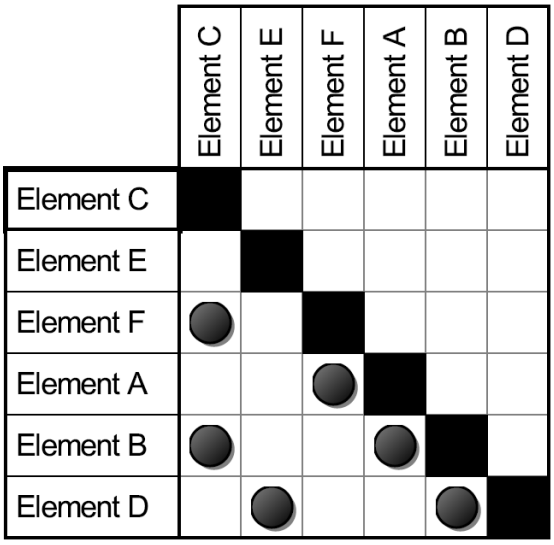

Figure 5.3: Design Structure Matrix manipulated with the partitioning process

fore the related tasks should be solved in an iterative working flow (Figure 5.2c).

The application of a DSM to a project allows to quickly understand which parameters feed or need for what. In this way, the order of tasks may be organized to be more efficient and incisive. Taking for example the DSM in Figure 5.1, it is clear that the tasks could be manipulated in order to better spot their interdependency and to improve the whole process. In Figure 5.3 the proper order to process easily and quickly the flow of information represented by the DSM is shown.

This process is called *partitioning*, it consists of manipulating the order of rows and columns to arrange the DSM without any feedback marks above the main diagonal. In general, the optimal results would be to obtain a lower triangular matrix, even if this is not always possible to be achieved, especially for complex systems. In that cases, the objective of the re-arrangement becomes to lowering the number of marks above the main diagonal and to move them as closer as possible to it. In doing so, the fewer process tasks are involved within the remaining iterative cycle making faster the whole processes. An exhaustive description of this operation applicable to DSM is given by Yassine in [142], moreover other

relevant DSM processes are described such as *tearing* or *banding*.

5.3 Application to the SGIS criteria

Within the thesis, the DSM technique has been applied to the first and second vulnerability level of SGISc. The procedure to evaluate a criterion is rendered into a set of specific data and derived parameters, which are logically ordered into a DSM. The DSMs developed in this perspective are graphically represented in Appendix B. It is worthwhile to mention that all the DSMs presented in this paper, have been modeled thanks to the software Cambridge Advanced Modeler (CAM) developed by Wynn *et al.* [143].

Beginning from the rule text of each stability failure, data required by the criterion for the assessment are identified. Then, they have been organized into the matrix according to the order of appearance within the criteria. Thereafter, by virtue of the properties of DSM, the set of parameters has been rearranged applying the partitioning method described in § 5.2. Thanks to the new arrangement of the DSM, it is straightforward to subdivide the set of elements in three main categories:

1. *Design parameters*, highlighted in blue;
2. *Dependent parameters*, highlighted in white
3. *Output*, highlighted in green.

It is considered as a *Design parameter* each element that does not directly depend on another one. The *Design parameters* category is subdivided in two other sub-category: *Main elements* and *Secondary elements*. The first sub-category consists of all those parameters that may be set directly by the designer or defined by the agreement between the ship owner and the yard, i.e. length between perpendicular, service speed, as well as, bilge keel dimension and vertical position of the center of gravity. The secondary elements can generally derive from the first ones, such as hull overall geometry or can even be independent like environmental conditions.

Dependent parameters are those parameters that should be evaluated according to the formulas defined by the rule. They deterministically depend on the *Design parameters* and they cannot be tuned by the designer. Finally, the *Output* category is made up of two elements: the criterion that evaluates the vulnerability of the vessel and the standard that is the threshold against which to compare the calculated criterion. Once the DSM is created and its elements are categorized, the *Design parameters* common to every stability failures have been highlighted. The *Main elements* common to all the criteria are listed in Table 5.1 and an excerpt of pure loss of stability DSM is represented in Figure 5.4 (all DSM are collected in Appendix B).

Once the DSMs have been made for each stability failure and levels, it has been decided to formulate a index able to evaluate the influence of *Main parameters* on the final results. The index formulated it has been called K-index and it is described in the following section.

Table 5.1: Main elements common to all stability failure identified by DSM

Main parameters		
Bilge keel area	A_{BK}	(m^2);
Breadth	B	(m);
Depth	D	(m);
Draught	d	(m);
Length between perpendicular	L_{PP}	(m);
Service speed	V_S	(m/sec);
Vertical position of Centre of gravity	VCG	(m);
Coordinate of the assessed point	P(x,y,z)	(m).

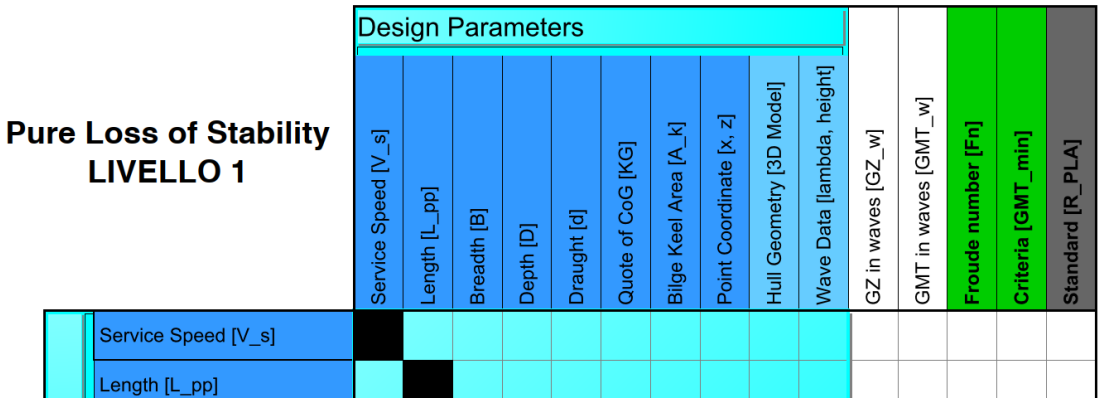

Figure 5.4: Excerpt of Design Structure Matrix of first vulnerability level of pure loss of stability

5.3.1 An index to compare criteria

The need of a non-dimensional index measuring the dependency of the criterion from a parameter, comes from the significant difference among the outcome formulation of each criterion. For example, the criterion for pure loss of stability - first level is simply the minimum metacentric height GM_{min}, but the outcome for parametric roll - first level is instead a ratio between the variation of metacentric height in wave and GM in still water; at the same time, for the excessive acceleration failure, the computed criterion is the transverse acceleration measured on board. This is not the same in the second vulnerability level criteria where the outcomes are expressed in terms of the probability of a failure in a long term analysis, even if obtained by means of different calculations and models. Therefore the K-index has been developed focusing mainly on the first levels, excluding the surf riding criterion because of its extremely simplified structure.

The slope coefficient of the regression line is a first attempt to express the link between a selected parameter and the final criterion by a numerical index. The regression line slope dependency on the unit of measurement for the specified criterion is an inconvenience for the comparison among all stability failures. In order to overcome this problem, K-index is proposed in the following form:

$$K = {}^{\Delta Y_{\%}}/_{\Delta X_{\%}} \tag{5.1a}$$

$$= \frac{Y - Y_{ref}}{Y_{ref}} \cdot \frac{X_{ref}}{X - X_{ref}} \tag{5.1b}$$

$$= \frac{Y - Y_{ref}}{X - X_{ref}} \cdot \frac{X_{ref}}{Y_{ref}} \tag{5.1c}$$

where X_{ref} is the design value of the selected *Main parameter*, Y_{ref} is the outcome value of the criterion referred to the design condition extrapolated from the linear regression line and X, Y are the coordinates of the assessed parameter evaluated along the linear regression line (Figure 5.5).

K-index does not depend on the specific unit of measurement of each criterion, so it can be assumed as a good coefficient for a comparison among all stability failures. As it is formulated, the coefficient K is based on the assumption of a linear relationship between the criterion and the considered parameter. This is valid if the parameter is changed in a limited neighborhood of the design value. Moreover, the value of K is strictly related to the selected point of reference as baseline: in my studies the parameters and criteria referred to the initial design condition have been chosen.

The sign of K-index represents the direction of the relationship between a main parameter and the criterion: a positive sign means there is a direct relationship, so increasing the parameter increases the criterion, vice versa for negative signs. Instead, the strength of the relationship is evaluated by the numerical value of the K-index. A high value of K corresponds to a strong link, which means that a limited variation of the parameter produces a large variation of the criterion. A null value of K means no relationship exists between the parameter and the final criterion.

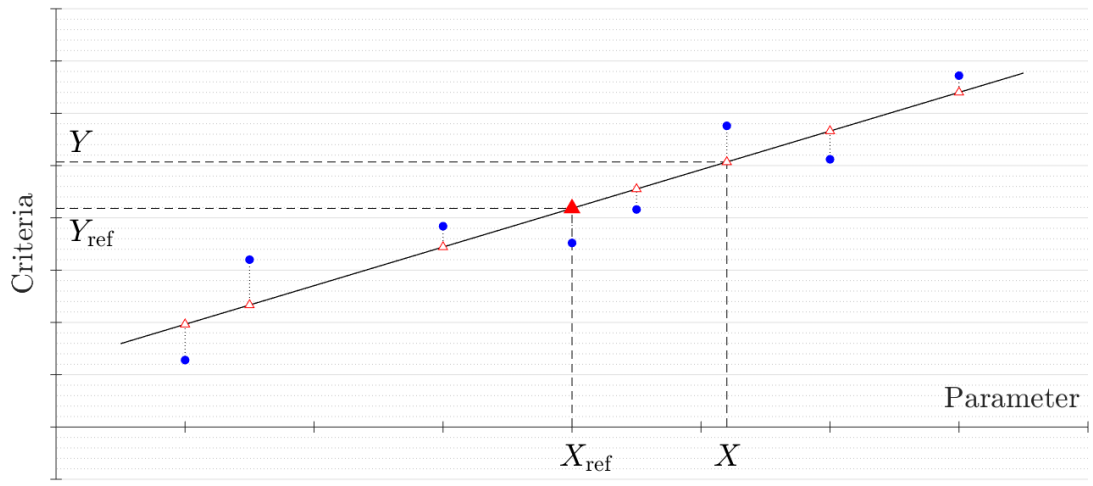

Figure 5.5: Exemplification of the K-index structure

Chapter 6

Application cases

In this chapter, in order to verify and validate the developed computational tools, a campaign of application has been conducted, with the complementary target to gain expertise for the design of ships with enhanced stability performance. In the followings, the results obtained by the applications of the SGISc to a set of vessels will be presented. In particular, an extensive analysis on a representative unit of mega-yacht is carried out, moreover a Ro-Ro pax ferry is analysed as well. The results are presented in terms of maximum KG curves (minimum KG curve only for the excessive acceleration stability failure). Finally, taking into account what about in Chapter 5, a set of systematic modification have been carried out, in order to identify the relationship among main design parameters and the criteria.

With the aim to find a tool able to evaluate the stability performance of naval vessels in a seaway condition, the SGISc have been also applied to three different typologies of naval vessel: an Offshore Patrol Vessel (OPV), a destroyer unit and a helicopter carrier. Furthermore, the results of applications have been presented together with those computed for a representative navy intact stability code obtained from the merge of different Navies regulations.

6.1 Mega yacht unit: a comprehensive analysis

A representative mega-yacht unit of about 70 (m) length has been analysed as an application case [136], [144]. In Table 6.1 the principal dimensions and technical data available for this ship are listed, while the construction plan is shown in Figure 6.1.

Since information about the interior of the mega yacht unit are not available, the general arrangement has been drawn as a contribution from a graduation thesis in MSc Naval architecture [145]. An internal and external layout have been designed taking into account solutions adopted on a set of similar units, also in terms of sizes. In Appendix C, from Figure C.1 to Figure C.6, the external and internal arrangements are shown. These technical drawings will be useful to identify the coordinates of the highest place where crew or passenger may be present on board as requested by the excessive acceleration criteria. At the same time, from the same drawings the exposed lateral area, as required within the dead ship condition criterion, has been quantified.

Table 6.1: Megayacht unit main dimensions

Main dimensions			
Length overall	L_{OA}	74.39	(m);
Length between perpendicular	L_{PP}	64.94	(m);
Maximum breadth	B_{max}	13.20	(m);
Design draught	d	3.30	(m);
Depth	D	7.50	(m);
Displacement	Δ	1669	(t);
Service speed	V_S	17.4	(kt);
Froude number	Fn	0.354	(-);
Block coefficient	C_B	0.586	(-);
Midship section coefficient	C_m	0.935	(-);
Bilge keel length	L_{BK}	23.0	(m);
Bilge keel span	b_{BK}	0.18	(m);
Design vertical centre of gravity	KG	5.50	(m);
Design metacentric height	GM_{design}	1.91	(m).

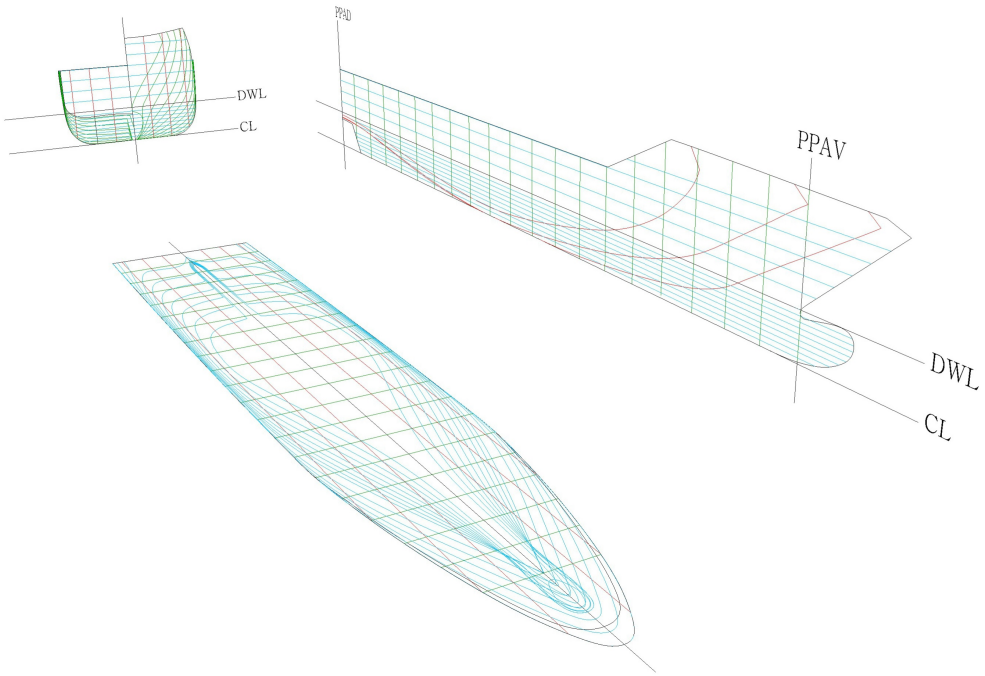

Figure 6.1: Three dimensional view of the megayacht construction plan

Table 6.2: Analysed draughts in the SGISc investigations

	d_{I}	$d_{10\%}$	d_{II}	d_{III}	d_{design}	d_{full}
(m)	2.5	2.7	2.9	3.1	3.3	3.5

It is expected the mega-yacht might present vulnerability to stability failures affected by interaction between wave profile and hull shape, i.e. parametric roll and pure loss of stability. In fact, they can be characterized by a significant difference in breadth while the draught is changing between volume below and above the waterline. Once above the waterline the hull volume of mega-yacht unit might grow quickly in order to house passenger accommodations as large as possible. Moreover, the extended longitudinal area up to the fourth tier deck, namely Sun Deck, it could make the unit vulnerable to the dead ship condition. The mega-yacht has been assessed with both first and second vulnerability levels of all criteria, except the second level of surf-riding because of the need of information not ready available for this specific unit, such as hull resistance and propeller characteristic curves. The results are all represented in terms of maximum KG curves but for excessive acceleration failure, which is represented as minimum KG curve due to intrinsic criterion structure. The KG curves indicate the maximum or minimum height above the keel line complying with the SGISc as a function of the draught; therefore, if a loading condition lies on the limit KG curve the ship still complies with the criterion; this is not the case when her KG is above the maximum KG curve (vice-versa for the minimum KG curve). One of the main reasons to assume this kind of results representation is the comparison between first and second levels outcomes and among the different stability failure modes. Besides the design draught, other five have been selected for the KG curve analysis, as reported in Table 6.2. Since no information about loading conditions other than the design one are available, they have been assumed from an investigation carried out on units of the same typology and similar dimensions. The payload of a yacht unit is made up of only a restricted number of passengers, therefore a change in the loading condition is mainly due to consumable variation, mainly fresh water and fuel oil. Since the consumable weight variation is limited compared to the lightship weight, it follows that the change range for draught among loading conditions is limited as well.

To assess the criterion for the dead ship condition stability failure, the exposed lateral area A_{lat} is required; its value is measured from the longitudinal profile (Figure C.1) at the corresponding loading condition. Finally, the longitudinal and vertical positions of the highest place where crew or passengers may be present, is to be derived for the excessive acceleration assessment. In Table 6.3 the supplementary information, beside the main dimensions, requested for the complete analysis are listed.

Table 6.3: Supplementary dimensions required to evaluate dead ship condition and excessive acceleration criteria

Supplementary information			
Design lateral exposed area	A_{lat}	663.7	(m^2)
Design quote of the exposed area center	Z_{lat}	8.60	(m)
Longitudinal position of the assessed point	X_P	25.98	(m)
Vertical position of the assessed point	Z_P	14.0	(m)

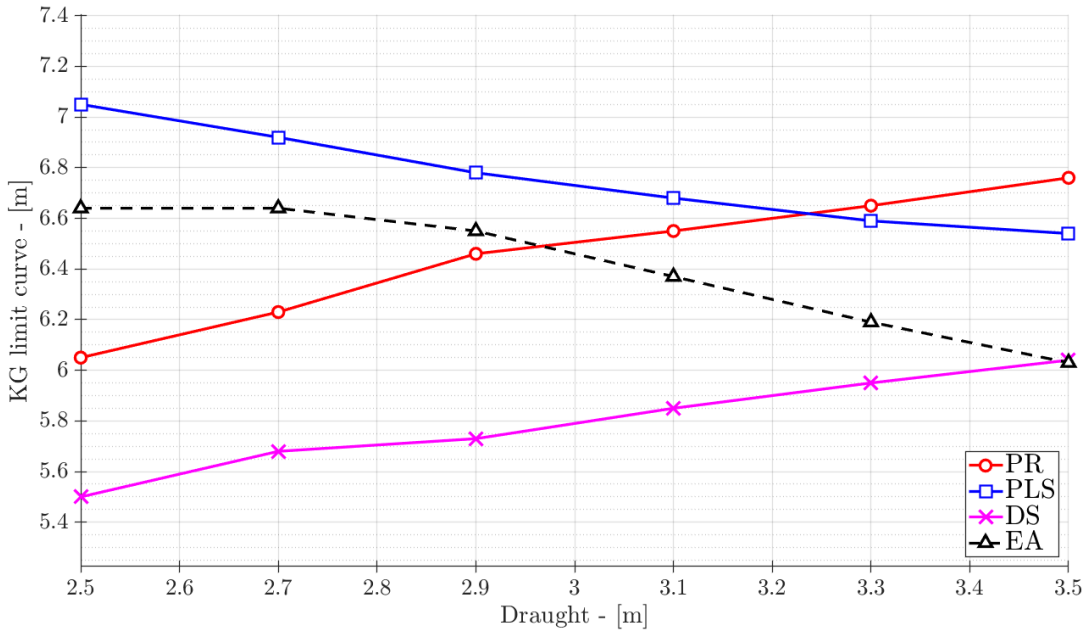

Figure 6.2: Megayacht unit - First vulnerability levels

6.1.1 Results

First vulnerability level analysis

The KG curves are shown in Figure 6.2, for all first levels except for surf-riding criterion, since it doesn't get influenced by the center of gravity position. On the vertical axis the maximum permitted KG (the minimum for the excessive acceleration failure) can be found, while on the x-axis the draughts listed in Table 6.2 are reported. Moreover, the maximum KG curves are depicted with colored continuous lines, while the minimum KG curve relative to the excessive acceleration phenomena is represented by a black dashed line.

Considering only the maximum KG curve, i.e. the continuous lines, it appears that in this range of draughts for the mega-yacht unit, the most severe criteria is the one referred to the dead ship condition. In fact in this case, the maximum KG curve is generally about 0.50 (m) below the curves relevant to the other two failures. Both the parametric roll and dead ship condition curves increase with the increasing of the draught, while pure loss of stability has the opposite trend. Comparing all the stability failures, hence the maximum and minimum

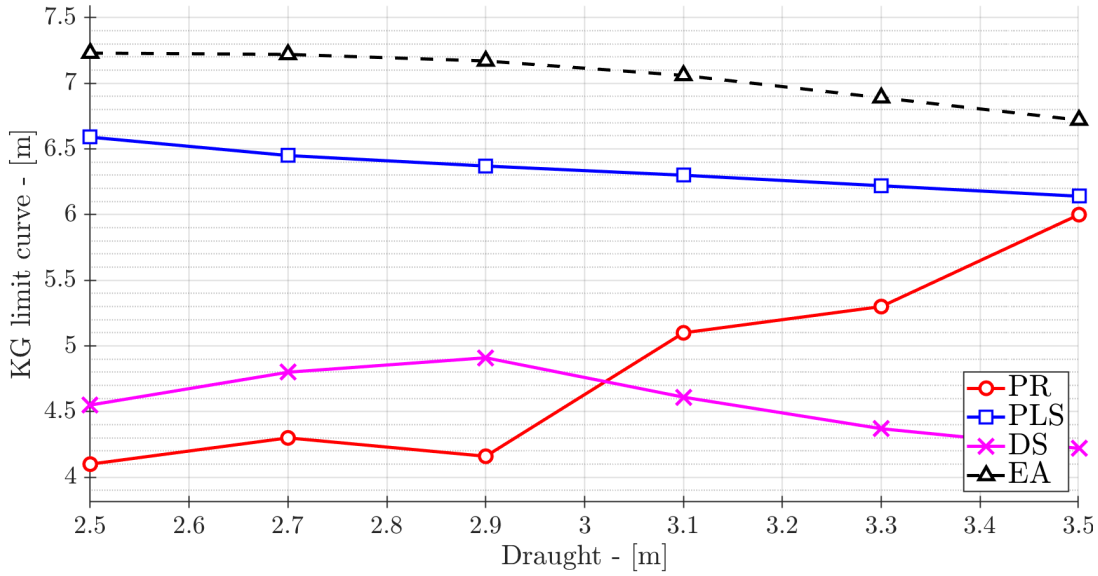

Figure 6.3: Megayacht unit - Second vulnerability levels

KG curves, it appears that no KG values along the whole draught range may satisfy all the criteria at the same time. In particular, there is no intersection between the minimum KG curve and the most severe maximum KG curve, except for $d = 3.5$ (m), where they correspond. A possible conclusion is that no *design space* is available to comply with all the first vulnerability criteria for the assessed draughts.

Second vulnerability level analysis

Adopting the same representation of the previous paragraph, the outcomes obtained by the application of the second vulnerability criteria to the mega-yacht unit are given in Figure 6.3. Also in this case the minimum KG curve referred to the excessive acceleration criteria is represented by a black dashed line, while other stability failures for maximum KG curves are continuous lines. Considering only the maximum KG curves it appears that, for draught values less than 3.0 (m), the parametric roll criterion is the one imposing the most severe KG threshold, even though the permissible KG value increases with increment of the draught. In fact, above $d = 3.0$ (m) the most severe curve becomes the one referred to the dead ship condition criterion. Also in this case, there is no *design space*, in terms of combination of KG and draught, where the ship can be designed, since the minimum KG curve (referred to excessive acceleration) stands well above all the others.

Consistency analysis between levels

In this section, each stability failure is analysed individually and a comparison between first and second vulnerability levels has been carried out. The results obtained are given from Figure 6.4 to Figure 6.7. Again, the representation adopted in the previous paragraph of maximum or minimum KG curves is used.

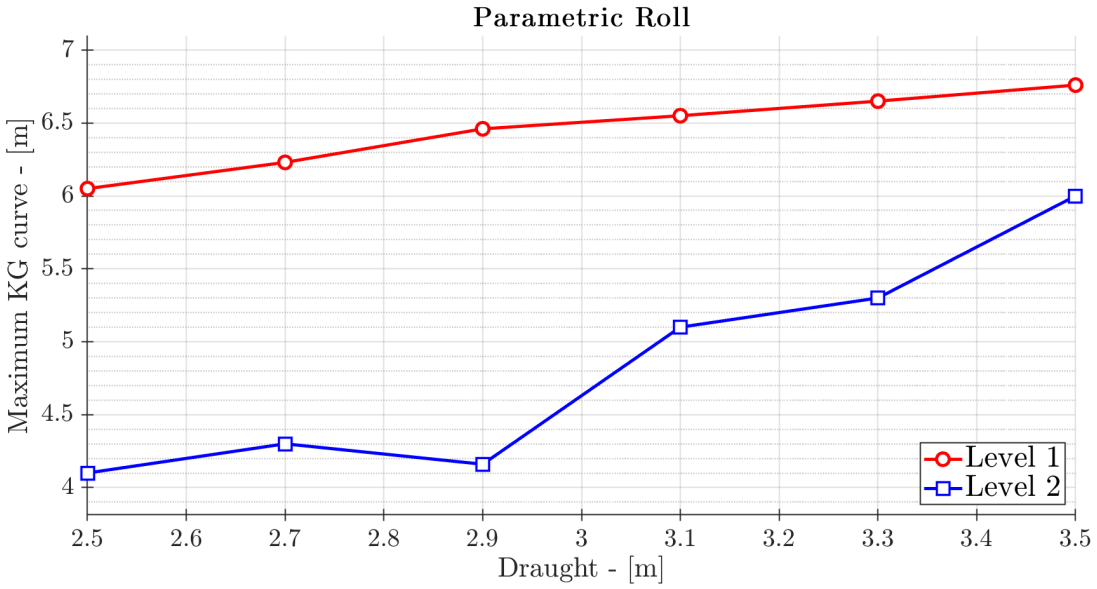

Figure 6.4: Megayacht unit - Comparison between first and second vulnerability levels for parametric roll

The outcomes of first vulnerability level are represented with red lines, while the blue curves refer to results of applications of the second vulnerability levels.

According to the philosophy of the SGISc, the first vulnerability level criterion should result more severe than the second one. In the KG limit curves representations, it means that the maximum KG curves of first levels should be located below the second level lines. The opposite should happen when the excessive acceleration phenomenon is considered, i.e. the first level minimum KG curve should stand above the second level one.

Unfortunately, it seems that in all the stability failures assessments there is a consistency problem between first and second criteria. In all cases, the first vulnerability limit curves stand above those evaluated for the second vulnerability criterion; vice-versa for the case of minimum KG curve for excessive acceleration phenomenon. The occurrence of these issues have been sometimes highlighted in literature and presented during IMO Sub-Committee meetings [26], [146], [147].

Furthermore, the outcomes show that for all the stability failures assessed, the trend of each level curve is the same, i.e. both first and second levels curves behave in a similar way in relation with the draught. This is not true, however, for the dead ship condition. This means that the criteria well describe the physics of the phenomena and that the issue of their relative position could be investigated in the definition of the vulnerability thresholds. As concerns the dead ship condition assessment, the different trend between curves, as a function of the draught, could be caused by the relevant differences at the basis of the methodologies adopted for the two levels.

In the case of second vulnerability assessment of parametric roll where dynamic issues are important, in particular for the second check, an alternative representation of results by matrix calculations could be more representative. The resonant nature of this phenomenon leads to identify isolated dangerous zone in

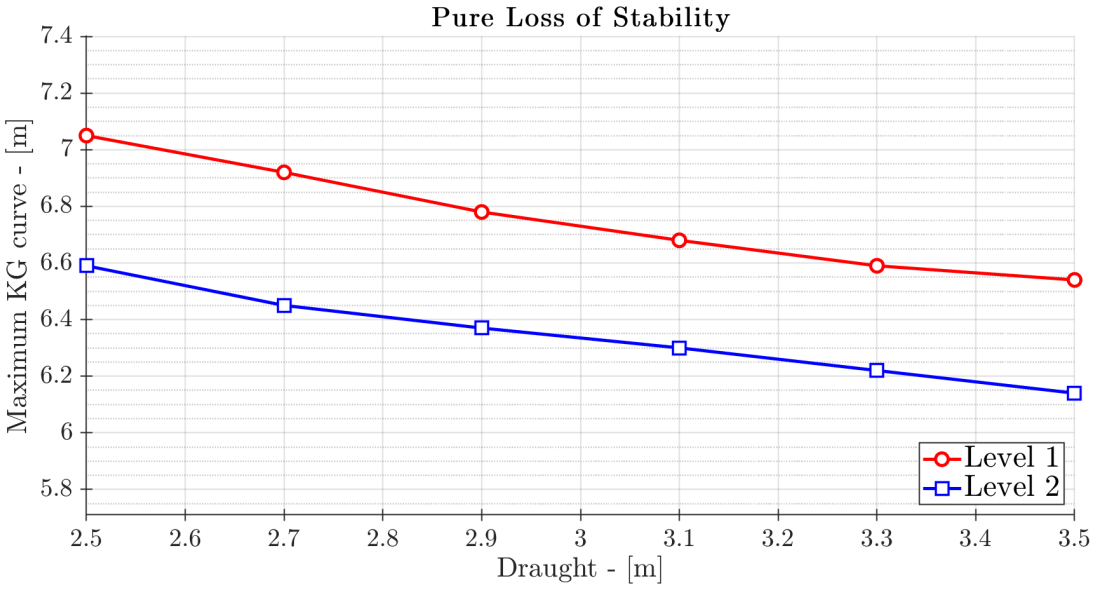

Figure 6.5: Megayacht unit - Comparison between first and second vulnerability levels for pure loss of stability

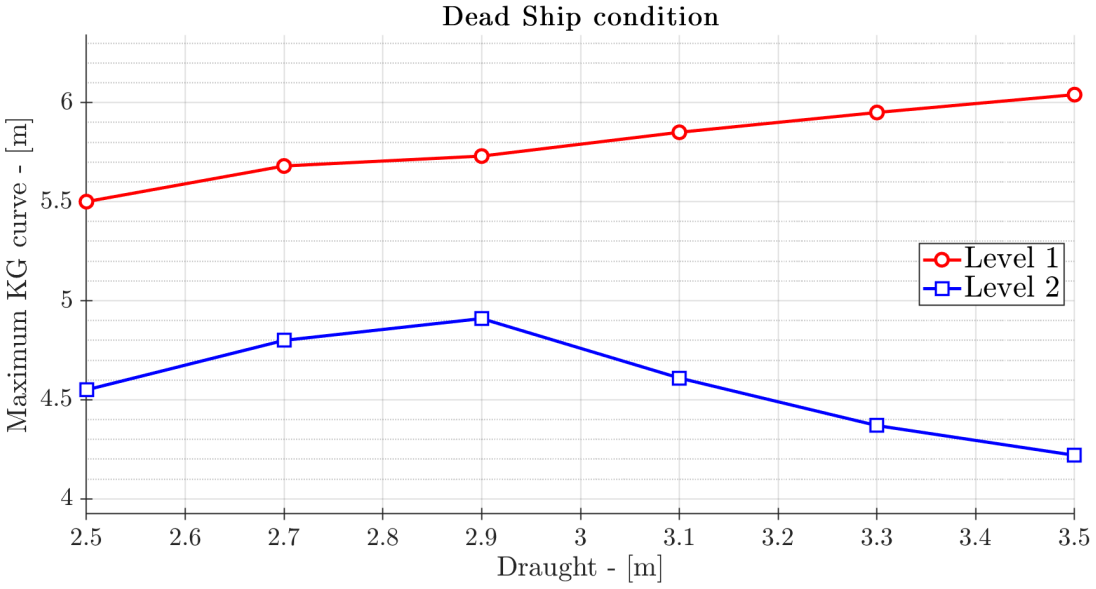

Figure 6.6: Megayacht unit - Comparison between first and second vulnerability levels for dead ship condition

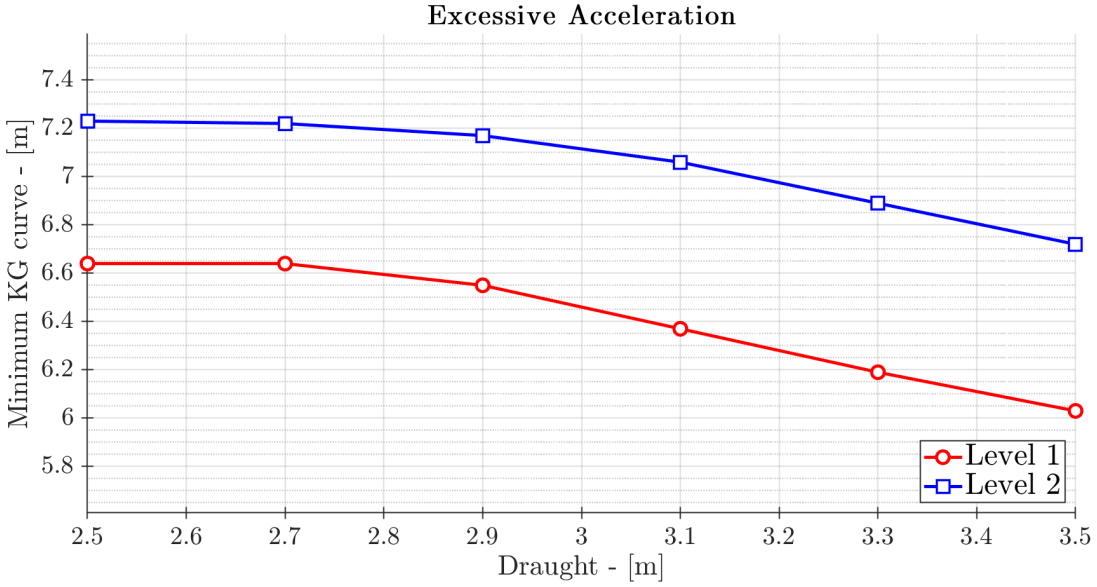

Figure 6.7: Megayacht unit - Comparison between first and second vulnerability levels for excessive acceleration

terms of KG and draughts, i.e. the KG value alone is not always representative of a vulnerable or not vulnerable ship to parametric roll. With the aid of Figure 6.8, it is possible to better understand this behaviour, e.g. considering the loading condition equal to $d = 3.30$ (m), it is possible to see that the vessel is considered vulnerable to parametric roll when KG is included between 4.90 (m) and 5.50 (m); above KG = 5.50 (m) the vessel turns out to be not vulnerable again until KG = 5.80 (m) (excepting for three isolated KG values); for KG values higher than 5.80 (m) the ship is always considered vulnerable.

K-index analysis

With reference to one of the aims of this thesis, the K-index has been calculated for each first vulnerability level, as formulated in Eq. 5.1. Thanks to this index, it has been possible to identify the relationship between each criterion and the main parameters available at the early stage ship design, as identified in Table 5.1. Part of this work has already been presented in [148].

To calculate the K-indexes, a set of modifications has been selected, five B_{wl}/d values have been identified and for each ratio, two different hulls have been modeled, for a total of ten different units. The block coefficient has been kept constant for all the configurations. Modified hulls may be collected in two main groups: in the first group, only the breadth has been modified for each unit (Table 6.4), while in the other one only the underwater depth has been changed (Table 6.5). The influence of breadth or draught modification on the stability failures has been evaluated. The influence of bilge keels area modification has been investigated as well. The bilge keel area effects on the outcomes can be simply evaluated by changing the input value within the formula of the criterion. It has been decided to change the bilge keel span from –10% to +40% of the design bilge keel span,

Matrix calculation for Parametric roll - Level 2 - check 2						
KG (m)	d = 2,5 (m)	d = 2,7 (m)	d = 2,9 (m)	d = 3,1 (m)	d = 3,3 (m)	d = 3,5 (m)
4,00	0,00E+00	0,00E+00	0,00E+00	7,69E-02	1,10E-01	5,07E-01
4,05	0,00E+00	0,00E+00	0,00E+00	1,10E-01	0,00E+00	5,12E-01
4,10	0,00E+00	0,00E+00	0,00E+00	1,24E-01	0,00E+00	5,24E-01
4,15	1,13E-01	0,00E+00	1,24E-01	1,24E-01	4,71E-03	4,24E-01
4,20	1,26E-01	0,00E+00	2,00E-01	3,66E-03	1,82E-02	5,60E-01
4,25	2,50E-01	0,00E+00	2,49E-01	9,36E-03	1,82E-02	4,50E-01
4,30	2,50E-01	0,00E+00	2,63E-01	1,82E-02	1,82E-02	4,50E-01
4,35	2,50E-01	9,19E-02	2,92E-01	1,82E-02	1,82E-02	5,11E-01
4,40	2,51E-01	1,33E-01	3,04E-01	1,82E-02	1,82E-02	3,74E-01
4,45	2,51E-01	1,33E-01	2,80E-01	1,82E-02	1,82E-02	4,98E-01
4,50	2,03E-01	2,58E-01	3,10E-01	1,82E-02	3,09E-02	4,98E-01
4,55	2,53E-01	2,67E-01	3,26E-01	1,73E-02	3,08E-02	4,98E-01
4,60	2,67E-01	2,67E-01	3,26E-01	1,82E-02	1,82E-02	5,17E-01
4,65	2,67E-01	2,67E-01	3,51E-01	1,82E-02	1,82E-02	6,41E-01
4,70	2,67E-01	2,01E-01	3,62E-01	1,82E-02	1,82E-02	6,41E-01
4,75	2,50E-01	2,53E-01	2,39E-01	1,82E-02	1,82E-02	5,48E-01
4,80	2,50E-01	2,67E-01	2,53E-01	1,82E-02	1,82E-02	4,28E-01
4,85	2,57E-01	2,67E-01	2,53E-01	1,82E-02	1,82E-02	4,29E-01
4,90	2,68E-01	2,58E-01	2,53E-01	1,82E-02	3,92E-01	5,53E-01
4,95	2,68E-01	2,58E-01	2,52E-01	1,25E-02	2,50E-01	5,53E-01
5,00	2,68E-01	1,34E-01	2,35E-01	0,00E+00	2,49E-01	5,53E-01
5,05	2,68E-01	1,43E-01	2,49E-01	0,00E+00	2,49E-01	5,53E-01
5,10	3,94E-01	1,43E-01	2,49E-01	0,00E+00	0,00E+00	4,29E-01
5,15	3,77E-01	4,10E-01	2,49E-01	1,25E-01	1,25E-01	4,29E-01
5,20	3,77E-01	4,10E-01	3,26E-01	0,00E+00	0,00E+00	5,44E-01
5,25	3,77E-01	4,10E-01	3,74E-01	1,25E-01	1,44E-02	5,52E-01
5,30	3,77E-01	2,67E-01	3,74E-01	1,29E-02	1,82E-02	5,53E-01
5,35	3,77E-01	4,00E-01	4,98E-01	1,42E-01	1,43E-01	5,53E-01
5,40	3,77E-01	4,00E-01	5,11E-01	1,82E-02	3,52E-02	4,29E-01
5,45	3,77E-01	4,31E-01	5,17E-01	1,82E-02	3,65E-02	4,29E-01
5,50	3,77E-01	2,67E-01	5,17E-01	1,43E-01	3,74E-02	5,53E-01
5,55	3,90E-01	5,25E-01	5,02E-01	1,43E-01	3,65E-02	5,71E-01
5,60	4,87E-01	5,14E-01	3,92E-01	3,08E-02	1,79E-01	5,71E-01
5,65	3,77E-01	5,34E-01	3,78E-01	3,65E-02	5,47E-02	5,71E-01
5,70	3,85E-01	5,34E-01	3,92E-01	3,65E-02	5,47E-02	5,71E-01
5,75	5,18E-01	5,34E-01	5,29E-01	4,54E-02	5,47E-02	5,71E-01
5,80	5,19E-01	5,43E-01	5,35E-01	5,47E-02	3,74E-02	5,71E-01
5,85	5,19E-01	5,43E-01	5,36E-01	1,79E-01	1,61E-01	5,71E-01
5,90	5,19E-01	5,43E-01	3,00E-01	3,74E-02	2,86E-01	5,71E-01
5,95	5,19E-01	5,43E-01	5,49E-01	1,61E-01	3,03E-01	5,71E-01
6,00	5,19E-01	4,19E-01	5,35E-01	3,65E-02	3,04E-01	4,47E-01
6,05	5,19E-01	4,19E-01	4,10E-01	3,03E-01	3,04E-01	4,47E-01
6,10	5,12E-01	5,57E-01	4,10E-01	3,04E-01	4,46E-01	4,37E-01
6,15	3,77E-01	5,56E-01	5,35E-01	4,45E-01	4,47E-01	4,29E-01
6,20	5,10E-01	5,53E-01	5,53E-01	4,47E-01	4,47E-01	4,29E-01
6,25	5,14E-01	5,53E-01	4,45E-01	4,47E-01	4,47E-01	4,29E-01
6,30	5,27E-01	4,19E-01	4,47E-01	4,47E-01	4,47E-01	4,29E-01
6,35	4,02E-01	4,24E-01	4,47E-01	5,71E-01	5,71E-01	4,29E-01
6,40	4,11E-01	4,29E-01	4,47E-01	4,29E-01	5,71E-01	4,29E-01
6,45	4,20E-01	4,32E-01	3,17E-01	5,71E-01	5,71E-01	4,29E-01
6,50	4,29E-01	4,32E-01	4,37E-01	5,71E-01	4,47E-01	4,29E-01
6,55	3,04E-01	4,38E-01	4,47E-01	4,47E-01	4,47E-01	6,78E-01
6,60	3,20E-01	4,38E-01	5,71E-01	4,47E-01	4,47E-01	9,12E-01
6,65	4,46E-01	4,29E-01	4,47E-01	4,47E-01	4,47E-01	9,96E-01
6,70	4,46E-01	4,38E-01	4,47E-01	4,47E-01	4,46E-01	9,99E-01
6,75	4,37E-01	4,38E-01	4,47E-01	4,47E-01	4,29E-01	0,00E+00
6,80	4,46E-01	4,38E-01	4,47E-01	4,47E-01	4,29E-01	0,00E+00
6,85	4,46E-01	4,38E-01	4,47E-01	4,46E-01	4,29E-01	0,00E+00
6,90	4,46E-01	4,38E-01	4,47E-01	4,29E-01	4,29E-01	0,00E+00
6,95	4,46E-01	4,38E-01	4,47E-01	4,29E-01	4,29E-01	0,00E+00
7,00	4,46E-01	4,38E-01	4,47E-01	4,29E-01	4,29E-01	0,00E+00
7,05	0,00E+00	0,00E+00	0,00E+00	0,00E+00	4,29E-01	0,00E+00
7,10	0,00E+00	0,00E+00	0,00E+00	0,00E+00	4,29E-01	0,00E+00
7,15	0,00E+00	0,00E+00	0,00E+00	0,00E+00	4,29E-01	0,00E+00
7,20	0,00E+00	0,00E+00	0,00E+00	0,00E+00	4,29E-01	0,00E+00

Figure 6.8: Results of parametric roll second level - second check by matrix calculations

Table 6.4: Main dimensions of the new hulls keeping constant the draught

Hull family * - Main dimensions						
B_{wl}/d	(-)	4.00	3.85	3.75	3.60	3.50
B_{wl}	(m)	13.20	12.71	12.38	11.88	11.55
d	(m)	3.30	3.30	3.30	3.30	3.30
D	(m)	7.50	7.50	7.50	7.50	7.50
T_ϕ	(sec)	7.74	8.56	9.28	10.79	12.32

Table 6.5: Main dimensions of the new hulls keeping constant the draught

Hull family # - Main dimensions						
B_{wl}/d	(-)	4.00	3.85	3.75	3.60	3.50
B_{wl}	(m)	12.97	12.97	12.97	12.97	12.97
d	(m)	3.24	3.37	3.46	3.60	3.71
D	(m)	7.44	7.57	7.66	7.80	7.91
T_ϕ	(sec)	7.99	8.21	8.36	8.58	8.76

with step of 10%.

As concerns the other main parameters identified in Table 5.1, the following considerations are pointed out:

- For the first level of each stability failure, service speed is a shared parameter only between Pure Loss of Stability and Surf-Riding. Due to the binary nature of its influence on the criteria, sped has been disregarded in the sensitivity assessment;
- The effects of the vertical position of centre of gravity on SGISc is well evident in literature and all along this Ph.D. thesis. Nevertheless, the sensitivity assessment is carried out with constant KG in order to gain insight about geometry effect;
- As shown in [136], the effects of a modification on length does not affect significantly the final outcomes of criteria, also in the case when wave profile is important like pure loss of stability and parametric roll for which the relation between the ship and the wave length, together with the wave height, is deemed to be relevant.

In order to compare the results obtained by changing each parameter (i.e. breadth, draught and bilge keel area) in the same graphic, on the horizontal axis the values of the assessed parameter divided by the corresponding design value have been reported. The square red markers represent the draught influence, the blue triangles stand for the sensitivity to breadth change while the pink diamonds show the effect of bilge keel area variation. To better represent the points and the calculated regression lines, the x-axis has been limited from 0.85 to 1.15.As a consequence, some sample points representative of bilge keel area parameter have been cut off from the graphs. In addition, to show the trend within each set

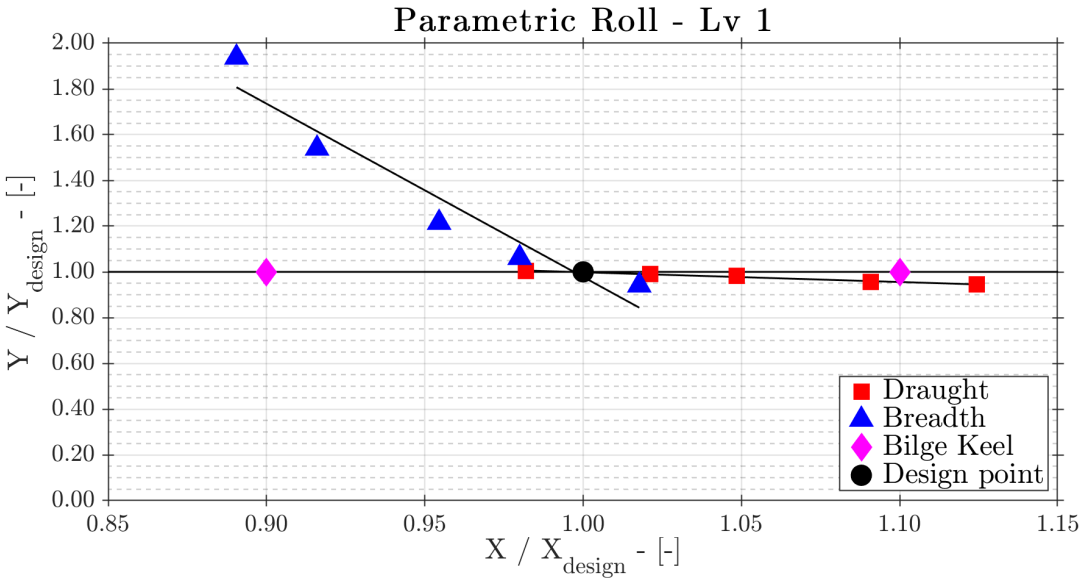

Figure 6.9: Influence of main parameters on parametric roll

of results, continuous lines are represented in the graphs. They are obtained by means of linear regression analysis. Criteria outcomes for each stability failures and hulls family are shown from Figure 6.9 to Figure 6.12. On the vertical axis the criterion values divided by the criterion value relevant to the design condition are represented.

The outcomes are summarized in Table 6.6. As expected, it is evident how the most important parameter is the breadth: in all cases the criterion values present the regression line with the highest slope, this is also confirmed by its K-index value which is up to seven time more than the other one. The influence of breadth on the final criterion value is less pronounced only for excessive acceleration phenomenon.

As regards the variations of draught, pure loss of stability phenomenon is the most influenced by this parameter. A particular explanation is needed when the bilge keel area variation is considered: results show a weak influence on the excessive acceleration failure, while the other failures appear not to be linked with this parameter. It is necessary to highlight that, as far as parametric roll and dead ship condition failure modes, the bilge keel area affects only the standards. The criterion for pure loss of stability assessment does not include this parameter at all.

Table 6.6: K-index values for each stability failures and assessed parameters

Stability failure	d	B_{wl}	A_{bk}
Pure loss of stability	-1.259	+7.672	0.000
Parametric roll	-0.427	-7.749	0.000
Dead ship condition	-0.441	+7.509	0.000
Excessive acceleration	-0.869	+2.921	-0.167

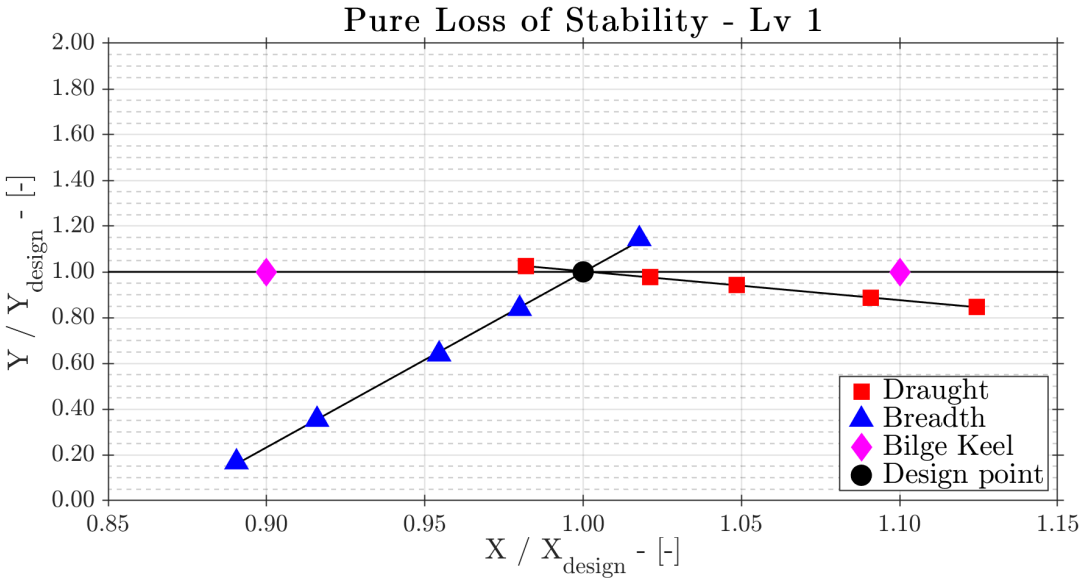

Figure 6.10: Influence of main parameters on pure loss of stability

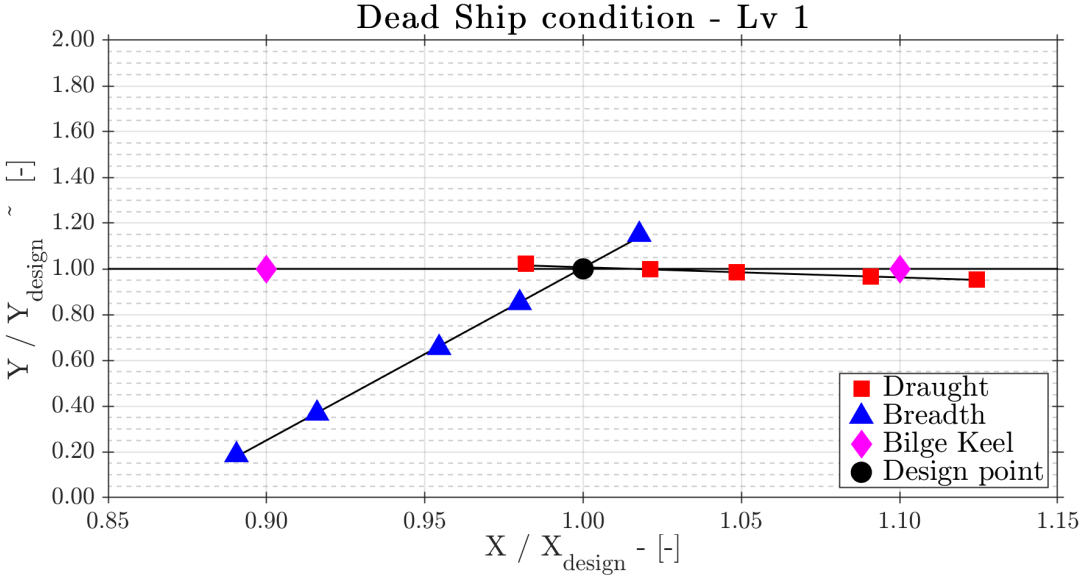

Figure 6.11: Influence of main parameters on dead ship condition

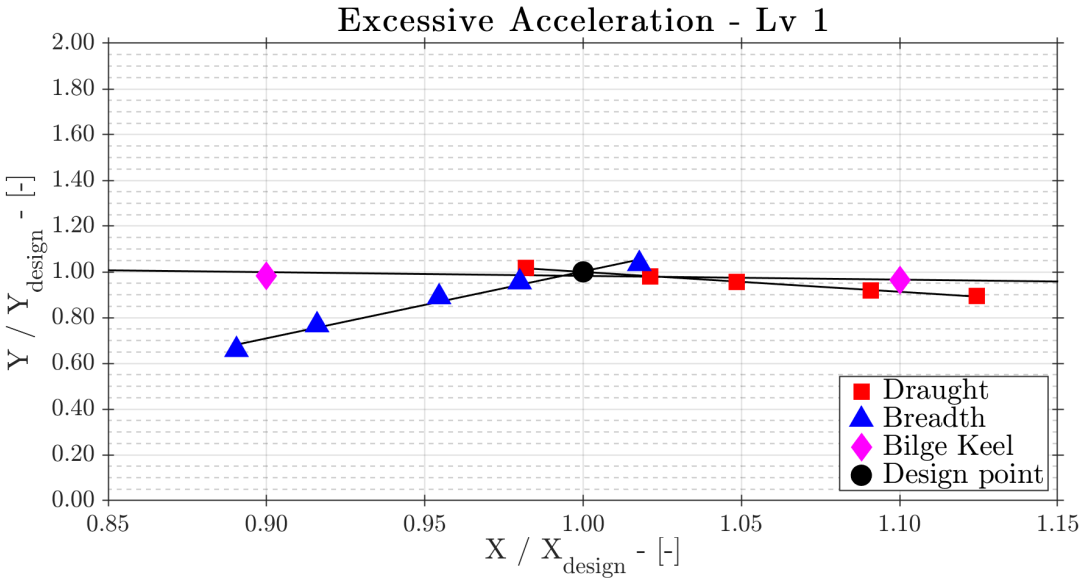

Figure 6.12: Influence of main parameters on excessive acceleration

Focusing on the trend between main parameters and criteria values, it is possible to deduce the following: an increment of hull draught leads to a decrement of criteria outcomes for all the failure modes considered; this decrement is also confirmed for bilge keel area variations in the case of the excessive acceleration phenomenon. As far as the breadth variation is concerned, the results point out that a direct relationship exists for all the failures excepting parametric roll. It is worthwhile to remind that, to judge a ship vulnerable or not to a stability failure, the criterion should be compared with the standard. For parametric roll and excessive acceleration, a ship is considered to be not vulnerable if the criterion value is lower than the standard; for pure loss of stability and dead ship condition, a ship is considered not to be vulnerable if the criterion value is higher than the standard.

6.2 Application to another relevant ship typology: Ro-Ro pax ferry

Another interesting case is the vulnerability assessment of a Ro-Ro pax ferry. Usually this typology of ships has a low draught, slender immersed volume, high cruise speeds and a huge windage area: these characteristics may lead to be vulnerable in terms of SGISc, in particular for parametric roll or pure loss of stability and dead ship condition. The main particulars of the Ro-Ro pax ferry are given in Table 6.7, a longitudinal view of the vessel is given in Figure 6.13.

Also for this unit, both the first and the second vulnerability levels criteria have been applied except for the surf-riding stability failure. In the following paragraphs the results are shown, the graphs keep the same representation for both levels, i.e. on the horizontal axis the draughts considered are reported while on the y-axis the maximum or minimum KG values are represented. For the

Table 6.7: Ro-Ro pax ferry main dimensions

Main dimensions			
Length overall	L_{OA}	211.2	(m);
Length between perpendicular	L_{PP}	186.2	(m);
Maximum breadth	B_{max}	30.40	(m);
Design draught	d	7.82	(m);
Depth	D	21.60	(m);
Displacement	Δ	28234	(t);
Service speed	V_S	22.0	(kt);
Froude number	Fn	0.265	(-);
Block coefficient	C_B	0.650	(-);
Midship section coefficient	C_m	0.995	(-);
Bilge keel length	L_{BK}	66.0	(m);
Bilge keel span	b_{BK}	0.30	(m);
Design vertical centre of gravity	KG	13.43	(m);
Design metacentric height	GM_{design}	1.43	(m).

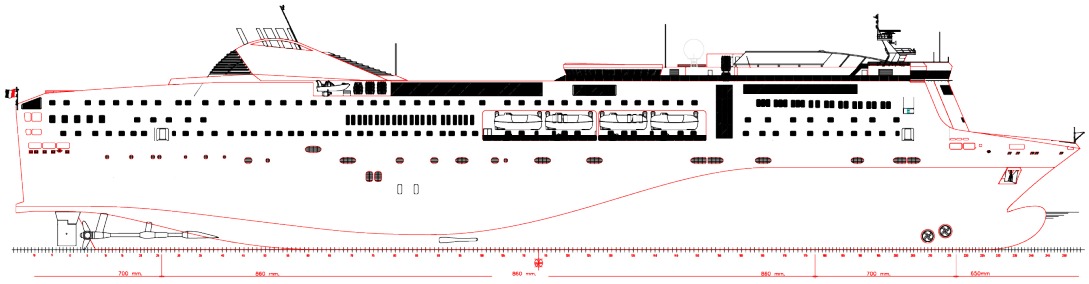

Figure 6.13: Longitudinal view of the Ro-Ro pax ferry

Table 6.8: Supplementary dimensions required to evaluate dead ship condition and excessive acceleration criteria

Supplementary information			
Design lateral exposed area	A_{lat}	5400	(m^2)
Design quote of the exposed area center	Z_{lat}	17.56	(m)
Longitudinal position of the assessed point	X_P	169.8	(m)
Vertical position of the assessed point	Z_P	34.0	(m)

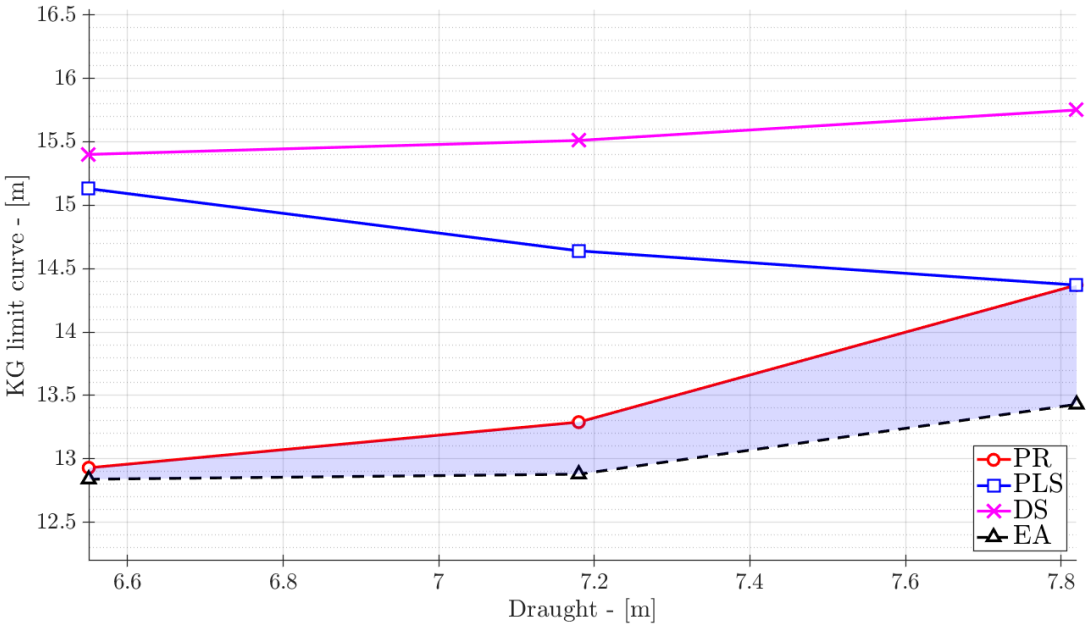

Figure 6.14: Ro-Ro pax ferry - First vulnerability levels

excessive acceleration analysis the wheel house coordinates have been considered as the critical point; these coordinates and the lateral exposed area corresponding to the design loading condition are reported in Table 6.8.

First vulnerability level analysis

In Figure 6.14, the results of first vulnerability level application are shown. For this typology of vessel, the *design space* exists and it is highlighted in light blue. At the design draught, equal to $d = 7.82$ (m), the KG may be set in a range of about 1 (m), from 13.5 (m) to 14.5 (m). At low draughts the area of *design space* dramatically reduces, becoming nearly zero around the lowest draught.

Considering the maximum KG curves, it appears that the parametric roll criterion is the most severe, in particular for low draughts. This behaviour was expected, since the Ro-Ro ferries well fit the geometrical issues that characterize parametric roll issue, as explained in § 3.2.1.

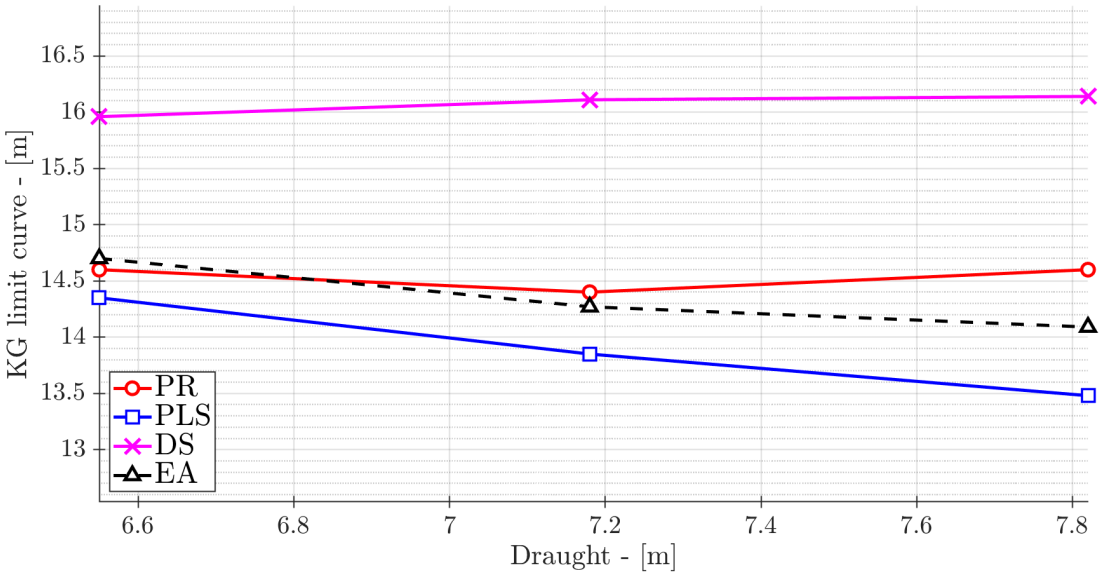

Figure 6.15: Ro-Ro pax ferry - Second vulnerability levels

Second vulnerability level analysis

According to the outcomes of second vulnerability assessments, it appears evident how in this case there is no *design space*, in contrast with the results of first vulnerability levels. The issues can be find within the inconsistency between first and second levels. The major difference between first and second level analysis occurs in the calculation of the excessive acceleration failure: in fact the second level curve is located more than 1.5 (m) above the first level line, in contrast with what expected (Figure 6.19). The same happens for pure loss of stability, the maximum KG curve of second level assessment is shifted below the corresponding first level curve as well (Figure 6.17). In this case, the consistent relation between levels for parametric roll and dead ship condition are ascertained (Figure 6.16 and Figure 6.19).

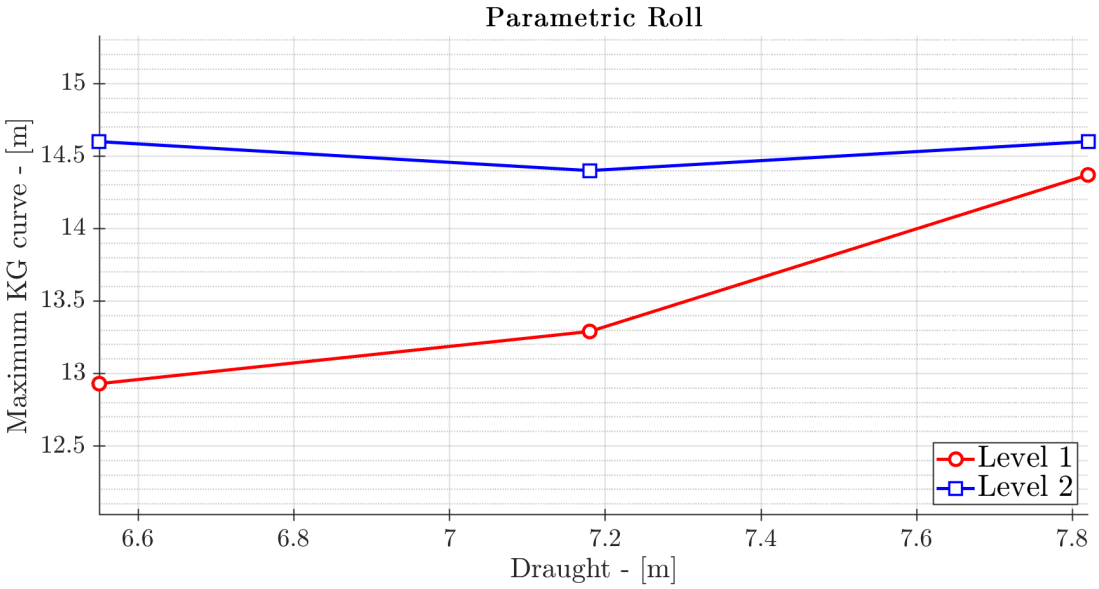

Figure 6.16: Ro-Ro pax ferry - Comparison between first and second vulnerability levels for parametric roll

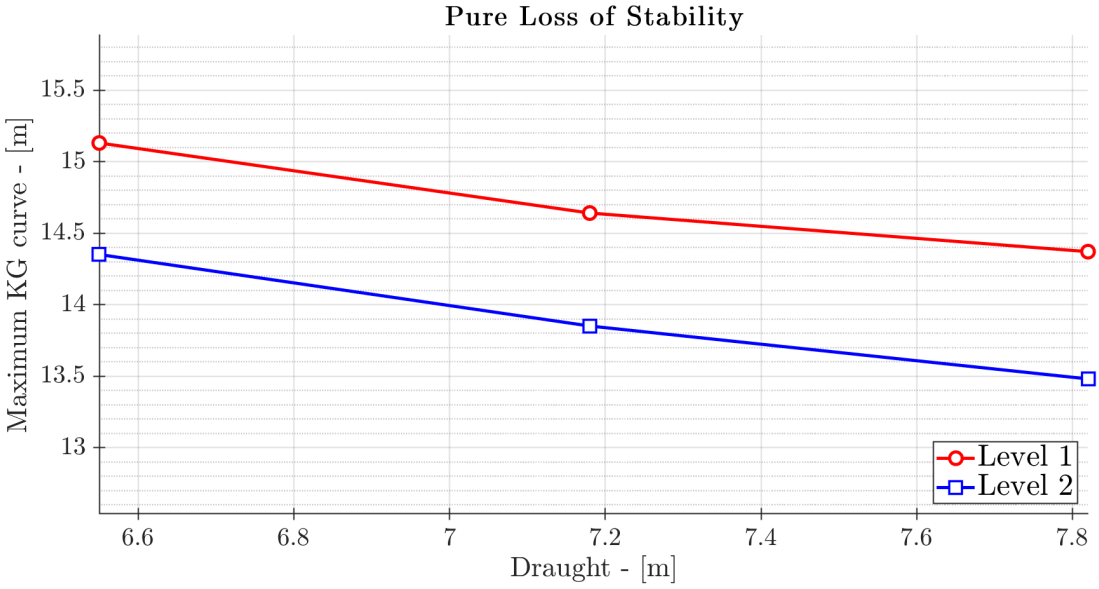

Figure 6.17: Ro-Ro pax ferry - Comparison between first and second vulnerability levels for pure loss of stability

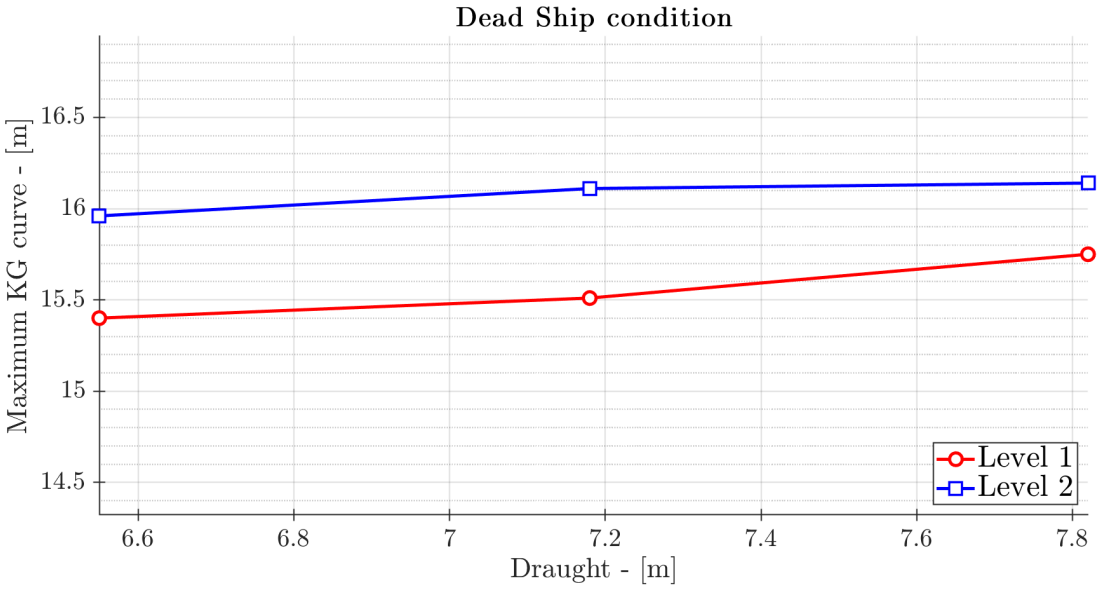

Figure 6.18: Ro-Ro pax ferry - Comparison between first and second vulnerability levels for dead ship condition

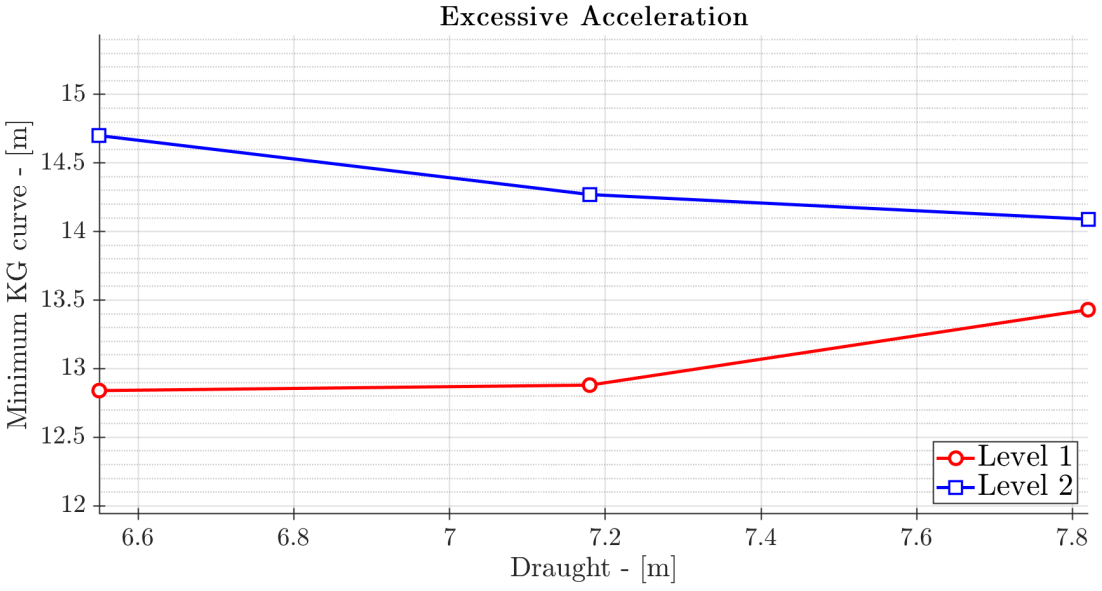

Figure 6.19: Ro-Ro pax ferry - Comparison between first and second vulnerability levels for excessive acceleration

6.3 An overview about naval ships

The importance to assess the stability performance of navy ships in extreme seas is well known, together with the implied challenges for large amplitude motions reliable prediction and identification of suitable performance–based criteria [149]. Naval ships in principles share with merchant ships the same general issues relative to stability failures but the safety rules framework to comply with is different, since Navies are not under IMO regulations. Another important difference is that naval vessels, due to their operational profile, often cannot avoid dangerous weather conditions when performing their missions, while a commercial vessel often can choose an alternative route. The attention to ship stability in waves is in parallel with an increasing interest in the development of risk based stability criteria. The trend is to frame the discussion about the ship performance within a risk assessment dealing with the risk of capsizing [150], [151]. In 2003, North Atlantic Treaty Organization (NATO) initiated the process toward a Goal Based Standard (GBS) for naval vessels that could guide navies and classification societies in the development of rules for naval vessels. The intent was to identify regulations for naval vessels that paralleled the IMO regulations for commercial vessels [152]. The Naval Ship code (NSc) does not provide specific dynamic-stability or capsize criteria, nor specify any procedures by which a vessel can be defined to be in compliance with the Code. A brief overview about the NSc is going to be developed in the following. The present navy stability standard are valuable reference to design safe ships. At the same time, it is recognized that they can be improved to truly reflect the dynamic behavior of ships in extreme conditions [153]. The hydrostatics-based standards have attempted to incorporate some considerations of dynamic issues through the so called beam winds combined with rolling criterion i.e. the effect of beam wind and seas on ship behavior. A way to overcome the limitations of the present standard seems to be the calculation of the probability of capsize as directly related to the probability of exceeding a critical roll angle. The methodology, most of the times, is developed using time domain simulations combined with probabilistic input data for the wave conditions and heading and speed [154]. Nevertheless, the vulnerability criteria developed by IMO, in particular the second level vulnerability criteria, can be reasonable tools for example in an early design stage [155]. As better explained in § 2.1.1, within the multi-layered framework of the SGISc the third and last level of assessment is in line with the probability of capsizing prediction coupled with a suitable ship motion computational tool able to capture all the non-linear phenomena necessary for capsizing prediction. The assessment tools developed as second level vulnerability criteria have been developed in order to be a good compromise between accuracy of results and computational engagement.

In this section, the second vulnerability criteria are applied to naval ships in order to gain insight for this category and to compare results with the present intact stability standards for naval ships. A part of this work has already been presented in [156]. A wider comparison is made between such standards and the SGISc, thanks to the application of all the first level vulnerability criteria for the whole set of stability failure modes, considering three different naval ship

typologies i.e. a helicopter carrier, a destroyer and a Patrol Vessel. Similar analysis has already been carried out in the latest years with interesting results by Grinnaert *et. al.* in [66] and by Tomaszek & Bassler in [157].

6.3.1 Navy ships intact stability criteria

In this section an analysis of different intact stability criteria has been carried out. United States Navy [158], United Kingdom Ministry of Defense (MOD) [159], France MOD [160] and Italy MOD [161] rule texts have been considered and a very similar structure in terms of criteria and standard values have been identified as expected. In fact, at a different extent, all of them are referable to approach and criteria developed by Sarching & Goldberg in [103]. Indeed it is possible to recognize, as a general scheme, the attention paid to the righting arm both alone and under the effect of different inclining moments i.e. turning at speed, the crowding of people on one side and the lifting of heavy list on one side. The influence of ice is taken into consideration as well. As far as sea-state conditions, the assessment of effect due to beam winds together with rolling (fixed angle of 25° for all the investigated rule texts) is requested.

The wind speed is actually differentiated, varying from 40 (kn) to 100 (kn), in relation with the rule text and the naval ship typology. In order to possibly improve or better validate the criteria, some investigations have been found in literature about the wind modeling in the beam winds combined with ship rolling with the support also of experimental test [162], [163]. As a general remark, the set of rules to be applied for naval ships is unquestionably more severe if compared with the IMO Intact Stability Code and this is coherent with the more severe operational profile warships have to fulfill with. For the same reason, usually a thorough investigation of the seakeeping performances are carried out for this ship category, both on short term and/or long term perspective, with attention to specific issues like for example accelerations, slamming events or to more comprehensive parameters like operational indexes. As already mentioned the stability assessment in a seaway, at the more exhaustive extent, in principle is a seakeeping problem with the need to capture all the necessary dynamic phenomena up to capsizing, often characterized by challenging non-linearities. This process, beside to be expensive and time consuming, requires the appropriate numerical tool for the ship dynamic behavior prediction. In line with a more thorough assessment of ship performance in waves the application of SGISc are assumed to be interesting also for navy ships, as an intermediate phase between the present intact stability criteria and a challenging seakeeping prediction at large angles.

The Naval Ship code

The concept of the formal risk assessment or design for safety approach is already implemented by IMO within its rulemaking activity. NATO has followed a similar attitude in adopting GBS as a basis for the NSc. GBSs are powerful tools able to establish a framework for integrating stability into a risk based design process [164]. Within a goal based standards, a goal or *safety objective* is defined through

a series of tiers or a framework for verification through design construction and operation. In NSc, the goal based standards approach is structured on five tiers as follows:

1. Aim (Philosophies and Principles);
2. Goal;
3. Functional Areas;
4. Performance Requirements;
5. Verification Methods;
6. Justification.

Performance requirements are defined in relation with ship operational profile and verified using appropriate criteria. As already mentioned the basic principle of a goal based approach is that the goals should represent the top tiers of the framework, against which ship is verified both at design and construction stages, and during ship operation. This approach has several advantages over more traditional prescriptive standards even though the NSc can become prescriptive if appropriate. Alternatively, it can remain at a high level applying other standards and relevant assurance processes. In this way GBS approach permits innovation by allowing alternative arrangements to be justified as complying with the higher level requirements. The NSc is recalled as significant in this paper because it can represent the background framework where application of SGISc to naval ships can find a possible rational collocation. Moreover in the introduction chapter of the NSc is stated that the overall aim of the Code is to provide a standard for naval surface ship safety based on and benchmarked against IMO conventions and resolutions. In this sense a continuous attention to IMO safety rules and their development is considered an appropriate attitude. In chapter *III - Buoyancy, Stability and Controllability* of [152] the main goals are identified:

> *The buoyancy, freeboard, main sub-division compartment and stability characteristics of the ship shall be designed, constructed and maintained to:*
>
> - *Provide an adequate reserve of buoyancy in all foreseeable intact and damaged conditions, in the environment for which the ship is to operate;*
> - *Provide adequate stability to avoid capsizing in all foreseeable intact and damaged conditions, in the environment for which the ship is to operate, under the precepts of good seamanship;*
> - *Permit embarked persons to carry out their duties as safely as reasonably practical;*
> - *Protect the embarked persons and essential safety functions in the event of foreseeable accidents and emergencies at least until the persons have reached a place of safety or the threat has receded including preventing the malfunction of the life-saving systems and equipment.*

Verification that the ship complies with this high level aims shall be responsability of the Naval Administration.

Table 6.9: Main dimensions of the naval vessels

Destroyer			
Length between perpendicular	L_{PP}	142.0	(m)
Maximum breadth	B_{max}	19.1	(m)
Draught	d	6.15	(m)
Displacement	Δ	8634	(t)
Froude number	Fn	0.397	(-)
Lateral exposed area	A_{lat}	1982.0	(m^2)
Bridge coordinates	(X; Z)	(95.1; 14.45)	(m)

Heli-Carrier			
Length between perpendicular	L_{PP}	172.0	(m)
Maximum breadth	B_{max}	24.0	(m)
Draught	d	6.50	(m)
Displacement	Δ	11768	(t)
Froude number	Fn	0.338	(-)
Lateral exposed area	A_{lat}	2607	(m^2)
Bridge coordinates	(X; Z)	(125.6; 15.17)	(m)

Offshore Patrol Vessel			
Length between perpendicular	L_{PP}	80.6	(m)
Maximum breadth	B_{max}	9.60	(m)
Draught	d	3.37	(m)
Displacement	Δ	1250	(t)
Froude number	Fn	0.457	(-)
Lateral exposed area	A_{lat}	506.5	(m^2)
Bridge coordinates	(X; Z)	(44.3; 7.47)	(m)

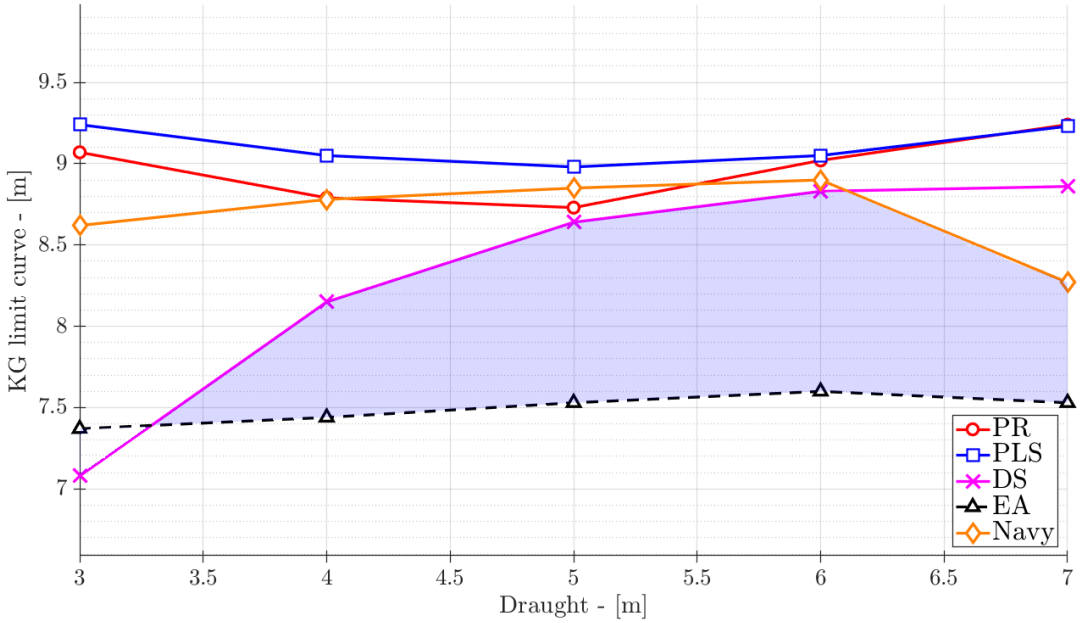

Figure 6.20: Destroyer - First vulnerability levels

6.3.2 Main data of the Naval vessels

In order to obtain an immediate flavor on the real feasibility about consistent integration between current navy intact stability rules and IMO new generation criteria, some investigations are carried out. The selected ships are a Destroyer unit derived from the DTMB 5415 model , a Helicopter carrier and a Patrol Vessel. In Table 6.9 their main data and dimensions are given. Due to the importance of the areas exposed to wind, special attention is given to the shape and dimensions of ship's higher part and superstructures that for each ship are appropriately designed on the basis of similar existing units. Moreover, the longitudinal profile it has been useful also to determine the longitudinal and vertical location of the bridge since, due to its importance, the wheelhouse has been selected as the reference point to assess in the excessive acceleration criterion.

6.3.3 Results

First vulnerability levels and Intact stability navy code

At first, the three ships are investigated calculating the maximum KG curves derived from the compliance with the SGISc first vulnerability level criteria. All the stability failure modes taken into account by IMO to frame the ship stability behavior in a seaway are considered, except for the surf riding condition. Results, for each vessel described above, are shown from Figure 6.20 to Figure 6.22. In the same figures, it is possible to put in evidence the maximum KG curves (indicated with *Navy*) that derive from the compliance with a set of criteria, representative of the present intact stability requirements for navy ships. In order to better understand the results, it is worthwhile to remind that for the case of excessive

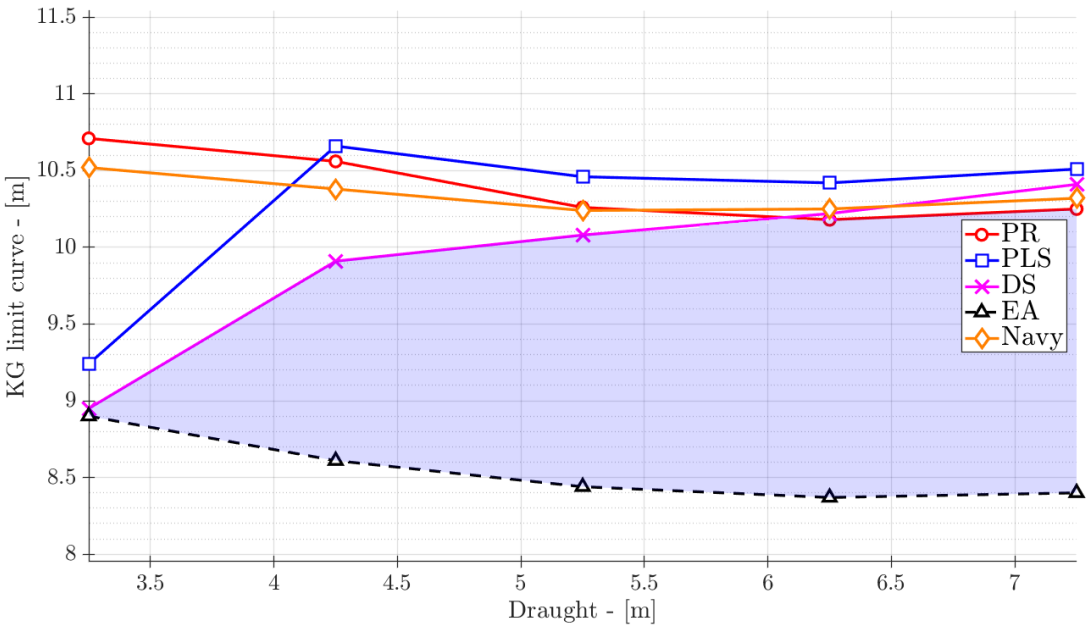

Figure 6.21: Heli-Carrier - First vulnerability levels

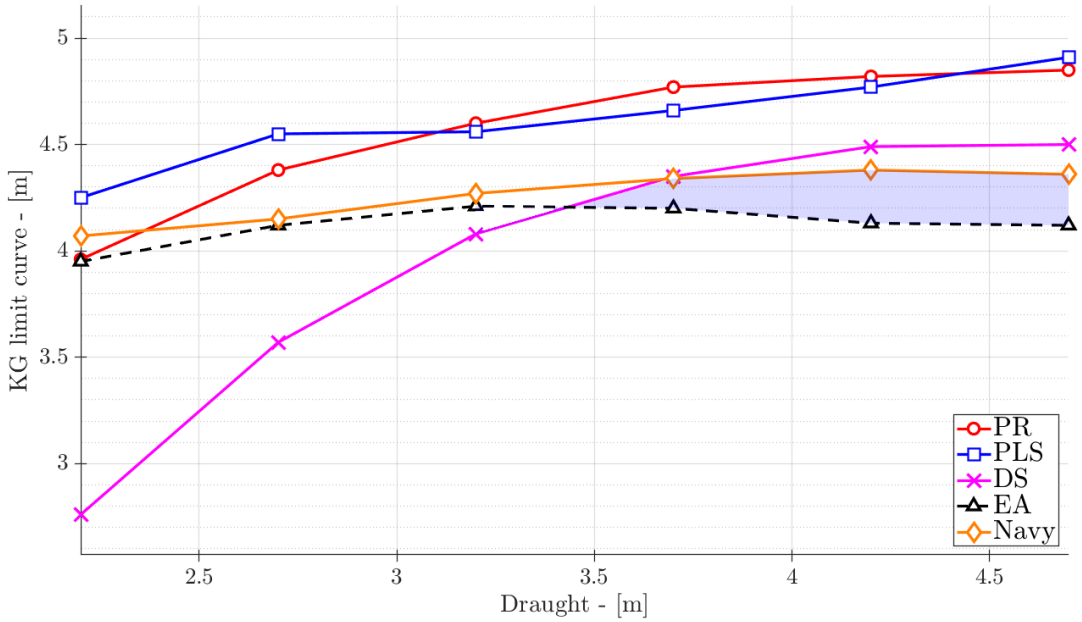

Figure 6.22: Offshore Patrol Vessel - First vulnerability levels

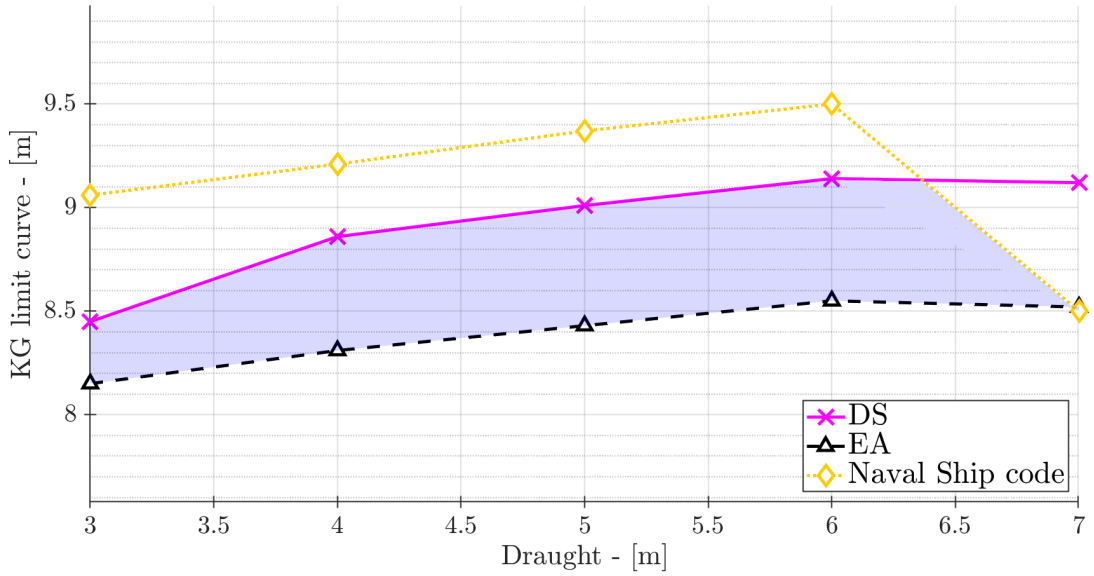

Figure 6.23: Destroyer - Second vulnerability levels

accelerations the curve should be named as the curve of the minimum KG i.e. it is required that the KG is higher than that curve. It is immediately evident how the *design space* (highlighted with a light blue area) is limited for all the vessels. Moreover, it is interesting to point out that the present intact stability standard for navy ships are well positioned in between the other curves, denoting a comparable and equivalent level of safety.

Second vulnerability level and Naval Ship code

As already mentioned, the Naval Ship Code is based on goal based approach i.e. a performance assessment perspective. In this sense it is not so easy to find a suitable methodology to carry out the assessment. The second vulnerability level criteria developed by IMO can be considered as a possible option, worth to be investigated. The second level criteria are defined to be a wide-ranging tool able to better frame the ship behavior and, even though not expressly meant, they are in principle suitable to be applied also to navy ship category. Thus, the second vulnerability levels for dead ship condition and excessive acceleration have been applied in this investigation. The beam winds combined with ship rolling criterion for a wind speed of 100 (kn), as described in the NSc, and an intact stability representative set of navy rules are applied as well. Finally, the maximum and minimum KG curves obtained by the application of SGISc and the NSc criterion are compared from Figure 6.23 to Figure 6.25.

It appears that maximum KG curve derived from second vulnerability level for dead ship condition criterion is significantly more severe than the NSc one. The results are not in line with what expected: the beam winds combined with ship rolling criterion, applied with 100 kn wind speed, was expected to be in principle more severe than the second vulnerability level approach for the dead ship condition. This one in fact is more extensive in terms of sea state condition

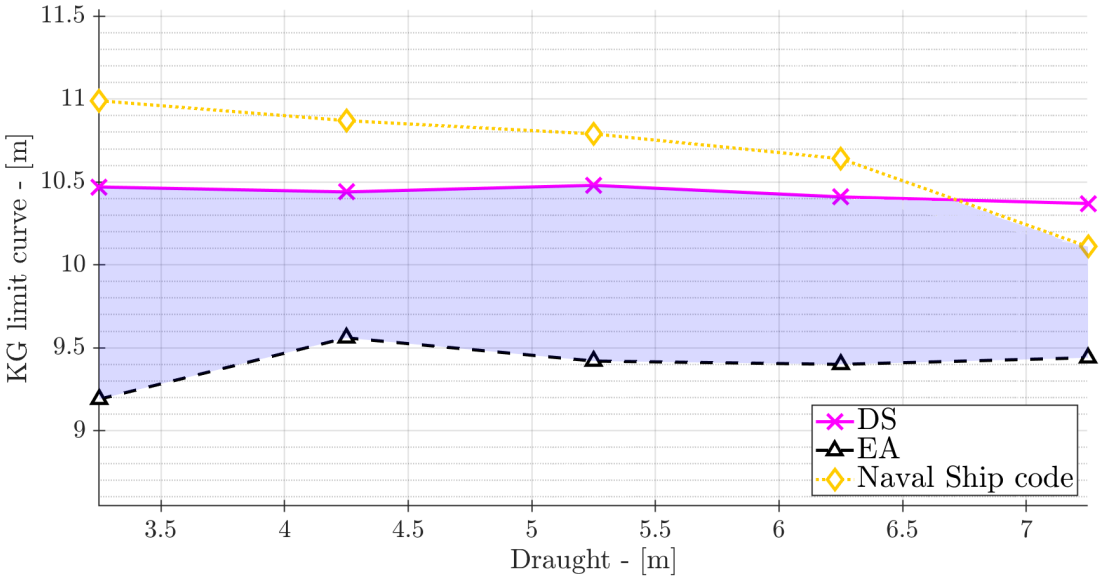

Figure 6.24: Heli-Carrier - Second vulnerability levels

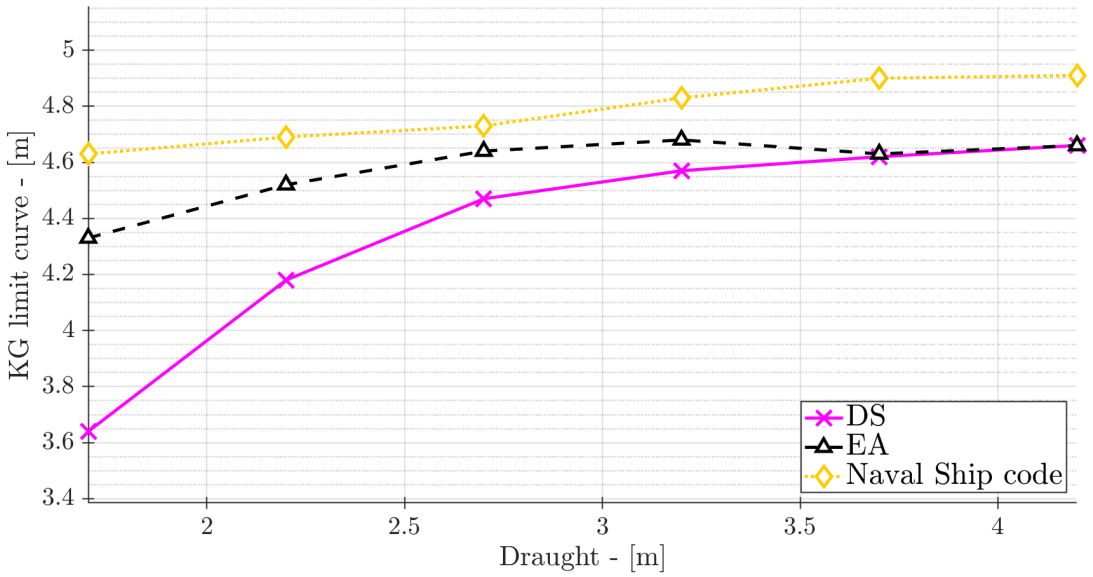

Figure 6.25: Offshore Patrol Vessel - Second vulnerability levels

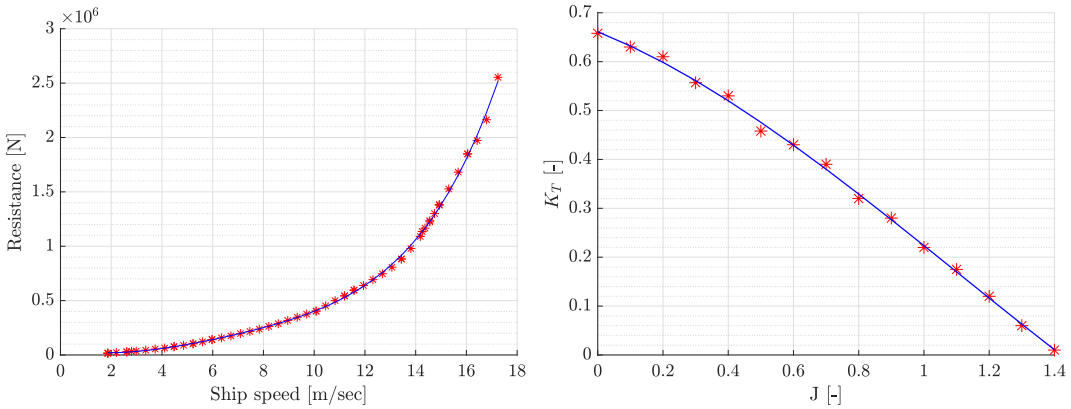

(a) Hull resistance (b) Propeller characteristic curve

Figure 6.26: Supplementary data required to evaluate surf-riding criterion

investigated, including environment conditions that are less severe.

Considering the minimum KG curve for excessive acceleration, sufficient *design space* area exists for both the destroyer and the heli-carrier. On the contrary, due to the high position of minimum KG curve for the OPV, it appears that there are no KG able to satisfy at the same time the dead ship condition, the naval ship code and the excessive stability criteria.

Application of surf-riding criterion

Finally, to conclude the comprehensive application of SGISc, the surf-riding criteria have been applied to the Destroyer vessel. The design loading condition has been considered, as defined in Table 6.9. Since its very simple structure, it is easy to determine that the ship is considered vulnerable according to the first level of vulnerability. In fact, the ship length is shorter than 200 (m) and the Froude number is higher than 0.300 (-), as defined in § 3.3.3. As a result, the second vulnerability level shall be applied.

In order to perform the second vulnerability assessment, further information about the ship are required, i.e. the hull resistance R and the propeller characteristic curve K_T (Figure 6.26). The results have been already presenter within the MSc thesis at UNIGE [165].

According to the second vulnerability level, the Destroyer unit has been considered vulnerable to the surf-riding phenomenon, since the criterion C evaluated at the service Froude number is higher than the standard R_{SR}. In order to further investigate the phenomenon, a sensitivity analysis on ship speed has been carried out. The criterion has been calculated changing the speed in a range from 21 (m/sec) to 26 (m/sec). The outcomes are given in Figure 6.27

On the horizontal axis, the Froude number is represented; while the final criterion is reported on the vertical axis in logarithmic scale. The horizontal dashed line represents the value of the standard R_{SR}. The outcomes point out that a slightly variation of the service speed leads to a huge variation of the final criterion: in fact, the slope of the curve is very pronounced.

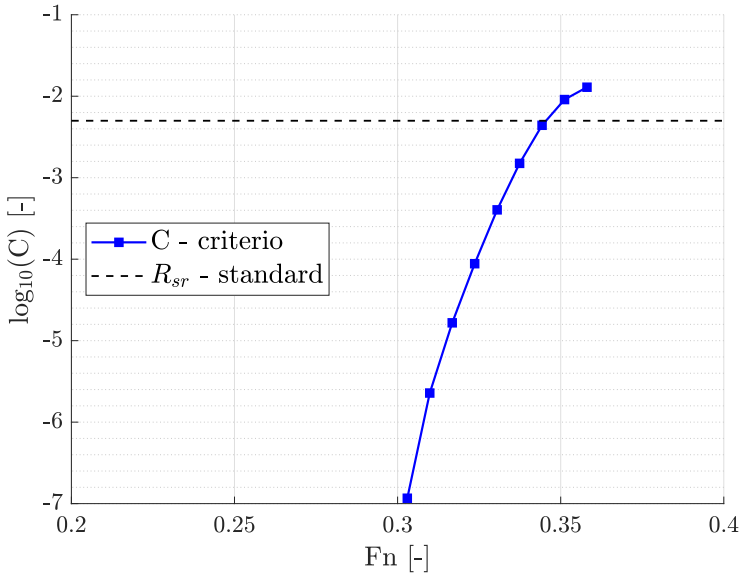

Figure 6.27: Relationship between Froude number and surf-riding criterion

Moving further into the structure of the criterion, the values of $C2$ is evaluated as a function of the wave steepness and of the wavelength to ship length ratio. To conduct this investigation, three different values of ship speed have been selected as parameters: 12 (m/sec), 13 (m/sec) and 14 (m/sec). It is useful to remind that the criterion $C2$ can assume the value of 1 or 0 according to a specified condition applied for a given set of waves. The results obtained are shown from Figure 6.28 to Figure 6.30. The red color is associated to the case of ship not vulnerable for the selected wave ($C2 = 0$), on the contrary when the ship is considered vulnerable ($C2 = 1$), she is represented by the yellow color.

As expected, the *Vulnerable zone*, highlighted in yellow, increases with the increasing of ship speed. The range of wave steepness s is defined by the criterion and should be noted that the maximum values of s is equal to 0.160 (-); that values can be considered very severe since wave having steepness greater than $1/10$ are not very common in nature.

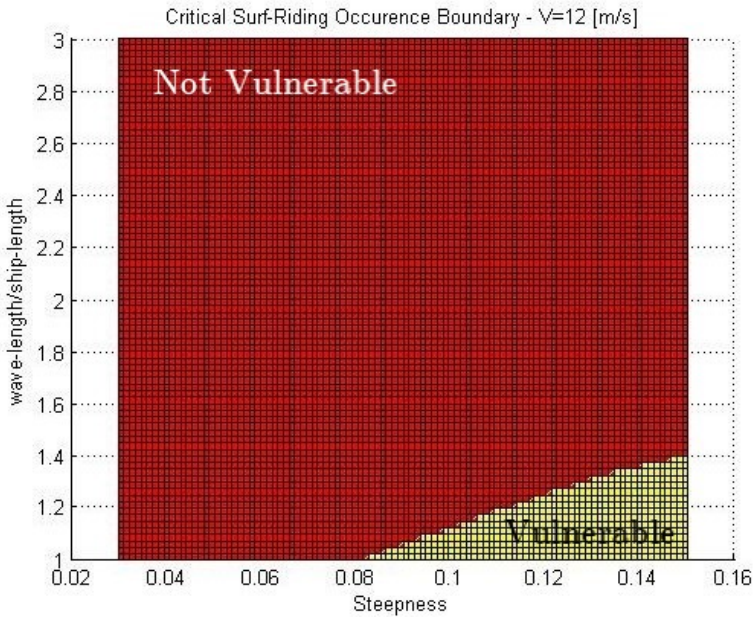

Figure 6.28: Further analysis of the $C2$ criterion - V = 12 (m/sec)

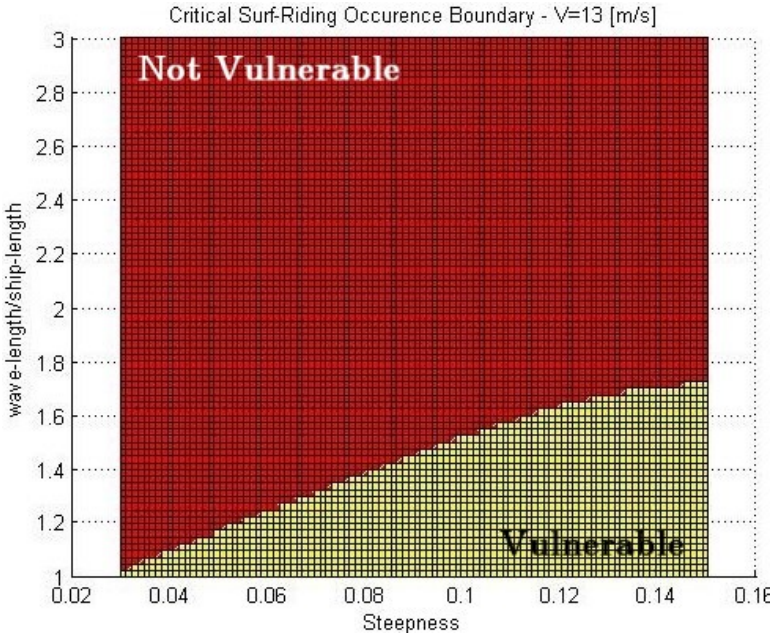

Figure 6.29: Further analysis of the $C2$ criterion - V = 13 (m/sec)

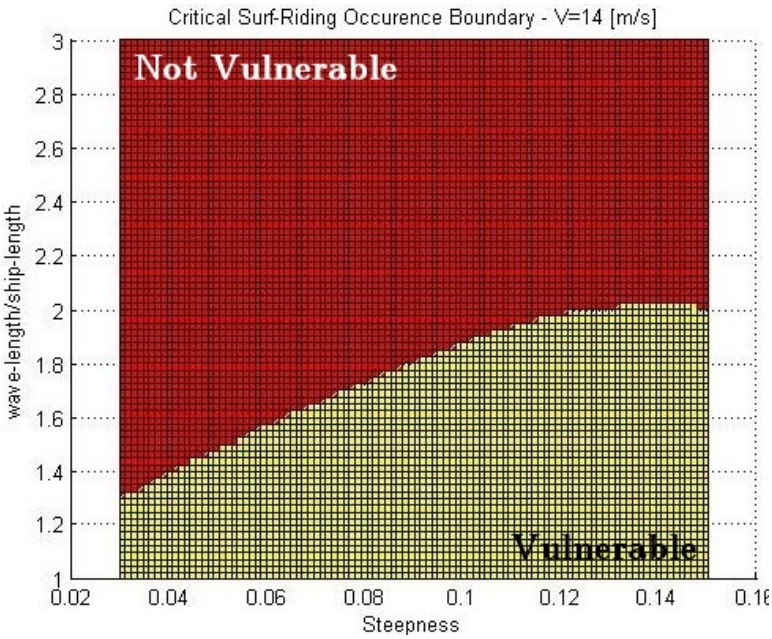

Figure 6.30: Further analysis of the $C2$ criterion - V = 14 (m/sec)

Chapter 7

Special problems dealing with Second Generation Intact Stability criteria

7.1 An analysis on damping coefficient

The accurate prediction of roll is much more complicated than other motions when engaged in a ship performance prediction in a seaway. This is due to the fact that roll motion is usually characterized by large angles and, also for this reasons, affected by significant non-linear effects. Another problem is the relevance of fluid viscosity and its inherent phenomena, which has still not been satisfactorily modeled. In addition, roll motion is strongly influenced by the presence of bilge keels, which are difficult to be analysed by the classical methods of hydrodynamics of an ideal fluid, especially at high roll angles [166]. The roll motion can be analysed addressing various kind of moments acting on the ship, such as: virtual and actual mass moments of inertia, roll damping moment, wave excitation and other moments caused by other modes of ship motion. Among them, the roll damping moment has been considered to be one of the most challenging term that should be correctly predicted. On the top of that, its evaluation is necessary sometimes at an early design stage in order to obtain a better understanding of ship motions in waves. However, using the *Strip Theory approach*, one of the most important and mature methodologies for seakeeping investigations, it is quite easy to evaluate all the terms in equation of ship motions in waves with practical accuracy, except for the roll damping. Difficulties in predicting the roll damping of ships arise from its nonlinear characteristics (due for instance to the effect of fluid viscosity as mentioned above) as well as from its strong dependence on the forward ship speed.

In the following sections, an analysis of the present roll damping prediction methods has been presented. In particular, two simplified methods have been selected because of their simplifications which permit to apply them in the early design phases. Moreover, they have been compared within the SGISc framework.

7.1.1 Damping coefficient prediction methods

Ikeda's method

The most adopted and studied damping prediction method is definitely the Ikeda's prediction method which was presented in 1978 by Prof. Y.Ikeda [167]. The main idea of Prof. Ikeda was to assume that the total roll damping coefficient could be divided into seven components [168], constituting the equivalent linear roll damping coefficient B_e :

$$B_e = B_F + B_E + B_L + B_W + B_{BK,N} + B_{BK,H} + B_{BK,L} \tag{7.1}$$

where:

- B_F = friction damping component, it is caused by the skin-friction stress on the hull during the roll motion;
- B_E = eddy damping component, it is caused by the pressure variation on the naked hull, excluding the effect of waves and bilge keels;
- B_L = lift damping component, it is a consequence of the forward speed of the ship;
- B_W = wave damping component, it denotes the increment of the hull-pressure damping due to the presence of free surface waves, including the effect of the interaction between the waves and lift;
- $B_{BK,N}$ = normal force damping component of bilge keels, it is related to the action of the normal force on the bilge keels themselves;
- $B_{BK,H}$ = hull pressure damping component of bilge keels, it corresponds to the pressure change on the hull caused by the installation of bilge keels;
- $B_{BK,L}$ = lift damping component of bilge keels, due to the effect of the forward speed on the bilge keels.

It is worth pointing out that, although these coefficients are assumed linear, their values may depend and vary with the roll amplitude and the frequency. Moreover, Ikeda decided to take into account the forward speed effect on all the terms since it might influence significantly their values.

As said before, Ikeda's method is the most established semi-empirical formulation for roll damping estimation and it is also recommended by ITTC [137]. The formula used in the method derived from a combination of theory and systematic model testing using different hull shapes and bidimensional sections. However in the latest year, the accuracy of Ikeda's method turned out to be unsatisfying for moder unconventional vessels having a high centre of gravity. Moreover the prediction method is valid only in large roll angle for modern type of ships with buttock flow stern and overestimates the roll damping for a very flat ship with large bilge keels.

Simplified Ikeda's methods

However, Ikeda's method cannot be used in the early design stages of ships because of the detailed information required. To overcome this limitation, in 2011 the prediction method was revised introducing some simplification. For this reason the method was renamed simplified Ikeda's method, which was also the method adopted within the SGISc framework.

As done in the first prediction method, the roll damping coefficient was divided into five different components:

$$B_{44} = B_F + B_E + B_L + B_W + B_{BK} \tag{7.2}$$

The simplified prediction formula has been developed on the basis of the Ikeda's original method using systematic series ships. These series ships are derived from Taylor Standard Series and their hull shapes are systematically changed by changing length, beam, draft, midship sectional coefficient and longitudinal prismatic coefficient. As a result, a simplified prediction method requiring parameters available in the early design phase, such as the principal characteristics and the bilge keel dimensions, has been obtained.

The friction and the lift damping components result to be exactly the same expression presented by the Ikeda's original method, while the other three components (eddy, wave and bilge keel component) are calculated through proposed formulas based on fitting experimental results. The complete prediction method is presented in [107].

Revisited Ikeda's method

In 2017 another method for the prediction of roll damping (renamed Revisited Ikeda's method) has been presented by Söder [169]. The modification of Ikeda's original method has been carried out to well represent the damping characteristics of modern car carriers. It is assumed as an extension that the revisited methodology could be applied with better results also to other ships, such as container carriers, Ro-Ro vessels and cruise vessels. For this type of ships, the hull lift component B_L and bilge keels component B_{BK} are considered as very important contribution for damping, therefore a new formulation for the just mentioned components have been developed. Both have been studied in a semi-empirical manner and model tests have been performed with the vessels considered in different bilge keels configurations and speeds. Furthermore non-viscid CFD calculations have been made with the case vessels to improve generic formulation for the hull lift damping component. As a result, it was found that Ikeda's original method seems to have underestimated the speed influence on the bilge keels damping and this may be ascribed to the low value of the lift force acting on the bilge keels considered in the original method. On the contrary, it has also been concluded that hull lift damping component is significantly overestimated with the original method. Taking into account these improvements, Revisited Ikeda's method may be extended to the new generation of volume carriers.

Blended Ikeda's method

Within the MSc thesis at UNIGE [170], a merge of the Simplified and Revisited Ikeda's methods has been done. It is well known that some components of Revisited Ikeda's Method, in particular the *wave damping component* B_W and the *eddy damping component* B_E are too heavy to implement specially in a preliminary design phase. For this reason these coefficients have been calculated by means of the same formulations proposed in Simplified Ikeda's Method. This new version of the method has been named as Blended Ikeda's Method. The following formula shows the relationship between the new proposal and the previous:

$$B_{44}^{\text{Blended}} = B_F^{\text{Revisited}} + B_E^{\text{Simplified}} + B_L^{\text{Revisited}} + B_W^{\text{Simplified}} + B_{BK}^{\text{Revisited}} \tag{7.3}$$

7.1.2 Comparison between prediction methods

In light of the methods presented above, it can be deemed that the problem of roll damping is mainly influenced by three main variables:

$$B_{44} = B_{44}(KG, V_S, \phi)$$

where:

KG	=	vertical distance of the centre of gravity,	(m);
V_S	=	ship forward service speed,	(m/s);
ϕ	=	heel angle,	(deg).

From the design point of view, it would be interesting to study the variation of roll damping coefficient as a function of the ship speed V_S and of KG for each of the two prediction methods, as well as the influence of heel angle ϕ has been taken into account. Finally, a comparison between $B_{44,\,\text{Blended}}$ and $B_{44,\,\text{Simplified}}$ has been made.

In order to carry out the analysis, the Ro-Ro pax ferry, previously presented in § 6.2, has been selected. Ikeda's original method could have some limited range of vertical center of gravity and ship's forward speed as well, where results reliability can be guaranteed. For this reason, it would be interesting to investigate how ship roll damping may change using different methods of estimation, for different values of vertical centre of gravity and ship forward speed.

With the aim to compare the simplified method with the proposed blended method, based both on the Ikeda's prediction method, an analysis on each component have been done considering different values of the parameters identified above. As first analysis, the simplified Ikeda's method has been applied and the roll damping coefficient has been expressed as a function of KG, keeping constant the other two variables selected. In Table 7.1, the selected constant values of ϕ and V_S are listed.

From Figure 7.1 to Figure 7.4, the trends of each component of the roll damping coefficient are given as a function of the vertical position of center of gravity KG. For the zero-forward speed condition, the total roll damping coefficient B_{44} decreases when KG is increasing (Figure 7.1 and Figure 7.2); this is not true when

Table 7.1: Parameters kept constant in the first analysis

ϕ (deg)	5°	15°
V_S (m/s)	0	15

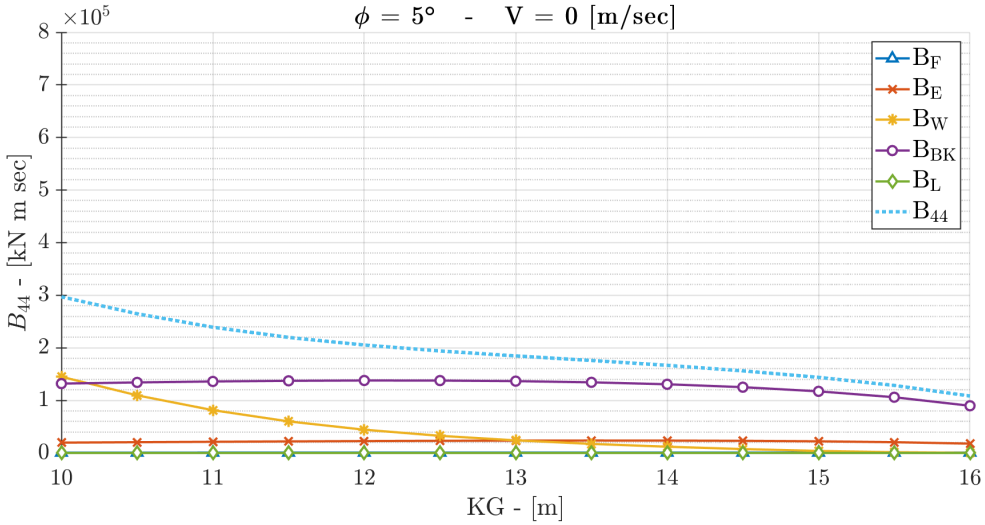

Figure 7.1: $B_{44}(KG)$ keeping constant $V_S = 0$ (m/sec) and $\phi = 5°$

the ship sails at high speed, in fact, the trend of B_{44} curve changes significantly because of the additional contribution given by the lift component B_L, which is directly related to the forward speed (Figure 7.3 and Figure 7.4). Considering each single component, results point out the following considerations:

- The bilge keel component B_{BK} keeps the same trend as function of KG even if it is affected by the heel angle ϕ. Moreover, while KG increases up to 13 meters B_{BK} increases as well and, it decreases immediately after that value;
- The wave component gives a significant contribution to the total damping coefficient for low values of KG. When KG assumes higher values, the wave component decreases dramatically;
- The eddy component B_E seems to be not affected by the KG, while the friction component B_F gives a negligible contribution to the total damping coefficient.

In a second analysis, the heel angle ϕ has been chosen as a variable, while the KG and the service speed V_S have been considered as fixed parameters, the simplified Ikeda's method has been applied again. The selection of parameters values are given in Table 7.2.

Table 7.2: Parameters kept constant in the second analysis

KG (m)	10	16
V_S (m/s)	0	15

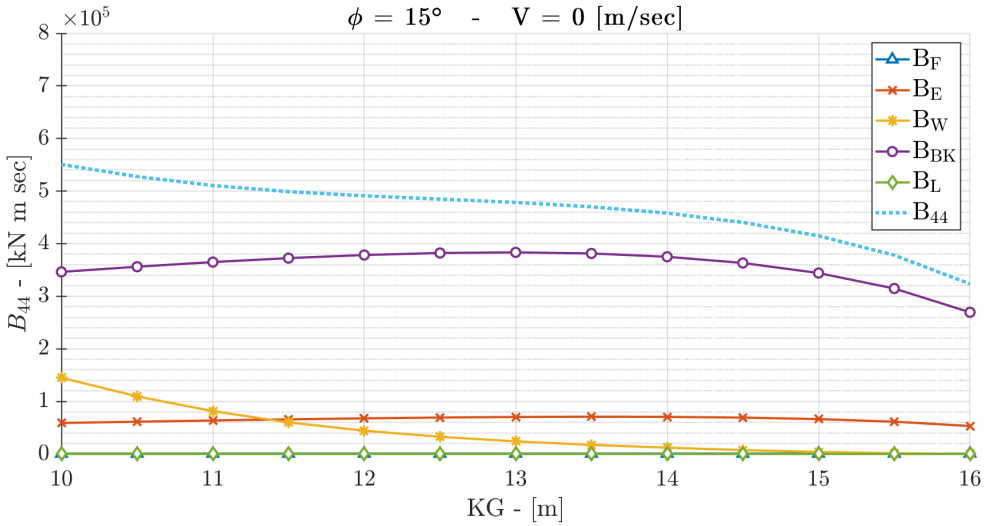

Figure 7.2: $B_{44}(KG)$ keeping constant $V_S = 0$ (m/sec) and $\phi = 15°$

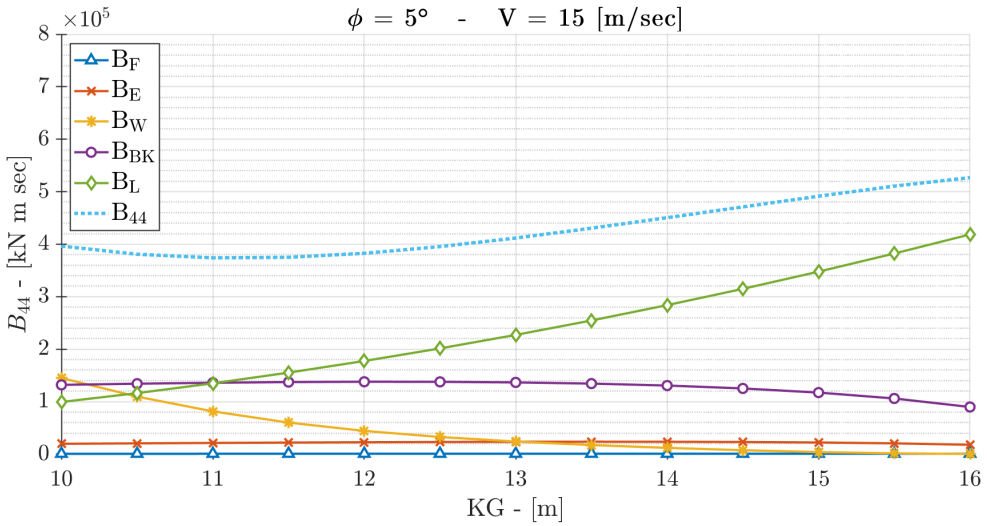

Figure 7.3: $B_{44}(KG)$ keeping constant $V_S = 15$ (m/sec) and $\phi = 5°$

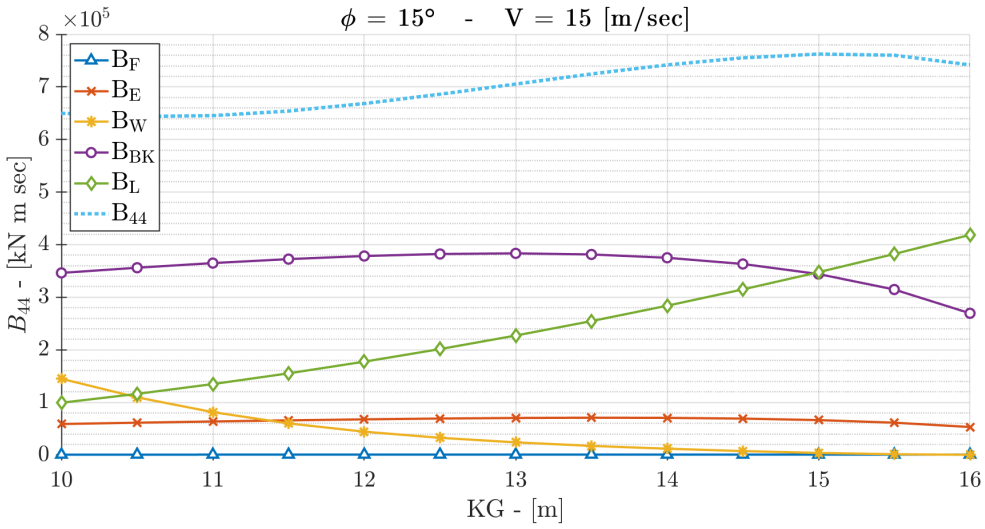

Figure 7.4: $B_{44}(KG)$ keeping constant $V_S = 15$ (m/sec) and $\phi = 15°$

From Figure 7.5 to Figure 7.8, the outcomes point out that the whole roll damping coefficient B_{44} always increases with increasing the heel angle, moreover this relationship seems to be nearly linear for low values of KG. Analysing in depth the coefficient, the following considerations can be assumed:

- the bilge keel component B_{BK} gives always the major contribution to the total coefficient, moreover it increases with increasing the heel angle as well as the eddy component B_E;
- in the zero-speed condition, the contribution to B_{44} of the wave component is relevant for low values of KG, but it decreases dramatically becoming negligible for high values of KG. Moreover, it seems that neither the heel angle nor the ship speed affect the values of wave damping component;
- the lift damping component B_L obviously is null at zero-speed and it grows with the increasing of speed giving a relevant contribution to the total damping coefficient, furthermore it does not depend on the heel angle being constant in the whole range of ϕ considered;
- once again, the friction component B_F results to be negligible for all possible values of heel angle.

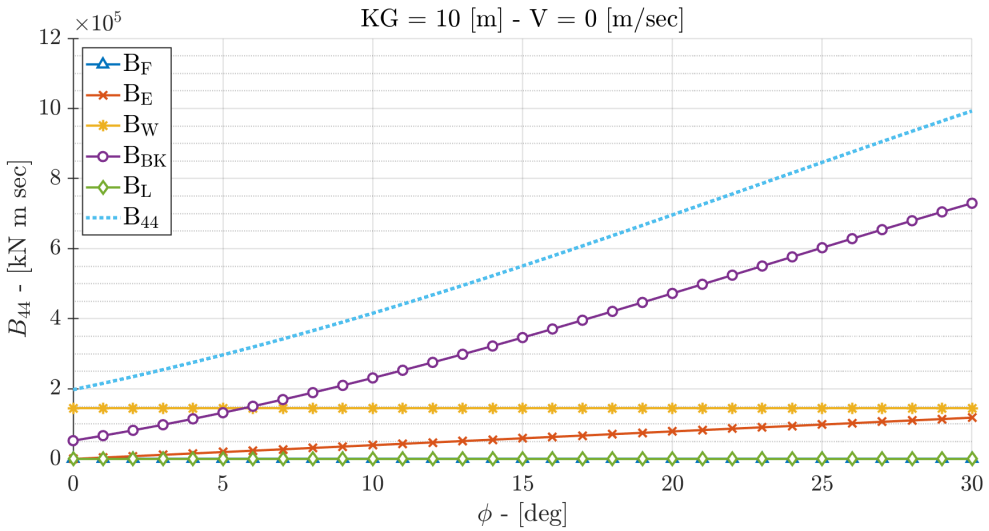

Figure 7.5: $B_{44}(\phi)$ keeping constant $V_S = 0$ (m/sec) and $KG = 10$ (m)

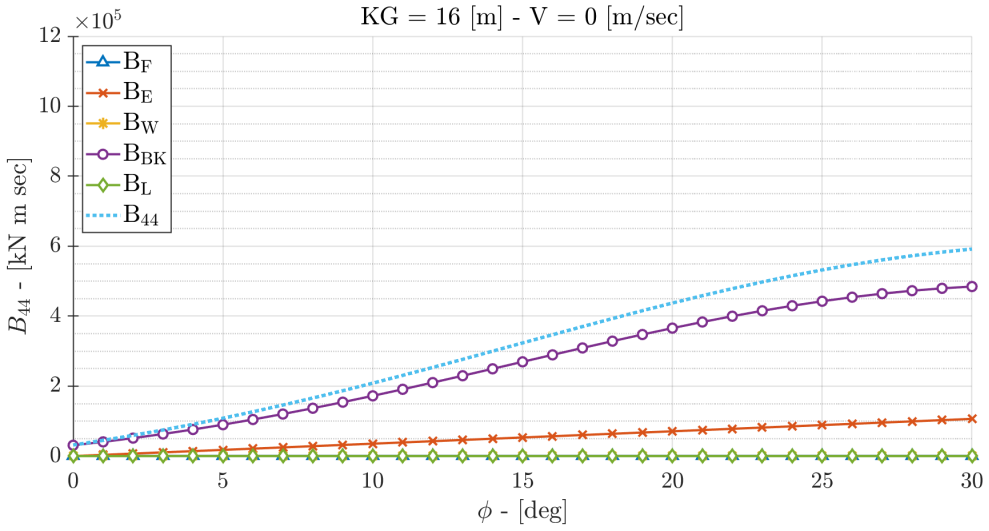

Figure 7.6: $B_{44}(\phi)$ keeping constant $V_S = 0$ (m/sec) and $KG = 16$ (m)

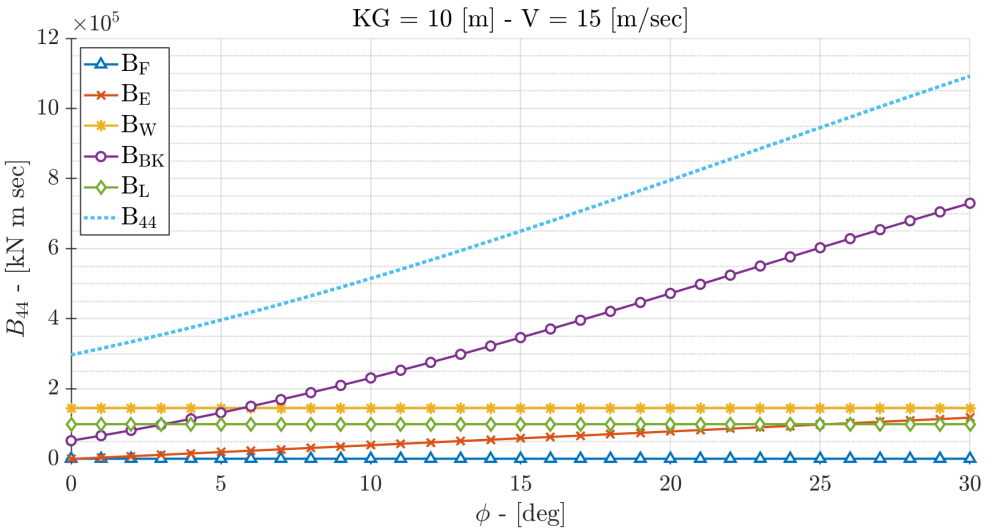

Figure 7.7: $B_{44}(\phi)$ keeping constant $V_S = 15$ (m/sec) and $KG = 10$ (m)

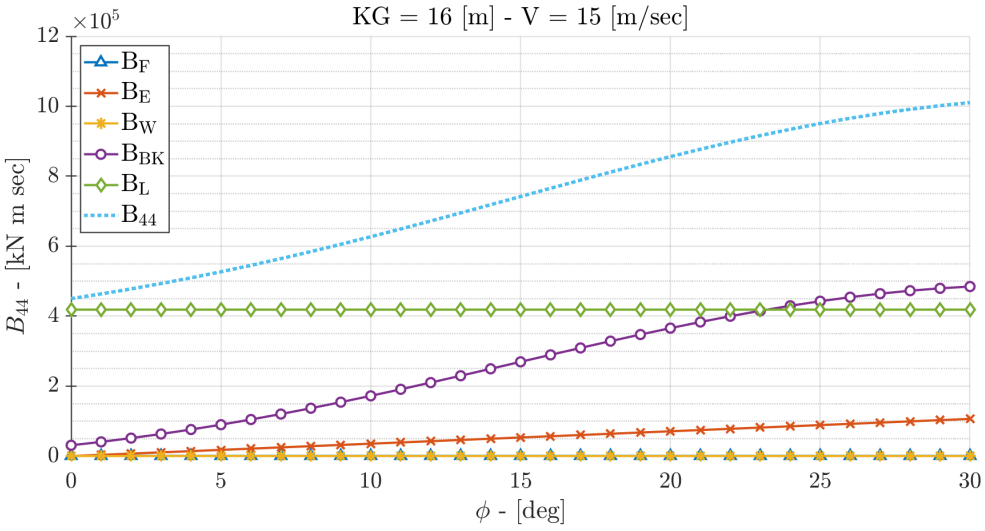

Figure 7.8: $B_{44}(\phi)$ keeping constant $V_S = 15$ (m/sec) and $KG = 16$ (m)

Since the sole difference between the simplified and the blended methods is the formulation of the bilge keel and of the hull lift components, the comparison of them has been carried out. From Figure 7.9 to Figure 7.16 the results obtained by the comparing analysis are shown; V_S and ϕ are kept fixed according to Table 7.1.

Considering the cases of zero-forward speed the bilge keel components of both methods have a similar trend with varying of KG, even if the higher the heel angle, the greater the bilge keel component evaluated with the blended method. Nearly the same values of B_{BK} are computed by the two methods for low values of heel angle, but those calculated with the blended method increase faster than those obtained with the simplified method when ϕ increases. In both cases, the hull lift components are null since the forward speed is zero.

In case of non-zero forward speed the same conclusions of previous cases can be given as concern the bilge keel damping component, it is worth mentioning that the overall values of $B_{BK,\,\text{Blended}}$ are a bit larger than those obtained at zero forward speed keeping exactly the same trend. This could depend on the fact that the original method of Ikeda underestimated the lift force acting on the bilge keels. Considering the hull lift component, it can be deduced that both methods keep a constant trend with varying of heel angles for B_L and they increase it with increasing of KG. As expected, the values of $B_{L,\,\text{Blended}}$ are always larger than $B_{L,\,\text{Simplified}}$.

To give an overall view of the differences of the total roll damping coefficient of both prediction methods, 3-D plots are shown in Figure 7.17. The considered sole parameter is the ship speed while the heel angle is represented on the x-axis and KG on the y-axis. Two different cases of forward speed have been considered: $V_S = 0$ (m/sec) and $V_S = 15$ (m/sec).

In case of zero forward speed the roll damping coefficients, in both the prediction methods, are quite similar for low heel angles; however the simplified Ikeda's method seems to have slightly overestimated roll damping with respect to the blended one. For higher values of heel angle, the total roll damping coefficient, obtained with the blended Ikeda's method, results to be considerably greater than the other method. This result may be interpreted as an overestimation of roll

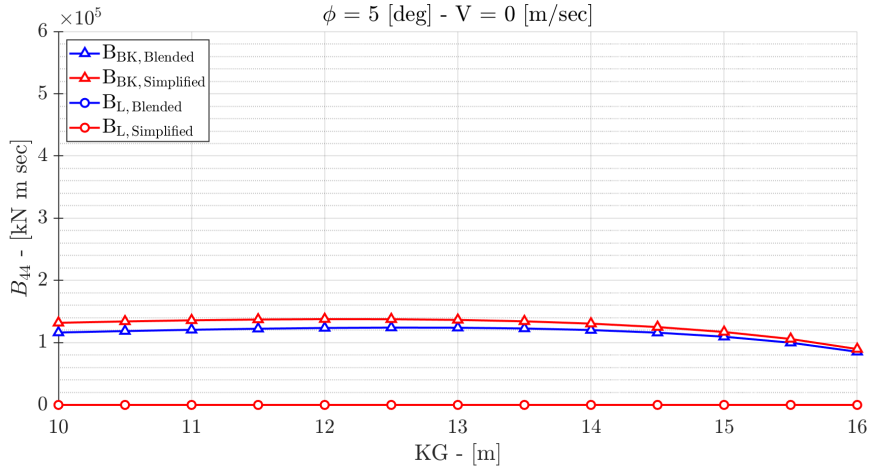

Figure 7.9: $B_{BK}(\phi)$ and $B_L(\phi)$ keeping constant $V_S = 0$ (m/sec) and $\phi = 0°$

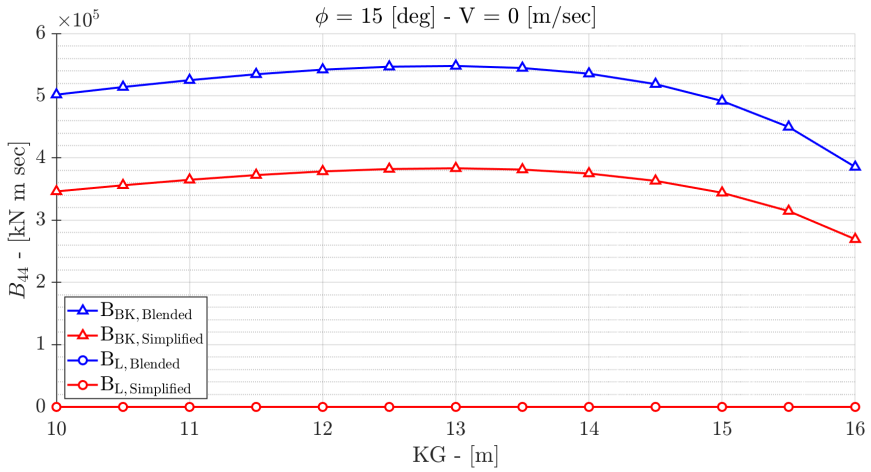

Figure 7.10: $B_{BK}(\phi)$ and $B_L(\phi)$ keeping constant $V_S = 0$ (m/sec) and $\phi = 15°$

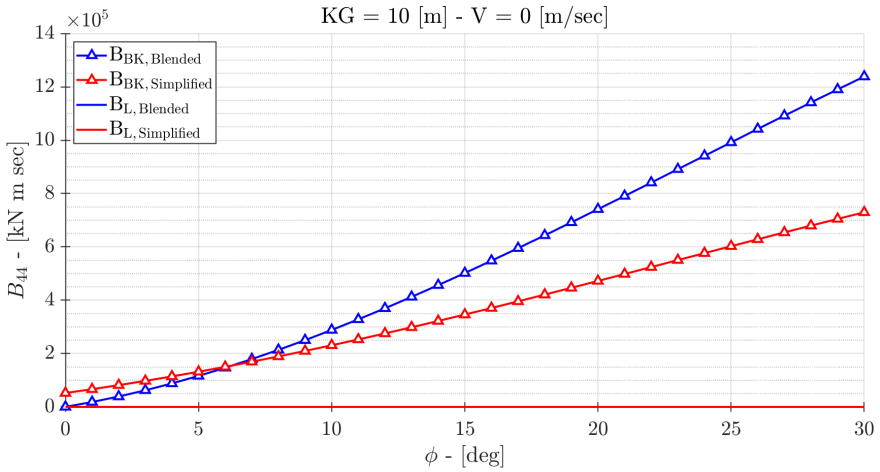

Figure 7.11: $B_{BK}(\phi)$ and $B_L(\phi)$ keeping constant $V_S = 15$ (m/sec) and $\phi = 0°$

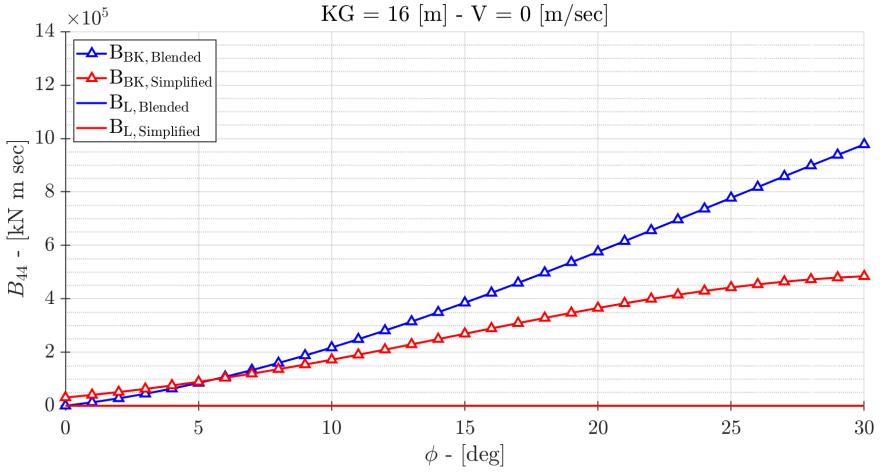

Figure 7.12: $B_{BK}(\phi)$ and $B_L(\phi)$ keeping constant $V_S = 15$ (m/sec) and $\phi = 15°$

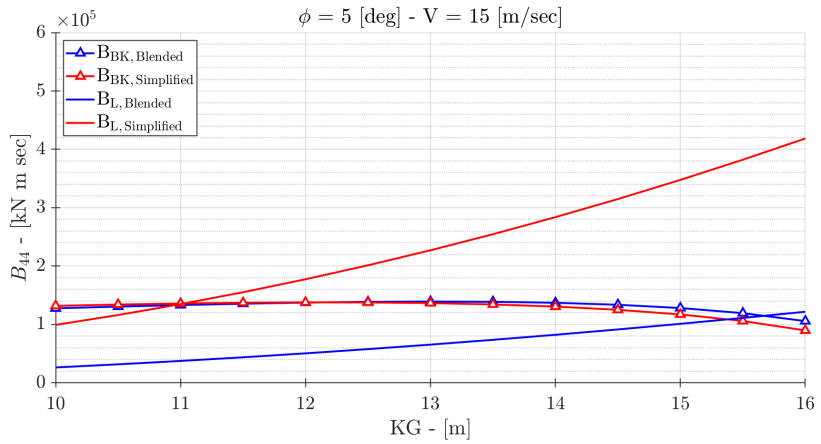

Figure 7.13: $B_{BK}(\phi)$ and $B_L(\phi)$ keeping constant $V_S = 0$ (m/sec) and $KG = 10$ (m)

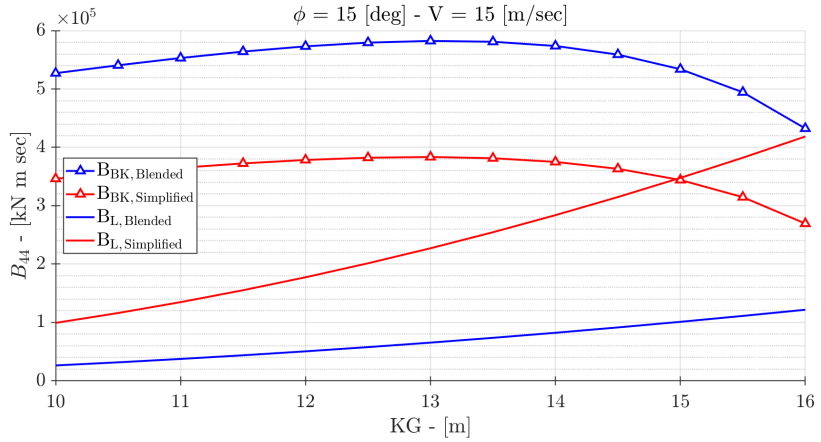

Figure 7.14: $B_{BK}(\phi)$ and $B_L(\phi)$ keeping constant $V_S = 0$ (m/sec) and $KG = 16$ (m)

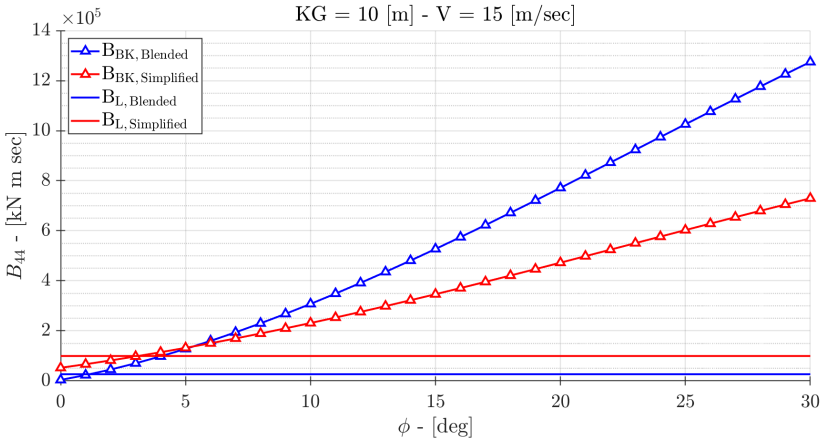

Figure 7.15: $B_{BK}(\phi)$ and $B_L(\phi)$ keeping constant $V_S = 15$ (m/sec) and $KG = 10$ (m)

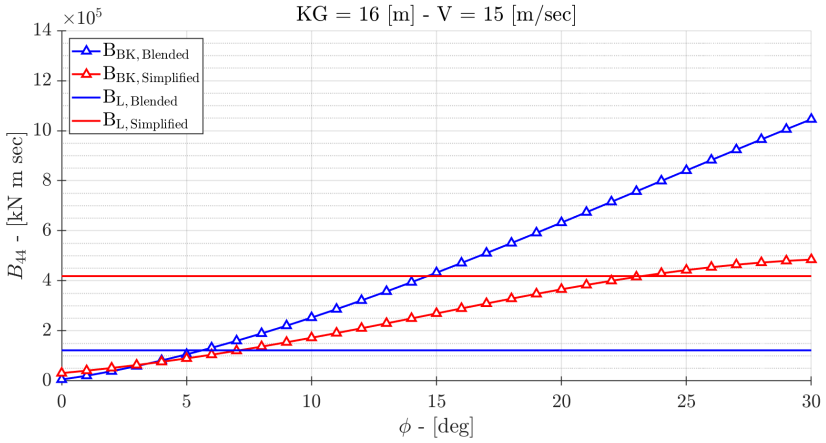

Figure 7.16: $B_{BK}(\phi)$ and $B_L(\phi)$ keeping constant $V_S = 15$ (m/sec) and $KG = 16$ (m)

damping for high heel angles which might imply great disadvantages in terms of ship's safety.

In case of non-zero-forward speed at low heel angles, the blended Ikeda's method has underestimated roll damping respect to the other method, therefore this might imply advantages in term of ship's safety. On the contrary, for high values of heel angles, the considerations of zero speed are still valid.

7.1.3 Damping coefficient within the Second Generation Intact Stability criteria

In this section the role of roll damping within the SGISc has been investigated. For this reason, the attention has been focused only on the criteria which contain the explicit calculation of roll damping coefficient, in particular:

- Dead Ship Condition - Level 2;
- Parametric Roll - Level 2;
- Excessive Acceleration - Level 2;

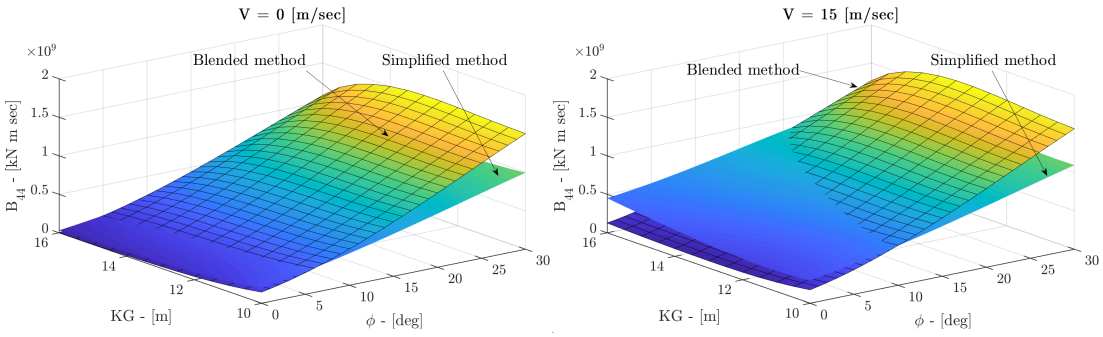

(a) $V_S = 0$ (m/sec) (b) $V_S = 15$ (m/sec)

Figure 7.17: Comparison between simplified and blended Ikeda's method

Table 7.3: Failure indexes and maximum allowable KG for the dead ship condition criterion

Simplified Ikeda's method			Blended Ikeda's method		
d (m)	C (-)	KG_{max} (m)	d (m)	C (-)	KG_{max}
6.55	1.71 x10^{-09}	15.8	6.55	3.82 x10^{-11}	15.8
7.18	6.05 x10^{-11}	16.1	7.18	5.55 x10^{-13}	16.1
7.82	1.91 x10^{-11}	16.1	7.82	1.07 x10^{-13}	16.1

Since the evaluation of roll damping within excessive acceleration criterion is the same of that reported in dead ship condition, only the latter and the paramertric roll stability failure have been analysed by the methods presented above.

Dead ship condition - Level 2

Analysing the scenario of dead ship condition, all the components of roll damping influenced by forward ship's speed, such as the lift damping component, have not been taken into account. This is obviously due to the fact that the ship speed is zero because of the assumed black out condition. The Ro-Ro pax, previously analysed in § 6.2, has been selected and three loading conditions have been considered: the departure condition with a draft of $d = 7.82$ (m); the arrival condition with a draft of $d = 6.55$ (m) and an intermediate case with a draft of $d = 7.18$ (m). The aim of this analysis is to assess the influence of roll damping prediction methods on the failure index of the second vulnerability level of dead ship condition criterion.

Implementing the procedure of IMO for both cases (i.e. Simplified Ikeda and Blended Ikeda methods) of roll damping, it is evident how the results obtained are substantially the same (Table 7.3). This means that a different expression of roll damping does not change the output of dead ship condition criterion, due to the formulation itself of the specific criterion . Considering the risk threshold of the criterion, the failure index is always smaller than R_{DS0}, therefore the ship turns out to be not vulnerable for all the examined cases. The research of the maximum VCG shows the negligible differences between the two methods when implemented in the criterion, in fact, the maximum VCG practically does not change using the two methods for each loading condition (Table 7.3).

Parametric Roll - Level 2

The analysis carried out in the previous section has been applied also to the parametric roll stability failure. The ship vulnerability has been investigated by the second check of level 2 of parametric roll, identifying the most unfavourable loading condition, in terms of draught and relevant KG. The procedure described in § 3.2.3 has been applied and the Ro-Ro pax ferry has been selected to carry out the investigation (§ 6.2). The failure index has been evaluated distinguishing the two different methodologies for damping prediction. The results obtained

for each loading condition, selected in the previous section, are listed below, in Table 7.4.

Reminding that the threshold is equal to $R_{PR0} = 0.06$, it is evident that the ship results to be vulnerable to the parametric roll only for the loading condition with $d = 7.18$ (m). This observation is valid for both cases of roll damping, therefore, it has been concluded that the ship's vulnerability for the second check of parametric roll level 2 is not influenced by the choice of the roll damping estimation method. It is worth mentioning that for $d = 7.18$ (m) the C_2 index outcomes are, on the contrary, very different in terms of order of magnitude for the two methodologies. Nevertheless, results agree in evaluating the ship as not vulnerable. In order to gain further insight into the problem, a specific investigation for the loading condition corresponding to $d = 7.18$ (m) has been further developed and reported in the following.

Numerical simulation of parametric roll Even though the different formulations for roll damping are not able to have an influence on C_2 as a whole, for sure they have an influence on the response in term of heel angle amplitude. For this reason it would be interesting to analyse the variation of the heel angle in the time domain. In order to perform these simulations, the worst scenario for parametric roll has been chosen considering the ship at the draught $d = 7.18$ (m), a natural roll period T_ϕ equal to 12.4 (sec) and the wave crest located midship. The investigated speeds have been calculated according to the criterion and are 11.3 (m/sec), 9.8 (m/sec) and 5.7 (m/sec). As expected, the development of the parametric roll phenomenon occurs when the ship roll natural period is about twice the encounter wave period. Moreover, the frequency range for roll resonance becomes larger with increasing of the wave height. From Table 7.5, it is evident that the case of ship proceeding in heading waves is a typical case where parametric roll might happen, thus only heading seas condition has been further analysed.

From the results, it has been deducted the maximum values of heel angle in relation with the wave height for the three cases of speed. From Figure 7.18 to 7.20, the results are given choosing the ship speed as a fixed parameter; on the horizontal axis the analysed wave heights are represented while on y-axis the maximum heel angle simulated is reported. The straight line represents the threshold heel angle as defined by the criterion.

In the case of ship speed equal to 5.7 (m/sec), the curves evaluated with different formulations of roll damping correspond for low value of wave heights

Table 7.4: Failure indexes and maximum allowable KG for the parametric roll criterion

Simplified Ikeda's method		Blended Ikeda's method	
d (m)	C_2 (-)	d (m)	C_2 (-)
6.55	0.045	6.55	0.051
7.18	0.074	7.18	0.074
7.82	0.049	7.82	0.009

Table 7.5: Ship natural roll period and encounter period ratio

	Heading seas	
	T_{enc} (sec)	T_ϕ/T_{enc} (-)
$V_1 = 5.7$ (m/sec)	8.2	1.5
$V_2 = 9.8$ (m/sec)	6.9	1.8
$V_3 = 1.3$ (m/sec)	6.6	1.9

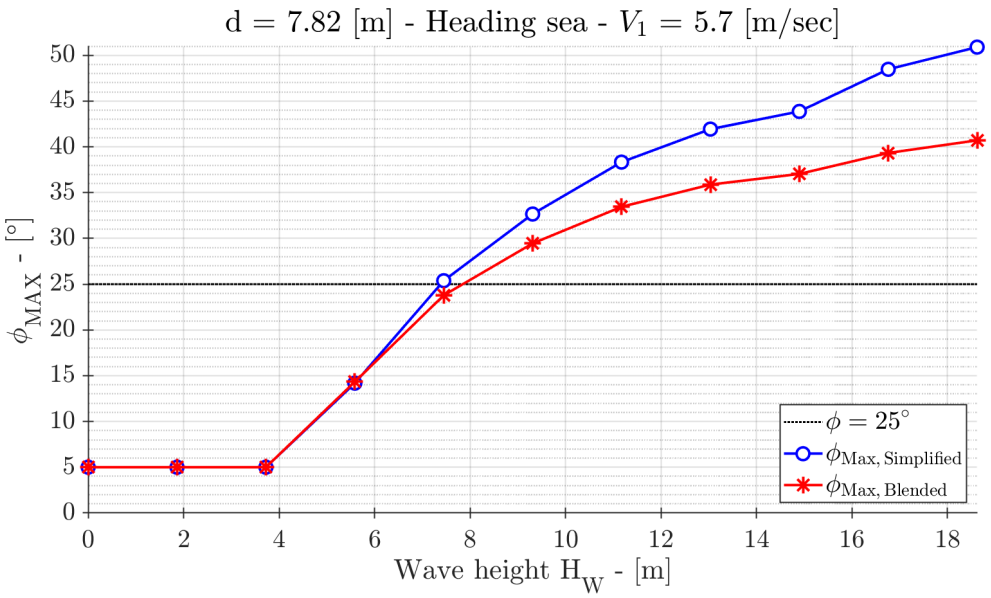

Figure 7.18: Maximum heel angle as a function of wave height at $V_S = 5.7$ (m/sec)

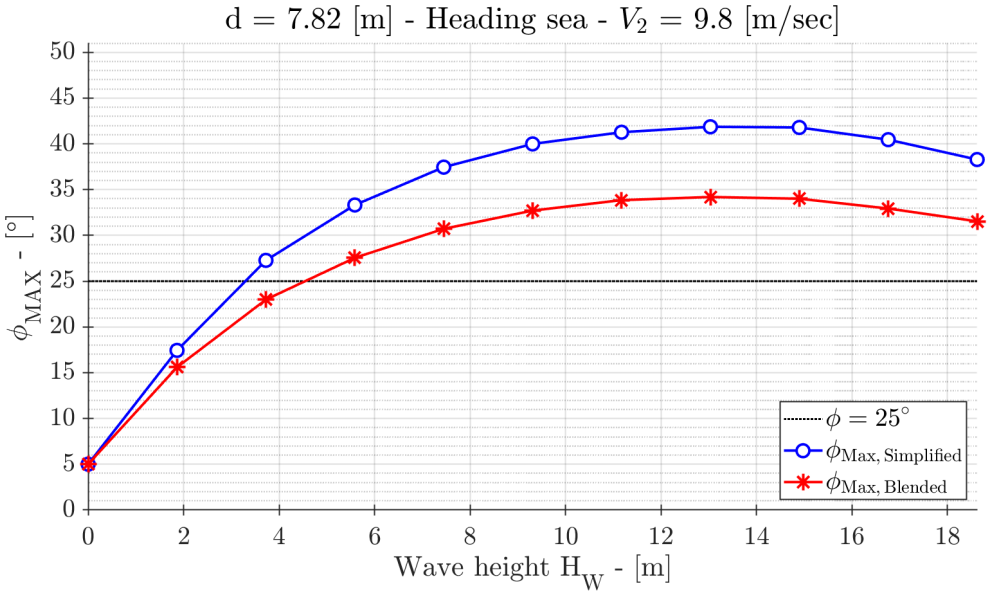

Figure 7.19: Maximum heel angle as a function of wave height at $V_S = 9.8$ (m/sec)

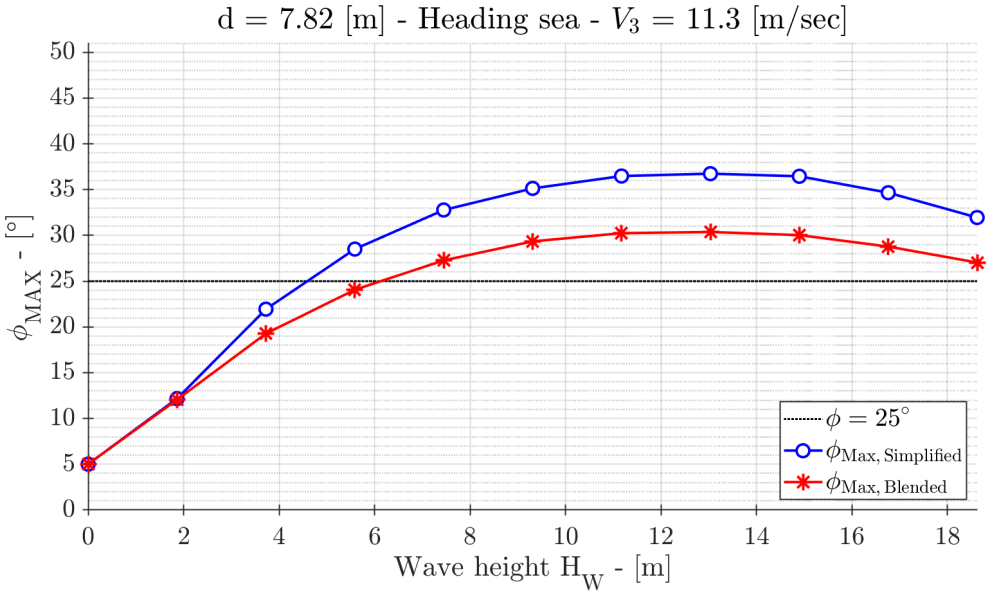

Figure 7.20: Maximum heel angle as a function of wave height at $V_S = 11.3$ (m/sec)

up to $H_W = 8$ (m); after this value the curve calculated with $B_{44,\,\text{Simplified}}$ grows faster (Figure 7.18). In the other two cases, the difference between curves is always large except for the first two wave heights. Considering the wave height which guarantees a maximum value of heel angle equal to the threshold ($\phi_{max} = 25°$), it appears that the difference between the roll damping prediction methods becomes larger for low speeds: the difference between the wave height is more than 1.2 (m). As it can be seen in Figure 7.20, only in the case of speed equal to 11.3 (m/sec) the difference between the wave heights at around 25° is similar, i.e. less than 0.4 (m). It is clear that, in case of ship in heading waves, the amplitude of roll angles obtained using simplified Ikeda's method is larger than the other. This is due to the fact that, considering high values of heel angle, $B_{44,\,\text{simplified}}$ resulted to be smaller than $B_{44,\,\text{blended}}$. Therefore, this latter allows a larger wave height to obtain the same maximum angle.

7.1.4 Comments to the results

In the previous sections, two roll damping prediction methods have been presented. They derive from the Ikeda's prediction method and both can be applied to the early design phase thank to their simplified structure. In order to compare them, a Ro-Ro pax ferry has been selected and analysed. The results put in evidence that in case of zero forward speed and also considering low heel angles, the simplified Ikeda's method slightly overestimates roll damping with respect to the other method. On the contrary, for higher heel angles the opposite results are obtained. In case of non-zero-forward speed and also considering low heel angles, the simplified Ikeda's method seems to strongly overestimate roll damping. However, at high values of heel angle, results obtained by the blended Ikeda's method rapidly overcame those obtained by the simplified one.

Furthermore, the second vulnerability level for the dead ship condition failure

mode has been applied to the Ro-Ro pax ferry using both roll damping prediction methods and also distinguishing three different cases of loading condition. It has been concluded that the ship appears to be not vulnerable for all loading conditions. Furthermore, from the ship vulnerability point of view the results do not depend on the choice of the prediction method, as far as damping concern.

Even in the application of the second check of Level 2 of parametric roll, the Ro-Ro pax ferry has been used as a case study; also the same cases of loading condition have been taken into account. The ship results to be vulnerable only for an intermediate case of loading condition. This behaviour is valid for both formulations of roll damping, therefore, it has been concluded that the ship vulnerability has not been influenced by the choice of prediction method of roll damping.

However, it is worth mentioning that for the design loading condition the C_2 index outcomes are very different in terms of order of magnitude for the two methods.

In light of this, an in-depth analysis has been carried out for this case, focusing on the results obtained by the time-domain model. From a comparison between the outputs, adopting the blended Ikeda's method leads to require a higher wave height to obtain the same heel angle compared to the simplified Ikeda's method. This difference it considerable also in the values of C_2, in fact, the indexes are very different in terms of order of magnitude for the two methodologies of prediction of roll damping. Nevertheless, the results agree in evaluating the ship as not vulnerable for Parametric Roll.

It is evident that the procedure proposed by IMO containing a long term analysis, tends to weaken the effect of each sea state (and damping formulation in turn) on the final index value C_2. From what above in this specific case, in fact, the use of different formulation for damping has not changed the conclusion that the ship is not vulnerable.

7.2 Toward the Direct Stability Assessment

The activities reported below have been developed during the exchange study period at the TUHH. The excessive acceleration failure mode within the framework of SGISc is the focus of this work. The ships analysed are a navy vessel and a Ro-Ro ferry; moreover, to benchmark the results of DSA tool, three container ships that have suffered of excessive acceleration failure have been analysed. The aim of this work is to compare the results computed by a DSA tool against those obtained by the application of Level 1 and Level 2 criteria for the excessive acceleration failure mode. It comes that the safety level of the investigated ships is evaluated by means of two different procedures. The first one is developed and applied in order to fit as much as possible the scenario adopted in Level 1 and Level 2, in terms of sea state. This procedure is a semi-automatic process and the outputs of the seakeeping code are elaborate by a Matlab® script. The second one has been developed at TUHH and implemented in the seakeeping code. It has been fully tested and validated along the past years. All possible scenarios that may happens in a seaway condition, i.e. sea state, encounter angle, ship

speed, are taken into account by this procedure, thus this is a complete tool to assess the vulnerability of a ship in term of stability.

7.2.1 Computational procedure

The DSA has been carried out by means of the seakeeping code *E4ROLLS* originally developed by Söding [171], Kröger [172] and Petey [173]. The previous references are written in German language, thus an English description is given in [174]. *E4ROLLS* simulates all six degrees of freedom. The basic concept is that those degrees of freedom, which are governed by nonlinearities effects, are computed through a non-linear simulation in time domain, whereas a linear simulation using RAOs (e.g. strip theory or panel code) is performed for those degrees of freedom that are governed by hydrodynamic effects. A more detailed description of the seakeeping code is given in [175], [176].

As pointed out above, this section deals with the excessive acceleration failure in the framework of SGISc. Since technical guidelines on DSA are still under development [36] during my PhD studies, the following two assessing procedures have been applied.

Direct procedure

One of the final aim of this research is to compare the results obtained by the application of Level 1 and 2 of SGISc against those obtained using a direct assessment tool, like as *E4ROLLS*. Therefore, the analysed scenario should be as comparable as possible with the formulation of simplified criteria (Lv 1 and Lv 2); both the criteria consider the vessel in a zero-speed condition in a pure beam seas scenario. This procedure is based on that proposed in [177] with some adjustment in the final part. It is summarized as follows:

- For each sea state (H_W and T_Z) a simulation is computed;
- Maximum transverse accelerations are taken into account as criterion and the upper threshold is chosen equal to 9.81 (m/sec^2);
- The short-term stability failure probability p_{fail} is defined as the ratio between the numbers of failure occurrences over the number of occurrences simulated. Within each roll period are recorded two lateral accelerations, one directed to portside (positive) and the other one to starboard side (negative);

$$p_{\text{fail}} = \frac{\text{n.failures}}{\text{n.totoccurrences}} \tag{7.4}$$

- A long-term stability failure probability p_{LongTerm} is estimated by multiplying the several short-term probability p_{fail} by the relevant scatter diagram weight W_{S}:

$$p_{\text{LongTerm}} = \sum p_{\text{fail}} \cdot W_{\text{S}} \tag{7.5}$$

– The average rate of stability per ship year (1/year), required by the SGISc, is evaluated according to the following formula:

$$r = \frac{-\log\left(1 - p_{\text{LongTerm}}\right)}{t} \tag{7.6}$$

where t is period of time analysed; Eq. 7.6 is given in [35], it derives from the exponential cumulative distribution function.

– The average rate of stability per ship year r is compared to the standard value proposed by the last draft of the rule text [36]. A ship is considered to be vulnerable to the assessed failure if:

$$r > 10^{-4} \qquad (1/\text{year})$$

Insufficient Stability Event Index (ISEI) procedure

In order to compare the results obtained with the above procedure, the ISEI has been implemented. Again, some adjustments are required to fit the excessive acceleration failure mode. Below a brief description of the index is given, for a detailed explanation see [178]. The operating conditions may be summarized in two categories: environmental condition (wave period and wave height) and ship specific operating data (speed and course). All these elements are joined together to compute the ISEI:

$$\begin{aligned}\text{ISEI} = \int\int\int\int p_{\text{sea}}(\mathrm{d}\mu, \mathrm{dH_W}, \mathrm{dT_1}, \mathrm{dv_s}) \cdot \mathrm{p_{fail}}(\mathrm{d}\mu, \mathrm{dH_W}, \mathrm{dT_1}, \mathrm{dv_s}) \cdot \mathrm{p}_\mu(\mu) \cdot \\ \cdot\, p_{\text{speed}}(\mathrm{d}\mu, \mathrm{dH_W}, \mathrm{dT_1}, \mathrm{dv_s}) \cdot \mathrm{d}\mu \cdot \mathrm{dH_W} \cdot \mathrm{dT_1} \cdot \mathrm{dv_s}\end{aligned} \tag{7.7}$$

$\boldsymbol{p_{\text{sea}}}$ **– Sea state** The probability of occurrence of given sea state is evaluated by this element of ISEI. The sea state is characterized by the significant wave height and the mean period. Their stochastic nature is collected in the scatter diagrams. These tables are published in [179] and they cover 126 locations. The computation of the ISEI uses the area n° 125.

$\boldsymbol{p_{\text{speed}}}$ **– Speed distribution** Usually, the speed in a direct assessment is set as the design speed or a percentage of that. The minimum threshold value is defined to 2 (kn), moreover the maximum speed is limited by the ship resistance, the propulsion power and the sea state encountered.

$\boldsymbol{p_\mu}$ **– Course probability distribution** The encounter angle is assumed to be equally distributed, thus the probability density function is the following:

$$p_\mu(\mu) = \frac{\pi}{2}$$

Seven encounter angles are considered between 0° and 180° (following and heading seas respectively) with an increment of 30°. Within the range of encounter angles, three sector areas are defined:

1. Following seas = $-45° \leq \mu \leq +45°$;
2. Heading seas = $+135° \leq \mu \leq -135°$;
3. Beam seas = the other sectors.

p_{fail} – Failure coefficient The coefficient is reduced to a failure binary coefficient: its values is 0 for all wave heights smaller than the limiting wave heights and it is 1 for those values equal or larger than the limiting wave heights. The limiting wave heights are evaluated fixing to 9.81 (m/sec^2) the maximum value of lateral acceleration in a specified point.

7.2.2 Scenario conditions

In the following paragraphs, the environmental and operational condition applied to each simulation are reported.

Sea states

Each possible wave condition is evaluated as indicated in IACS Recommendation No.34 (Appendix A). It means that only waves with non-zero occurrences have been taken into account. Each sea state, defined by a significant wave height H_W and a zero-crossing period T_Z, is represented by a Pierson-Moskovitz spectrum. To take into account the short crested effects, a spreading $\cos^2$–function is applied.

Encounter angle

Parametric roll and synchronous resonance are the two main physical mechanisms that, when coupled with low roll period, lead to excessive acceleration failure. Parametric roll happens when a ship is sailing along the same direction of waves (following or heading seas) and the encounter period is about half of the natural rolling period. Synchronous resonance happens when an external force, such as wind or waves, encounters the ship with a frequency close to her natural roll frequency. In this condition, the roll motion grows more and more, leading to large roll angles. Taking into account the above mentioned phenomena, the condition of beam and heading seas have been analysed for all the assessed ships. A quartering seas ($\mu = 150°$) is added only for the Ro-Ro pax ferry, the OPV navy vessel and the Containerships#1.

Ship speed

Level 1 and Level 2 of excessive acceleration criteria consider the ship in a condition of zero speed. With the aim to compare the first two levels with the DSA, the former analysis studies the ships at zero speed in a beam seas condition; subsequently two other speeds are added. As stated in the accident reports of the three considered cases, the ships were sailing at a low speed between 2 and 5 (kn), therefore it has been decided to analyse also a speed of 3 (kn). Finally, a

Table 7.6: Summary of environmental conditions

Encounter angle	Assessed ship speed		
	$V_S = 0$ (kn)	$V_S = 3$ (kn)	Fn = 0.216 (-)
Following seas ($\mu = 0°$)	N	N	N
Beam seas ($\mu = 90°$)	Y	Y	Y
Quartering seas ($\mu = 150°$)	Y	Y	Y
Heading seas ($\mu = 180°$)	Y	Y	Y

Froude number of about 0.22 (-) is computed for each ship, in order to analyse also a sailing condition.

Summary

In Table 7.6, all the assessed conditions are summarized. For each ship, a total of six different scenarios have been considered.

7.2.3 Case studies

The sample vessels for the investigation are presented in this paragraph. It has been selected an OPV, a Ro-Ro ferry and three different Containerships. It is reported that the last three ships have suffered of excessive acceleration in the past. They have been considered to check if the proposed procedure can recognise the stability failure at the loading condition of the accident. In order to evaluate the lateral acceleration, the assessed points have been always located in the wheelhouse on the bridge deck. In Table 7.7, the main dimensions and the loading condition assessed are reported, together with the longitudinal X_P and the vertical Z_P coordinates of the considered point, required in the excessive acceleration analysis.

7.2.4 Results and comments

In the following, a brief description of the obtained results and some relevant comments are given. Moreover, a comparison between the two procedures in terms of results is carried out.

Average rate per ship year

In Table 7.8 results of the Direct procedure, in terms of average rate per ship year, are listed for each vessel, speed and encounter angle. According to [36], a ship is considered vulnerable at excessive acceleration failure if the average rate per ship year is greater than 10^{-4}. The values above the threshold highlighted in red denote a vulnerability to the stability failure for the considered environmental condition.

Table 7.7: Main data of the sample vessels

OPV		
L_{PP}	80.2	(m)
B	10.2	(m)
d	3.37	(m)
Δ	1298	(t)
GM	1.134	(m)
T_ϕ	7.69	(sec)
X_P	44.5	(m)
Z_P	14.5	(m)

Ro-Ro pax ferry		
L_{PP}	186.2	(m)
B	30.4	(m)
d	7.80	(m)
Δ	29486	(t)
GM	3.160	(m)
T_ϕ	17.04	(sec)
X_P	170.0	(m)
Z_P	34.0	(m)

Containership #1		
L_{PP}	319.0	(m)
B	42.8	(m)
d	8.08	(m)
Δ	66649	(t)
GM	7.712	(m)
T_ϕ	11.86	(sec)
X_P	82.0	(m)
Z_P	52.0	(m)

Containership #2		
L_{PP}	195.0	(m)
B	29.8	(m)
d	5.70	(m)
Δ	18741	(t)
GM	5.627	(m)
T_ϕ	10.77	(sec)
X_P	13.0	(m)
Z_P	41.0	(m)

Containership #3		
L_{PP}	195.4	(m)
B	29.8	(m)
d	5.59	(m)
Δ	17921	(t)
GM	4.56	(m)
T_ϕ	11.79	(sec)
X_P	13.0	(m)
Z_P	40.0	(m)

The Fn = 0.216 corresponds in term of speed for the different ships as follows:

- Off-shore Patrol Vessel - $V_S = 12$ (kn);
- Ro-Ro pax ferry - $V_S = 18$ (kn);
- Containership#1 - $V_S = 23$ (kn);
- Containership#2 - $V_S = 18$ (kn);
- Containership#3 - $V_S = 18$ (kn);

According to the results obtained, the worst case seems to be the beam seas condition for all the speeds. This is in contrast with the trend outlined by real accidents, where the bow quartering seas condition is happened to be the worst. For example, the actual environmental conditions at the moment of the accident for Containership#1 are described by the quartering seas scenarios: the average rate confirms the vulnerability of this ship at large acceleration for the specific loading condition. This inconsistency may be caused by the approximation within *E4ROLLS*: the roll motions in beam seas are overestimated by the seakeeping code because it neglects the nonlinear effects of the sway. These effects are negligible for longitudinal seas but they assume a relevant influence in beam seas, where the drift motion considerably increases the roll damping. As regards the pure heading seas condition, it appears that no ship is vulnerable to large lateral accelerations for each assessed speed. Investigating the influence of speed on the phenomenon, the results point out that the worst situations happen for the zero speed condition, while an increase of speed decreases substantially the average failure rate.

ISEI procedure

Table 7.9 summarizes the values of the ISEI stability index for each ship. It is worthwhile to note that ISEI considers all the probable encounter directions and speeds, as described above. Furthermore, ISEI is made up of the three components as function of sea direction: heading, beam and following seas.

Since we are not aware of ISEI application to excessive acceleration phenomenon, a threshold value was not available yet. In order to define it, the ISEI value of Containership#1 has been taken as reference, since this is the Chicago Express container-ship and it represents the reference ship for the development of Level 1 and Level 2 of the excessive acceleration stability failure in the SGISc framework. Considering the threshold equal to the ISEI value of Containership#1, the outcome shows that all the assessed ships are considered vulnerable to excessive acceleration failure, except the Ro-Ro pax ferry whose index is null. A comparison between ISEI and Direct procedure results is not trivial because the first one analyses the ship in a comprehensive way, taking into account more combinations of speed and encounter angle within the final value. Instead, the Direct procedure analyses separately case by case a restricted amount of combinations, as shown in Table 7.6. Comparing the results of beam seas state with the ISEI, the two procedures appear to be consistent in judging

Table 7.8: Average rate of stability failure in beam seas condition

Average rate per ship year - Beam seas (μ = 90°)			
Speed	0.0 (kn)	3.0 (kn)	Fn = 0.216 (-)
Offshore Patrol Vessel	1.42 x10^{-4}	1.07 x10^{-4}	1.40 x10^{-6}
Ro-Ro pax ferry	1.91 x10^{-8}	4.09 x10^{-8}	0.00
Containership #1	4.21 x10^{-3}	5.65 x10^{-4}	5.20 x10^{-8}
Containership #2	3.29 x10^{-3}	1.24 x10^{-3}	1.75 x10^{-7}
Containership #3	2.05 x10^{-4}	5.81 x10^{-5}	1.66 x10^{-9}

Average rate per ship year - Quartering seas (μ = 150°)			
Speed	0.0 (kn)	3.0 (kn)	Fn = 0.216 (-)
Offshore Patrol Vessel	1.30 x10^{-5}	2.34 x10^{-5}	8.60 x10^{-7}
Ro-Ro pax ferry	1.96 x10^{-9}	0.00	0.00
Containership #1	4.11 x10^{-4}	1.94 x10^{-4}	5.93 x10^{-10}
Containership #2	–	–	–
Containership #3	–	–	–

Average rate per ship year - Heading seas (μ = 180°)			
Speed	0.0 (kn)	3.0 (kn)	Fn = 0.216 (-)
Offshore Patrol Vessel	2.76 x10^{-6}	3.95 x10^{-6}	2.49 x10^{-8}
Ro-Ro pax ferry	9.78 x10^{-10}	0.00	0.00
Containership #1	4.69 x10^{-5}	4.43 x10^{-5}	0.00
Containership #2	1.37 x10^{-5}	1.59 x10^{-5}	0.00
Containership #3	6.75 x10^{-8}	8.19 x10^{-8}	8.47 x10^{-9}

Table 7.9: Insufficient Stability Event Index of all ships

	ISEI			
Sea direction	All direction	Heading	Beam	Following
Offshore Patrol Vessel	7.50 x10^{-3}	2.60 x10^{-3}	2.60 x10^{-3}	2.30 x10^{-3}
Ro-Ro pax ferry	0.00	0.00	0.00	0.00
Containership #1	2.40 x10^{-6}	1.40 x10^{-6}	1.00 x10^{-6}	0.00
Containership #2	1.41 x10^{-4}	2.50 x10^{-5}	1.10 x10^{-4}	5.70 x10^{-6}
Containership #3	1.42 x10^{-5}	4.60 x10^{-6}	9.30x10^{-6}	3.20 x10^{-7}

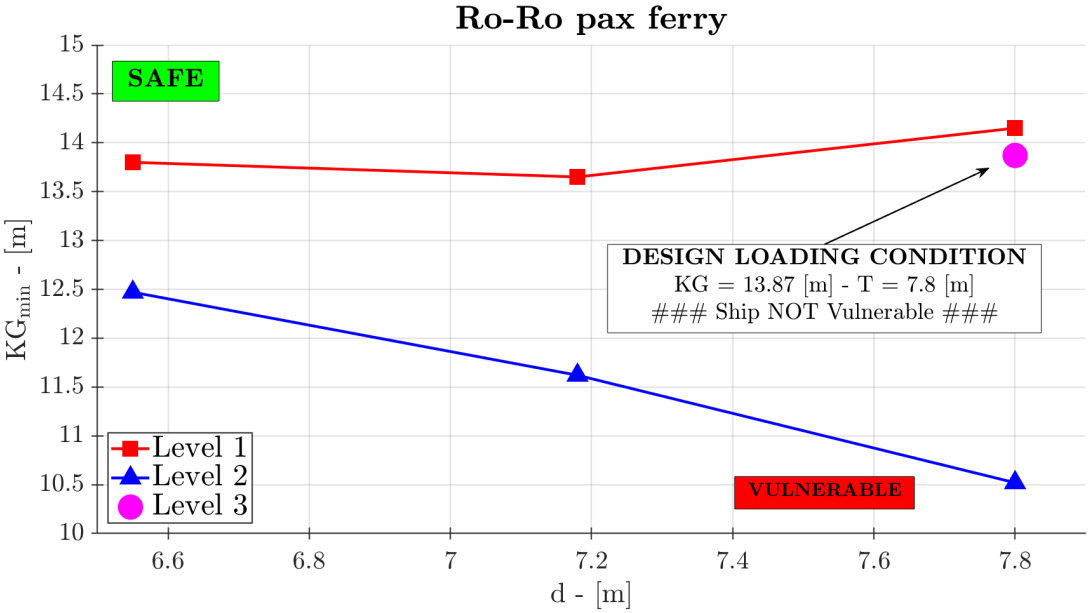

Figure 7.21: Ro-Ro pax ferry: Minimum KG according to SGISc

the ship performance in terms of vulnerability for the first two speeds (i.e. 0.0 and 3.0 knots) but this is not true for the third one (Fn = 0.216). The same comparison is done for the heading seas seaway: in this case there is no agreement between the two procedures. The Direct procedure points out that all ships do not suffer the excessive acceleration phenomenon in heading seas, whilst the ISEI results declare the ships as vulnerable excepting for the Ro-Ro pax ferry.

Stability Assessment VS Level 1 and Level 2

Coming back to the multi-layered approach at the base of SGISc, in this paragraph the results of the Level 1 and 2 are compared to those of Direct Stability Assessment, namely the Level 3. The scenario described in the first two levels of vulnerability considers a ship in zero-speed situation and a beam sea state; for this reason only the Direct procedure outcomes corresponding to this scenario are taken into account.

In Figure 7.21 and Figure 7.22, the limiting curves according to Level 1 and Level 2 of SGISc are shown for the OPV and the Ro-Ro pax ferry. On the

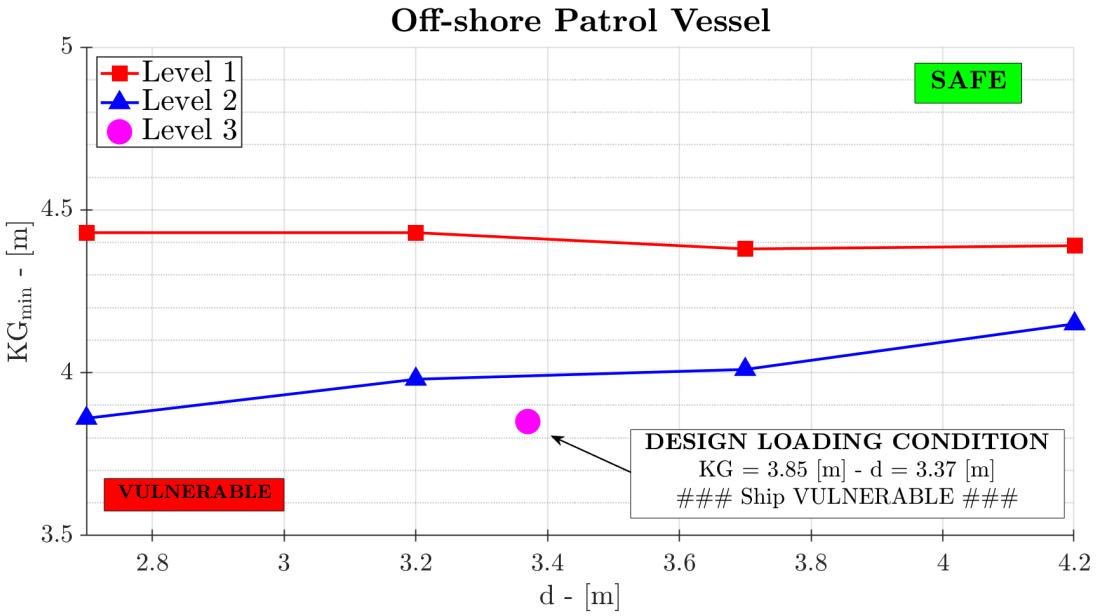

Figure 7.22: OPV: Minimum KG according to SGISc

horizontal axis the assessed draughts are reported, while the minimum permitted KG is reported on the vertical axis. The red limiting line is referred to the Level 1 of excessive acceleration while the blue line represents the Level 2. The outcomes of the Direct procedure are shown in the graph by means of a pink dot and a corresponding label. A ship is considered to be vulnerable to excessive acceleration failure if her vertical center of gravity stands below the limiting line. As concerns the first two levels of vulnerability, it appears that the relationship between them is in line with the multi-layered approach defined by the SGISc. The lower line in both cases is always represented by the first level of vulnerability, disclosing its higher severity. It is important to note that in the evaluation of roll damping the alternative procedure has been adopted in the evaluation of damping coefficient of Level 2, as stated by the code. The alternative procedure assumes the roll damping coefficient equal to those computed by the simplified Ikeda's method at 15° of heel angle and keeping fixed the value. Considering the third vulnerability level, also in this case what expected is confirmed by the results. The design loading condition referred to OPV is above the limiting curves, thus the ship should be considered vulnerable to the stability failure; this has been confirmed by the result of the Direct procedure. Regarding the loading condition analysed for the Ro-Ro pax ferry, it stands between the two limiting curves and it defines the vessel not vulnerable to excessive acceleration. In this case, the Direct procedure confirms what is stated by the Level 2. Moreover, it shows the greater severity of Level 1 due to the simplifications included within its structure.

Chapter 8

Discussion & Conclusions

The main goal of this thesis is the development and the application of a set of computational codes able to carry out a vulnerability assessment within the SGISc framework. They could become useful tools to analyse and study how the ship stability performance in a seaway, assessed by the criteria, can be affected by a selection of parameters which are the most important in the early design phases.

After an introduction where the regulatory context and a selection of real accidents are framed, a complete analysis of the physics at the basis of each stability failure and of the criteria structure has been carried out in Chapter 3. Once the criteria structure was tackled, the main part of the work is presented in Chapter 4: the flow chart of each computational tool is shown and the script functions, needed during the development process, are listed and explained. Moreover in Chapter 5, another in-depth analysis on the criteria has been addressed, focusing on the relationship between the input parameters and the final criterion. Chapter 6 summarizes the results of the application of the developed computational tools on a set of different typologies of vessel. An analysis on specific problems related to SGISc application is presented in Chapter 7 .

Finally, in this chapter a brief summary of the whole work carried out, toghether with an analysis of the achieved outcomes is given. In conclusion, an outlook on further possible improvements to the codes is attached.

8.1 Summary

In the latest years, a series of accidents all over the word put in evidence the need of new intact stability criteria. Vessels judged as safe by the current intact stability regulations were involved in serious accidents. The dynamics of incidents were investigated by the authorities and the outcomes point out that the current intact stability criteria cannot forecast and avoid the phenomena. New generation of vessels have been designed with hull shapes, dimensions and operability tasks setting a substantial gap with the most traditional ships. The need of new criteria able to describe the real physics of ship stability failures began to pool the experts' opinion. The methodology adopted by old criteria, which are based on empirical information and statistical records of previous accidents, is deemed to be not

sufficient anymore. In light of this, the IMO decided to revise the current Intact Stability code, during the Sub-Committee meetings were identified three main stability failures never addressed before:

- Restoring moment variation due to waves profile (parametric roll and pure loss of stability);
- Stability failure in the Dead Ship condition;
- Maneouvring-related stability failure (surf-riding/broaching-to).

Later, the excessive acceleration failure was introduced in the criteria development process. Since the relevance of the topic, an ad hoc working group was established with the aim to develop a set of new criteria, the so called Second Generation Intact Stability criteria. A fundamental disruption from the previous criteria is that the ship behaviour in a seaway condition has been considered and the effects of wave and hull interaction are tackled in detail. Another innovation introduced by the SGISc was the multi-tired approach: it consists of three different criteria with an increasing level of accuracy for each stability failures. The first two levels could be evaluated by computational tools using the available data in the early design phase. The third one consists in a direct stability assessment requiring detailed information of the project, and especially, a powerful tool able to simulate the ship dynamics with at least four degrees of freedom. Derived from the direct assessment, operational guidance or operational limitation could be issued. The first one defines a set of advice to the master on how to handle the vessel sailing in specific environmental conditions, while the operational limitation imposes constraint to the navigation, i.e. maximum permitted wave heights or other environmental restrictions.

After the five phenomena have been identified (i.e. parametric roll, pure loss of stability, surf-riding, dead ship condition and excessive acceleration) the working group started to develop the criteria structure for both the first and the second level. Not without difficulties, at the Sub-Committee meeting in early 2018 a complete version of all criteria has been presented and it is forecast to finalize and issue the final version of SGISc by the IMO meeting in 2020. It is worthwhile to mention that this thesis is based on the documents available up to the fifth SDC Sub-Committee session (January 2018).

Following an in depth analysis of the physics and criteria structure carried out in Chapter 3, a set of computational tools have been developed for all the criteria both the first and the second level. A flow chart for each tool has been drawn up in order to facilitate the writing process of the computational tools in Matlab® language. The choice of this programming software is based on the concept that Matlab® is widespread among UNIGE researchers but also because a Matlab® script able to compute the stability properties (hydrostatiscs and GZ calculation) considering the hull and wave interactions was already available within the University at the beginning of my Ph.D.

Once the computational tools have been developed, a campaign of applications on different hulls has been carried out in order to verify and validate them. In particular, a representative mega-yacht unit of about 70 (m) and a Ro-Ro pax

ferry have been assessed in a comprehensive way. With reference to this two units, the outcomes point out that some tuning operations on the criteria are needed, in fact for both vessels, the *design space* does not exist except for the first levels of Ro-Ro pax ferry. The *design space* is defined as the area where the combination of draughts and KG makes complying the vessel with all the criteria at the same time.

Another issue registered in the comparison of first and second level within the same stability failure is the consistency of the results. According to the multi-layered approach, the first level should be more severe than the second one, thus in the outcome representation by KG limit curves, it means that the first level maximum KG curve must be below the second level limit curve, vice-versa for the minimum KG curve; when this does not happen an inconsistency is registered. Inconsistencies between levels have been found in all the stability failures in the case of the mega-yacht unit, while the results are consistent only for the dead ship condition and parametric roll phenomena in the case of the Ro-Ro pax ferry.

As a further analysis, an useful tool already adopted in system engineering, has been applied to the SGISc: for each stability failure and level a DSM has been drawn up in order to reveal the relationship between parameters and, most important, to identify the main parameters which are considered to be relevant in the early design phase. Thanks to the application of DSM, each failure has been systematically analysed and a set of eight main influencing parameter has been selected, also in a transversal perspective among the different stability failures. By means of a set of parent hulls of the mega-yacht unit, the effects of a variation in breadth, draught and bilge keels area on the final criteria values have been studied. In order to quantify and compare each influence magnitude, a coefficient has been proposed, the so called K-index. As expected, it resulted that the modification in breadth is the most significant for all the phenomena assessed, with the lower influence on the excessive acceleration phenomenon. Regarding the draught and bilge keel area, their influences on the criteria in terms of absolute values appear to be limited, moreover the outcomes point out the inverse relationship between these parameters and the criteria. As a final comment to get advantage of such approach, it is important to keep in mind what follows: the criterion value, therefore the trend pointed out by the K-index, should be framed in the logic of comparison with the standard; e.g. for excessive acceleration and parametric roll, since the criterion should be lower than the respective standard to consider the ship not vulnerable, a negative sign of K-index means the ship improvement in her stability performance; the opposite for the dead ship condition and pure loss of stability failure.

Due to the need to find efficient tools to investigate dynamic stability in waves of navy vessels as stated in the Naval Ship code, the SGISc are applied to three different warships, i.e. a helicopter carrier, a destroyer and an OPV. A special attention is paid to the ship performance assessment for beam winds combined with ship rolling, since naval ships cannot limit in principle their operational profile because of weather and sea state adverse conditions. The application of the first vulnerability level criteria, for all the stability failure modes, to the three ships has evidenced the nearly equivalent level of safety of the present intact

stability rules for naval ships when compared with the SGISc curves. A critical issue is that the maximum KG curve for the excessive acceleration failure mode, when combined with other curves, practically limits the *design space* to a very narrow area, especially for the OPV. As regards the application of the second level vulnerability criterion for the dead ship condition stability failure, results give evidence about the higher severity of the criterion when compared with the one applied by the NSc. Also in this case, the excessive acceleration stability failure sets a severe constraint in the design of these ships. After a general analysis of navy vessels by SGISc, the destroyer unit has been selected to be assessed with the second level of surf-riding criterion. Considering the design service speed, the vessel has been judged vulnerable to this stability failure. Moreover, the influence of ship speed on the criterion value has been investigated by means of a sensitivity analysis: outcomes point out how the magnitude of the relationship between speed and criterion value is outstanding, in fact, a slightly variation of the Froude number leads to a huge variation of the criterion value.

Finally, two specific topics are investigated: the role of roll damping within the SGISc and an application of direct stability assessment for the excessive acceleration failure. As concerns the first topic, the Ikeda's prediction method, also in its simplified and revised versions have been studied. By the merge of the simplified and revised Ikeda's method, a blended prediction method has been formulated and applied to SGISc; in particular, second levels of parametric roll and dead ship condition are selected. The outcomes point out that the influence of the roll damping prediction method on the criterion value is very slightly and no relevant effects are registered.

The application of the direct stability assessment for the excessive acceleration failure has been carried out by means of the software developed at TUHH. The software is called *E4ROLLS*, it is able to simulate ship behaviour in six degrees of freedom, with the roll and surge motion modeled taking into account non-linearities. In this analysis, the OPV, the Ro-Ro pax ferry and three container-ships have been investigated. To evaluate the ship vulnerability, two procedures are considered, the first one was developed within the TUHH and it is called ISEI; the second procedure was presented at IMO meeting and it takes into account the average failure rate. The main difference in the two procedures is that the ISEI procedure carries out a widespread investigation considering a set of ship speeds and headings, while the average failure rate is computed only for a specific combination of speed and wave direction. In both the procedures, all the sea states included in the North Atlantic scatter diagram are considered. Outcomes show how for the beam seas condition all the vessels, except for the Ro-Ro pax ferry, are considered to be vulnerable for excessive acceleration failure at low speed. Increasing the speed, it appears that all the vessels become not vulnerable to the phenomenon, the same happens considering heading seas. This could be ascribable to an increase of roll damping, in particular for the roll damping lift component. As conclusion, the results of the average failure rate procedure for the Ro-Ro pax ferry and OPV in the design condition are compared to those obtained by the application of both first and second level of excessive acceleration failure. In order to better compare the direct assessment procedure with the vulnerability

levels, the same scenario is considered, i.e. the beam seas direction and zero speed condition. In this case, agreement in the vulnerability outcomes has been found: the average failure rate of the OPV confirms what point out by both the vulnerability levels; considering the Ro-Ro pax ferry as not vulnerable, the outcome of direct assessment confirms the second vulnerability level and retracts the first level result.

8.2 Contributions and outlooks

The development of a set of computational tools able to assess the ship stability performance is very important because it permits to further study the structure of each criterion applying them to real vessels. In fact, once the codes are developed, it has been possible to begin a campaign of application with the goal to investigate the influence of the new generation criteria on the vessel design. Carrying out systematic variations to a parent hull and applying the SGISc, it could be possible to define a database of information that might provide to the designer an important aid in the early phases of ship design. Moreover, the developed codes have been a useful tool to outline an insight view of the criteria structure, e.g. the relation between the first and second level and the roll damping prediction method. For example, the relevance of the environmental condition, represented by the wave scatter diagram table on the criteria values, might be interesting to investigate as well. Currently, the computational codes are not user friendly and a good knowledge about the SGISc and programming skills are required to work with them; further improvement of this aspect will be carried out. Besides, the modularity feature of each script should be enhanced, according to the concept introduced by the multi-layered approach.

Finally, probably the most important but for sure the most challenging further step will be to set the basis to develop a complete direct assessment tool. According to what published during the IMO meetings, the direct stability assessment tool should be able to simulate at least four degrees of freedom, taking into account non-linear coupling factors between motions. The development of this tool needs expertise on different branch of naval architecture and for sure, a deep knowledge about the most promising method to implement a well defined physically based ship performance model.

The analysis and investigations carried out during this PhD activity are based on the premises that some methodologies and criteria are to be developed to address the stability of a ship in a seaway. In fact, this is clearly stated in the first paragraphs of Intact Stability code. It is to be recognized that to this aim the researchers' community in the ship stability field has put a significant effort in the latest ten/fifteen years. The suitability of the SGISc to design safer ships is to be demonstrated in the following years by the applications of the ship designers' community. At present, the criteria will not be made mandatory nor included in the Part A of Intact Stability code, rather they will be issued as a suggested assessments and their application should be endorsed by IMO and other organizations. The application of the criteria on a wide amount of vessel typologies by ship designer as well as the collection of the obtained results by

interested organization will be, for sure, the best benchmark for the purpose of enhance the robustness of SGISc structure. Focusing on the results of the application of SGISc, it appears evident that there are inconsistencies between first and second levels for some vessels analyzed. In particular for the megayacht unit, the application of SGISc reports inconsistencies between vulnerability levels for all stability failures. In light of these results, it might be advisable that the SGISc are further refined in order to tune the standard thresholds making them applicable to all typologies of vessel.

Bibliography

[1] F. Grinnaert. *Analysis and implementation of Second generation criteria in a stability computer code.* PhD thesis, Université de Bretagne Occidentale, 2017.

[2] C.J. Söder. *Controlling the roll responses of volume carriers.* PhD thesis, KTH Royal Institute of Technology, 2017.

[3] IMCO. Recommendation on intact stability for passenger and cargo ships under 100 metres in length. Resolution A.167(AS.IV), Inter-Governmental Maritime Consultative Organization, London, UK, 1968.

[4] IMCO. Recommendation on intact stability of fishing vessels. Resolution A.168(ES.IV), Inter-Governmental Maritime Consultative Organization, London, UK, 1968.

[5] J. Rahola. *The judging of the stability of ships and the determination of the minimum amount of stability especially considering the vessels navigating Finnish waters.* PhD thesis, Technical University of Finland, Helsinki, Finland, 1939.

[6] IMO. Recommendation on a severe wind and rolling criterion (Weather Criterion) for the intact stability of passenger and cargo ships of 24 metres in length and over. Resolution A.562(14), International Maritime Organization, London, UK, 1982.

[7] IMO. Code on intact stability for all types of ships covered by IMO instruments. Resolution A.749(18), International Maritime Organization, London, UK, November 1982.

[8] IMO. Adoption of the international code on Intact Stability. Resolution MSC.267(85), International Maritime Organization, London, UK, December 2008.

[9] A. Francescutto. Intact stability criteria of ships - Past, present and future. *Ocean Engineering*, 120:312–317, 2016.

[10] L. Kobyliński. Stability Criteria - Present status and perspectives of improvement. *The internationa jurnal on marine navigation and safety of sea transportation*, 8(2), 2014.

[11] L. Kobyliński. Rational stability criteria and the probability of capsizing. In *Proceedings of* 1^{st} *International Ship Stability Workshop*, Glasgow, UK, 1975.

[12] A. Francescutto. Is it really impossible to design safe ships? *Transaction of Royal Institute of Naval Architect*, 135:163–173, 1993.

[13] K.J. Spyrou. Ship capsize assessment and non linear dynamics. In *Proceedings of the* 4^{th} *International Workshop Theoretical Advance in Ship Stability and Pratical Impact*, St John's, Canada, 1998.

[14] K.J. Spyrou and A.D. Papanikolaou. Ship design for dynamic stability. In *Proceedings of the* 7^{th} *International Marine Design Conference*, pages 167–178, Kyongju, Korea, 2000.

[15] SLF 48/4/7. Dynamic intact stability or stability problems in waves. Submitted by Germany, International Maritime Organization, London, UK, 2005.

[16] SLF 48/WP.2. Review of the Intact Stability code. Report of the working group (part 1), International Maritime Organization, London, UK, 2005.

[17] SLF 52/WP.1. Development of new generation intact stability criteria. Report of the working group (part 1), International Maritime Organization, London, UK, 2010.

[18] IMO. Guidance to the master for avoiding dangerous situations in following and quartering seas. Circular MSC/707, International Maritime Organization, London, UK, October 1995.

[19] IMO. Revised guidance to the master for avoiding dangerous situations in adverse weather and sea conditions. Circular MSC.1/1228, International Maritime Organization, London, UK, January 2007.

[20] SLF 52/17. Report to the Maritime Safety Committe. Report, International Maritime Organization, London, UK, 2008.

[21] SLF 53/3/5. Comments on the structure of new generation intact stability criteria. Submitted by Poland, International Maritime Organization, London, UK, 2010.

[22] SLF 53/19. Report to the Maritime Safety Committee. Report, International Maritime Organization, London, UK, 2010.

[23] SLF 53/INF.8. Sample calculations on the Level 2 Vulnerability criteria for parametric roll. Submitted by Sweden, International Maritime Organization, London, UK, 2010.

[24] SLF 54/3/5. Sample verification and proposal of draft Level 1 criteria on parametric roll and pure loss of stability. Submitted by China, International Maritime Organization, London, UK, 2011.

[25] SLF 55/INF.5. Sample calculations for level 1 and level 2 vulnerability criteria. Submitted by Germany, International Maritime Organization, London, UK, 2012.

[26] SLF 55/INF.14. Verification of the draft Levels 1 and 2 vulnerability criteria for parametric rolling and pure loss of stability. Submitted by IACS, International Maritime Organization, London, UK, 2012.

[27] SDC 1/INF.8. Information collected by the Correspondence Group on Intact Stability regarding the second generation intact stability criteria development. Submitted by japan, International Maritime Organization, London, UK, 2013.

[28] S. Krüger and H. Hatecke. The impact of the 2nd generation of intact stability criteria on RoRo - ship design. In *Proceedings of the* 12^{nd} *International Symposium on Practical Design of Ships and other Floating Structures*, pages 641–649, Changwon city, Korea, October 2013.

[29] S. Krüger et al. Investigation of the 2nd generation of intact stability criteria for ships vulnerable to parametric rolling in following seas. In *Proceedings of the* 32^{nd} *International Conference on Ocean, Offshore and Artic Engineering*, Nantes, France, June 2013.

[30] SLF 54/WP.3. Development of second generation intact stability criteria and any other business. Report of the working group (part 1), International Maritime Organization, London, UK, 2012.

[31] SDC 2/WP.4. Development of Second Generation Intact Stability criteria. Report of the working group, International Maritime Organization, London, UK, 2015.

[32] SDC 3/WP.5. Finalization of Second Generation Intact Stability criteria. Report of the working group, International Maritime Organization, London, UK, 2016.

[33] SDC 4/5/1. Finalization of Second Generation Intact Stability Criteria - Report of the correspondence group. Submitted by Japan, International Maritime Organization, London, UK, 2016.

[34] SDC 4/INF.4/Add.2. Information collected by the Correspondence Group on Intact Stability (part 3). Submitted by japan, International Maritime Organization, London, UK, 2016.

[35] SDC 4/INF. 8. Direct stability assessment - Information for further discussion. Submitted by germany, International Maritime Organization, London, UK, 2016.

[36] SDC 4/WP. 4. Draft guidelines of direct stability assessment procedures for use with the second generation intact stability criteria. Report of the working group, International Maritime Organization, London, UK, 2016.

[37] SDC 5/15. Report to the Maritime Safety Committee. Report, International Maritime Organization, London, UK, 2018.

[38] SLF 52/WP.2. Revision of the Intact Stability code. Report of the working group (part 1), International Maritime Organization, London, UK, 2008.

[39] SLF 55/3/7. Comments on present status of development of second generation intact stability criteria. Submitted by Italy, International Maritime Organization, London, UK, 2013.

[40] SDC 3/INF.10. Information collected by the Correspondence Group on Intact Stability regarding second generation intact stability criteria. Submitted by japan, International Maritime Organization, London, UK, 2015.

[41] S. Krüger. Evaluation of the cargo loss of a large container vessel due to parametric roll. In *Proceedings of the* 9^{th} *International Marine Design Conference*, Michigan, USA, 2006.

[42] SLF 54/INF.6. Theoretical investigation into the loss of containers of the Pacific Adventurer off Cape Morton Queensland. Submitted by Germany, International Maritime Organization, London, UK, 2011.

[43] Federal Bureau of Marine Casualty Investigation. Fatal accident on board the CMV CCNI GUAYAS during Typhoon 'KOPPU' on 15 September 2009 in the sea area off Hong Kong. Investigation Report 391/09, Federal Higher Authority subordinated to Ministry of Transport, Hamburg, Germany, June 2011.

[44] W.N. France et al. An investigation of head-sea parametric rolling and its influence on container lashing systems. *Marine Technology*, 40(1):1–19, 2003.

[45] Federal Bureau of Marine Casualty Investigation. Fatal accident on board the CMV CHICAGO EXPRESS during Typhoon 'HAGUPIT' on 24 September 2008 off the coast of Hong Kong. Investigation Report 510/08, Federal Higher Authority subordinated to Ministry of Transport, Hamburg, Germany, November 2009.

[46] Federal Bureau of Marine Casualty Investigation. Loss overboard of 10 containers from JRS CANIS at estuary of Elbe River on 12 January 2007 at 02:40. Investigation Report 45/07, Federal Higher Authority subordinated to Ministry of Transport, Hamburg, Germany, October 2008.

[47] V. Belenky, J.O. de Kat, and N. Umeda. Toward performance-based criteria for intact stability. *Marine Technology*, 45(2):101–120, 2008.

[48] V. Belenky, C.C. Bassler, and K.J. Spyrou. Development of second generation intact stability criteria. Hydromechanics Department Report, Naval Warfare Center Carderock Division, Carderock, USA, 2011.

[49] A. Francescutto and N. Umeda. Current status of new generation intact stability criteria development. In *Proceedings of* 11^{st} *International Ship Stability Workshop*, Wageningen, The Netherlands, 2011.

[50] N. Umeda. Current status of second generation intact stability criteria development and some recent efforts. In *Proceedings of* 13^{rd} *International Ship Stability Workshop*, Brest, France, 2013.

[51] C.C. Bassler et al. A review of available methods for application to second level vulnerability criteria. In *Proceedings of* 10^{st} *International Ship Stability Workshop*, Daejeon, Korea, 2008.

[52] M. Hamamoto and K. Nomoto. Transverse stability of ships in a following seas. In *Proceedings of* 2^{nd} *International Conference on the Stability of Ships and Ocean Vehicles*, Tokyo, Japan, 1982.

[53] G. Helas. Intact stability of ships in following waves. In *Proceedings of* 2^{nd} *International Conference on the Stability of Ships and Ocean Vehicles*, Tokyo, Japan, 1982.

[54] J.R. Paulling. The transverse stability of a ship in a longitudinal seaway. *Journal of Ship Research*, 4(4), 1961.

[55] Y. Watanabe. On the dynamic properties of the transverse instability of a ship due to pitching. *Journal of the Society of Naval Architects of Japan*, 53, 1934.

[56] J.R. Paulling, O.H. Oakley, and P.D. Wood. Ship motions and capsizing in astern seas. In *Proceedings of* 10^{th} *Symposium on Naval Hydrodynamics*, Office of Naval research, MIT, 1974.

[57] J.R. Paulling, O.H. Oakley, and P.D. Wood. Ship capsizing in heavy seas: the correlation of theory and experiments. In *Proceedings of* 1^{th} *International Conference on the Stability of Ships and Ocean Vehicles*, Glasgow, UK, 1975.

[58] L. Kobyliński and S. Kastner. *Stability and Safety of ships: Regulation and Operation*, volume 9. Elsevier Science, first edition, 2003.

[59] Nechaev, Yu.I. Stability of Ships in Following seas. Document in russian, Sudostroenie Publishing, Leningrad, Russia, 1978.

[60] V.L. Belenky and N.B. Sevastianov. *Stability and Safety of ships: Risk of Capsizing.* The Society of Naval Architects and Marine Engineers, second edition, 2007.

[61] O. Grim. Beitrag zu dem Problem der Sicherheit des Schiffes im Seegang. *Schiff und Hafen*, 6, 1961.

[62] G. Bulian. On an improved grim effective wave. *Ocean Engineering*, 35:1811–1825, 2008.

[63] N. Umeda and Y. Yamakoshi. Experimental study on pure loss of stability in regular and irregular following seas. In *Proceedings of* 3^{nd} *International Conference on the Stability of Ships and Ocean Vehicles*, Gdansk, Poland, 1986.

[64] H. Vermeer. Loss of stability of ships in following waves in relation to their design characteristics. In *Proceedings of* 4^{th} *International Conference on the Stability of Ships and Ocean Vehicles*, Naples, Italy, 1990.

[65] SLF 54/3/8. Level 1 assessment of parametric roll - direct calculation of GM variation in regular waves. Submitted by SYBAss, International Maritime Organization, London, UK, 2011.

[66] F. Grinnaert et al. Application of 2^{nd} generation intact stability criteria on naval ships. In *Proceedings of the* 15^{th} *International Ship Stability Workshop*, Stockholm, Sweden, 2016.

[67] M.M. González et al. Application of Second Generation IMO Intact Stability Criteria to medium-sized fishing vessels. In *Proceedings of* 14^{st} *International Conference on the Stability of Ships and Ocean Vehicles*, pages 269–277, Kuala Lumpur, Malaysia, September 2014.

[68] SLF 53/INF.10. Information collected by the Correspondence Group on Intact Stability. Submitted by Japan, International Maritime Organization, London, UK, 2010.

[69] N. Umeda and Y. Yamakoshi. Probability of ship capsizing due to pure loss of stability in quartering seas. *Naval Architecture and Ocean Engineering*, 30:73–85, 1992.

[70] H. Hashimoto. Pure loss of stability of a tumblehome hull in following seas. In *Proceedings of the* 19^{th} *International Offshore and Polar Engineering Conference*, volume 3, pages 626–631, 2009.

[71] SLF 55/INF.15. Information collected by the intersessional Correspondence Group on Intact Stability. Submitted by Japan, International Maritime Organization, London, UK, 2012.

[72] W. Froude. On the rolling of ships. *Transaction of the Institution of Naval Architects*, 2:180–227, 1861.

[73] A. Pollard, J.and Dudebout. Theorie du Navire. Paris, France, 1892.

[74] J.R. Paulling. On parametric rolling of ships. In *Proceedings of* 10^{th} *Intl. Symp. on Practical Design of Ships and Other Floating Structures*, Huston, USA, 2007.

[75] J.R. Paulling. Parametric rolling of ships – Then and Nows. In M.A.S. Neves, V. Belenky, J. de Kat, K. Spyrou, and N. Umeda, editors, *Contemporary Ideas on Ship Stability and Capsizing in Wave*, volume 93 of *Fluid Mechanics and Its Applications*. Springer, Dordrecht, NL, 2011.

[76] J.R. Paulling and R.M. Rosenberg. On unstable ship motions resulting from nonlinear coupling. *Journal of Ship Research*, 3(1):36–46, 1959.

[77] R.P. Dallinga. Hydromechanic aspects of the design of fin stabilisers. In *Proceedings of International Conference on Ship Motion & Manoeuvrability*, London, UK, 1993.

[78] W.S. Peters, V. Belenky, and C.C. Bassler. On vulnerability criteria for righting lever variations in waves. In *Proceedings of* 11^{th} *International Ship Stability Workshop*, Wageningen, The Netherlands, 2010.

[79] SLF 52/INF.2. Information collected by the intersessional Correspondence Group on Intact Stability. Submitted by Japan, International Maritime Organization, London, UK, 2009.

[80] SLF 54/INF.12. Information collected by the intersessional Correspondence Group on Intact Stability. Submitted by Japan, International Maritime Organization, London, UK, 2011.

[81] P. Du Cane and G.J. Goodrich. The following sea, broaching and surging. *Transactions of Royal Institution of Naval Architects*, 104(2):109–140, 1962.

[82] S. Motora, M. Fujino, and T. Fuwa. Mechanism of broaching-to phenomena. In *Proceedings of* 2^{nd} *International Conference on the Stability of Ships and Ocean Vehicles*, pages 535–550, Tokyo, Japan, 1982.

[83] P. Boese. Steuern eines Schiffes im schweren achterlichen Seegang. *JSTG*, 63:337–355, 1969.

[84] O. Grim. Das Schiff in von achtern kommenden Seegang. *JSTG*, 30:84–94, 1983.

[85] M. Kan. Guidelines to avoid the dangerous surf riding. In *Proceedings of* 4^{th} *International Conference on the Stability of Ships and Ocean Vehicles*, Naples, Italy, 1990.

[86] N. Umeda et al. Broaching prediction in the light of an enhanced mathematical model, with higher order terms taken into account. *Journal of Marine Science and Technology*, 145(7):145–155, 2003.

[87] Z. Ayaz, D. Vassalos, and K.J. Spyrou. Manoeuvring behavior of ships in extreme astern seas. *Ocean Engineering*, 33(17-18):2381–2434, 2005.

[88] R. Skejic and O.M. Faltinsen. A unified seakeeping and manoeuvring analysis of ships in regular waves. *Journal of Marine Science and Technology*, 13(4):371–394, 2008.

[89] B. Horel et al. Experimental database for surf-riding and broaching-to quantification based on captive model tests in waves. In *Proceedings of* 14^{st} *International Conference on the Stability of Ships and Ocean Vehicles*, pages 94–104, Kuala Lumpur, Malaysia, September 2014.

[90] N. Umeda et al. Stability assessment for intact ships in the light of model experiments. *Journal of Marine Science and Technology*, 45(4):45–57, 1999.

[91] M.R. Renilson. An investigation into the factors affecting the likelihood of broaching-to in following seas. In *Proceedings of* 2^{nd} *International Conference on the Stability of Ships and Ocean Vehicles*, pages 551–564, Tokyo, Japan, 1982.

[92] N. Umeda et al. Model experiments on extreme motions of a wave-piercing tumblehome vessel in following and quartering waves. *Journal of the Japan Society of Naval Architects and Ocean Engineers*, 8:123–129, January 2008.

[93] S. Hosseini et al. Cfd, system-based and efd study of ship dynamic instability events: Surf-ridings, periodic motion and broaching. *Ocean Engineering*, 38(1):88–110, 2010.

[94] H. Hashimoto, N. Umeda, and A. Matsuda. Broaching prediction of a wave-piercing tumblehome vessel with twin screws and twin rudders. *Journal of Marine Science and Technology*, 16(4):448–461, 2011.

[95] K.J. Spyrou. Surf-riding, yaw instability and large heeling of ships in following/quartering waves. *Shiffstechnik*, 42(2):103–112, 1995.

[96] Y. Makov. Some results of theoretical analysis of surf-riding in following seas. *Transactions of the Krylov Society*, 126:124–128, 1969. (In Russian).

[97] K.J. Spyrou. Surf-riding and oscillations of a ship in quartering seas. *Journal of Marine Science and Technology*, 1:24–36, 1995.

[98] K.J. Spyrou. Dynamic instability in quartering seas: the behaviour of a ship during broaching. *Journal of Ship Research*, 40(1):46–59, 1996.

[99] T. Tsuchiya. An approach for treating stability of fishing boats. In *Proceedings of* 1^{nd} *International Conference on the Stability of Ships and Ocean Vehicles*, pages 1–9, Glasgow, UK, 1975.

[100] Y. Watanabe et al. A proposed standard of stability for passenger ships (part iii: Ocean-going and coasting ships). *Journal of Society of Naval Architects of Japan*, 99:29–46, 1956.

[101] M. Yamagata. Standard of stability adopted in japan. *Transactions of Institution of Naval Architects*, 101:417–443, 1959.

[102] Register of Shipping of the USSR. Standards of stability of sea-going vessels and coasters. Technical report, Mosrskoi Transport, Moscow, RU, 1961. Also available in IMCO STAB/77, USSR (1979).

[103] L.L. Goldberg and T.H. Sarchin. Stability and buoyancy criteria for u.s. naval surface ships. *Transactions of American Society of Naval Architects and Marine Engineers*, 70:418–458, 1962.

[104] L.K. Kobyliński and S. Kastner. *Stability and safety of ships*, volume 1. Elsevier, Oxford, UK, 2003.

[105] IMO. Interim guidelines for alternative assessment of the weather criterion. Circular MSC.1/1200, International Maritime Organization, London, UK, May 2006.

[106] A.G. Davenport. The spectrum of horizontal gustiness near the ground in strong wnids. *Journal of the Royal Meteorological Society*, 87:194–211, April 1961.

[107] Y. Kawahara, K. Maekawa, and Y. Ikeda. A simple prediction formula of roll damping of conventional cargo ships on the basis of ikeda's method and its limitation. In *Proceedings of* 10^{th} *International Conference on Stability of Ships and Ocean Vehicles*, St. Petersburg, Russia, 2009.

[108] E. Perrottet. A standard of stability for ships. *Transaction of the Institution of Naval Architects*, page 208, 1935.

[109] IMO. Explanatory notes to the international code on intact stability. Circular MSC.1/1281, International Maritime Organization, London, UK, December 2008.

[110] SLF 48/4/6. A modular methodology for the estimation of the ship roll safety under the action of stochastic wind and waves. Submitted by Italy, International Maritime Organization, London, UK, 2005.

[111] G. Bulian and A. Francescutto. A simplified modular approach for the prediction of the roll motion due to the combined action of wind and waves. *Proc. Instn Mech. Engrs, Vol. 218, Part M - Journal of Engineering for the Maritime Environment*, pages 189–212, 2004.

[112] A. Cardo, A. Francescutto, and R. Nabergoj. On damping models in free and forced rolling motions. *Ocean Engineering*, 9:171–179, 1982.

[113] Y. Ogawa. A study for the effect of correlation between winds and waves on the capsizing probability under dead ship condition. In *Proceedings of* 10^{th} *International Conference on Stability of Ships and Ocean Vehicles*, St. Petersburg, Russia, 2009.

[114] A. Francescutto et al. Experiment-support weather criterion and its design impact on large passenger ships. In *Proceedings of* 2^{nd} *International Maritime Conference on Design for Safety*, Sakai, Japan, October 2004.

[115] H. Parkus. *Random process in mechanical sciences*. Springer-Verlag Wien, 1969.

[116] A.H.S. Ang and W.H. Tang. Basic principles. In *Probability concepts in Engineering Planning and Design*, volume 1. John Wiley and Sons, 1984.

[117] S.H. Crandall and W.D. Mark. *Random vibration in mechanical system.* Academic Press, New York, USA, 1973.

[118] G. Bulian and A. Francescutto. Safety and operability of fishing vessels in beam and longitudinal waves. *International Journal of small craft technology*, 148(2):1–16, 2006. Transaction of the Royal Institution of Naval Architects - Part B.

[119] G. Bulian, A. Francescutto, and A. Maccari. Possible simplified mathematical model for roll motion in the development of performance-based intact stability criteria - Extended and revised version. Quaderno di Dipartimento 46, University of Trieste - DINMA, Trieste, Italy, January 2008.

[120] SLF 52/3/5. Proposal with regard to the scope of new generation criteria. Submitted by Germany, International Maritime Organization, London, UK, 2009.

[121] J.L. Colwell. Human factors in the naval environment: a review of motion sickness and biodynamic problems. DREA Technical memorandum 89/220, Canadian National Defence Research Establishment Atlantic, Dartmouth, Canada, November 1989.

[122] S.C. Stevens and M.G. Parsons. Effects of motion at sea on crew performance: a survey. *Marine Technology*, 39(1):29–47, 2002.

[123] A. Scamardella and V. Piscopo. Passenger ship seakeeping optimization by the overall motion sickness incidence. *Ocean Engineering*, 76:86–97, 2014.

[124] T.A. Applebee, T.M. McNamara, and A.E. Baitis. Investigation into the seakeeping characteristics of the US Coast Guard 140-ft WTGB class Cutters: Sea trial aboard the USCGC MOBILE BAY. NCRDC Report SPD 0938-01, Naval Ship Research and Development Center, Bethesda, USA, March 1980.

[125] A.E. Baitis, T.A. Applebee, and T.M. McNamara. Rudder roll stabilization for coast guard cutters and frigates. *Naval Engineers Journal*, 95(3):267–282, 1983.

[126] A.E. Baitis, T.A. Applebee, and T.M. McNamara. Human factors considerations applied to the operations of the FFG-8 and LAMPS Mk III. *Naval Engineers Journal*, 97(4), 1984.

[127] F. Warhurst and A.J. Cerasani. Evaluation of the performance of human operators as a function of ship motion. ELECLAB Report 225/68, Naval Ship Research and Development Laboratory, Maryland, USA, April 1969.

[128] S.F. Wiker, R.L. Pepper, and M.E. McCauley. A vessel class comparison of physiological, affective state and psychomotor performance changes in men at sea. Report USCG-D-07-81, US Coast Guard, USA, August 1980.

[129] J.P. O'Hanlon and M.E. McCauley. Motion sickness incidence as a function of the frequency and acceleration of vertical sinusoidal motion. Technical Report 1733-1, Human Factors Research division, Goleta, USA, September 1973.

[130] M.E. McCauley et al. Motion sickness incidence: Exploratory studies of habituation, pitch and roll, and the refinement of a mathematical model. Technical Report 1733-2, Human Factors Research division, Goleta, USA, April 1976.

[131] V.L. Lewis, editor. *Principles of Naval Architecture*, volume III. The Society of Naval Architects and Marine Engineers, second edition, 1988.

[132] A.R.J.M. Lloyd. *Seakeeping : ship behaviour in rough weather*. Ervis Horwood limited, 1989.

[133] R. Bhattacharyya. *Dynamics of marine vehicles*. John Wiley & Sons Ltd., 1978.

[134] ITTC Seakeeping Committee. Seakeeping experiments. Recommended procedures and guidelines 7.5-02-07-02.1, International Towing Tank Conference, 2017.

[135] A. Coraddu, P. Gualeni, and D. Villa. Vulnerability assessment for the loss of stability in waves: some application cases for a further insight into the problem. In *Proceedings of* 11^{st} *International Conference on the Stability of Ships and Ocean Vehicles*, Athens, Greece, 2012.

[136] N. Petacco and P. Gualeni. Second generation intact stability criteria for mega-yachts: application and design consideration. In *Proceedings of* 3^{rd} *International Conference on Maritime Technology and Engineering*, Lisbon, Portugal, 2016.

[137] ITTC Stability Committee. Numerical estimation of roll damping. Recommended procedures and guidelines 7.5-02-07-04.5, International Towing Tank Conference, 2011.

[138] L. Qiao and M. Ryan. Applying the design structure matrix (DSM) to SAR satellite formation flying design. In *Proceedings of System Engineering and Test & Evaluation conference*, Canberra, Australia, 2015.

[139] J. Bartolomei et al. *Analysis and applications of design structure matrix, domain mapping matrix and engineering system matrix frameworks*. Massachussetts Institute of Technology, MIT, USA, 2007.

[140] Ş.T. Petkaş and M. Pultar. Modelling detailed information flows in building design with the parameter-based design structure matrix. *Design Studies*, 27(1):99–122, 2006.

[141] S.D. Eppinger and T.R. Browning. *Design structure matrix methods and applications*. The MIT press, 2012.

[142] A.A. Yassine. An introduction to modelling and analyzing complex product development processes using the design structure matrix (DSM) method. In *Maine IEEE/PMI joint meeting*, USA, 2002.

[143] D.C. Wynn et al. An introduction to the cambridge advanced modeller. In *Proceedings of* 1^{st} *International Conference on Modelling and Management of Engineering Processes*, Cambridge, UK, 2010.

[144] N. Petacco and P. Gualeni. IMO second generation intact stability criteria: Application to a set of mega-yacht parent hulls in a ship design perspective. In *Design & Construction of Super & Mega Yachts*, Genoa, Italy, 2017.

[145] M. Tosi, P. Gualeni, and N. Petacco. *CRITERI DI STABILITÀ ALLO STATO INTEGRO DI SECONDA GENERAZIONE: Applicazione del primo livello di verifica per il fenomeno di Excessive Acceleration ad unità megayacht.* M.Sc. Thesis in yacht design, Università degli studi di Genova, 2017.

[146] SDC 1/5/2. Sample calculation results of the proposed second-generation intact stability criteria regarding the failure modes Parametric Rolling, Pure Loss of Stability (Levels 1 and 2) and Broaching (Level 1). Submitted by germany, International Maritime Organization, London, UK, 2013.

[147] SDC 4/INF. 5. Supplementary sample ship matrix calculations for parametric rolling, pure loss of stability and excessive acceleration criteria. Submitted by china, International Maritime Organization, London, UK, 2016.

[148] N. Petacco and P. Gualeni. A system approach for second generation intact stability criteria compliance. In *Proceedings of* 13^{rd} *International Conference on the Stability of Ships and Ocean Vehicles*, Kobe, Japan, 2018.

[149] A.M. Reed. A naval perspective on ship stability. In *Proceedings of the* 10^{th} *International Conference on the Stability of Ships and Ocean Vehicles*, St. Petersburg, Russia, 2009.

[150] A. Peters. Tolerable capsize risk of a naval vessel. In *Proceedings of the* 11^{th} *International Ship Stability Workshop*, Wageningen, The Netherlands, 2010.

[151] D. Tellet. Incorporating risk into naval ship weight and stability control. In *Proceedings of the* 12^{th} *International Ship Stability Workshop*, Washington, USA, 2011.

[152] NATO. Nato standard naval ship sode. Intact stability regulations Anep 77 - edition E - version 1, NATO Standardization Agency (NSA), 2014.

[153] D. Perrault. Examination of the probability results for extreme roll of naval vessels. In *Proceedings of the* 13^{th} *International Ship Stability Workshop*, Brest, France, 2013.

[154] B. Beaupuy et al. Operability of french naval ships over 50 years. In *Proceedings of the* 11^{th} *International Conference on the Stability of Ships and Ocean Vehicles*, Athens, Greece, 2012.

[155] P.R. Alman. Approaches for evaluating dynamic stability in design. In *Proceedings of the* 11^{th} *International Ship Stability Workshop*, Wageningen, The Netherlands, 2010.

[156] N. Petacco et al. An integration of present navy ships intact stability criteria in the perspective of ship performance assessment in a seaway. In *Proceedings of* 16^{th} *International Ship Stability Workshop*, Belgrade, Serbia, 2017.

[157] H. Tomaszek and C.C. Bassler. Dynamic stability assessment of naval ships in early-stage design. In *Proceedings of the* 12^{th} *International Conference on the Stability of Ships and Ocean Vehicles*, Glasgow, UK, 2015.

[158] Naval Sea System Command. Design practices and criteria for U.S. Navy surface ship stability and reserve buoyancy. Intact stability regulations T9070-AF-DPC-010/079, Ministry of Defense, 2016.

[159] UK-MOD. Stability standards for surface ships - part 1 - conventional ships. Intact stability regulations NES 109, Ministry of Defense, 2000.

[160] FR-MOD. Stabilité des batiments de surface de la marine nationale. Intact stability regulations N° 6018 A, Ministry of Defense, 1999.

[161] IT-MOD. Norme per la stabilità e la riserva di galleggiabilità delle navi di superficie. Intact stability regulations NAV-04-A013, Ministry of Defense, 1980.

[162] R. Luquet et al. Aerodynamics loads on a heeled ship. In *Proceedings of the* 12^{th} *International Conference on the Stability of Ships and Ocean Vehicles*, Glasgow, UK, 2015.

[163] A. Ariffin, S. Mansor, and J.M. Laurens. Conduction of a wind tunnel experiment to investigate the ship stability weather criterion. In *Proceedings of the* 15^{th} *International Ship Stability Workshop*, Stockholm, Sweden, 2016.

[164] P.R. Alman. Thoughts on integrating stability into risk based methods for naval ship design. In *Proceedings of the* 12^{th} *International Ship Stability Workshop*, Washington, USA, 2011.

[165] A.G. Di Mare, P. Gualeni, and N. Petacco. *I criteri di stabilità allo stato integro di seconda generazione: sviluppo e applicazione di un metodo per la verificia relativa al fenomeno di surf-riding/broaching.* M.Sc. Thesis in naval architecture and marine engineering, Università degli studi di Genova, 2017.

[166] H.P. Phiel. *Ship roll damping analysis.* PhD thesis, Universität Duisburg Essen, April 2016.

[167] Y. Ikeda, Y. Himeno, and N. Tanaka. A prediction method for ship roll damping. Report 45, University of Osaka, Osaka, Japan, 1978.

[168] Y. Himeno. Prediction of ship roll damping - state of the art. Report 239, Department of Naval Architecture and Marine Engineering - University of Michigan, Michigan, USA, 1981.

[169] C.J. Söder, A. Rosén, and M. Huss. Ikeda revisited. *Journal of Marine Science and Technology*, pages 1–11, November 2017.

[170] A. Pollicardo, P. Gualeni, and N. Petacco. *Second Generation Intact Stability criteria: Analysis and Application with Specific Reference to Roll Damping.* M.Sc. Thesis in naval architecture and marine engineering, Università degli studi di Genova, 2018.

[171] H. Söding. Gutachten über die Belastungen des Schiffes E.L.M.A. Tres durch Seegang am Vormittag des 26.11.1981. Report No. 2327, Technische Universität Hamburg-Harburg, Hamburg, Germany, 1982.

[172] P. Kröger. Simulation der Rollbewegung von Schiffen. Technical report, Technische Universität Hamburg-Harburg, Hamburg, Germany, 1987.

[173] F. Petey. Ermittlung der Kentersicherheit lecker Schiffe im Seegang aus Bewegungssimulationen. Technical report, Technische Universität Hamburg-Harburg, Hamburg, Germany, 1988.

[174] H. Söding et al. Method ROLLS for simulating roll motions of ships. *Ship Technology Research*, 60(2):70–84, 2013.

[175] TUHH/M6. *Analysis of seakeeping for surface condition.* Hamburg, Germany.

[176] N. Rox. *Examination of the intact stability and the stability behaviour of container vessels within the ballast condition.* PhD thesis, Technische Universität Hamburg-Harburg, 2010.

[177] SDC 5/6/13. Comments on document 5/6 - Application example of direct stability assessment for excessive aceleration failure mode. Submitted by japan, International Maritime Organization, London, UK, 2017.

[178] F. Kluwe. Development of a minimum stability criterion to prevent large amplitude roll motions in following seas. Master's thesis, Technische Universität Hamburg-Harburg, 2009.

[179] H. Söding. Global seaway statistics. *Schriftenreihe Shiffbau*, 48:147–153, 2001.

Appendix A

North Atlantic Wave Scatter Diagram

Table A.1: North Atlantic wave scatter diagram - IACS Recommendation N° 34

	T_z (s) = average zero up-crossing wave period																	
H_s	1,5	2,5	3,5	4,5	5,5	6,5	7,5	8,5	9,5	10,5	11,5	12,5	13,5	14,5	15,5	16,5	17,5	18,5
0,5	0,0	0,0	1,3	133,7	865,6	1186,0	634,2	186,3	36,9	5,6	0,7	0,1	0,0	0,0	0,0	0,0	0,0	0,0
1,5	0,0	0,0	0,0	29,3	986,0	4976,0	7738,0	5569,7	2375,7	703,5	160,7	30,5	5,1	0,8	0,1	0,0	0,0	0,0
2,5	0,0	0,0	0,0	2,2	197,5	2158,8	6230,0	7449,5	4860,4	2066,0	644,5	160,2	33,7	6,3	1,1	0,2	0,0	0,0
3,5	0,0	0,0	0,0	0,2	34,9	695,5	3226,5	5675,0	5099,1	2838,0	1114,1	337,7	84,3	18,2	3,5	0,6	0,1	0,0
4,5	0,0	0,0	0,0	0,0	6,0	196,1	1354,3	3288,5	3857,5	2685,5	1275,2	455,1	130,9	31,9	6,9	1,3	0,2	0,0
5,5	0,0	0,0	0,0	0,0	1,0	51,0	498,4	1602,9	2372,7	2008,3	1126,0	463,6	150,9	41,0	9,7	2,1	0,4	0,1
6,5	0,0	0,0	0,0	0,0	0,2	12,6	167,0	690,3	1257,9	1268,6	825,9	386,8	140,8	42,2	10,9	2,5	0,5	0,1
7,5	0,0	0,0	0,0	0,0	0,0	3,0	52,1	270,1	594,4	703,2	524,9	276,7	111,7	36,7	10,2	2,5	0,6	0,1
8,5	0,0	0,0	0,0	0,0	0,0	0,7	15,4	97,9	255,9	350,6	296,9	174,6	77,6	27,7	8,4	2,2	0,5	0,1
9,5	0,0	0,0	0,0	0,0	0,0	0,2	4,3	33,2	101,9	159,9	152,2	99,2	48,3	18,7	6,1	1,7	0,4	0,1
10,5	0,0	0,0	0,0	0,0	0,0	0,0	1,2	10,7	37,9	67,5	71,7	51,5	27,3	11,4	4,0	1,2	0,3	0,1
11,5	0,0	0,0	0,0	0,0	0,0	0,0	0,3	3,3	13,3	26,6	31,4	24,7	14,2	6,4	2,4	0,7	0,2	0,1
12,5	0,0	0,0	0,0	0,0	0,0	0,0	0,1	1,0	4,4	9,9	12,8	11,0	6,8	3,3	1,3	0,4	0,1	0,0
13,5	0,0	0,0	0,0	0,0	0,0	0,0	0,0	0,3	1,4	3,5	5,0	4,6	3,1	1,6	0,7	0,2	0,1	0,0
14,5	0,0	0,0	0,0	0,0	0,0	0,0	0,0	0,1	0,4	1,2	1,8	1,8	1,3	0,7	0,3	0,1	0,0	0,0
15,5	0,0	0,0	0,0	0,0	0,0	0,0	0,0	0,0	0,1	0,4	0,6	0,7	0,5	0,3	0,1	0,1	0,0	0,0
16,5	0,0	0,0	0,0	0,0	0,0	0,0	0,0	0,0	0,0	0,1	0,2	0,2	0,2	0,1	0,1	0,0	0,0	0,0

Appendix B

Design Structure Matrix applied to SGISc

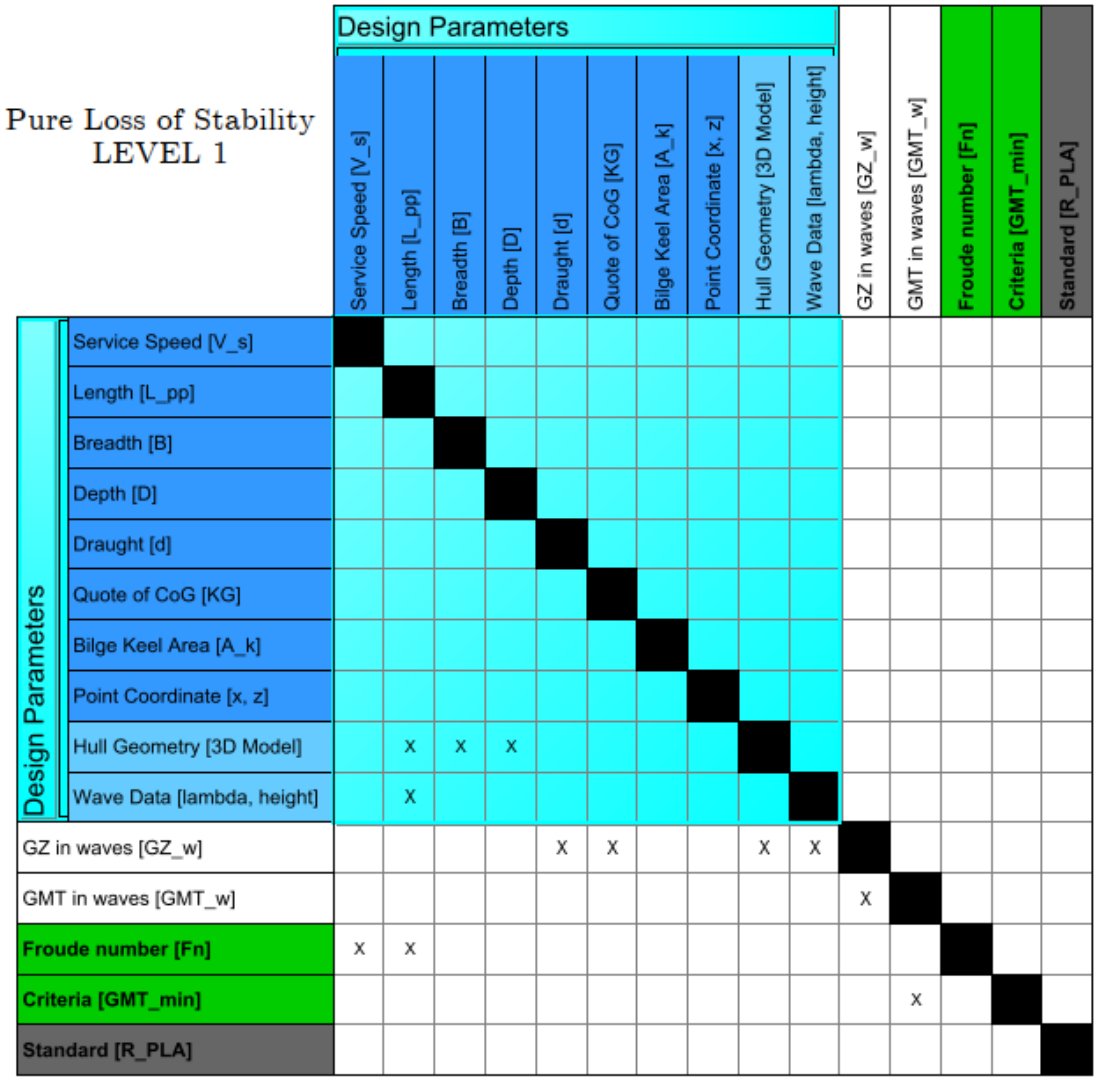

Figure B.1: Design Structure Matrix of first vulnerability level of pure loss of stability

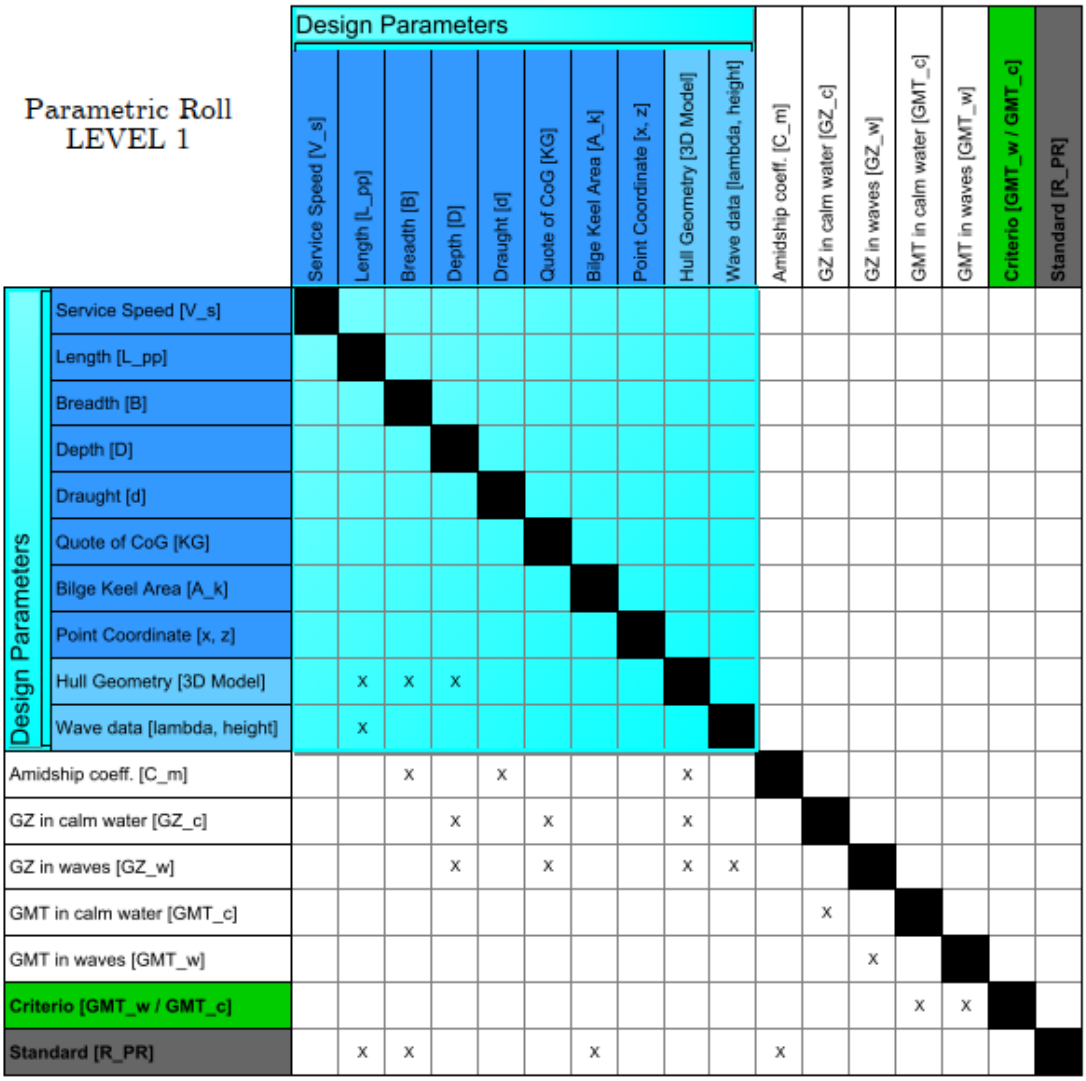

Figure B.2: Design Structure Matrix of first vulnerability level of parametric roll

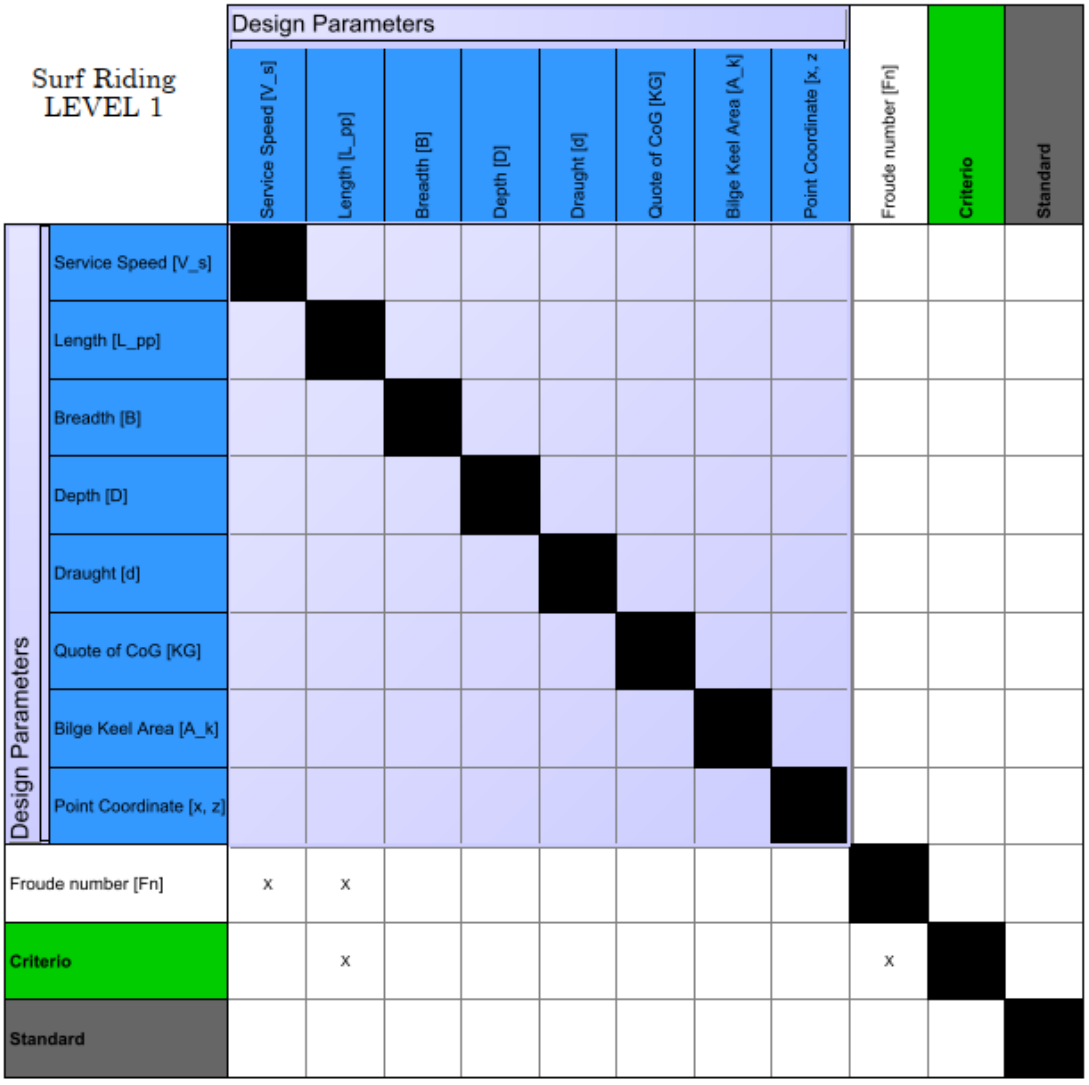

Figure B.3: Design Structure Matrix of first vulnerability level of surf-riding

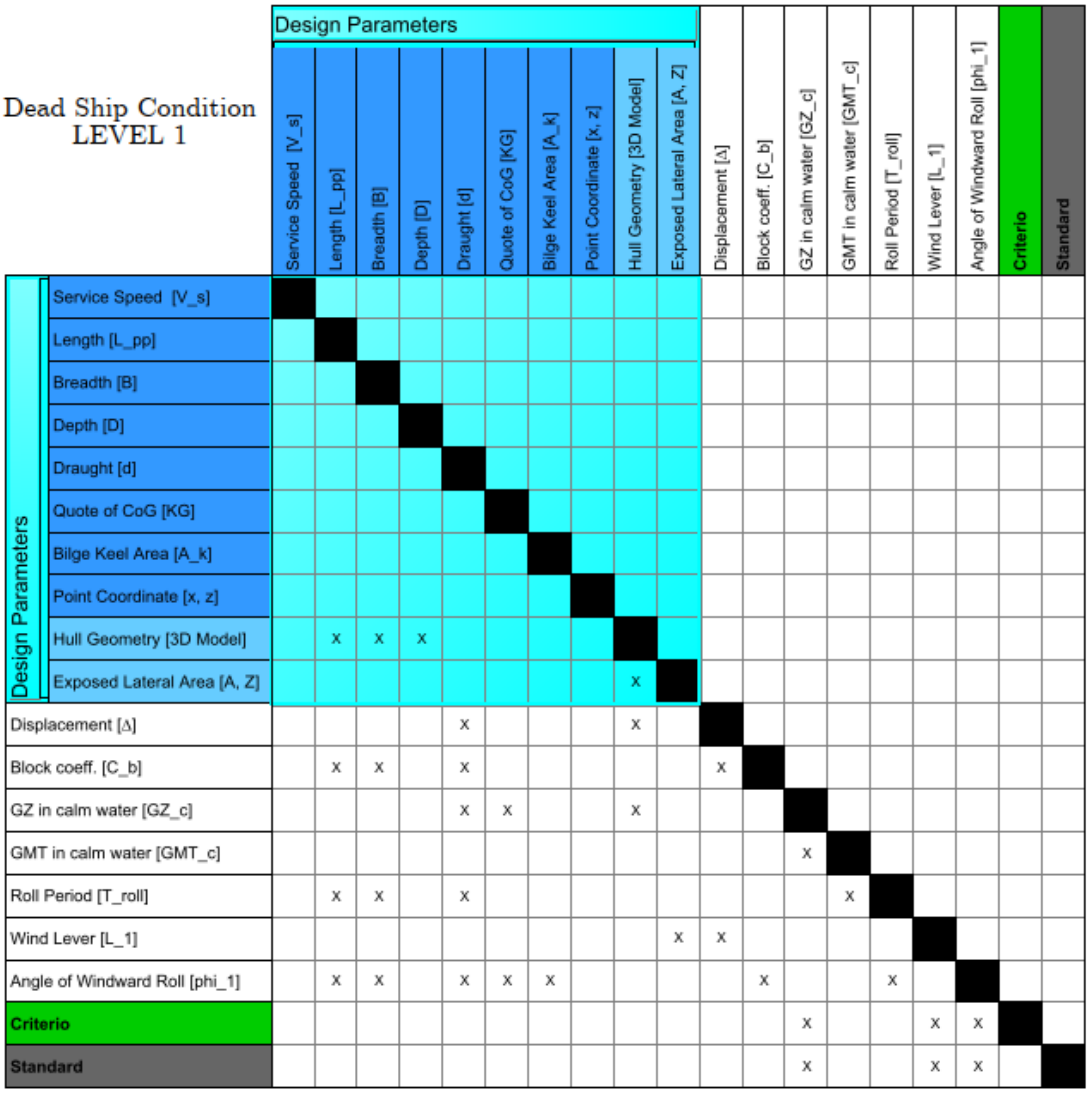

Figure B.4: Design Structure Matrix of first vulnerability level of dead ship condition

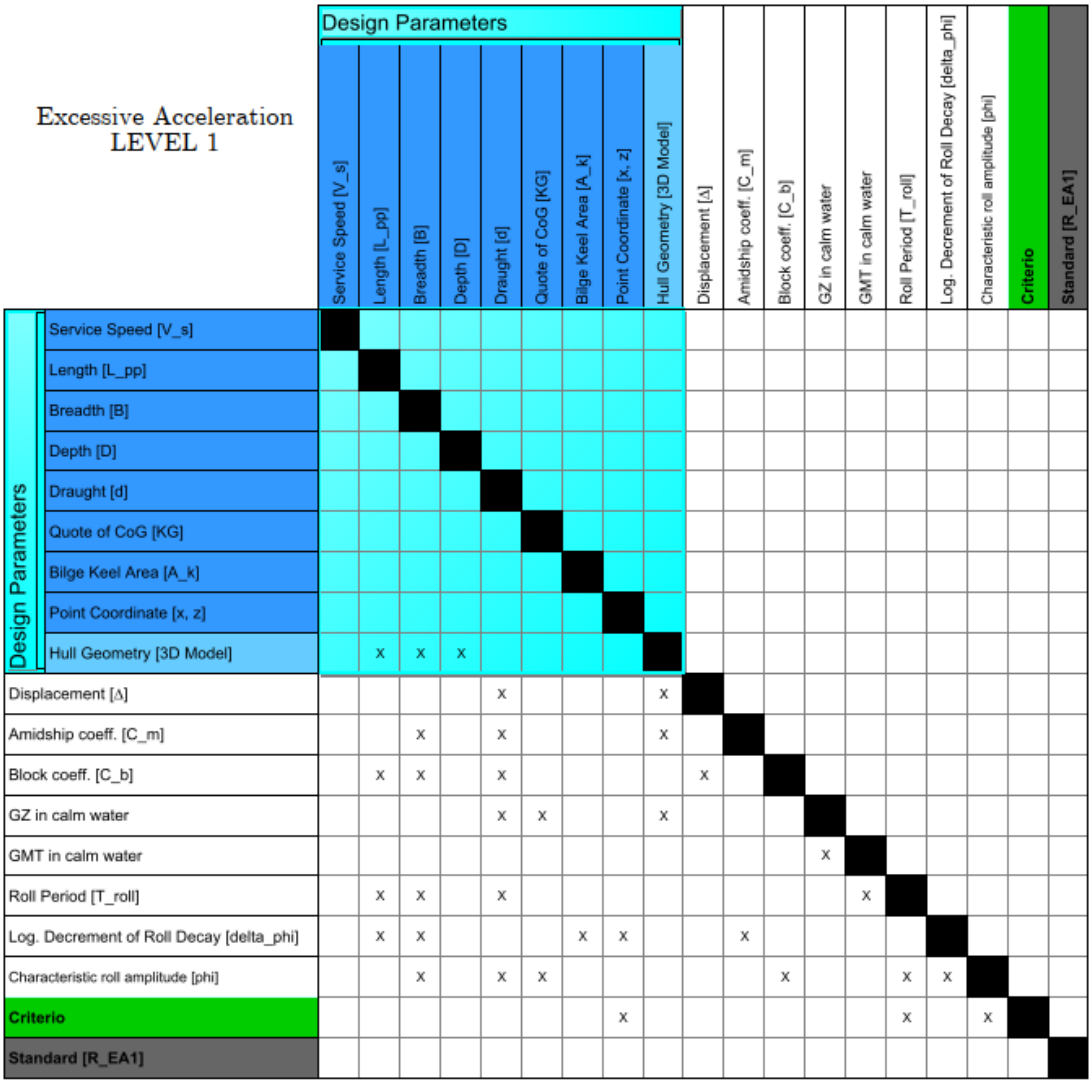

Figure B.5: Design Structure Matrix of first vulnerability level of excessive acceleration

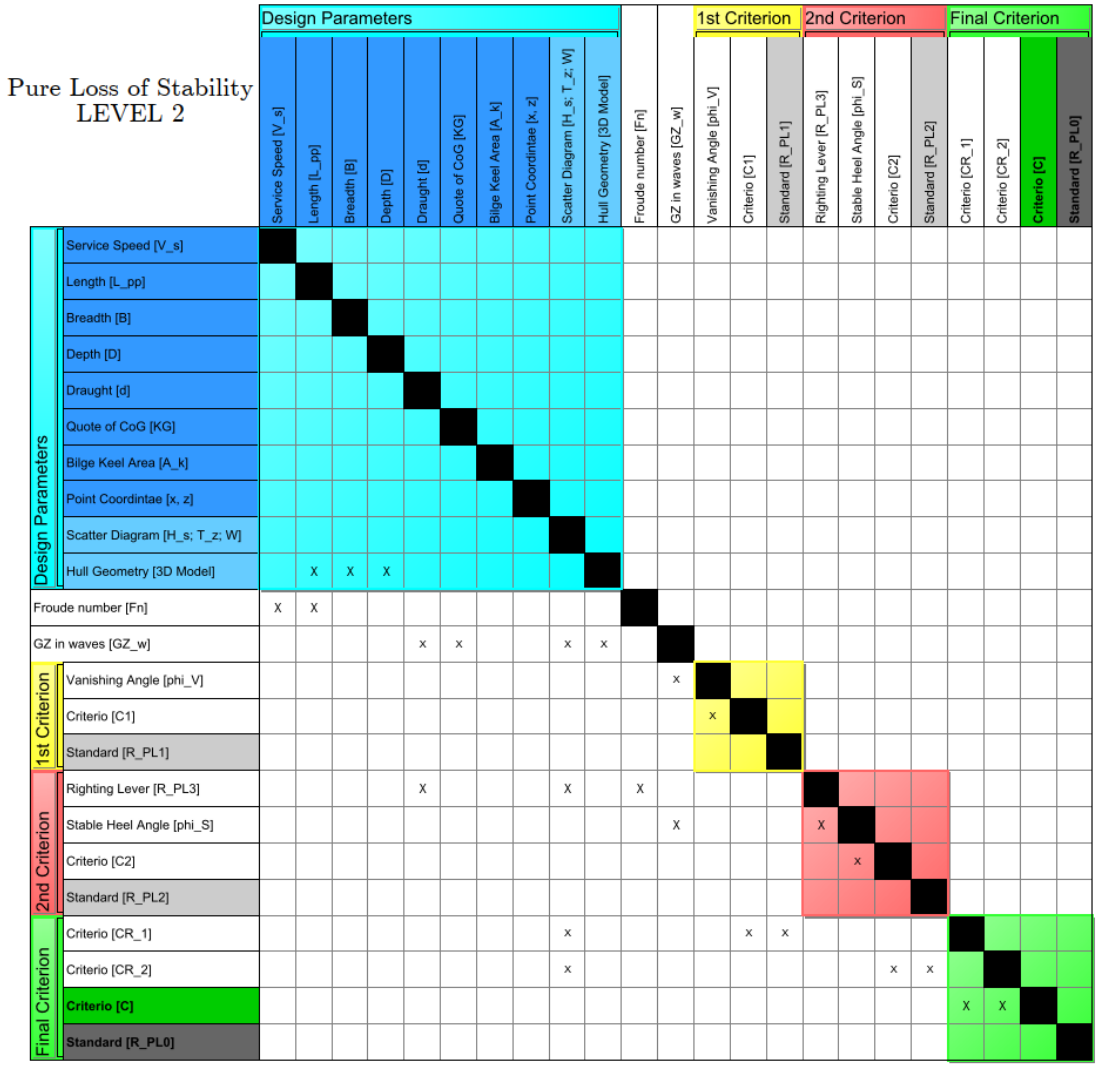

Figure B.6: Design Structure Matrix of second vulnerability level of pure loss of stability

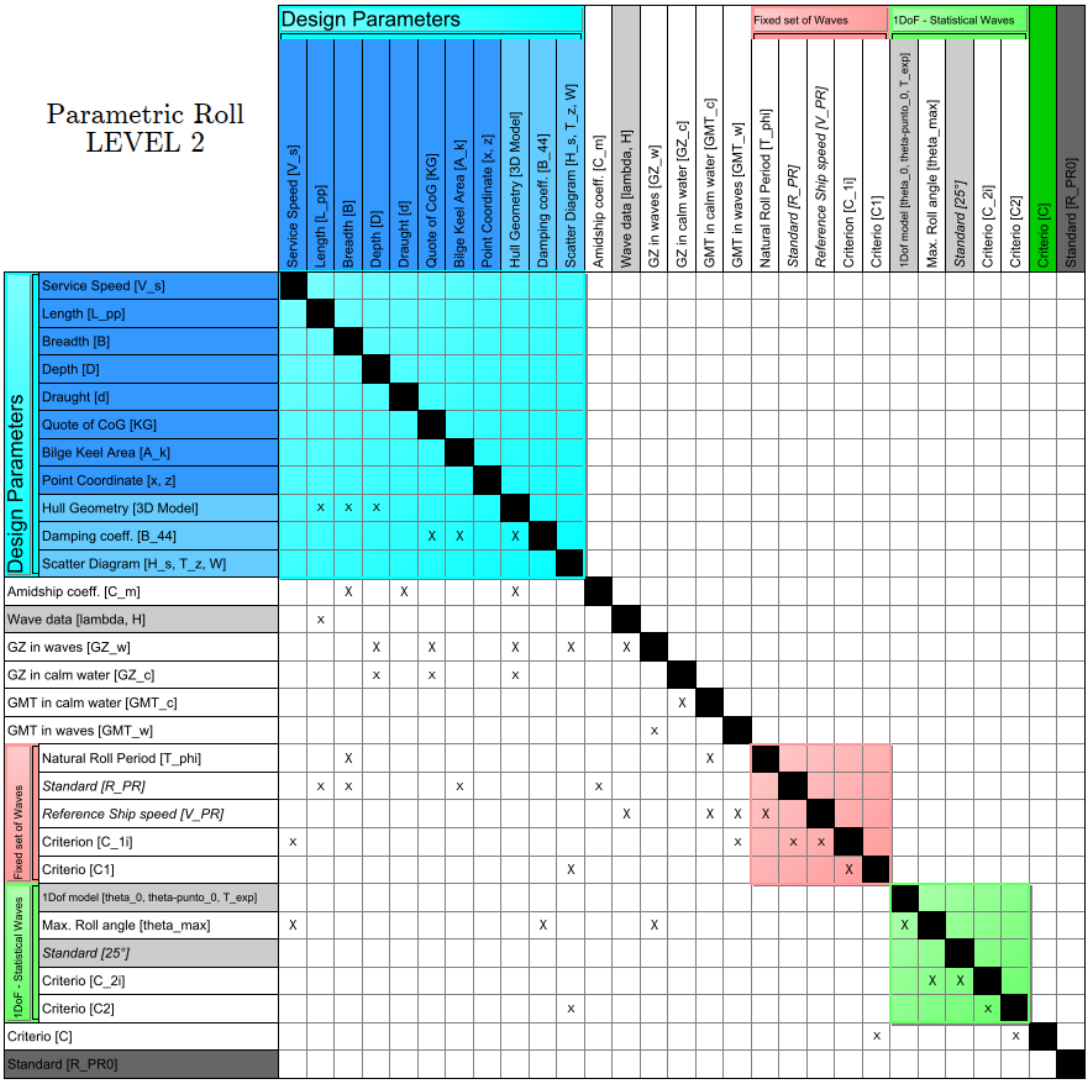

Figure B.7: Design Structure Matrix of second vulnerability level of parametric roll

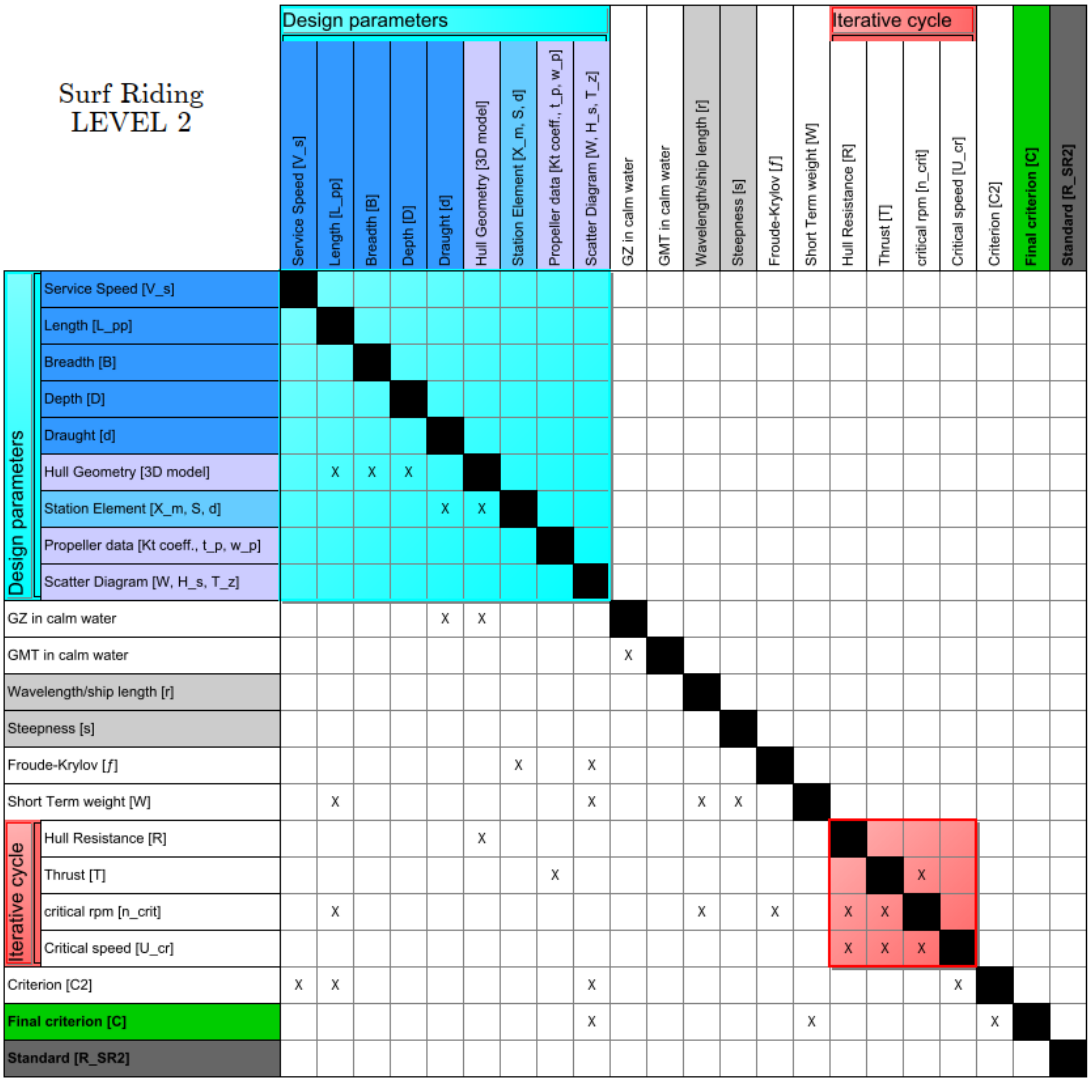

Figure B.8: Design Structure Matrix of second vulnerability level of surf-riding

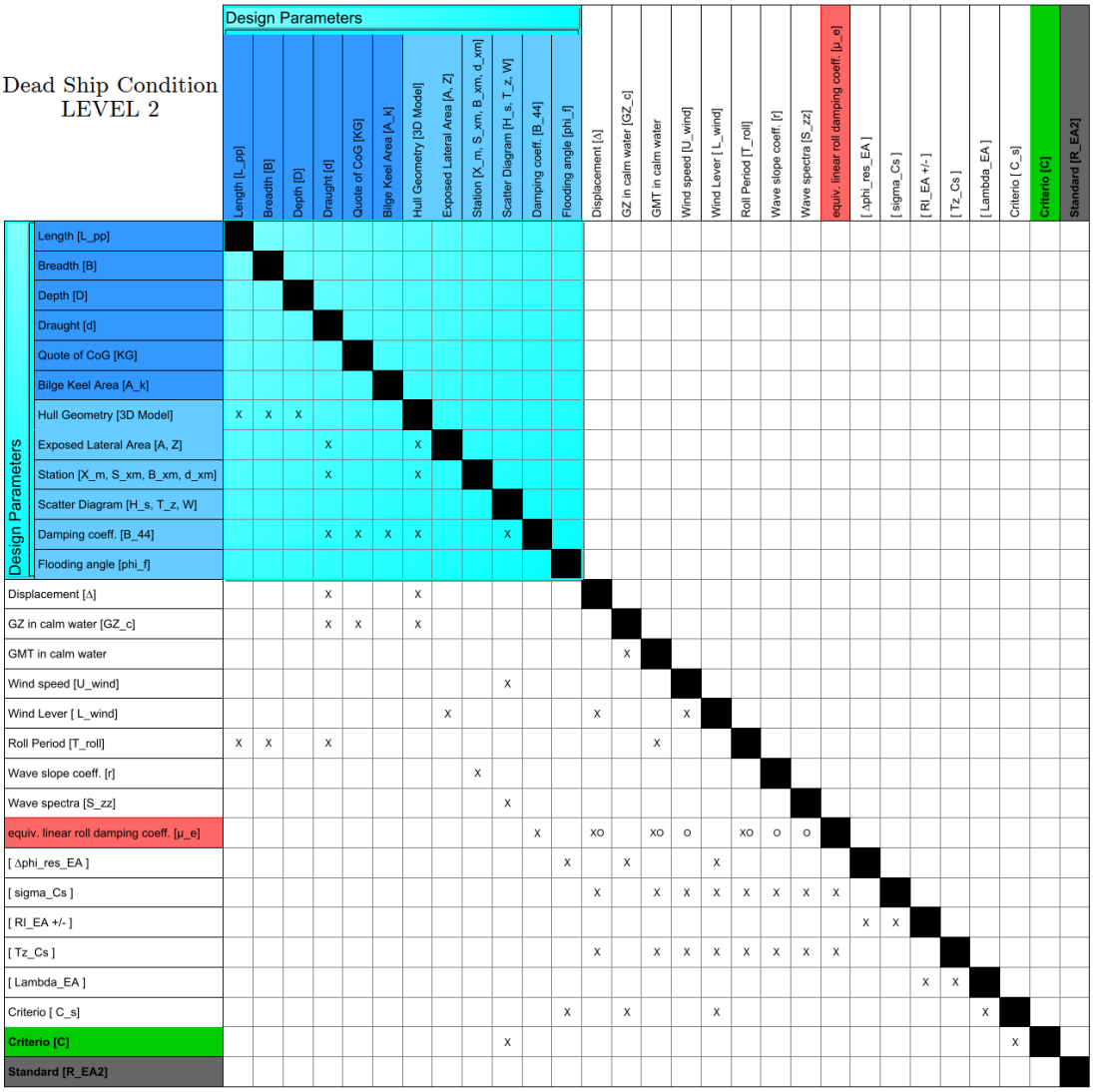

Figure B.9: Design Structure Matrix of second vulnerability level of excessive acceleration

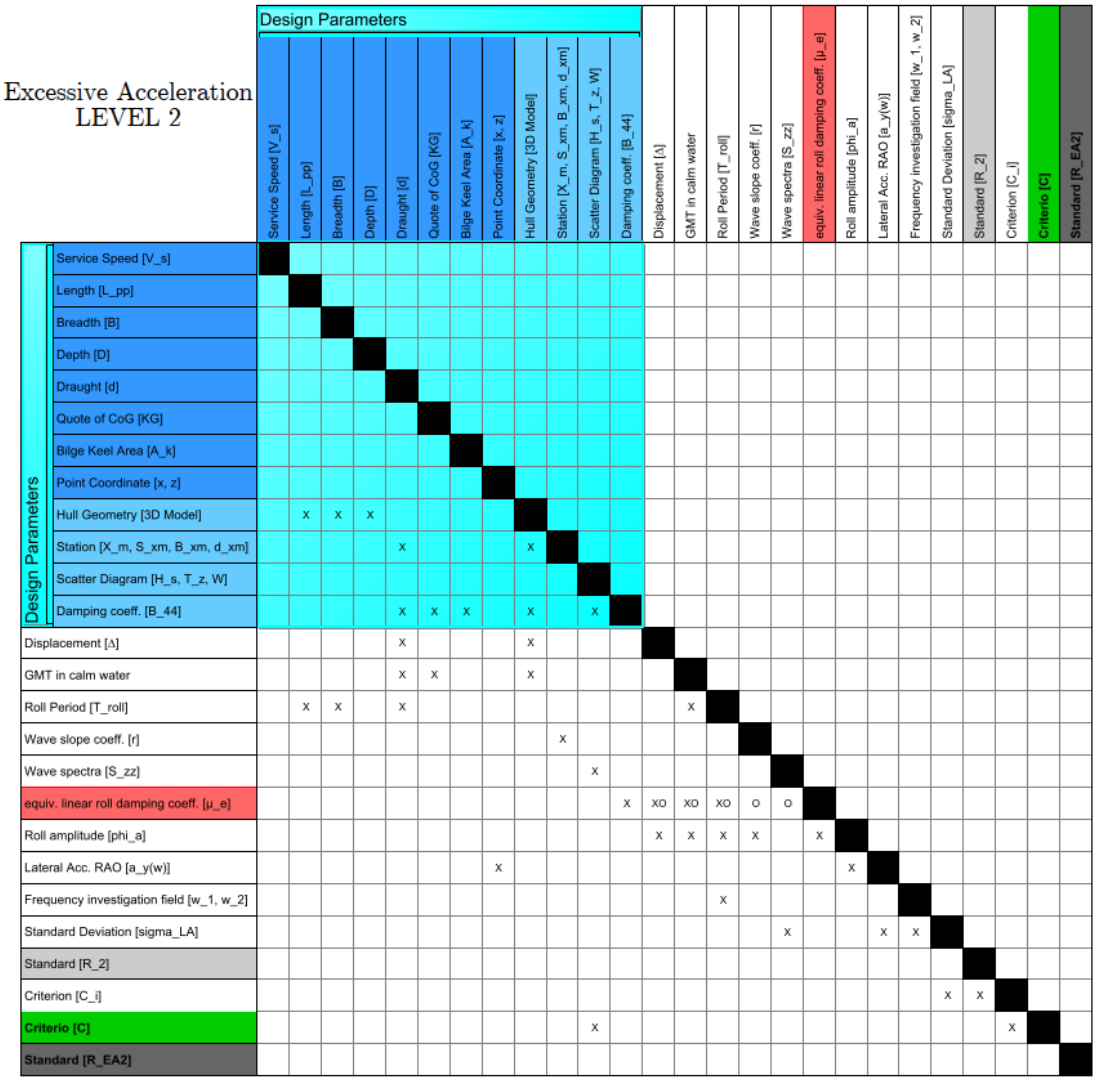

Figure B.10: Design Structure Matrix of second vulnerability level of dead ship condition

Appendix C

General Arrangement of megayacht unit

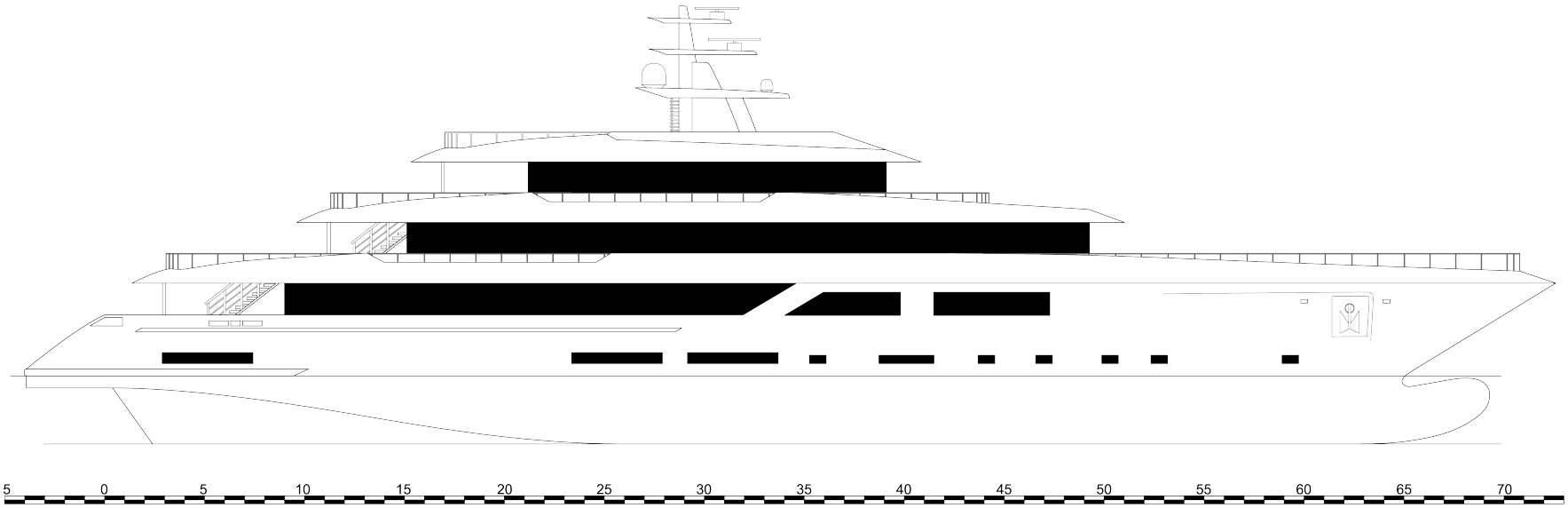

Figure C.1: Megayacht - Longitudinal view

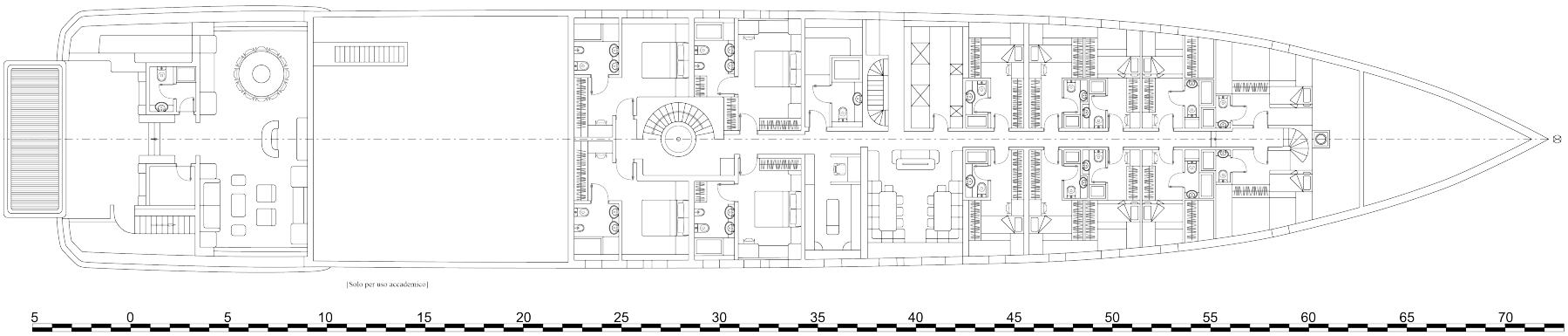

Figure C.2: Megayacht - Lower Deck

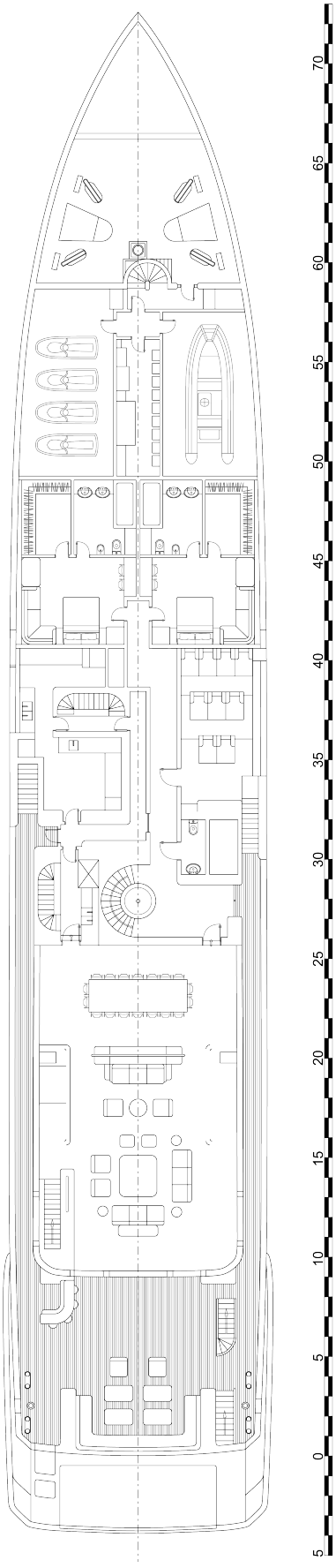

Figure C.3: Megayacht - Main Deck

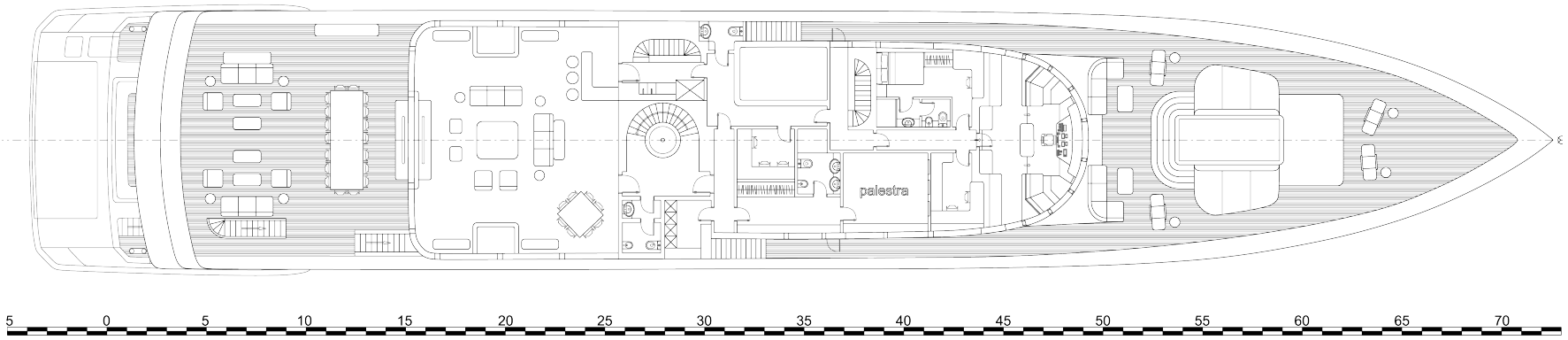

Figure C.4: Megayacht - Upper Deck

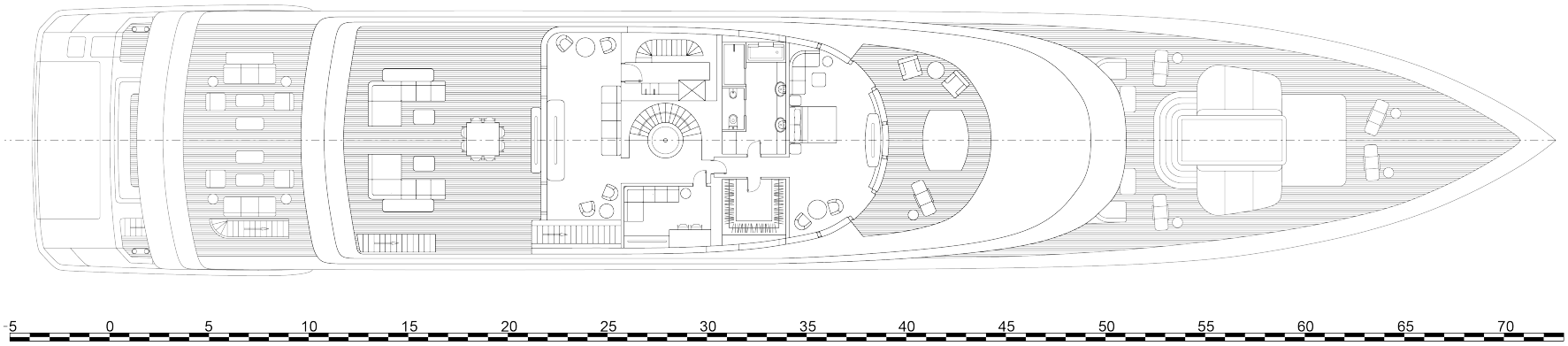

Figure C.5: Megayacht - Fly Bridge

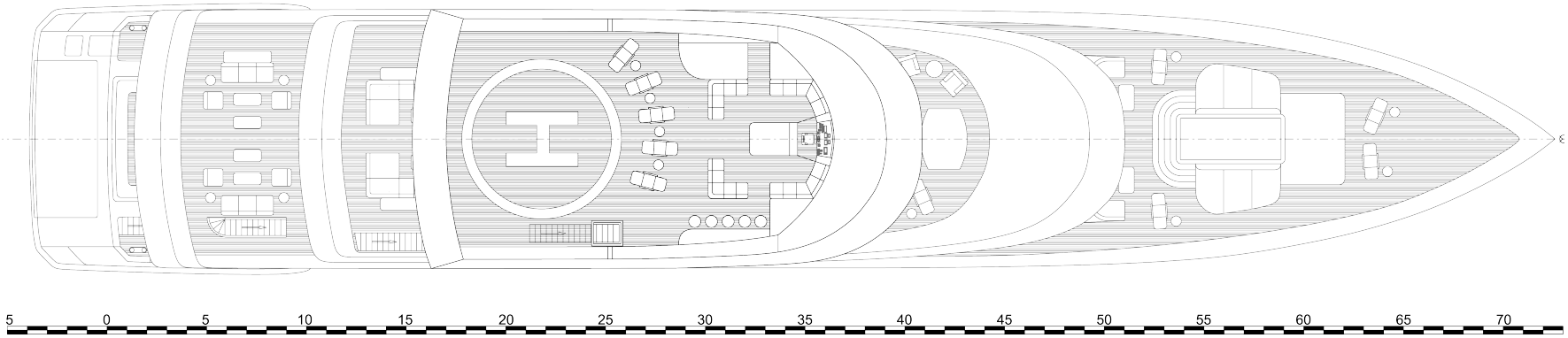

Figure C.6: Megayacht - Sun Deck